Imperial College London

The development of novel sustainable carbonaceous materials as substitutes for carbon black in rubber-based products

Yiran Fan

A thesis submitted to Imperial College London for the degree of Doctor of Philosophy

August 2017

Department of Civil and Environmental Engineering

Faculty of Engineering

Imperial College London

Declaration of Originality

I, YIRAN FAN, confirm that the work presented in this PhD thesis is my own original work.

Signature: FAN YIRAN

Date: 16/08/2017

The copyright of this thesis rests with the author and is made available under a Creative Commons Attribution Non-Commercial No Derivatives licence. Researchers are free to copy, distribute or transmit the thesis on the condition that they attribute it, that they do not use it for commercial purposes and that they do not alter, transform or build upon it. For any reuse or redistribution, researchers must make clear to others the licence terms of this work.

Abstract

Carbon black is a commodity material which is used mostly as a reinforcing filler in rubber and plastic production. Its manufacture is not only energy-consuming, contributes significantly to global CO_2 emissions, but uses non-renewable feedstock making it unsustainable. Given the increasing pressure against the continued use of non-renewable sources of feedstock, there is an exciting opportunity to develop alternative materials to act as rubber fillers for environmental and economic reasons.

This research has focused on the development of novel carbonaceous rubber fillers produced through the pyrolysis of coconut shell and raw sewage sludge. The basic properties of feedstock were evaluated to assess the efficacy of final filler performance; a Response Surface Methodology was applied to model the relationship between pyrolysis conditions and the key physical and chemical properties of the char filler and to optimise the pyrolysis process. Feedstock were pyrolysed using a laboratory-scale furnace using various temperatures, heating rates, holding times and atmospheres. A comparison was made between char fillers and commercial carbon blacks to establish the optimum production conditions. The selected char fillers were mixed with styrene-butadiene rubber and the rubber products were evaluated for their technological performance. Therefore, a fundamental understanding of the rubber-char filler interaction and the performance of the sustainable fillers was developed. By-products (oil and gas) were also studied as a wider sustainability study embedded within the research.

The coconut shell and raw sewage sludge have significant potential for use as a sustainable feedstock for carbon black replacement in rubber manufacture. These fillers were found to have equivalent surface area (2.9 – 318.2m^2/g) to a semi-reinforcing filler and provide 52 – 59° hardness, 482 – 962% elongation at break to the rubber products. Further research has been identified to improve post-production processing and rubber formulation which would help further optimize and improve the product for in-rubber use.

Acknowledgement

I would like to express my deepest gratitude to my wonderful supervisor Dr Geoff Fowler for his continuous guidance, support and encouragement throughout the last three and half years. Thank you for everything and thank you for believing I could, for always being there to help. I am also thankful to Mrs Carol Edwards and Dr Ángel Nievas Pino in the Roger Perry lab for their technical support and suggestion.

I would like to thank Dr Chris Norris, Mr Martyn Bennett and the Avon Rubber (Artis UK) for their technical advice and the rubber products analysis. I would like to express thanks to Mr Darryl A Walters from Cabot Performance Materials UK Ltd and Avon Rubber (Artis UK) for supply carbon black samples.

I would like to thank all my colleagues and friends: Miss Emma Fryer, Dr Ruben Menke, Dr Athanasios Bourtsalas, Dr Ding Zhou, Dr Nicolas Schaeffer and others in the two labs, office 411 and EWRE group for their sincere advice and help for both research and life. I am also thankful to the staff of Department of Civil and Environmental Engineering.

Finally, I am very grateful to my parents for their care, concern and support, without whom I would not be able to fulfil my PhD. Thank you for always being standing behind me, silently supporting me and encouraging me.

Table of Contents

Chapter 1 Introduction and Literature Review.....17

1.1 Introduction 17

1.2 Global Warming and Waste Management 19

1.2.1 Greenhouse Gases and Global Warming.....19

1.2.2 Waste Management and GHG Emission Control.....21

1.2.2.1 European Community (EC) Directive 1999/31/EC on the Landfill of Waste ..21

1.2.2.2 Directive 2000/76/EC on the Incineration of Waste.....22

1.2.2.3 Directive 2008/98/EC Waste and Repealing Certain Directives 22

1.2.2.4 Waste Hierarchy.....23

1.3 Sewage Sludge and its Management.....24

1.3.1 Sludge Characteristics 24

1.3.2 Sludge Disposal in Practice 28

1.4 Carbon Black.....30

1.4.1 Rubber 30

1.4.2 Carbon Black 32

1.4.2.1 Classification.....35

1.4.3 Characterisation of Carbon Black.....36

1.4.3.1 Particle and Aggregate Size 37

1.4.3.2 Surface Area.....39

1.4.3.3 Structure.....40

1.4.3.4 Chemical Properties of the Surface.....41

1.5 Rubber – Carbon Black System 42

1.5.1 Carbon Black Reinforcement Mechanism.....42

1.5.1.1 Small Particle Size 44

1.5.1.2 Slippage at Interface 46

1.5.1.3 Chemical Reaction 47
1.5.2 New Direction for Carbon Black 50
1.5.2.1 Surface Modification on Carbon Black 50
1.5.2.2 Alternative Feedstock for Carbon Black Substitute 52
1.6 Response Surface Methodology (RSM) 57
1.6.1 Experimental Design for Multi-level Variable 59
1.6.2 Multi-objective Optimization 62
1.7 Summary 63
Chapter 2 Research Aim and Objectives 64
Chapter 3 Materials and Methodology 66
3.1 Introduction 66
3.2 Materials 66
3.2.1 Sources of Char Filler 66
3.2.1.1 Coconut Shell 66
3.2.1.2 Sewage Sludge 67
3.2.2 Commercial Carbon Blacks 68
3.2.2.1 Carbon Black N115 68
3.2.2.2 Carbon Black N220 69
3.2.2.3 Carbon Black N330 69
3.2.2.4 Carbon Black N550 71
3.2.2.5 Carbon Black N660 71
3.2.2.6 Carbon Black N772 71
3.2.3 Chemical Reagents 72
3.3 Methodology 72
3.3.1 Preparation of a Series of Char Fillers 72
3.3.1.1 Thermogravimetric Analysis (TGA) 72

3.3.1.2 Proximate Analysis 75
3.3.1.3 Carbon Hydrogen Nitrogen Sulphur Analysis 76
3.3.1.4 Conventional Thermal Pyrolysis 76
3.3.1.5 Response Surface Methodology (RSM) Design 78
3.3.1.6 Post-pyrolysis Grinding by Wet TEMA Milling 80
3.3.2 Characterization Methods 80
3.3.2.1 Textural Characterization 80
3.3.2.2 Toluene Extraction 81
3.3.2.3 pH Value 82
3.3.2.4 Boehm Titration 82
3.3.2.5 Transmission Electron Microscopy 82
3.3.3 In-rubber Testing 83
3.3.4 Scanning Electron Microscopy 85
3.3.5 Oil Calorific Value Analysis 85
3.4 Summary 86
Chapter 4 Coconut Shell Derived Char Fillers 87
4.1 Characterisation of Coconut Shell 87
4.1.1 Thermal Analysis of Coconut Shell 87
4.1.1.1 TGA-DTG Curves 87
4.1.1.2 Proximate Analysis 90
4.2 Overview of Pyrolysis 91
4.3 Characteristics of Commercial Carbon Blacks and Char Fillers 93
4.4 RSM Process Optimization 97
4.4.1 Char Filler pH Value Response Analysis 97
4.4.1.1 Statistical Analysis 97
4.4.1.2 Optimization of Pyrolysis Process on pH Value and Interaction between Independent Variables 97

4.4.1.3 Statistical Analysis and Validation of Model 100

4.4.1.5 Optimization of Pyrolysis Process based on pH Value and Model Verification 107

4.4.2 Char Filler t-plot Surface Area Response Analysis 108

4.4.2.1 Statistical Analysis 108

4.4.2.2 Optimization of Pyrolysis Process on t-plot Surface Area and Interaction between Independent Variables 108

4.4.2.3 Statistical Analysis and Validation of the Model 109

4.4.2.4 Interaction among Parameters Influencing Pyrolysis Process and t-plot Surface Area 111

4.4.2.5 Optimization of Pyrolysis Process based on t-plot Surface Area and Model Verification 115

4.5 Coconut Shell Derived Char Fillers In-rubber Tests 116

4.5.1 Transmission Electron Microscope (TEM) Results 116

4.5.2 Carbon Hydrogen Nitrogen Sulphur Tests 122

4.5.3 In-rubber Characterization 123

4.6 Conclusion 137

Chapter 5 Raw Sewage Sludge Derived Char Filler 138

5.1 Characterisation of Raw Sewage Sludge 138

5.1.1 TGA-DTG Curves 138

5.1.2 Proximate Analysis 139

5.2 Overview of Pyrolysis of Raw Sewage Sludge 140

5.3 Characteristics of Commercial Carbon Blacks and Sludge Char Fillers 142

5.4 RSM Process Optimization 144

5.4.1 Sludge Char Filler pH Value Response Analysis 145

5.4.1.1 Statistical Analysis 145

5.4.1.2 Optimization of Pyrolysis Process on the pH Value and Interaction between Independent Variables 145

5.4.1.3 Statistical Analysis and Validation of Model 148
5.4.1.4 Optimization of Pyrolysis Process based on pH Value and Model Verification 151
5.4.2 Sludge Char Filler t-plot Value Response Analysis 152
5.4.2.1 Statistical Analysis 152
5.4.2.2 Optimization of Pyrolysis Process on the t-plot Surface Area and Interaction between Independent Variables 152
5.4.2.3 Statistical Analysis and Validation of Model 153
5.4.2.4 Optimization of Pyrolysis Process based on t-plot Surface Area and Model Verification 156
5.4.3 Sludge Char Surface Acidic Groups Response Analysis 156
5.4.3.1 Statistical Analysis 156
5.4.3.2 Optimization of the Pyrolysis Process on Surface Acidic Groups and Interaction Between Independent Variables 157
5.4.3.3 Statistical Analysis and Validation of the Model 158
5.4.3.4 Interaction among Parameters Influencing the Pyrolysis Process and the Surface Acidic Group Values 161
5.4.3.5 Optimization of the Pyrolysis Process based on Acidic Groups Value and Model Verification 165
5.5 Raw Sewage Sludge Derived Char Fillers In-rubber Test 166
5.5.1 Transmission Electron Microscope (TEM) Result 167
5.5.2 Carbon Hydrogen Nitrogen Sulphur Tests 169
5.5.3 In-rubber Characterization 171
5.6 Conclusion 183
Chapter 6 Environmental Impact Evaluation 184
6.1 Calculation of Energy Consumption 184
6.1.1 Life Cycle Assessment 184
6.2 Methodology 185

6.3 Energy Assessment 187
6.3.1 Energy Consumption Assessment 187
6.3.2 The Calorific Value of Oil Output 188
6.4 Energy Analysis 190
6.5 Carbon Dioxide Emission Saving 192
6.6 Conclusion 193
Chapter 7 Conclusions and Future Work 194
7.1 Conclusions 194
7.2 Contributions to Knowledge 197
7.3 Future Work 198
References 200
Appendix I 228
Appendix II 231

List of Figures

Figure 1-1 Waste Hierarchy (EC, 2008) 23
Figure 1-2 Typical wastewater treatment process (after Lenntech, 2017) 25
Figure 1-3 1-2 cis-1,4-polyisoprene (Chiang, 2013) 30
Figure 1-4 Chemical structure of natural rubber. Head α and end group ω are not proven (Chiang, 2013) 31
Figure 1-5 Carbon black 34
Figure 1-6 Carbon black structure (Wang et al., 2000) 35
Figure 1-7 Comparison between filled and unfilled rubber matrix (Edwards, 1990) 43
Figure 1-8 Schematic illustration of the effect of particle size on rubber reinforcement (Edwards, 1990) 45
Figure 1-9 Changes in the microstructure of a filled rubber system under strain (Dannenbery, 1966) 46
Figure 1-10 Chemical function on carbon black surface (after Bueche, 1960) 47
Figure 1-11 Example of (a) 3D plot and (b) contour plot of response surface for two variables (Myers et al., 2009) 58
Figure 1-12 Design points for CCD designs with (a) 2 variables and (b) 3 variables (Sharifan, 2014) 59
Figure 1-13 Design points for BBD design with (a) 2 variables and (b) 3 varibales (Sharifan, 2014) 60
Figure 1-14 Doehlert design with (a) 2 variables and (b) 3 variables (Sharifan, 2014) 61
Figure 2-1 Flow diagram of the process for the production of carbon black substitutes 65
Figure 3-1 Dried coconut shell 67
Figure 3-2 Dried raw sewage sludge 68
Figure 3-3 STA 1500 Simultaneous Thermal Analyser 74
Figure 3-4 Carbolite 11/50 rotary furnace 78
Figure 3-5 Parr 6100 Calorimeter 86
Figure 4-1 TG and DTG curves of coconut shell under N_2 88
Figure 4-2 Proximate analysis of coconut shell 90
Figure 4-3 Perturbation plots with four pyrolysis parameters on char yield 93
Figure 4-4 Pareto chart showing the effects of different independent variable on pH value 100
Figure 4-5 (a) Experimental values and predicted values for the model & (b) Normal probability plot of the residues 103

Figure 4-6 (a-f) Response surface plots of pH value, illustrating the interaction between two variables: selected for temperature, heating rate, holding time and nitrogen flow rate.....106
Figure 4-7 Pareto chart showing the effects of different independent variable on pH value 109
Figure 4-8 (a) Experimental values and predicted values for the model & (b) Normal probability plot of the residuals 111
Figure 4-9 (a-f) Response surface plots of t-plot surface area, illustrating the interaction between two variables: selected for temperature, heating rate, holding time and nitrogen flow rate.....114
Figure 4-10(a-h) TEM-micrographs of Run 20, Run 30, N330 and N772 at 6K and 25K magnification, showing particle shape, size and distribution 120
Figure 4-11 3D surface roughness maps highlighting filler dispersion, scale in micron 125
Figure 4-12(a-i) SEM plots of compounded rubber sheets at 25K magnification, illustrating rubber-filler bonding system.....130
Figure 4-13 MDR cure profiles of coconut shell chars in the SBR system.....133
Figure 4-14 Elastic modulus plots against double strain amplitude of the compounds containing N772 and coconut char 134
Figure 4-15 ΔE'networking efficiency versus surface area of coconut chars 135
Figure 4-16 Coconut char Run 20 compared to N330.....136
Figure 4-17 Coconut char Run 20 compared to calcined clay.....136
Figure 5-1 TG and DTG curves of sewage sludge under N_2 138
Figure 5-2 Proximate analysis of raw sewage sludge.....139
Figure 5-3 Perturbation plots with four pyrolysis parameters on the sludge char yield.....142
Figure 5-4 (a) Experimental pH values and predicted pH values for the model & (b) Normal probability plot of the residues 149
Figure 5-5 Diagnostic plots for pH value (a) residual versus predicted pH value and (b) residual versus run number 151
Figure 5-6 (a) Experimental t-plot surface area values and predicted t-plot surface area values for the model & (b) Normal probability plot of the residuals.....154
Figure 5-7 Diagnostic plots for t-plot surface area value (a) residual versus predicated value and (b) residual versus run number.....155
Figure 5-8 Pareto chart showing the effects of different independent variables on surface acidic groups 157

Figure 5-9 (a) Experimental surface acidic group values and predicted surface acidic group values for the model & (b) Normal probability plot of the residues.....160
Figure 5-10 Diagnostic plots for surface acidic group value (a) residual versus predicted value and (b) residual versus run number.....161
Figure 5-11 (a-f) Response surface plots of surface acidic groups, illustrating the interaction between two variables: selected for temperature, heating rate, holding time and nitrogen flow rate.....165
Figure 5-12 TEM-micrographs of Run 13 and Run 20 at 6K and 25K magnification, showing particle shape, size and distribution.....169
Figure 5-13 3D surface roughness maps highlighting filler dispersion, scale in micron 173
Figure 5-14(a-i) SEM plots of compounded rubber sheets at 25K magnification, illustrating rubber-filler boning system.....177
Figure 5-15 MDR cure profiles of sludge chars in the SBR system.....178
Figure 5-16 Elastic modulus plots against double strain amplitude of the compounds containing N772 and sludge chars 180
Figure 5-17 ΔE'networking efficiency versus surface area.....181
Figure 5-18 Char samples compared to N772 182
Figure 5-19 Carbon black N990 appearance 183
Figure 6-1 Three systems in this study 186
Figure 6-2 The input and output of the three production processes 191

List of Tables

Table 1-1 Typical composition and properties of sewage sludge (Tchobanoglous et al., 2003) 26
Table 1-2 Indicative metal content in wastewater solids (Tchobanoglous et al., 2003) 27
Table 1-3 Classification and typical particle size of carbon blacks 36
Table 1-4 Mean particle size of typical carbon blacks 38
Table 1-5 SBR (Styrene-Butadiene Rubber) Formulation 44
Table 1-6 Theories on filled elastomer 49
Table 1-7 Materials used as rubber fillers 56
Table 1-8 Comparison of CCD, BBD and DM (Ferreira et al., 2004) 62
Table 3-1 Main technical characteristics of carbon blacks 70
Table 3-2 Chemical reagent 72
Table 3-3 Proximate analysis protocol 75
Table 3-4 Variables and their levels used in the experimental design 79
Table 3-5 SBR formulation 84
Table 3-6 Mixing procedure 84
Table 4-1 Char, oil and gas yield from pyrolysis 92
Table 4-2 Characterization of carbon black and char filler 95
Table 4-3 Experimental design matrix with experimental and predicted values 98
Table 4-4 Analysis of variance of the fitted quadratic regression model 101
Table 4-5 Optimum condition solution for optimum pH value 108
Table 4-6 Analysis of variance of the fitted quadratic regression model 110
Table 4-7 Optimum conditions solutions for t-plot surface area 115
Table 4-8 Selection of coconut shell derived char fillers for in-rubber tests 116
Table 4-9 Elemental composition of coconut shell, char fillers and commercial carbon black 122
Table 4-10 Rheology and physical data of coconut shell chars 131
Table 5-1 Char, oil and gas yield from pyrolysis of sewage sludge 141
Table 5-2 Characterization of carbon black and sludge char filler 143
Table 5-3 Experimental design matrix with experimental and predicted values 146
Table 5-4 Analysis of variance of the fitted linear regression model 148
Table 5-5 Optimum condition solution for optimum pH value 152
Table 5-6 Analysis of variance of the fitted linear regression model 153

Table 5-7 Optimum condition solution for optimum t-plot surface area 156
Table 5-8 Analysis of variance of the fitted quadratic regression model 158
Table 5-9 Optimum conditions solution for acidic group value 166
Table 5-10 Selection of coconut shell derived char fillers for in-rubber tests 166
Table 5-11 Elemental composition of sewage sludge and sludge char fillers 170
Table 5-12 Rheology and physical data of sludge chars 179
Table 6-1 The energy consumption sources during pyrolysis 187
Table 6-2 Energy usage of feedstock pyrolysis 188
Table 6-3 Calorific value of oil output 188
Table 6-4 Energy obtained from oil output per batch 189
Table 6-5 Final net energy consumption 189
Table 6-6 Carbon dioxide emissions of the different system 192

List of Abbreviation

ANOVA	Analysis of Variance
ASTM	American Standard for Testing and Materials
BBD	Box-Behnken Design
BET	Brunauer-Emmett-Teller
BS	British Standard
CCD	Central Composite Design
CCFD	Central Composite Face Centred Design
CHNS	Carbon Hydrogen Nitrogen Sulphur
DEFRA	Department of the Environment, Food and Rural Affairs
DM	Doehlert Matrix
DMA	Dynamic Mechanical Analysis
DSA	Double Strain Amplitude
DTG	Derivative Thermogravimetry
GHG	Greenhouse Gas
IEA	International Energy Agency
IPCC	International Panel on Climate Change
ISO	International Organisation for Standardization
M100	Modulus at 100% Elongation
M300	Modulus at 300% Elongation
MDR	Moving Die Rheometer
NR	Natural Rubber
NSA	Nitrogen Surface Area
phr	Parts per Hundred Rubber
RSM	Response Surface Methodology
SBR	Styrene Butadiene Rubber

SEM	Scanning Electron Microscopy
TEM	Transmission Electron Microscopy
TG	Thermogravimetry
TGA	Thermogravimetric Analysis

Chapter 1 Introduction and Literature Review

1.1 Introduction

There is a significant use of carbon black as a reinforcing material and additive in the fields of elastomers and materials manufacture. Over 11 million tonnes of carbon black are used every year in tyre manufacture alone. The carbon filler in rubber can make up over 30% of the material by weight (Kühner & Voll, 1993). The key property of carbon black fillers is the ability to bond with the elastomer component, hence providing mechanical strength as well as imparting durability to the materials.

The manufacturing process of carbon black requires a partial combustion of fossil-origin hydrocarbon fuels (such as heavy oil, coal tar and natural gas etc.) under reduced oxygen conditions. The production is not only energy intensive, but also unsustainable in the long-term as a source of feedstock to produce carbon black. Due to the increasing demand for non-renewable materials in industrial and manufacturing processes, coupled with the need to reduce the release of fossil-origin carbon dioxide and the widespread recognition, that the adoption of the circular economy model is important for the long-term development of society; there is a major need to research and develop the potential of alternative and waste materials to be used in polymeric products which can replace carbon black fillers.

There has been a significant shift in industrial societies through recognition of the finite nature of materials and resources. Hence, growing focus on the treatment and disposal of waste material is becoming a priority. A variety of legislation on waste management has been approved by the European Union in recent decades. The waste framework directive of 1975 required Member States to manage waste by encouraging prevention and responsible disposal. The treatment and disposal of waste materials is becoming a problem of increasing urgency in industrialized societies (McAllister, 2015; Strange, 2002). There is no doubt that the concern about environmental issues is gradually increasing. At the same time, environmental issues have been constantly broadened with concepts, such as sustainable development, which implies not only ecological, but also economic and social responsibilities.

There is an exciting innovation opportunity to develop alternative materials to act as rubber fillers. Recently, increasing attention has been given to "green" fillers, which come from industrial by-products and other waste materials having potential "renewability" (Chaudhary et al., 2004). The use of bio-based fillers would further help to reduce the dependence upon fossil fuel and move towards a sustainable material basis for rubber filler production.

Previous work has successfully recovered carbon black from end-of-life tyres and reapplied this material to new types of rubber filler and related materials. The aim of this research project was to build upon previous research to develop new types of fillers for elastomers and related materials based on the char produced during pyrolysis of biomass (coconut shell) and raw sewage sludge derived from wastewater treatment processes, which are wholly renewable in origin.

In this project, these two new and different materials are being considered as alternative feedstock for carbon black-like materials as a reinforcing filler in rubber. Coconut shell, a cellulosic and lignocellulosic waste, is available in large quantities. It has been reported that there were about 31.2 million of tonnes coconut shell produced in 2013 (FAO, 2017). It has relative uniformity and potential to be used as a low-cost parent material for rubber fillers. The production of a carbon black substitute from a biodegradable waste would be beneficial as it reduces the demand on non-renewable carbon black feedstock, such as fuel oils or natural gas and also helps to combat global warming by converting the biodegradable waste material into solid char, stabilising the carbon and preventing its release as CO_2 or methane (CH_4). It is also widely known that coconut shell can be used as a bio-fuel and is also a commercial source of charcoal and activated carbon. The activated carbon made from coconut shell is considered to be superior to those obtained from other feedstock, due to its highly microporous and complementary mesoporous structure. In particular, the mesopores make it potentially suitable for in-rubber applications. Research into this potential application for coconut shell char is needed (Zhou et al., 2012; Xiong et al., 2011; Kuratani et al., 2011; Jain & Tripathi, 2014).

The second problematic waste material is raw sewage sludge. The treatment and safe disposal of sewage sludge is one of the most significant challenges in wastewater management. Without enough regard to the environmental effects, the significant amount of sludge generated every year inevitably leads to a material with a high pollution potential. Sewage sludge, as a high-volume, carbon rich/high organic content material, offers great promise as a feedstock for the production of a renewable filler for application in elastomer manufacture using a pyrolysis-based process.

With the pressures on reducing waste disposal and growing emphasis upon resource recovery, increasing attention has been paid to reusing materials which would be otherwise discarded. There have been several studies reported in the literature using alternative materials as fillers in rubber materials, although most of this work has focussed on using recovered rubber, pyrolytic rubber, or naturally occurring materials such as lignin, nut shells, egg shells, fly ash or rice husks (Chaudhary et al., 2004; Intharapat et al., 2013; Sareena et al., 2012; Sae-oui et al., 2009; Gopalan & Dufresne, 2003). The results show that the performance of these "green fillers" in the rubber matrix and the production requirements has limited their application in rubber manufacture. Only under some production conditions can comparable performance be achieved, for example the tensile strength of a rubber material containing 20 phr (parts per hundred of rubber) of treated rice husk ash can reach 26.0 MPa compared to 22.0 MPa obtained by commercial carbon black N774 (Chaudhary et al., 2004). The physical properties, such as tensile strength and modulus reported, indicate that the fillers can be grouped as semi to non-reinforcing fillers. The key properties of interest will be discussed in more detail later (See Section 1.4). This thesis reports for the first time an analysis of coconut shell char and raw sewage sludge char as a novel and sustainable filler for rubber and related materials.

1.2 Global Warming and Waste Management

1.2.1 Greenhouse Gases and Global Warming

Greenhouse gases (GHGs) refer to a group of gases in the atmosphere including carbon dioxide, water vapour, ozone and methane, which absorb infrared radiation and reflect it back towards the surface of the planet, causing warming of the atmosphere. Life on earth cannot

live without the energy from the sun. Although greenhouse gases only make up about 1% of the atmosphere, they control climate by absorbing heat and holding it to the planet.

Global warming describes a rapid increase in the average surface temperature on earth over the past century due to the greenhouse gases released by burning fossil fuels, which is a change that may permanently affect the climate of the planet. Over the past 50 years, the average global temperature has unusually increased at a high speed. According to the Intergovernmental Panel on Climate Change (IPCC) fourth assessment in 2007, the linear trend of temperature increase in 0.74 ± 0.18 ˚C from 1906 to 2005, which has increased by 23.3% comparing to its 100-year increase from 1901 to 2000 (IPCC, 2007). However, it is reported by experts that the trend is still accelerating, all but one of the 16 hottest years have happened since 2000 in the NASA's (North American Space Agency) 134-year record (MacMillan, 2016). IPCC has also predicted that the average global temperatures could increase between 1.4 and 5.8 °C by the year 2100. Several severe outcomes may occur from global warming, such as rising sea levels due to the melting of the polar ice caps, as well as storms and other negative weather events.

Global warming happens when too much carbon dioxide (CO_2) and other greenhouse gases in the atmosphere act as a blanket, absorbing solar radiation and warming the planet. These pollutants can last for decades in the atmosphere trapping heat, so they cause the planet to warm (Lashof & Ahuja, 1990). This is also known as the greenhouse effect, which is always at the centre of the climate debate. The burning of fossil fuel to make electricity or for transportation of goods is regarded as the largest sources of GHGs.

In order to reduce the GHG emissions, the Climate Change Act (2008) in the UK developed a long-term legislative framework to reduce emissions by 34% and 80% by 2020 and 2050 respectively (IPCC, 2007). It should be noted that although much progress has been made in enabling especially the UK and other western economies to achieve their GHG emission targets, this has been as a result of deindustrialisation. The products and materials needed for societal operation are now manufactured in developing economies, using the same technologies as in the past. This means that many of the heating processes in the industrial

sector, including both high and low temperature activities, requires attention to enable the required emission reductions to be achieved. Thus, the research described in this thesis has potential for application across the globe.

1.2.2 Waste Management and GHG Emission Control

In the European Union Directive 2008/98/EC on waste (2008), waste refers to any substance or object which the holder discards or intends or is required to discard. Waste is unavoidable, and undesirable in all human activities. Several legislative tools have been introduced to help to manage waste by the EU and hence the UK. These are described below.

1.2.2.1 European Community (EC) Directive 1999/31/EC on the Landfill of Waste

About 28 million tonnes of municipal waste is produced in the UK every year, of which 83% ends up in landfill. It is also reported that about 60% of the municipal waste is biodegradable, which decays anaerobically in the landfill producing methane, a potent greenhouse gas (DEFRA, 2011). There are also many other problems related to the landfill, such as leaching, pests, litter and discarding of material of value.

The overall objective of the European Community (EC) Directive 1999/31/EC (1999) on the landfill of waste was to prevent or reduce as far as possible the negative effects on the environment and the risk to human health by setting uniform technical standards and operational and technical requirements for the landfills. This directive also contains requirements on the characteristics of the waste to be landfilled.

The EU Landfill Directive aims to reduce the biodegradable waste sent to landfill as 75% of the 1995 level by 2010, 50% of the 1995 level by 2013 and 35% of the 1995 level by 2020. For example, in the UK, 40% of household waste need to be reduced for landfill by 2020 assuming all of this is biodegradable. Due to the Packaging Directive and a new Directive on electronic waste, it is necessary to divert other waste from landfill. These result in around 55 per cent of waste needing to be diverted from landfill by 2020 (DEFRA, 2011).

The Government's Waste Strategy 2000 (DETR, 2000) is the framework for England for improving the management of waste and responding to the EU Landfill Directive. Some actions are introduced by the strategy for reducing the dependence on landfill: (1) Greater efforts to reduce waste, (2) Substantial increase in re-use, recycling and composting, (3) Where waste cannot be recycled, recovery of energy from waste, through incineration.

1.2.2.2 Directive 2000/76/EC on the Incineration of Waste

The Directive 2000/76/EC on the Incineration of Waste (2000) is composed with the objective of preventing or limiting the negative environmental effects by emissions from the incineration and the co-incineration of waste into air, soil, surface and groundwater and the resulting risk to human health.

The Directive describes incineration plants as plants that thermally treat wastes by oxidizing it, with or without combustion heat recovery. It has also covers other thermal treatment processes including pyrolysis, gasification, or plasma processes as long as the substances obtained by these processes are subsequently incinerated.

1.2.2.3 Directive 2008/98/EC Waste and Repealing Certain Directives

Article 6 of the Directive 2008/98/EC (2008) on waste develops conditions when waste stop being a waste after a recovery operation and meet the following requirements:

(1) "the substance or object is commonly used for specific purposes

(2) a market or demand exists for such a substance or object

(3) the substance or object fulfil the technical requirements for the specific purposes and meets the existing legislation, and

(4) the use of the substance or object will not lead to overall adverse environmental or human health impacts"

1.2.2.4 Waste Hierarchy

Waste management strategies are ranked in to a hierarchy, which has been adopted and reiterated in the Directive 2008/98/EC on waste. The waste hierarchy is shown in Figure 1-1, which indicated the level of priority in order to deliver the best environmental outcome. Five steps have been identified in hierarchy according to the Article 4 of Directive 2008/98/EC (2008).



Figure 1-1 Waste Hierarchy (EC, 2008)

Prevention: Reducing the waste quantity before a product becomes waste, reducing the waste quantity and the negative environmental effects and risk to human health.

Preparing for re-use: Any operation by which products or materials are used again for their original purpose.

Recycling: Any resource recovery operation, which involves collection and treatment of waste material for using as feedstock for producing same or another product.

Recovery: Energy recovery: any operations by which original materials can be replaced by waste, such as gasification and pyrolysis.

Disposal: Any option which is not lead to recovery, such as landfills.

Although the hierarchy of waste management focuses on reducing the production of waste, it is not well suited for many biomass-based wastes due to the high market demand for the foodstuffs which result in the waste (e.g. consumption of rice producing rice husks and

coconut flesh & oil producing shells). However, these biomasses can be efficiently used for making carbonaceous products and generating energy. According to the hierarchy, this option must be undertaken only when waste cannot be reduced, recycled or reused, leading to waste biomass being a good material for application as a renewable energy source.

1.3 Sewage Sludge and its Management

Water plays a vital and crucial role for all forms of life in the world. As a result, wastewater becomes inevitable and needs to be treated in wastewater treatment plants (WWTPs) before being discharged into the environment preventing it from contaminating the environment and harming lives.

After the treatment procedure, the cleaned water is discharged to the receiving water and the majority of the residual solid from the WWTP is known as sewage sludge (sludge). Sludge primarily consist of human faeces, toilet paper and dead microbes, and may also contain a significant amount of pathogens, parasites and undesirable chemicals. Therefore, the treatment of sewage sludge is one of the most significant challenges in wastewater management. A tremendous quantity of sludge is produced in WWT process every day and it is reported that the amount of the sludge produced has increased even more rapidly recently (Smith et al., 2009; Laturnus et al., 2007). The estimated mass of sludge produced in the European Union is around 60g per person-day, approximate 8.4 – 10.1 million tonnes of dried matter per year and is predicted to reach 13 million by 2020. In the UK, more than 1.4 million dry tonnes of treated sludge is produced each year (Rio et al., 2005; Fytili & Zabaniotou, 2008; Smith et al., 2009; Agrafioti et al., 2013; Samolada & Zabaniotou, 2014). This huge amount of sludge unavoidably leads to a significant potential pollution load. Therefore, the treatment of sewage sludge produced from WWTP remains an important global issue.

1.3.1 Sludge Characteristics

Different types of sludge are produced from different individual biological wastewater treatment processes. Figure 1-2 shows a typical wastewater treatment process. There are 5

major steps within the WWT process: preliminary, primary, secondary, tertiary (advanced WWT) and disinfection steps.

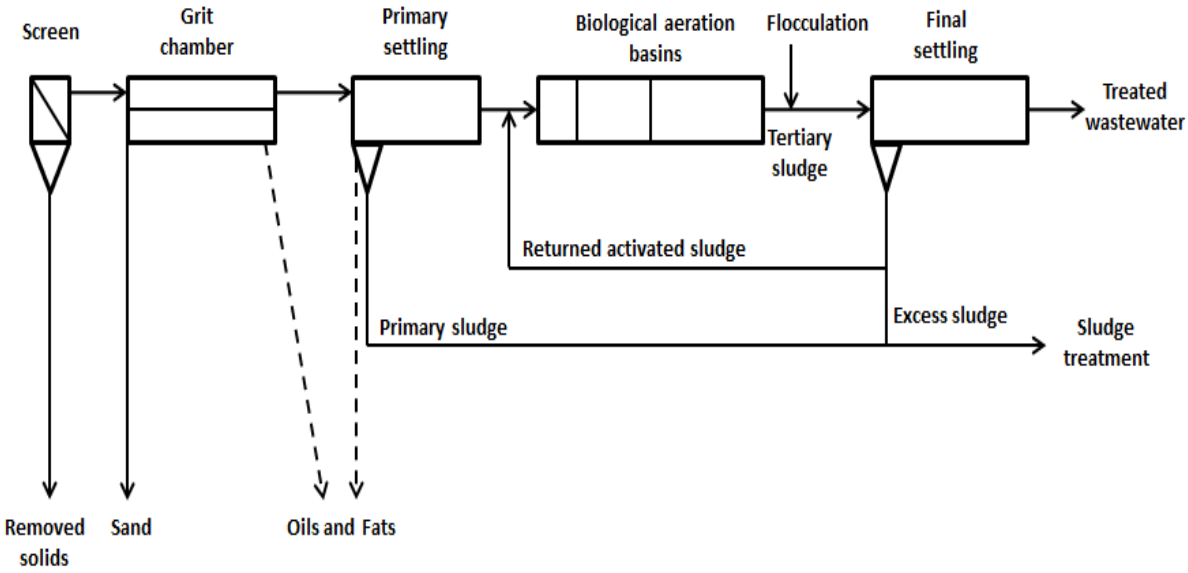


Figure 1-2 Typical wastewater treatment process (after Lenntech, 2017)

The sludge removed after the primary treatment is named as "primary solid" or "primary sludge". The sludge removed from the clarifier in the secondary treatment is called "waste activated sludge" or "secondary sludge", some of which is recycled back to the aeration tank and the excess is removed for further treatment. The term sludge includes primary sludge and secondary sludge. These sludge are combined and called undigested sludge or raw sludge. Further treatment is needed for the undigested sludge before being reused in agriculture, incineration or to landfill disposal (Tchobanoglous, 2003).

Water is the main component of sludge. The amount of water depends on the sludge type (primary, secondary or tertiary sludge) and the way of stabilisation (aerobic, anaerobic). Raw sludge usually has a water content of 93% to 99%. Therefore, a dewatering (up to about 35% dry substance content) or drying (to over 85% dry substance content) process is necessary for further sludge utilization.

The second main component in sewage sludge is solid matter, which is comprised of organic and inorganic substances. The sludge after the wastewater treatment process may contain:

Carbon (50-70 %), Oxygen (21-24%), Nitrogen (15-18%), Hydrogen (6.5-7.3%), Phosphorus (1-1.5%) and Sulphur (0-2.4%). The composition of sludge depends on the source of wastewater and the WWT method used in each plant. The typical compositions of sewage sludge are shown in Table 1-1 and the typical metal content is summarised in Table 1-2.

Table 1-1 Typical composition and properties of sewage sludge (Tchobanoglous et al., 2003)

Item	Untreated primary (% of TS)		Digested primary (% of TS)	
	Range	Typical	Range	Typical
Total dry solids	5-9	6	2-5	4
Volatile solids	60-80	65	30-60	10
Protein	20-30	25	15-20	18
Nitrogen	1.5-4	2.5	1.6-3.0	3
Phosphorous (P_2O_5)	0.8-2.8	1.6	1.5-4.0	2.5
Cellulose	8-15	10	8-15	10
Iron (not as sulphide)	2.0-4.0	2.5	3.0-8.0	4.0
Silica (SiO_2)	15-20	-	10-20	-
pH	5.0-8.0	60	6.5-7.5	7.0
Alkalinity (mg/L as $CaCO_3$)	500-1500	600	2500-3500	3000
Organic acids (mg/L as HAc)	200-2000	500	100-600	200
Energy content (kJ/kg TSS)	23000-29000	25000	9000-14000	12000

Table 1-2 Indicative metal content in wastewater solids (Tchobanoglous et al., 2003)

Metal	Dry solids, mg/Kg	
	Range	Medium
Arsenic	1.1 – 230	10
Cadmium	1 – 3410	10
Chromium	10 – 99000	500
Cobalt	11.3 – 2490	30
Copper	84 – 17000	800
Iron	1000 – 154000	17000
Lead	13 – 26000	500
Manganese	32 – 9870	260
Mercury	0.6 – 56	6
Molybdenum	0.1 – 214	4
Nickel	2 – 5300	80
Selenium	1.7 – 17.2	5
Tin	2.6 – 329	14
Zinc	101 – 49000	1700

As sewage sludge is held in an aqueous suspension, it may also contain a number of microorganisms, including protozoa, bacteria, nematodes, micro fungi and algae. Within the microbial community there is always the potential for pathogens to be incorporated, as well as several potentially harmful or toxic elements and compounds; hence safe and effective alternative treatment and suitable disposal methods need to be explored (Arundel, 2000).

All sewage sludge is treated before disposal by approved procedures to guarantee that hazards are controlled and mitigated. The most common sludge treatments before further

reuse consist of anaerobic digestion, aerobic digestion, lime stabilisation, thermal drying, composting and sludge pasteurization (Fytili & Zabaniotou, 2008; Tchobanoglous et al., 2003). In the UK and EU, anaerobic digestion is the most popular method, which treated 66% of the sludge in 2010. It is regarded as the most cost-effective process among all the methods based on the Renewable Energy Directive (2009/28/EC), due to the limited environmental impact and high energy recovery.

1.3.2 Sludge Disposal in Practice

There are three traditional disposal routes for sludge in the UK: farmland application (80.3%), landfill (0.7%), and incineration (18%) (Water UK, 2017). Farmland application is one of the most common practices for decades to tackle the sludge issue in the UK and many other countries. Approximate 150,000 hectares of farm land receives the treated sludge annually in the UK, of which arable crop land occupied the majority. Treated sewage sludge for agriculture is regarded as the best practicable environmental method in the EU and UK, since the sludge can provide valuable quantities of nutrients and stable organic matter to soil (Water UK, 2016). However, there are still a few problems which restrict the use of sewage sludge in agriculture. The possible accumulation of undesirable chemicals such as heavy metals, toxic organics, and pathogens can be the main concern, as they may pass along the food chain (Arundel, 2000; Eddy et al., 2003). Many regulations and codes of practices need to be followed for sludge to farmland application to protect human and soil health, and the wider environment, particularly the EU Sludge Directive (1986), the Sludge (Use in Agriculture) Regulations (1989), the Urban Waste Water Directive 91/271/EEC (1991), the Code of Practice for the Agricultural Use of Sewage Sludge (1996), the Safe Sludge Matrix (1998), the EC Nitrates Directive (1991), and the Biosolid Nutrient Management Matrix (2014). Due to the inherent chemical energy lost and associated health problems, the disposal of stabilized sewage sludge in sanitary landfills is also not ideal. Based upon the European Landfill Directive 1999/31/EC, landfill has been generally eliminated for the increasing disposal costs. Although incineration is helpful for sterilisation, volume reduction and thermal efficiency improvement, it is not a practical option since the cost of the following treatment of gases released has become even greater (Eddy et al., 2003) and the production of furans, dioxins and heavy metals may also cause environmental concern (Shen et al., 2008).

The above disadvantages of each disposal methods have become the motivation and limiting factors in the development of new technologies for sewage sludge treatment. Several techniques, such as wet oxidation, gasification and pyrolysis, have been found promising. Of these alternate processes pyrolysis is believed as a feasible alternative method for sludge treatment. When researching for economical and consistently available precursor feedstock, sewage sludge is believed to have the potential as a promising material to be converted into sustainable carbonaceous materials and energy. In the past decade, pyrolysis of sewage sludge in an inert atmosphere at relatively low-temperatures (500°C) has been given a lot of attention. This process involves heating the sludge in an oxygen-free atmosphere, which leads to the production of char, oil and gases. Half the original mass of sludge can be removed through this process. Meanwhile, pyrolysis offers the possibility of recovering the oils from the sludge which can be eventually used as a fuel. After some treatment, the char residue can also be reused as active carbon in industry. This conversion offers a combined benefit of reducing the sludge mass and obtaining a valuable product at lower cost (Shen et al., 2008; Inguanzo et al., 2002; Domínguez et al., 2005; 2006; Conesa et al., 1997; Shen & Zhang, 2005; Stuart et al., 2006).

Many papers have investigated the effects of operating parameters such as temperature and residence time on both quality and quantity of the pyrolytic products. The yields of the products obtained from a pyrolysis process mainly depend on the raw material decomposition (primary reactions) and on the reactions suffered by the primary volatised components (secondary reactions). As a result, it is important for the sewage sludge to undergo chemical characterisation to ascertain its organic and inorganic content before pyrolysis, as this has a direct effect on the porosity, surface chemistry of the char produced and the chemical composition of the oils and gases (Chen et al., 2002, Shen et al. 2008).

1.4 Carbon Black

1.4.1 Rubber

The history of processing rubber dates back to 1600 B.C. by Ancient Mesoamerican peoples, which is about 3500 years earlier than the development of vulcanization process by Charles Goodyear in 1839. The Mesoamerican made solid rubber balls and other rubber artefacts; they also used liquid rubber for medicines and painting (Hosler et al., 1999; Slacks, 2002).

Natural rubber is acquired from the latex, which is an aqueous and insoluble emulsion composed of a cis-1,4-polyisoprene phase from the rubber-producing plants (shown in Figure 1-3) (Kroschwitz et al., 1985). Given the high rubber contents and quality, the Brazilian rubber tree (*Hevea brasiliensis*) is currently the only commercial sources of natural rubber (Backhaus, 1985). The exact structure of natural rubber is still not clear, even though a lot of research has been done (Puskas et al., 2006). Normally, natural rubber is a polymer made up of 320 to 35,000 isoprene molecules (shown in Figure 1-4).

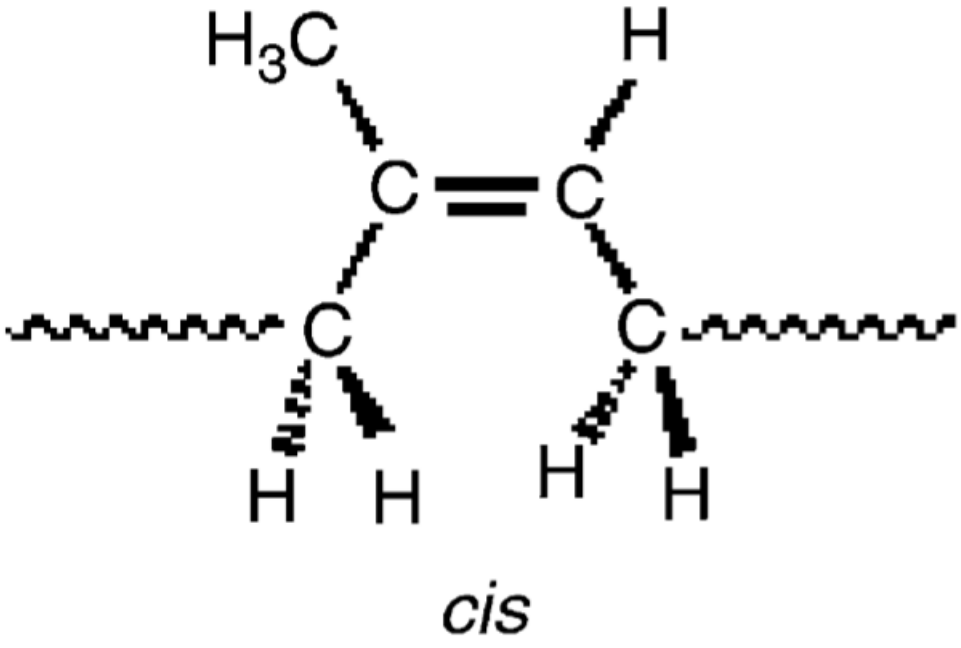


Figure 1-3 1-2 cis-1,4-polyisoprene (Chiang, 2013)

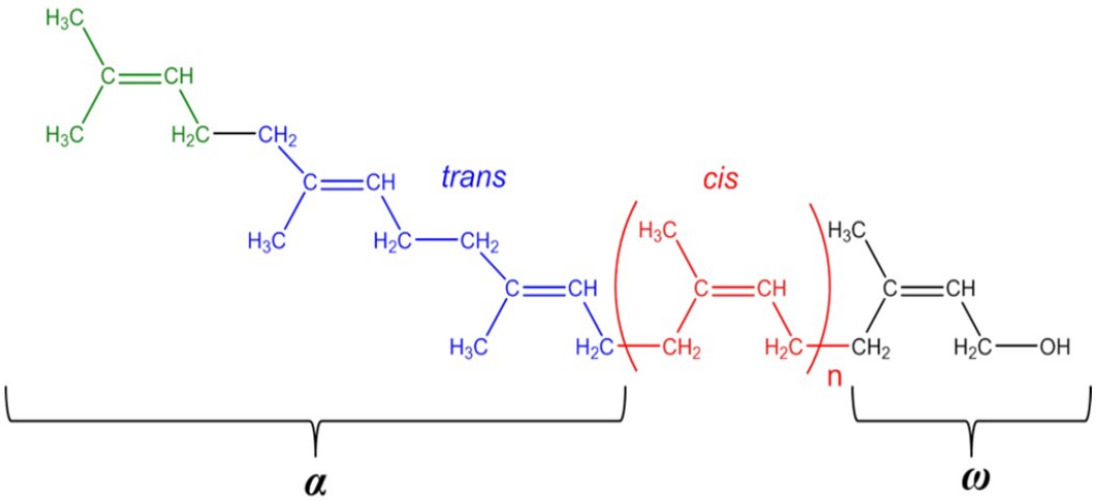


Figure 1-4 Chemical structure of natural rubber. Head α and end group ω are not proven (Chiang, 2013)

Over the past century, the importance of natural rubber to human society has increased gradually. It might not be recognized, but rubber plays an essential role in about everything (e.g. transportation, industry, agriculture and even the kitchen and office areas) whether directly or indirectly with long usage (Morton, 1963). Almost the whole world is dependent on rubber and it is being used by everyone on a daily basis. There will be approximately 10.9 million tonnes of natural rubber produced in 2017, more than 90% of which is grown is Asia. Thailand, Malaysia and Indonesia are the three largest producers (ANRPC, 2017).

Natural rubber exhibits the advantages of advanced elasticity, high strength, great toughness and manufacturing versatility. A rubber band can be stretched to 9 or 10 times its original length before returning to its original condition as soon as the outside pressure is released. Similarly, a block of rubber can also be compressed, and after the load is released the block will display its original shape and dimensions in a very short time. As to the extent to which it can be distorted, in the rapidity of recovery and in the degree to which it recovers its original shape and dimensions, rubber is unique. Strength and toughness are almost equal essential properties with elasticity of rubber. The higher strength and greater toughness of rubber provide more powerful elastic qualities in some situations where most other elastic materials may fail. Due to these properties and its dependence on them, rubber shows excellent resistance toward cutting, tearing and abrasion. Furthermore, this combination of

useful physical properties is well maintained over a wide range of temperature, from low temperatures (-40 or -45°C) to relatively high temperatures (100 or 120°C), which covers the most commonly used range of climatic conditions. Also, rubber is relatively inert, resisting to the deteriorating effects due to the atmosphere and many chemicals. Therefore, it has a relatively long and useful life under a wide variety of conditions (Division, 1995). Natural rubber is biodegradable and can be decomposed spontaneously in soil by a specific group of microorganisms (Ikram, 2002; Ali Shah et al., 2013). The rubber products being used in real life need to be in their vulcanised forms to be resistant to natural degradation mechanisms. Therefore, scientists in rubber related industries are always looking for new means to improve rubber products.

1.4.2 Carbon Black

At present, various components are added during manufacturing since engineering rubber cannot be in its natural state. It is hard to see an application of elastomers using the polymer in an unfilled state. A wide range of particulate fillers have been used in rubber manufacture, for different purposes, which are based on reinforcement, low material cost and processing ease. The presence of fillers in rubber is important to achieve durable products, increase strength and prolong life. Fillers can also help improve the modulus of elasticity which is a measure of stiffness of the given materials and are sometimes applied for this purpose. Particulate fillers such as carbon black and silica are widely used to improve the strength of vulcanized rubbers more than tenfold (Li et al., 2008).

The use of carbon black can be traced back to the third century B.C in China and India. Carbon black is by far the most commonly used filler for rubber compounds and has the preeminent performance among all the reinforcing fillers since the World War I. The worldwide production of carbon black in 2012 was about 11 million metric tonnes (ICBA, 2016). It is added to rubber compounds to enhance the physical properties, such as hardness, tensile strength (a maximum load that a material can support without fracture when being stretched) and tear strength (a measure of how well a material can oppose when being torn). As reinforcing fillers, carbon blacks help to increase the hardness and viscosity of rubber-based compounds being the most effective of all filler materials (Medalia & Kraus, 1994). There are three main types of carbon black: furnace black, thermal black and channel black,

which are named because of their production processes. Furnace black is the most important black (occupies 95% of the market); about 70% of the furnace black is currently used for tyre production and other automotive products. Thermal black and channel black can only be used in a limited range of rubber compound (e.g., fluorocarbon rubbers) with only a few grades. Meanwhile, there are two specialist carbon blacks: lampblacks and acetylene black. Lampblack was invented by the Chinese for ink and lacquer formulations over 3,500 years ago; and acetylene black is conductive and used for conducting rubber products (Kühner & Voll, 1993; ICBA, 2016). After the middle of the 20th century until now, almost all the rubber-reinforcing carbon black used today is produced by the oil furnace process, namely furnace black. During the furnace process, a hydrocarbon fuel, such as natural gas or heavy aromatic residue oil from the petroleum or coal industries, is burned in a refractory-lines steel furnace with insufficient oxygen. After that, the black product is separated from the hot combustion gases by means of cyclones and filter bags. The black is then pelletized by either a dry or a wet procedure to satisfy different market purpose. The yield of the black produced in the furnace process varies from 25% to 70% of the available raw carbon materials, depending upon the particle size. Most of the furnace blacks have relatively low oxygen contents (usually less than 1%) and their surface is always neutral or alkaline (Forrest, 2001). The manufacture of carbon black usually has a considerable carbon footprint, due to the incomplete combustion of heavy hydrocarbons. 2.4 tonnes of CO_2 are estimated to be emitted per tonne of carbon black, which compares to 0.8 tonnes of CO_2 per tonne of cement for cement manufacture (Athanassiades, 2013; IEA, 2007).

Carbon black is an extremely pure form of elemental carbon which consists of very small, mostly spherical particles fuse together in clusters referred to aggregates. The aggregates themselves then group together as agglomerates which break up when mixing with rubber compounds, shown in Figure 1-5. The aggregates are regarded as the smallest dispersible unit of carbon black within the rubber matrix in usual conditions. As a result, aggregates are often considered as the actual reinforcing unit (Donnet et al., 1993). The structure of carbon black is defined as the types of aggregates. It can be observed directly by TEM as partly graphitic. The outer layers show more graphitic structure than those in the centre. Normally, the smaller the size of the carbon black the less graphitic it is in structure.

At a high magnification, the carbon atoms in the aggregates can be seen in overlapping graphitic layers that locally present a quasi-crystalline turbostratic structure with an approximately 0.35nm interlayer spacing. As evidenced by TEM, the morphology of carbon black can be simplified as an onion-like structure. Chemically reactive functional groups are in most cases attached to the graphitic edges. As shown in Figure 1-6, carbon black is composed of well-developed graphite platelets which roughly remain parallel to one another but random in orientation with adjacent layers (Wang et al., 2000). In other words, the edge of each layer can be regarded as the effective reactive zone of carbon black. The higher the structure, the more spherical particles in an aggregate. As the number of particles presenting in an aggregate increases, the space volume within the aggregate will also increase. However, this kind of space is not accessible for the rubber molecules due to the small size (Blow, 1975).

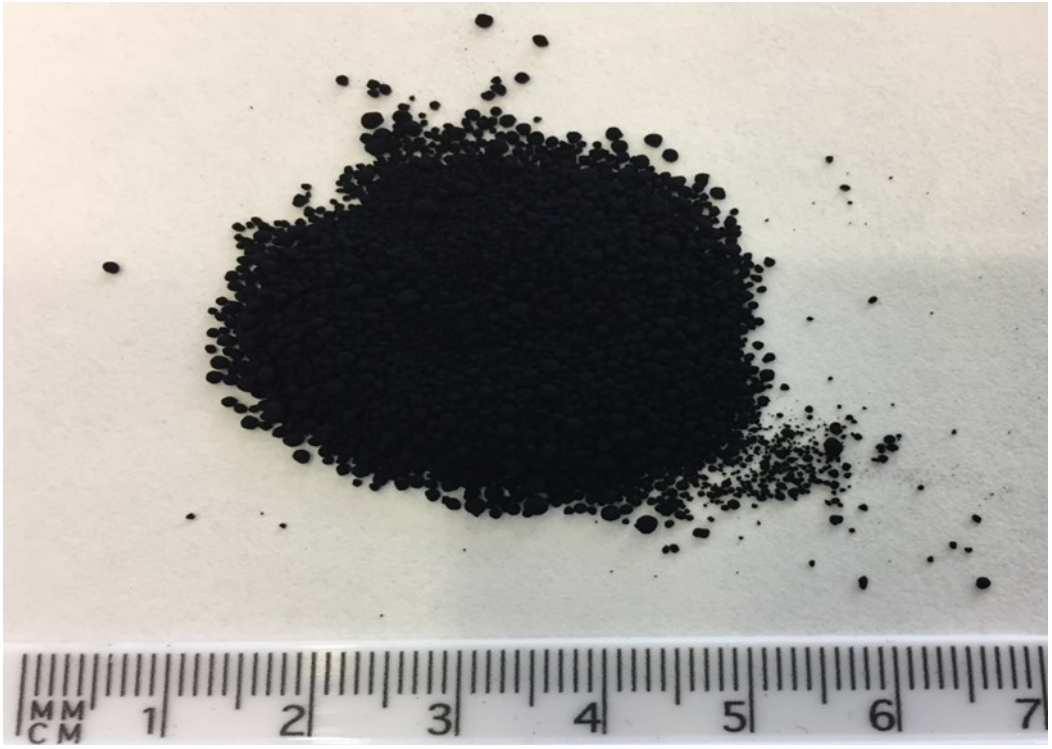


Figure 1-5 Carbon black

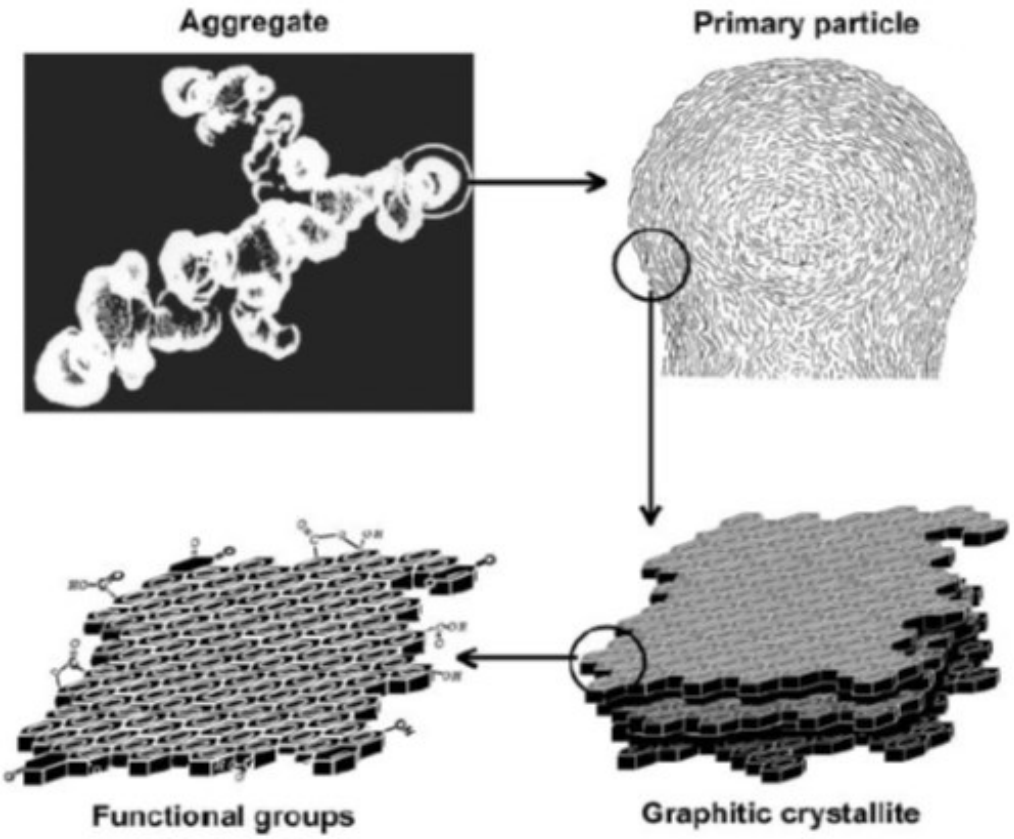


Figure 1-6 Carbon black structure (Wang et al., 2000)

1.4.2.1 Classification

A carbon black classification system has been built up by the American Society of Testing Materials (ASTM), which is essentially based upon particle size and degree of surface oxidation (which primarily affects the curing time of rubber - carbon black compounds). The N series comprises 'normal curing' furnace and thermal blacks, then S letter is defined as the 'slow-curing' channel blacks and deliberately oxidized furnace blacks. The first number of the three-digit suffix tells the particle size, as shown in Table 1-3. The remaining two digits are given randomly without meaning. For example, N330 series denotes fillers which were made at normal curing rate of the host rubber compound and with surface area between 70 and 99m^2/g (Wampler et al., 2004). Specification are given in terms of both analytical properties of carbon black and physical properties applied to the rubber in standard recipes (ASTM Classification D-1765); this is important, since a given set of analytical properties may not ensure the same rubber properties, especially in carbon blacks made by different manufacturers.

Table 1-3 Classification and typical particle size of carbon blacks

ASTM Series	Average particle diameter (nm)	Name	Abbreviation
N100	11-19	Super Abrasion Furnace	SAF
N200	20-25	Intermediate SAF	ISAF
N300	26-30	High Abrasion Furnace	HAF
N400	31-39	Special Conductive Furnace	XCF
N500	40-48	Fast Extruding Furnace	FEF
N600	49-60	General Purpose Furnace	GPF
N700	61-100	Semi-Reinforcing Furnace- High Structure	SRF-HS
N800	101-200	Fine Thermal	FT
N900	201-500	Medium Thermal	MT
S200	20-25	ISAF- Low Structure-Super Conducting	ISAF-LS-SC
S300	26-30	HAF- Low Structure-Super Conducting	HAF-LS-SC

1.4.3 Characterisation of Carbon Black

A variety of characteristics contribute to the reinforcement of elastomers offered by carbon black. Particle size, the morphology of aggregates and the microstructure can be considered as the key properties of carbon black that affect the interaction between carbon black and rubber-related elastomers. Further, the characteristics of the carbon black surface and its structural organization, particle porosity, surface area and its chemical composition are also essential. The development of a large polymer-filler interface is a very important variable. A

specific surface area of a spherical particle of 1μm in diameter can be $6m^2/cm^3$. And this is roughly the lower limit of significant reinforcement. The upper limit of useful specific surface area can reach 300 – $400m^2/cm^3$, and is determined by considerations of dispersibility, processability of the unvulcanised mix, and serious loss of rubbery characteristics of the composite (Maya, 2007).

1.4.3.1 Particle and Aggregate Size

Particle size and distribution remain probably the most fundamental physical properties important for the reinforcement capacity of carbon black. This may be the reason why particulate fillers obtained directly from grinding of minerals or by simple precipitation are often regarded as non-reinforcing fillers, because their fundamental particles are too "big". In most cases, non-reinforcing fillers are used in elastomers simply to provide a slight increase in modulus and a very significant drop in break properties (Mark et al., 2005).

Carbon black particle aggregates are reported to work as a unit in the rubber matrix, however the reinforcement imparted by the carbon black is not influenced by the aggregates units but by each individual particle within the unit. Usually, the average particle diameter of carbon black ranges from 10nm to 500nm. As the particle size decreases, the dispersion of carbon black in rubber compounds can be enhanced, the interface extension can be promoted, consequently resulting in good reinforcement ability (OEC, 2015; Donnet et al., 1993).

Several instrumental methods are available to measure the fundamental particle size and its distribution of carbon blacks. Scanning electron microscopy (SEM) has become the most popular method for estimating carbon black primary particle size distribution. Scanning tunnelling microscopy, atomic force microscopy, transmission electron microscopy (TEM) and X-ray diffraction (XRD) are also popular for carbon black particle size examination. In order to determine the size of individual particles, a TEM image is a helpful tool for visualising particle aggregates (Donnet et al., 1993).

According to the ASTM D-1765-17, the particle sizes of some typical carbon blacks are shown in Table 1-4. In this table, ASTM number has been mentioned before in the classification part, HI presents the aggregate size heterogeneity index, which is a dimensionless measure of the breadth of the particle size distribution (Donnet et al., 1993).

Table 1-4 Mean particle size of typical carbon blacks

ASTM number	Mean particle diameter (nm)	HI*
N110	18	1.59
N121	19	1.58
N220	21	1.51
N234	20	1.57
N299	24	1.44
N326	27	1.44
N330	30	1.59
N339	26	1.56
N351	32	1.44
N358	30	1.49
N472	21	2.32
N550	56	1.67
N630	58	1.76
N650	61	1.65
N660	67	1.65
N762	107	1.57
N774	79	1.68
N990	285	1.63

* HI = Aggregate size heterogeneity index

1.4.3.2 Surface Area

Surface area is an important morphological characteristic of reinforcing fillers when considering their role in rubber reinforcement. It indicates the extension of the interface such as the available surface for the interaction between the rubber and the filler surface. The result of surface area would determine how much of the area can be accessed by rubber molecules, provide the data of porosity of carbon black particulates. In most cases, carbon black with a small particle size may have a high external surface area, but this may also be influenced by the structure and the nature of surface. It is necessary to note that if the pores are significantly smaller than the very large (normally meso or macro-pore size) rubber polymer chains, then the polymer cannot access these pores. As a result, unlike micro-pores for the application of activated carbon, meso and macro pores may play the decisive role on the filler surface.

There are two main tools being widely used for the examination of a carbon black surface's area.

(1) Nitrogen adsorption (BET Method)

The BET method is the most widely used procedure to measure the surface area of carbon black. It is named after Brunauer, Emmett, and Teller, who published this procedure in 1938 (Gregg & Sing, 1982). According to the ASTM D6556-16 standard, the total and external surface areas of the carbon black can be evaluated by measuring the amount of nitrogen adsorbed at liquid nitrogen temperature and several partial pressures of nitrogen. The NSA (Nitrogen Surface Area) value is calculated from the adsorption data and includes the total surface area, inclusive of micropores, pore diameters less than 2 nm. The external surface area correlates to the specific surface area that is accessible to rubber is determined by the statistical thickness method.

Surface area and pore size distributions of the samples are characterized by the nitrogen adsorption and desorption method. Before gas adsorption measurements, the samples need to be degassed under vacuum condition at 300 ± 10 °C for a period of time. Subsequently, the adsorption and desorption analysis of N_2 can be conducted and the adsorption isotherm obtained. The BET surface area, micropore volume and pore size distribution can be

determined from N_2 adsorption. The BET model gives an estimate of surface area of the filler sample by the equation:

$$S_{BET} = V_m \times 4.35$$

Where: V_m = volume of nitrogen per gram that covers one monomolecular layer in standard cm^3/g,

4.35 = area occupied by 1 cm^3 of nitrogen = $\frac{(6.02\times10^{23})(16.2\times10^{-20})}{22400}$

6.02×10^{23} = Avogadro's number,

16.2×10^{-20} = area of nitrogen molecule in m^2, and

22400 = number of cm^3 occupied by one mole of gas at STP.

Since the particles are basically spheroidal, the BET measurement of surface area by adsorption methods can also be applied to the particle size test. As surface area is measured, the average particle diameter can be calculated assuming that each particle to be a true sphere.

(2) Iodine adsorption

During the iodine adsorption test, the excess iodine is titrated with standard sodium thiosulfate solution for the adsorption number after a unit weight of carbon black is mixed with a portion of standard iodine solution. The iodine adsorption number is related to the surface area of carbon blacks and generally correlates well with the BET surface area. The result may be affected by the presence of pores, volatiles or extractible components. Sometimes, the aging of carbon black might influence this result as well. Commercial reinforcing carbon blacks have iodine adsorption numbers typically in the 70 – 160mg/g range whilst semi-reinforcing blacks are in the 30 – 45mg/g range.

1.4.3.3 Structure

Two descriptions are applied to illustrate carbon black's structure: primary structure and secondary structure. The primary structure is the degree to which carbon particles join

together in aggregates. The secondary structure is used to define the agglomeration of aggregates due to Van der Waals force. The secondary structure is relatively weaker than the primary structure and much of it will be lost during the pelletisation process. Aggregation contributes nearly all of the structure-related effects observed in rubber compounds, while agglomeration is easily destroyed during rubber-mixing and has only minor effects on compounded rubber properties. Researchers have found that the higher the structure of the carbon black, the more irregular the shapes of the aggregates, thus the less these aggregates are capable of packing together (Blow, 1975). The determination of structure is of primary importance because structure is influenced by the quantity of the filler added for the reinforcement and therefore the level of strain amplification (definition) of the deformable phase.

The structure of carbon black is normally measured by determining the total volume of the air spaces between aggregates per unit weight of carbon black. This measure is achieved by testing the volume of liquid oil (dibutyl phthalate, DBP) (ASTM D2414 – 16e1) required to fill the voids. The oil absorption number of carbon black is related to the processing and vulcanizate properties of rubber compounds containing the carbon black. An absorptometer is the instrument used in this test, which consists of a small chamber where a weighed amount of the black is stirred by rotors as the liquid is added at a constant rate. As the DBP is added, the carbon black powder changes to a semi-liquid mass with an increase in torque. When all the voids are filled, the whole mass stiffens up abruptly with an increasing torque required to turn the rotors. The machine is set to shut off at this point and the DBP adsorption is read off and recorded as $cm^3/100g$ of black (ASTM, 2016). Low structure blacks have values in the range 60-80 ml/100g, while high structure types in excess of 120ml/100g (Loadman, 1998).

1.4.3.4 Chemical Properties of the Surface

Carbon blacks consist of 90-99% elemental carbon. It is believed that the nature of the carbon atoms on the surface may also affect the reinforcement. The carbon atoms can be relatively unreactive if they are an integral part of the layer plane, more reactive if attached to a hydrogen atom, and very reactive if present as a resonance-stabilised free radical, for example in an edge position (Wampler et al., 2004).

The other major constituents of carbon black are hydrogen and oxygen. The hydrogen comes from the original hydrocarbon and is distributed throughout the carbon black particle (Wampler et al., 2004). There is also evidence for the presence on the surface of at least four oxygen-containing groups: phenolic, ketonic, carboxylic and lactones (Lin, 2002; Boehm, 1994). Chemical surface groups are believed to have an effect upon the cure procedure within many vulcanizing systems. In addition to the oxygen and hydrogen groups, carbon blacks may also contain very small amounts of sulphur depending upon the nature of the hydrocarbon feedstock used in the manufacture. Most of the sulphur is chemically combined and appears to be inert and does not cause crosslinking of rubber (Pena et al., 2001).

The "Boehm titration" is regarded as a useful wet chemical method to measure oxygen surface groups on carbon materials (Goertzen et al., 2010). The principle of the Boehm titration method is based on the different acidities of oxygen groups on the carbon surface, so that they can be neutralized by bases with different strengths. Sodium hydroxide (NaOH) is the strongest base commonly applied and it can neutralize almost all Brønsted acids (including phenols, lactonic groups and carboxylic acids), while sodium carbonate (Na_2CO_3) would react with carboxylic and lactonic groups (e.g. lactone and lactol rings) while sodium bicarbonate ($NaHCO_3$) can only neutralize carboxylic acids. Through this process, the types of oxygen groups on carbon surface can be defined and quantified from the difference between the uptakes of bases (Tsechansky & Graber, 2014).

1.5 Rubber – Carbon Black System

1.5.1 Carbon Black Reinforcement Mechanism

The studies of the reinforcement of elastomers by fillers have been widely undertaken since 1960s (Mark et al., 2005). Many of the products of elastomers could not be without the use of fillers due to their significant improvement in mechanical properties. However, despite the efforts of generations of scientists the knowledge about particulate fillers reinforcement mechanism remains fragmentary today.

In most cases, the vulcanization process can only yield resilient products with elastic properties but very little strength. Strength properties are introduced by the addition of "reinforcement" fillers. In terms of "reinforcement", it conveys a range of different meaning when applied to different matrices and application, such as thermosets, thermoplastics, or elastomers. Normally, the partial replacement of the deformable matrix (e.g. thermosets, thermoplastics, etc.) by particulate fillers would decrease the matrix deformability. While the situation is very different when reinforcing fillers are added into the elastomers, as the fillers increase modulus and deformation of the elastomers at break simultaneously. After fillers are added to the compound, several changes may occur: (1) an increase in modulus, or stress at a particular strain, (2) an increase in elongation at break for vulcanizates having a given degree of cross-linking, and (3) consequently, an increase in tensile strength (Mark et al., 2005). The increase in stiffness and the improvement of physical properties such as tear resistance, tensile strength and abrasion resistance are regarded as the crucial standards for reinforcement evaluation. Even though this attractive paradox is not fully understood, there is a common view about the contribution to the stress-strain behaviour of filled vulcanizates from fillers. The reinforcing ability of a filler can be seen from Figure 1-7, where two SBR vulcanizates are compared, the only difference between them is the presence or absence of 50phr carbon black N220 in the rubber recipe. The formulation of the SBR (Styrene-Butadiene Rubber) vulcanizates can be seen from Table 1-5. It can be seen from the plot that with the addition of carbon black N220, the stress-train cure witnessed a sharp rise, almost ten-fold compared with the unfilled rubber.

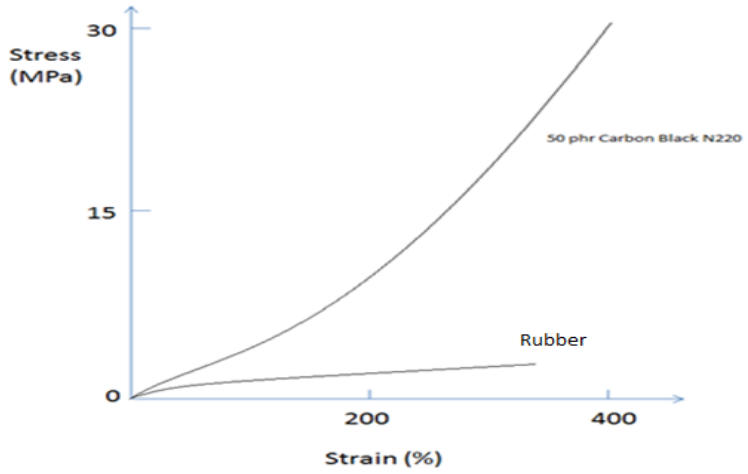


Figure 1-7 Comparison between filled and unfilled rubber matrix (Edwards, 1990)

(Rubber: SBR 1502, 100; zinc oxide, 3; stearic acid, 1.5; Santoflex 13, 0.5; Santoflex 77, 0.5; Sundex 8125, 3; DPG, 0.3; Santousure NS, 1.2; Sulphur, 2. Press cure: 40 min at 153°C. Same formulation with addition of 50 phr N220 carbon black)

Table 1-5 SBR (Styrene-Butadiene Rubber) Formulation

SBR (Styrene-Butadiene Rubber) Formulation	
SBR 1502	100phr
Zinc Oxide	3phr
Stearic Acid	1.5phr
Santoflex 13	0.5phr
Santoflex 77	0.5phr
Sundex 8125	3phr
accelerator DPG	0.3phr
Santousure NS	1.2phr
Sulphur	2phr
(Carbon Black N220)	50phr
Press cure: 40 min at 153°C	

The reinforcement property of fillers has been a subject of a very large body of literatures for decades. So far, more than eight theories have been applied to illustrate reinforcement mechanisms. Nevertheless, none of them can be expressed in simple or at least a comprehensible way. From the practical point of view, it is difficult to examine the vulcanized products so as to identify conditions at the polymer-filler interface as they are under service condition. Furthermore, this problem is strongly related to the polymer-filler bonding which is probably one of the most controversial topics about filler reinforcement. According to much research into the carbon black reinforcement mechanism, there are three postulations which have gained most of the agreement.

1.5.1.1 Small Particle Size

It has been reported that almost all the material that have been proved to have reinforcement effects represent diversity on the properties of their surface, but have a common feature of extremely small particle size. Therefore, several researchers have concluded that the

reinforcement mechanism is attributed to an interfacial effect consequent upon small particle size. A hypothesis has been pointed out that any finely divided solid material that can be dispersed in the polymeric matrix will reinforce rubber compounds. Schmidt (1951) who reported strong reinforcing effects in SBR filled with colloidal stannic oxide, silica, Prussian Blue, polystyrene and casein proved that "*small particle size of the pigment is of prime importance in elastomer reinforcement, whereas the chemical nature of the pigment appears to be of secondary importance*" (Edwards, 1990). Carbon blacks perfectly follow this rule. As the grade of black is above N330, whose particle diameter is larger than 300nm, the blacks are named as "semi-reinforcing". With the average particle diameter decreasing, the reinforcing ability of carbon blacks is improving. After the average diameter drops below 35nm, the blacks can be grouped as "super-abrasion" grades. Gent and Tompkins (1969) have reported that the pressure required to maintain a gas bubble in a liquid becomes very large as the bubble size is reduced, and suggest that this conclusion may be connected with the behaviour of rubber in relation to small particles. In the carbon black field, the gas bubble in the hypothesis is replaced by solid carbon black particles. However, how the reinforcement property changes when the diameter falls into the region below 10 nm remains unexplored. There must be a point below which the properties of carbon black would be closer to a molecular solution than solid particles. Thus, the best particle size, it is suggested, needs to be worked out (Edwards, 1990). Figure 1-8 illustrates this question schematically.

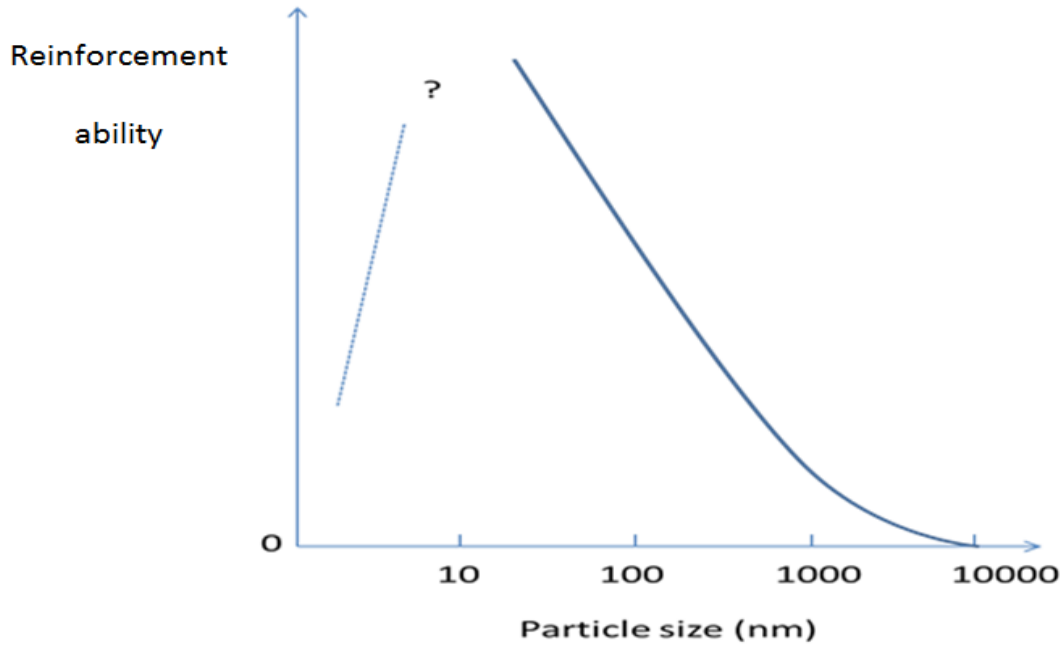


Figure 1-8 Schematic illustration of the effect of particle size on rubber reinforcement (Edwards, 1990)

1.5.1.2 Slippage at Interface

In the early 1960s, Danneberg (1966) proposed the mechanism of molecular slippage at the interface between rubber molecular chains and the fillers. Stress can be redistributed by the slippage of molecular chains, and then helps prevent the molecular rupture. Danneberg also reported that the frictional heat occurring during the relative motion between rubber molecular chains and filler can help release the strain energy so that hysteresis can be seen in the matrix instead of break up. Figure 1-9 shows the proposed changes in the filled rubber system under strain (Jha, 2008).

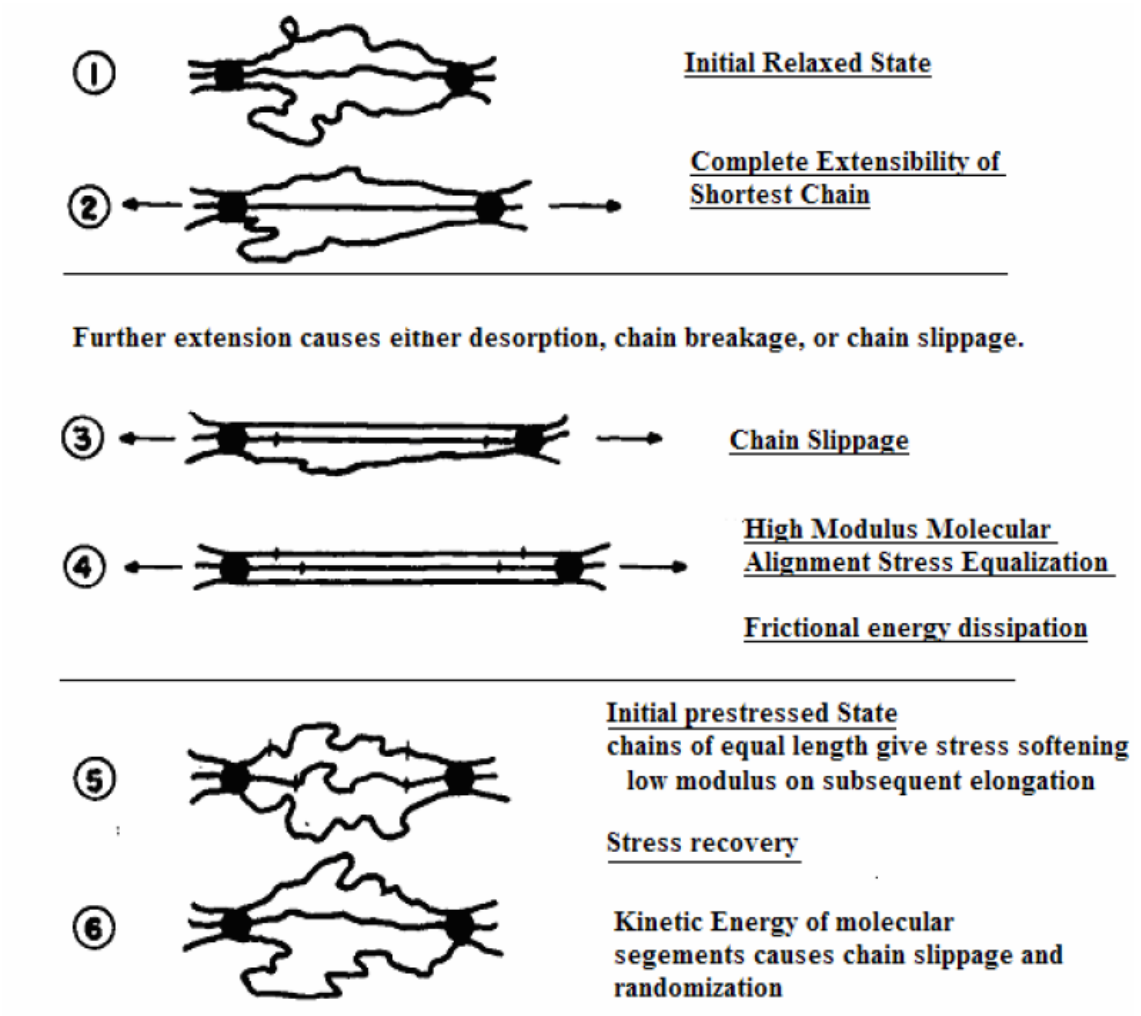


Figure 1-9 Changes in the microstructure of a filled rubber system under strain (Dannenbery, 1966)

1.5.1.3 Chemical Reaction

Functional groups on the surface of carbon black are most likely subjected to a variety of inter- and intra-molecular interactions. Acid/base reaction and hydrogen bonding are probably the main reactions that may occur between the rubber matrix and the carbon black. In the 1960s, Boehm (1994) characterized the oxygenated functions on the carbon black surface (as discussed previously in section 1.5.2). From that time, some researcher started to believe that the interaction between carbon black and natural rubber was the result of chemical reaction between the acidic groups on the carbon black surface and the basic moieties within the rubber matrix. The reaction sites were removed from the surface of carbon black and the change of the rubber product performance was observed to verify this mechanism. As postulated before, the removal caused a large reduction in the modulus and abrasion resistance properties imparted by the original carbon black. Strong chemical bonding is reported to contribute in two different aspects. First, it can help to make the filler agglomerates break up in the mixing step, and prevent any tendency toward the particle re-agglomeration. Also, it may have some advantage for the physical properties, like modulus and resilience, etc. during the vulcanization process. According to the above, the rubber industry has been developing the reactive processing of filled polymer during the mixing and/or even vulcanization step for many years. Some typical chemical functions on the carbon black surface can be seen from Figure 1-10 (Mark et al., 2013).

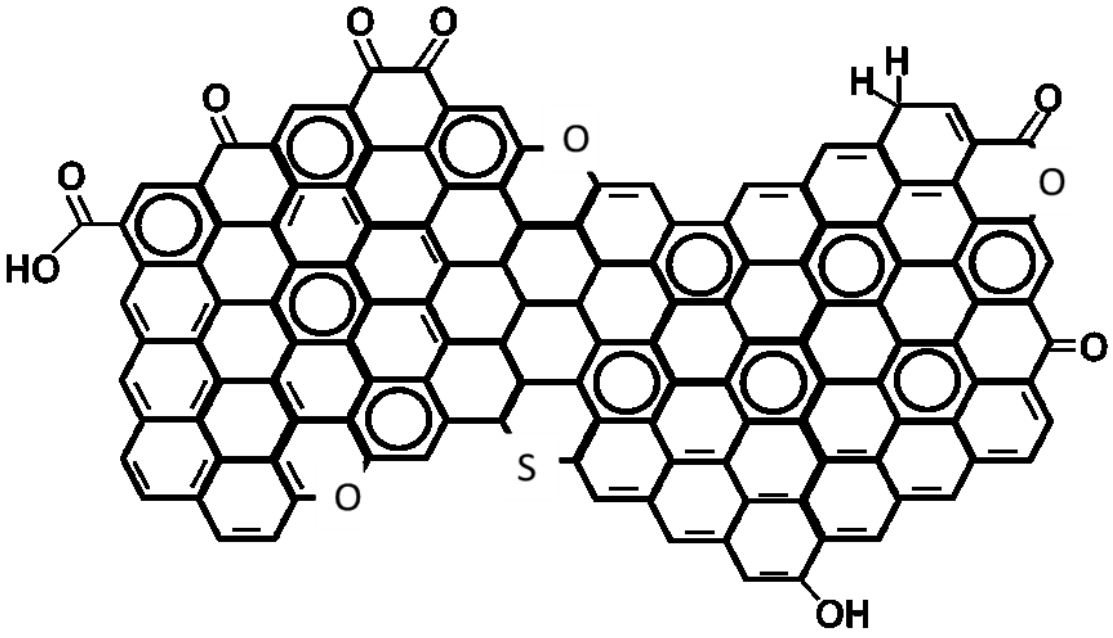


Figure 1-10 Chemical function on carbon black surface (after Bueche, 1960)

Nevertheless, there are not only chemical functional group on the carbon black surface, which can build chemical bonding between the carbon black and rubber molecules, a huge number of reactive double carbon bond have been observed on the black surface by STM (Scanning Tunnelling Microscope). As reported by Medalia and Kraus (1994), such double bonds could react with sulphur, olefins, and radicals to provide chemical bonding between the carbon black surface and natural rubber, but the numbers of this type of bond still cannot be illustrated quantitatively until now. Based on the huge amount of literature, there is suggested to be a correlation between the hydrogen content of carbon black, which is determined by isotopic exchange and their reinforcement capacity (Mark et al., 2005).

Even though, as several lines of evidence has suggested, strong polymer-filler bonding is not always necessary or desirable to provide optimum properties. A proper degree of strong interaction is highly expected in optimising the properties of practical rubber compositions. The polymer/filler slippage can occur with only minor bonding under stress and over most of the interfacial area. Meanwhile, the timing of bonding also has an effect on the final rubber compound. If the bonding is introduced to the mixture before vulcanization, the network between carbon black and rubber may be over-developed and make the whole system difficult to process. If excessive bonding happens during vulcanization, it may cause the extreme condition that the polymer connected to the filler would become totally immobile. Furthermore, result in a tremendous decrease in extensibility. Much evidence supports that the optimum degree of strong bonding should be quite low in relation to the surface area available to the rubber molecules (Mark et al., 2013).

The remaining five less supported postulations are summarised in Table 1-6 below.

Table 1-6 Theories on filled elastomer

Theories on filled elastomer	Summary	Reference
Stored energy function	Use thermodynamic concepts to study the relationship between stress and train. The order and disorder of system correlate to the extension of the molecular chains.	Treloar, 1943 Mooney, 1940 Rivlin, 1956 Gent, 1996
Hydrodynamic Theory	Rigid fillers typically increase the stiffness of the elastomer. The presence of the rigid fillers lead to local strains, which is greater than globally applied strains.	Guth & Gold, 1938 Guth, 1945 Payne, 1962
Strain Amplification	Modifications to hydrodynamic model at high strains.	Mullins & Tobin, 1965 Blanchard & Parkinson, 1948 Bueche, 1960
Model of weak and strong linkage	The filled rubber can be regarded to be made of strong and weak linkages. Different weak linkages can be broken by different stresses contributing to softening.	Blanchard & Parkinson, 1948; 1952
The Bueche model	The fillers are connected with the molecular network chains within a filled rubber.	Bueche, 1961; 1965

1.5.2 New Direction for Carbon Black

Despite the fact that the modern carbon black industry has existed for more than a century, there are still many opportunities for improving carbon black for certain applications. Carbon black with better characteristics and from alternative feedstock has recently been receiving increasing attention.

1.5.2.1 Surface Modification on Carbon Black

Since the surface is one of the most important characteristics for the interaction between blacks and rubber compound, modification of the surface chemistry has been investigated for several decades. The surface area and surface activity property of carbon black is recognized to be essential due to the presence of various reactive functional groups on the surface. Nowadays, carbon black manufacturers and researchers are making progress on altering the morphology of the carbon structure, increase the crystalline sites and the stress oriented active plane so as to obtain improved vulcanizate properties.

Chakraborty's group (Ganguly et al., 2003; 2005) has selected aromatic polyhydroxy compounds as a carbon black modifier and applied the treated carbon black into natural rubber. The rubber filled with modified carbon black resulted in having a higher modulus, heat build-up, hysteresis loss and other dynamic properties. The improvements can be attributed to a high charge density in the surface due to the proportion and nature of surface groups present in surface modified blacks. As a result, some form of higher crosslink density can occur. In addition, the fact that the higher stress induced crystallization due to interactive sites may also contribute to the system. The formation of crosslink density and the compactness of crystal structure are reported to increase the heat build-up properties. Usually a more ordered crystalized structure resulting in stronger bond formation occurs. The -OH group in aromatic linkages increases its degree of nuclrophilicity, which in turn improves linkages between polymer and filler surface. According to the results of secondary ion mass spectroscopy (SIMS) on dry carbon black, the complex hydrocarbon structures are suitable for chemical reactivity at the carbon black surface. These complex structures exist at the edges of the graphite-like layers and provide an environment suitable for bonding or other reactions. Furthermore, a considerable amount of hydrogen is present at the surface

associated with these structures, which supports the importance of hydrogen to the surface activity of carbon blacks. The concentration of hydrogen ions introduced by the surface modifiers is much higher than native carbon black.

The development of polar basic (KOH) and nonpolar (C_6H_6) chemical surface modification and the resulting mechanical properties of the carbon-black-filled rubber composites have been studied by Park (Park & Kim, 2000; Park et al., 2002). Their result showed that the two modification methods do lead to a considerable improvement of the nonpolar characteristics of the carbon black surface. It is believed that both the stable microstructures and the surface functional groups of the nanostructured carbon black surface can be enhanced by the chemical modification. The resulting rubber composite showed better cure behaviours, tensile stress and dynamic mechanical properties than the virgin (unmodified) carbon black filled rubber polymer. It has been noted that the degree of adhesion between the carbon black and rubber is linked to the increase of hardness, modulus and tensile strength of carbon black-filled rubber composites. This can be interpreted as demonstrating the interdependence of the active functional groups, surface energy, and energetically different crystallite faces of the filler surface.

For the basic modified carbon black, the increase in the vulcanization reaction as well as the improvement of the dispersive force of carbon blacks in the rubber matrix resins can be possibly explained as a result of improving the surface roughness (or increase in the specific surface area) and the chemical erosion of the carbon black surface. At the same time, an increase of basic functional groups can be observed on the carbon black surface edges. As to the nonpolar modified carbon black, the improvement for the final products can be attributed to the increase of aromatic nonpolar functional groups on carbon black surfaces and increases of both the viscosity and the crosslinking density (Park et al., 2005).

Rubber elastomers filled with carbon black having surfaces modified by vegetable oil obtain high tensile strength and elongation properties, but low abrasion and hardness compared with normal carbon blacks filled products. It is reported that carbon black modified by si-69, introduces higher hysteresis and improved abrasion resistance at both low and high

temperature. The same result can be also achieved by modifying the carbon black with aliphatic dihydric and trihydric alcohol. Surface modification with a phenolic plant product provides carbon black with a higher flex crack growth resistance. Some researches proved that diazonium salt modification is a very popular and efficient way in rubber and plastic application (Ganguly et al., 2003; 2005).

1.5.2.2 Alternative Feedstock for Carbon Black Substitute

With the rapid increase in the price of raw rubber and other compounding ingredients, the rubber industry has made great efforts to reduce the production cost and increase competitiveness. There are several concerns about the ongoing use of conventional petroleum based carbon black feedstock. On one hand, the price of carbon black oil witnesses a gradual increase every year. The Cooper Tire Company has suggested that carbon black oil is now the largest expense in the production of carbon black. The feedstock accounts for 30-35% of the carbon black sale price. Take tyre production as an example, the population of world vehicles was 1.0 billion in 2010; it is believed that the number will reach 2.5 billion by 2050 (Andrews, 2014). The consumption of carbon black will be immeasurable since at least 30% of the tyre weight is based on carbon black.

Due to the non-degradability of the petroleum based feedstock of carbon black, it may cause severe environmental problems. Concerns about the environment and its protection mean that many research are being undertaken with the objective to reduce the dependence of carbon black feedstock on fossil fuel and transform its sourcing to a sustainable material basis. Not only is the current feedstock & manufacture process energy intensive, it is unsustainable in the long-term as a resource of feedstock to make the carbon. The use of bio-based fillers would further help to reduce the dependence upon fossil fuel and move towards a sustainable material basis for rubber filler production.

Recently, the rubber industry has a newfound interest in fillers derived from biodegradable waste feedstock, which has potential for recycling, to replace the conventional crude oil based feedstock. Their recyclability and utilization has become a major driving factor in their acceptance and employability, as well as low cost and abundant availability. Therefore, bio-

based biodegradable composites have become the next generation materials in the carbon black industry. This new class of carbon black-like feedstock includes natural sources (e.g. natural fibres), industrial by-products (e.g., saw dust, rice husk, coconut shell), and even industrial waste material (e.g., rice husk ash). This field is very attractive from both the ecological and economic point of view, since it could enable rejected material to become valuable material, which could be reused in industry (Intharapat et al., 2013; Gopalan & Dufresne, 2003).

(1) Rice husk ash

Rice husk ash (RHA) is an industrial waste material produced by burning rice husk for energy generation. It has a tough, woody and abrasive nature along with a high silica content. Given that the main components of rice husk as is amorphous silica and residual unburned or charred carbon (carbon char/black), rice husk ash has already attracted increasing attention (Chaudhary et al., 2004). Arayapranee et al. (2005) studied the quality of the rubber products filled with rice husk ash and compared them with another two commercial rubber fillers, Hi-Sil 233s silica (SiO_2) and carbon black N330. Their observations from various tests indicates that the incorporation of RHA filler in rubber with loading from 0 to 40phr can help provide high hardness but low tensile strength and tear strength, the viscosity and cure time of the RHA filler rubber were also reduced. Only a better resilience property is observed in the product compared with silica or carbon black filled ones. No significant change appears in other properties, such as Young's modulus and abrasion loss. It can be seen from the scanning electron micrographs that the dispersion of RHA filler in the rubber matrix is not continuous, which results in a weak structure compared with that of carbon black and silica. Sea-oui and co-workers (2002) reported a similar conclusion. They found that both low- and high- carbon content grades of RHA gave inferior mechanical characteristics, such as tensile strength, modulus, hardness, abrasion resistance and tear strength, compared with the reinforcing filler (silica and carbon black). Costa et al. (2000; 2002) tested properties of rubber filled with 20phr milled rice husk, which showed slightly inferior physical properties compared with the commercial carbon black or silica filled compounds, except for abrasion resistance. The incorporation of RHA into polypropylene was tested by Faud and his group (1995), and an increased flexural modulus of the composites was obtained. Meanwhile, elongation at break (the ratio between changed length and initial length after breakage),

tensile strength and Izod impact strength (impact resistance of materials) saw a decrease (Crompton, 2012). According to these results, it can be concluded that rice husk ash can be used as a cheaper filler for rubber products when mechanical properties and improvements are not critical.

There is the option to undertake some surface modification of RHA. There are a few investigations which have suggested that the rubber compounds filled with 20phr surface-treated RHA, which was modified by means of chemical treatment with NaOH or HCl, shows slightly superior properties (such as tensile strength) than the commercial filler filled rubber (Arayapranee, 2004). Many groups also researched the compatibility between silanol groups of RHA and a polymer matrix having polar groups (reactive towards silanol groups) (Chaudhary, 2004). The influence of a compatibilizer [poly (propylene –ethylene acrylic acid)] and a silane coupling agent [3-aminopropyl-trithoxy silane (3-APF)] on mechanical properties of milled RHA-filled polypropylene/natural rubber blends have also been studied. Ismail et al. (2001) investigated RHA filled polypropylene/natural rubber blends and observed a slight improvement in mechanical properties of polypropylene-natural rubber blends after using amino-silane agents, which may introduce some enhancement in filler-matrix interaction upon silanation. The mechanical properties of RHA filled vulcanizates in Ishak and Bakar's study (1995) were comparable to carbon black vulcanizates, which indicated that it is possible to partially replace carbon black by RHA. It should be noted that the similarity was only obtained at low filler loading (approximately 20 wt.%). With an excessive filler loading, the interaction between filler and matrix will be inhibited, which will result in poorer tensile properties and reduced elongation at break (Genieva et al., 2008). Recently, further investigations were undertaken to gauge the effect of peroxide based silane on chain-scission and to study the bonding between the silanol groups of RHA and epoxy groups of rubber (Manna et al., 1999).

(2) Peanut shell powder

Peanut shell powder (PSP) is a waste from one of the major food crops in the world, with large quantities produced annually. There were around 43.9 million tonnes of peanuts (in shell) produced in 2014 (FAO, 2017). The chemical composition of peanut shell powder is similar to hard wood, but with high cellulose content having a bulk density of 0.10g/cm^3 and

moisture content of 25%. Its chemical composition makes PSP a promising material as a rubber filler, mainly from the ecological stand point. Sareena et al. (2012) suggested that PSP is most effective as a filler in natural rubber at 10phr loading. After chemical modification by alkali treatment, the filler reinforcement ability of modified PSP increased and the modified PSP-NR composites shows better physicomechanical properties. Until now, research into peanut shell powder has been limit; much potential for further works exists, such as modification methods and mixing process improvement etc.

(3) Limestone dust waste

Limestone dust waste (LDW) is obtained from the explosions during the mining of limestone to get raw materials for cement manufacturing. The large quantities of fine dust cause serious air pollution and health hazards. Due to this situation, using the LDW to replace the most commercial fillers has gained more and more attention.

According to Sae-oui and co-worker (2009), after LDW is added into the rubber matrix, it has a negative effect on most mechanical properties, such as tensile strength, tear strength and abrasion resistance. Whereas, the addition of LDW still has a little effect on compound processability. LDW has recently been grouped as a non-reinforcing filler, because of its relatively low specific surface area and thus low reinforcement ability.

Other materials which have been used as fillers in rubber have been summarised in Table 1-7.

Table 1-7 Materials used as rubber fillers

Material	Short Summary	Reference
Chicken Eggshell	The eggshell calcium carbonate filled epoxidized natural rubber showed superior vulcanization characteristics (higher maximum torque and cure rate index, lower cure time and scorch time), higher tensile properties and lower tension set value.	Intharapat et al., 2013
Fly ash	Fly ash (up to 60 phr) can be used as a non-reinforcing filler for ESBR compounds, where abrasion resistance is not significantly required. The 300% modulus values remained unchanged with increasing loading.	Dasgupta et al., 2012
Soy spent flakes	The soy spent flakes can partially replace carbon black as the reinforcement co-filler in rubber composites. The elasticity of the co-filler network structure is close to that of carbon black filled composites.	Jong. L, 2007
Lignin	Reinforcing properties of lignin as filler in nitrile rubber can be improved on suitable chemical treatment for good thermal stability.	Setua et al., 2000
Pyrolytic tyre	Chars obtained from pyrolytic tyre can be successfully reused as semi-reinforcing fillers in rubber formulations. The physical and mechanical properties of the rubber filled with pyrolytic tyre were found to be comparable to rubber containing N772 and with N772 and silica.	Athanassiades, E., 2013
Waste newsprint fibres	The sodium silicate and magnesium chloride treated newsprint fiber waste at 40phr can improve the electrical and mechanical properties of the rubber composite.	Nashar et al., 2003
Marble sludge with carbon black	Marble sludge can be used as a co-filler with carbon black in natural rubber. High tensile strength, modulus, tear strength and hardness can be achieved.	Ahmed et al., 2013

1.6 Response Surface Methodology (RSM)

Traditionally, optimization of analytical processes has been carried out by monitoring one factor at a time on an experimental response. Only one parameter is changed while keeping all other variables at a constant level. This optimization technique is called one-variable-at-a-time, which always requires a large number of experiments and relies on the experience of the analysts (Kincl et al., 2005). The major disadvantage of the one-variable-at-a-time methodology is that it doesn't consider the interactions between parameters, so that the complete effect of combined variables on the process and the optimum conditions cannot be clearly studied in an efficient way. Another drawback of this technique is that it calls for unnecessarily numerous experiments. It is greatly beneficial if a thorough analysis of a process and the interactions can be undertaken with as few experiments and with as low cost as possible (Bolton & Bon, 2010; Bloomfield & Bulter, 2000; Kincl et al., 2005). In order to overcome this problem, the optimization of analytical procedures has been developed to provide simultaneous comparisons of several variables at one time. Among them the most popular multivariate techniques applied in optimization is Response Surface Methodology.

Response Surface Methodology (RSM) refers to a combination of mathematical and statistical techniques to analyse, improve and optimise industrial processes. It is very powerful and widely used for the modelling and analysis of problems, especially in which a response of interest, including the quality and performance characteristic of a product or process, is influenced by several input variables, and the objective is to optimize this response (Myers et al., 2009). The RSM technique was first introduced by Box and Wilson in 1951 for optimization in the chemistry field (Box & Wilson, 1951). Since then, it has been widely applied in many other industrial fields to investigate the behaviour of a system at a selected region, optimize the process and develop the operating conditions for specific objectives. In addition, the RSM is still helpful when optimization is beyond the boundaries of the experiments, as it can identify new conditions for the experiment to achieve the desire target.

A multiple regression analysis of the results is conducted based on the well-designed experiments, which leads to a mathematical relationship between the independent factors and the response. The individual and interactive effects of the experimental factors in the process

can be indicated by the regression models. There are three typical classes for the regression models: (1) first order polynomial (indicative of main effects only), (2) first order polynomial enhanced with two factor interactions and (3) second-order models which contains complete quadratic effects (Myers et al., 2009, Banks, 1998). The response surface can be visualized graphically through 3D plots or by contour ploys as shown in Figure 1-11.

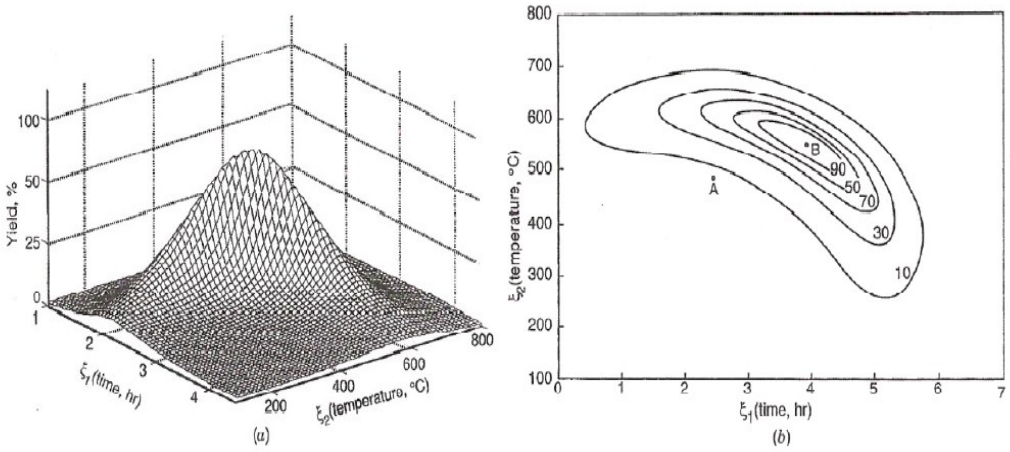


Figure 1-11 Example of (a) 3D plot and (b) contour plot of response surface for two variables (Myers et al., 2009)

RSM is a sequential optimization process and typically contains the same stages in the application as follows: (1) Screening tests. Through the first block of the response surface methodology, the independent variables of major effects on the system are investigated and the delimitation of the experimental region or the level of the independent factors can be identified according to the objective of the process and the experience of the researcher. (2) The experimental design is determined and the experiments are carried out based on the selected experimental matrix. Usually second-order models are employed at this stage to illustrate the surface curvature. (3) The obtained experimental data is then optimized through the fit of a polynomial function by the mathematic-statistical technique. (4) The fitness of the selected model is evaluated. (5) The necessity is identified and the possibility of performing a displacement in direction to the optimal region is verified. (6) The optimum values for each studied variable are obtained (Bezerra et al., 2008).

1.6.1 Experimental Design for Multi-level Variable

Good data collection and a scientific approach are needed in designing the experiment to guarantee that the outputs from the optimisation analysis are maximised. It is obvious that the statistical design of experiment is one of the most efficient and useful means to obtain the desirable output (Montgomery, 1976). Experimental design is a specific selection of combinations for the levels of variables that are applied experimentally to obtain the responses (Banks, 1998). A good fit of the regression model, time and cost effective and good distribution of data can be achieved by a successful experimental design.

Multi-level design is used when the variables are applied in more than two levels. The most popular multi-level design is the Central Composite Design (CCD), which was introduced by Box and Wilson (Box & Wilson, 1951). The CCD is powerful and flexible, considering the effects of variables and overall experimental error with fewer experiments. In order to gain a good estimate of pure error (experimental error), the centre points are usually repeated 4 to 6 times. Whereas, all factors are studied in five levels by default: alpha (the distance from the centre point to the end of the axial point), with negative, zero and positive values (-α, -1, 0, 1, +α). Figure 1-12 presents the full central composite design for two and three variables. The experiment number required by CCD can be calculated by $N = k^2 + 2k + c_p$, where k in the number of variable and c_p is the replicate number of the central point (Bezerra et al., 2008).

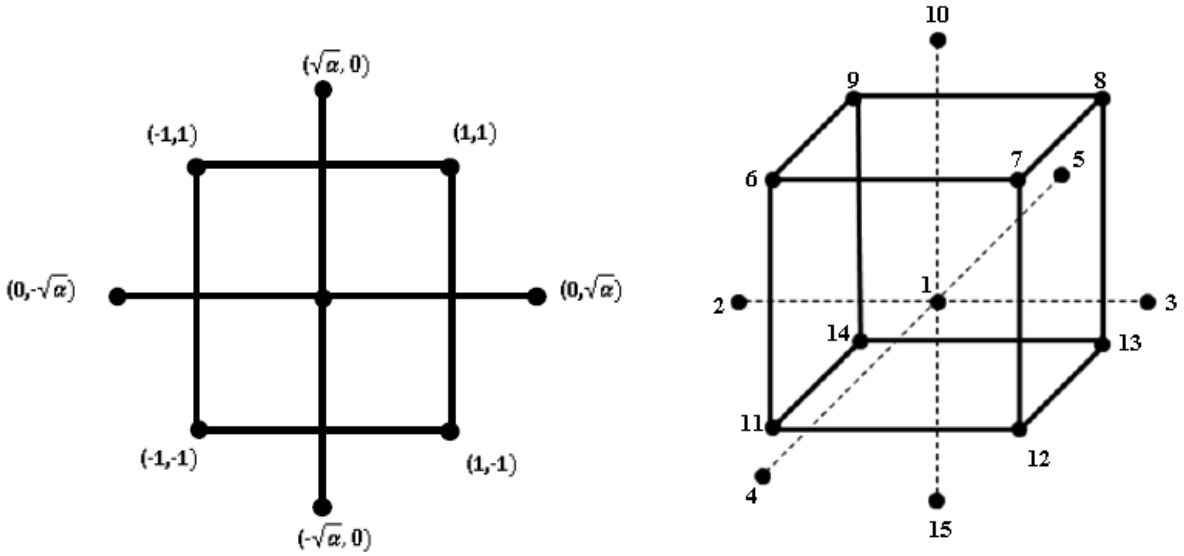


Figure 1-12 Design points for CCD designs with (a) 2 variables and (b) 3 variables (Sharifan, 2014)

Another widely employed multi-level design is Box-Behnken design (BBD) (Box & Behnken, 1960). It is a 3-level second-order designs and very efficient and economical mainly for a large number of variables. BBD is a spherical design since no points are at the vertices of the experiment region, all design points are either in a sphere or at the centre of a sphere. This design is well suited in examples where there is little or no interest in studying the response at the extremes i.e. the corners of the cube (Myers & Montgomery, 2002; Liyana-Pathirana & Shahidi, 2005), or where the edge points are experimentally expensive or difficult to achieve. Figure 1-13 illustrates the BBD design with 2 and 3 factors. The number of experiments required by BBD is based on $N = k^2 - 2k + c_p$, where k is the number of variables and c_p is the number of the centre points. All variable levels only need to be adjusted as three levels (-1, 0, +1) with equally spaced intervals between these levels (Ferreira et al., 2007; Bezerra et al., 2008).

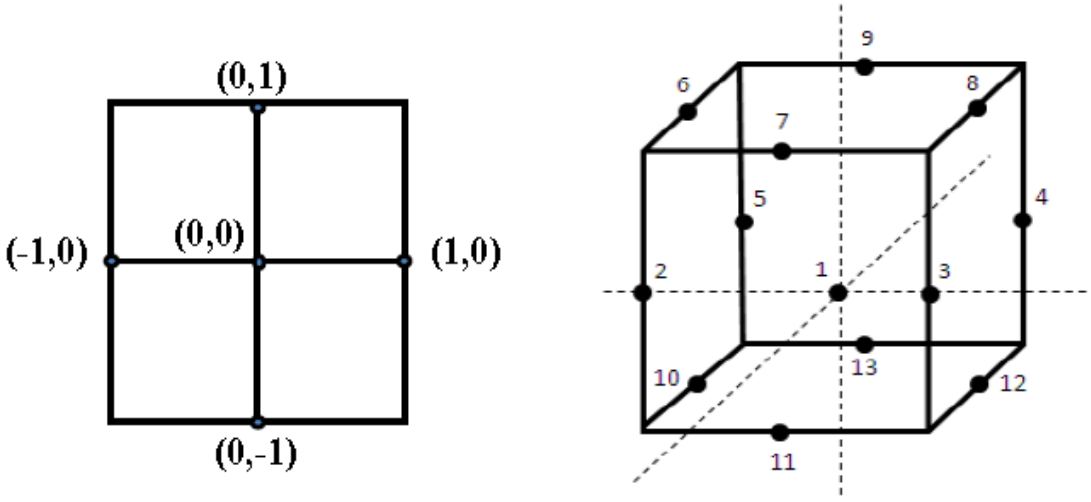


Figure 1-13 Design points for BBD design with (a) 2 variables and (b) 3 varibales (Sharifan, 2014)

Doehlert design, a uniform shell design, developed by Doehlert in 1970 is an alternative practical multi-level design. According to Ferreira et al. (2004), Doehlert is regarded as more efficient than CCD and BBD since fewer tests are required for the equivalent (or more) data, so that fewer experimental points are needed. This design describes a circular domain for 2 factors, spherical for 3 factors, and hyperspherical for more than four factors, which focus on the uniformity of the factors in the experimental domain. The experiment number required by

Doehlert design is $N = k^2 + k + c_p$, where k is the variable number and c_p is the replicate number of the central point. Figure 1-14 presents the DM design for two and three factors.

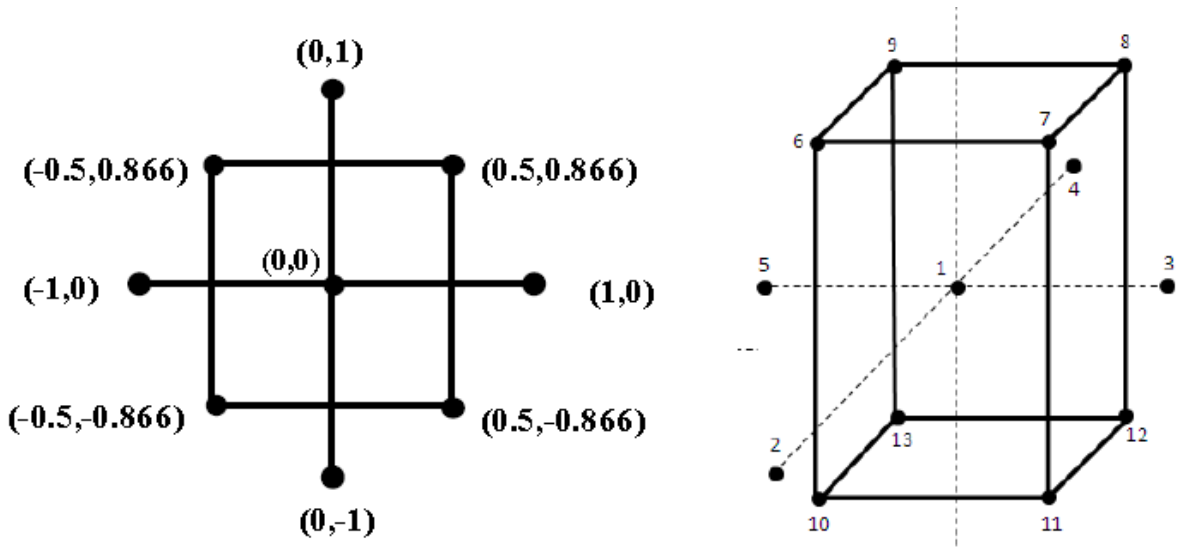


Figure 1-14 Doehlert design with (a) 2 variables and (b) 3 variables (Sharifan, 2014)

Unlike CCD and BBD all factors are at the same level, each variable in the DM can be studied at a different number of levels. For example, each variable in DM design can employ 3 to 5 levels, some variables at -1, -0.5, 0, +0.5 and +1, while others at -0.866, 0 and +0.866. This makes Doehlert design more flexible compared with CCD and BBD.

The most outstanding property of DM is its potential for sequential (Sharifan, 2014). When the boundaries are not selected correctly, or it is found necessary to develop a region out of the initial boundaries, the displacement of the experimental matrix to another experimental region can be achieved using previous adjacent points (Massart et al., 1997; Aujame et al., 2000). The application of Doehlert design has been paid more and more attention in analytical chemistry in recent year (Bezerra et al., 2008).

The efficiency of CCD, BBD and DM is summarised in Table 1-8, where efficiency refers to the ratio of the number of coefficients in a second order quadratic model for *k* factors, with the number of experiments in the analysis of those k independent factors.

Table 1-8 Comparison of CCD, BBD and DM (Ferreira et al., 2004)

Variables (k)	Number of Coefficients (p)	Number of experiments (n)			Efficiency (p/n)		
		CCD	BBD	DM	CCD	BBD	DM
2	6	9	-	7	0.67	-	0.86
3	10	15	13	13	0.67	0.77	0.77
4	15	25	25	21	0.60	0.60	0.71
5	21	43	41	31	0.49	0.61	0.68
6	28	77	61	43	0.35	0.46	0.65
7	36	143	85	57	0.25	0.42	0.63
8	43	273	113	73	0.16	0.40	0.62

1.6.2 Multi-objective Optimization

In most of the real industrial cases, the optimum is not only limited to one objective since lots of objectives need to be considered at the same time, such as cost, energy consumption and efficiency. Superimposed response surface of all objective function can be used to tackle this problem in term of two-dimensional problems (Lee et al., 1999). The contour plots or 3D surface from RSM can be applied and will result in a region of optimum condition considering all objective functions and limitations. Unlike single objective optimization analysis, the multi-objective problem does not have a single solution from one optimum point. Such problems then contribute to a set of "trade-off" optimal solutions, also known as "Pareto Optimal" solutions. A region where all the rest of the region has a higher value for at least one of the objective function can be found through Pareto Optimal; in other words, all Pareto Optimal solutions are regarded equally fit if there is no additional subjective preference. These solutions often come out with a set of curves; while any two of them contain a compromise between objective functions. (Deb, 2005; Caramia & Dell'Olmo, 2008; Konak et al., 2006).

1.7 Summary

This literature review has discussed the research on the characteristics of commercial carbon black and the production of carbon black substitutes from biomass and related materials. According to developing legislation related to GHG emission, new approaches need to be developed for the huge amount of these wastes which arise every year. Thus the invention of new approaches to enable the proper and sustainable management of coconut shell and sewage sludge are needed. Given that these two materials are carbon-rich, they have the potential to be converted through pyrolysis into reusable materials and applied as rubber fillers with potential reinforcing properties. Through the application of the Response Surface Methodology (RSM), which has been introduced in this chapter, in can be applied as a systematic method to study and optimise the pyrolysis parameters necessary for the production of optimal char fillers. In the following chapter, the aims and objectives to be achieved in this thesis will be introduced.

Chapter 2 Research Aim and Objectives

The key aim of this research is to develop, test and characterize novel types of sustainable fillers for rubber and related materials derived from the chars produced during the pyrolysis of biomass and other materials, derived from sustainable origins. Coconut shell and raw sewage sludge have been selected as materials which fulfil the required criteria and will be studied to test and understand their fundamental interaction in a rubber system.

The research aim will be addressed by achieving the following objectives:

a. Characterizing fully the physical and chemical properties of commercial carbon blacks and the influence of the filler upon the properties on the polymer.

b. Investigating the key physical and chemical properties of potential feedstock, such as thermal behaviour and proximate analysis using Thermogravimetric analysis (TGA).

c. Producing carbon-based fillers from feedstock through the application of conventional pyrolysis to convert into char fillers.

d. Examining physical and chemical properties of char filler products through: Nitrogen adsorption, toluene extractions, pH value, Boehm titration, Transmission Electron Microscopy (TEM), CHNS test and TGA.

e. Mixing char fillers with the most promising properties with rubber compounds through collaboration with the project industrial partner.

f. Optimising the manufacturing process for the production of a char filler.

g. Development of a screening tool to better enable selection of the most suitable materials as carbon black replacement fillers in the rubber system.

The approach to the work is summarised in the flow diagram shown in Figure 2-1.

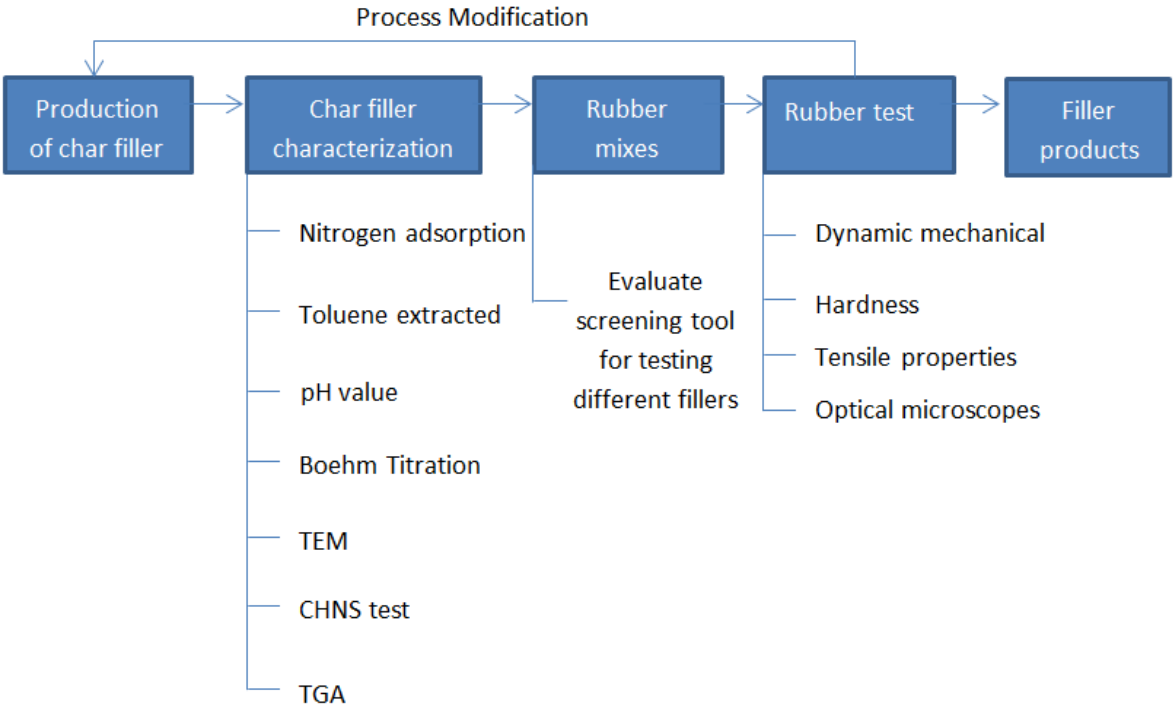


Figure 2-1 Flow diagram of the process for the production of carbon black substitutes

Chapter 3 Materials and Methodology

3.1 Introduction

In this chapter, the feedstock, reference materials (commercial carbon blacks) and the experimental methodologies used during the research are discussed. The feedstock examined were waste biomass: coconut shells and sewage sludge. Feedstock with different properties will lead to different characteristics of the produced char fillers and thus significantly influence the final performance of char fillers. Therefore, the first step of this research is to investigate the properties of the feedstock through their thermal behaviour, organic composition obtained from proximate analysis and CHNS content. In order to replace commercial carbon blacks, the study of carbon black characteristics is very important. The methods used to gain the knowledge of reference carbon blacks are discussed. After that, the production process of char fillers, which was thoroughly studied by the Response Surface Methodology (RSM), are explained in this chapter.

3.2 Materials

3.2.1 Sources of Char Filler

3.2.1.1 Coconut Shell

As a single and simple genus species, coconut grown everywhere exhibit similar properties. The coconut shells used in this project had already been shredded into random large pieces (approx. 15mm × 15mm) by the supplier. They were imported from India and shipped as 25Kg sacks.

In order to make the following experiments standardised, after being crushed into to small pieces (less than 10mm) by a laboratory-scale hammer miller (Glen Creston, UK) in the lab, the small pieces of coconut shell were then dried at 105 °C to constant weight, to reduce the moisture content (Figure 3-1).



Figure 3-1 Dried coconut shell

3.2.1.2 Sewage Sludge

The dewatered raw sludge cake used in this research was supplied by Thames Water from their Crossness treatment works. The raw sludge was dewatered by the belt press after collection on the site of the waste water treatment plant, then the dewatered sludge cake was firstly sterilized in the laboratory by using the Autoclave at 121°C for 15 minutes and then dried at 60°C to a constant weight, usually it takes around 48 hours, as shown in Figure 3-2. The texture of dried raw sludge was light and loose compared with the digested sludge. Subsequently, the dried sludge was grounded by hand using a pestle and mortar to less than 10 mm and then stored in air tight containers for further use, including sludge characterization and carbonization.



Figure 3-2 Dried raw sewage sludge

3.2.2 Commercial Carbon Blacks

Commercial carbon black (CAS-No. 133-86-4) N115, N220, N330, N550, N660 and N772 were used as the reference materials in this research. Among them, N115, N220, N330, N550 and N660 are supplied by Cabot Corporation. N772 is provided by Degussa AG. All of the commercial carbon black samples are made using the furnace procedure (Section 1.4.2) and in black pellet form, as shown in Appendix I. Carbon black N115 (N110 series) is super-abrasion furnace black; N220 (N200 series) is intermediate super-abrasion furnace black; N330 (N330 series) is high-abrasion furnace blacks, and is also used as the reference material in the in-rubber tests; N550 (N500 series) is fast-extrusion furnace black, N660 (the N600 series) is general-purpose furnace black; and N772 with (N700 series) is low to semi-reinforcing furnace black, which is also the reference material in the in-rubber tests.

3.2.2.1 Carbon Black N115

N115 has a very high degree of reinforcing ability to both natural and synthetic rubbers. The surface area per unit mass is very high, whereas the structure is low. N115 is often used in the high-performance passenger tyre treads, off-the-road tyres, aero-tyres and the premium tread

compound of truck tyre. The rubber products containing N115, such as high strength conveyor belt and industrial rubber articles, have outstandingly high abrasion resistance and high strength coupled with relatively low modulus and low resilience (high hysteresis). Table 3-1 shows the main typical characteristics of carbon black from N115 to N772.

3.2.2.2 Carbon Black N220

N220 is a high-amplifying fine active carbon black, which can disperse easily in the rubber matrix. When mix with rubber, N220 helps provide a high level extrudability, increased wear resistance, high resistance of tensile and tolerable tear resistance, with relatively low modulus. N220 is normally used in the manufacturing of high quality and durability rubber products, such as the tread rubber of tyres for passenger cars and trucks and high grade conveyor belts. Table 3-1 shows the main typical characteristics of carbon black N220.

3.2.2.3 Carbon Black N330

Carbon black N330 is the most widely used high abrasion furnace black, is a high-dispersing and amplifying black. N330 can provide good reinforcement, which resulting in good tensile strength, moderate abrasion resistance, elasticity and excellent extrusion characteristic.

N330 is an industry standard for many tyre application, including both truck tyre treads and sidewalls application. It is particularly suitable for the tyre treads that requires good wear resistance, including those made from emulsion SBR, solution SBR, PBR, NR or blends of any of these polymers. Due to its balanced properties, N330 is also used for conveyor/transmission belts, tube applications, hose covers, seals and moulded compounds etc. Carbon black N330 is one of the reference materials in later in-rubber test. Table 3-1 shows the main typical characteristics of carbon black N330.

Table 3-1 Main technical characteristics of carbon blacks

Properties	N115	N220	N330	N550	N660	N772	Analyse Method
Nitrogen Surface area, m^2/g	129-145	112-126	71-85	34-46	29-41	30 ± 5	ASTM D 3037
CTAB Surface area, m^2/g	119-137	102-120	73-91	35-49	29-43	29 - 37	ASTM D 3765
STSA, m^2/g	124±9	106±9	75±9	39±9	34±9	30±5	ASTM D 6556
DBP Absorption, $cm^3/100g$	113±7	114±7	102±7	121±7	90±7	65 ± 5	ASTM D 2414
Heat Loss, % max	3.0	2.5	2.5	1.5	1.5	0.3	ASTM D 1509
Sieve Residue, % max							
35 mesh	0.001	0.001	0.001	0.001	0.001	0.0001	ASTM D 1514
325 mesh	0.1	0.1	0.1	0.1	0.1	0.005	
pH Value	5-9	7-10	7-10	5-9	7-10	9 – 11	ASTM D 1512
Ash content, % max	0.5	0.7	0.7	0.7	0.7	0.4	ASTM D 1506
Pour density, kg/m^3	345±40	355±40	380±40	360±40	440±40	460	ASTM D 1513
Fine content, % max	7	7	7	7	7	7	ASTM D 1508
Iodine Absorption, g/kg	160±8	121±7	82±8	43±6	36±6	30±5	ASTM D 1510
Tinting Strength, %	115-131	108-124	96-112	59	59	23	ASTM D 3265
Stress at 300% Elongation, Mpa	-3.4±1.6	-2.3±1.6	-0.9±1.6	-0.9±1.6	-2.6±1.6	-4.1±1.6	ASTM D 3192
Sulfur content, % max		2.0	1.1	1.1	1.1	0.1	ASTM D 1619

3.2.2.4 Carbon Black N550

Carbon black N550, with high structure and smooth particle surface, is the best reinforcing black among soft carbon blacks, also called semi-reinforcing carbon black. Its medium-dispersion and medium-activity lead to highly enduring properties, high extrusion rate, high temperature resistance, high heat-conductivity, high reinforcement, high elasticity and rebounding properties and relatively high tear resistance. Carbon black N550 is suitable for both natural rubber and synthetic rubbers. It is widely used in fabric cord of tyres, tyre side compounds, extrusion and rolling compounds, and profiling articles, seal and hoses as well. Table 3-4 shows the main typical characteristics of carbon black N550.

3.2.2.5 Carbon Black N660

Carbon black N660 is a medium-dispersion, medium-active and low structure carbon black with high tensile stress, good processing performance, high rebounding performance and high flexibility. It is widely applied in various vulcanizates, such as fabric cord of tyre, inner tyre, bicycle tyre and footwear etc., providing good elasticity, moulded, extrusion and fatigue properties. The only deficiency of carbon black N660 is the low elongation. Table 3-1 shows the main typical characteristics of carbon black N660.

3.2.2.6 Carbon Black N772

Carbon Black N772 is obtained from continuous process in the furnace by a thermal-oxidative decomposition of natural gas, also called semi-reinforcing furnace carbon black. It belongs to low to semi-dispersion, middle-active grades of carbon black. Among rubber carbon blacks, N772 has the largest particle size and lowest structural and surface area, it normally disperses relatively slowly.

It can be applied as a filler with high load in both natural rubber and synthetic rubbers, mainly in the manufacture of frameworks, compounds of buffering layers, extruded rubber articles and tubes. N772 can give the rubber mixtures high elasticity, low heat-up, good aging-resistance and superior dynamic performance when used in tyre frames and technical rubber products. Table 3-1 shows the main typical characteristics of carbon black N772.

3.2.3 Chemical Reagents

Table 3-2 provides information on the chemical compounds used in this research, which including physical properties, such as molecular weights, solubility melting point, boiling point, purity and supplier companies.

Table 3-2 Chemical reagent

Reagent	MW (g/mol)	Melting point (°C)	Boiling point (°C)	Purity (%)	Company
Toluene	94.14	-95°C	110.6°C	≥ 99.5	VWR
Acetone	58.08	-94°C	56°C	≥ 99.0	SIGMA-ALDRICH
			Powder		
NaOH	40.00	-	-	≥ 98.8	VWR
Na_2CO_3	105.99	-	-	≥ 99.9	BDH
$NaHCO_3$	84.01	-	-	≥ 99.99	Fisher
Potassium hydrogen phthalate	204.22	-	-	≥ 99.9	BDH
KOH	56.11	-	-	≥ 85.0	BDH

3.3 Methodology

3.3.1 Preparation of a Series of Char Fillers

3.3.1.1 Thermogravimetric Analysis (TGA)

Thermogravimetry (TG) or thermal gravimetric analysis (TGA) is mainly considered as a range of techniques by which the thermo-physical and thermo-chemical characteristics of a sample are monitored as a function of time and temperature, in a defined atmosphere, under controlled temperature conditions (Haines, 1995). The composition of the given materials and their thermal stability at a high temperature up to 1000°C can be studied through this analysis.

The weight loss or gain of the materials due to decomposition, oxidation, or dehydration can be gained from this process at the same time. As the temperature increases, various components (e.g. moisture and organic content) of the sample are removed or decomposed and the weight percentage of each resulting mass loss can be recorded.

The thermo-gravimetric weight change (loss) curve was plotted against temperature. It provides a range of temperatures within which the maximum thermal degradation of feedstock takes place (Rout, 2013). According to the mass loss steps in a TGA curve, several characteristics of materials can be determined, such as thermal stability, composition, moisture and volatiles content, level of inorganic and organic components, ash content and decomposition kinetics. Pyrolysis is known as a heating process of a substance in the absence of oxygen at a particular temperature. Therefore, the temperature(s) for effective pyrolysis of the feedstock need to be determined at the first stage. By using the TG data, the derivative thermogravimetric (DTG) results can be studied according to the calculation of the rate of the mass loss. The Derivative Thermogravimetry (DTG) plots are the first derivatives of the original TG curve, which determines the information about the critical points with the highest decomposition rate in the thermal event (Mettler Toledo, 2012).

Thermogravimetric analysis (TGA) is applied in this research to identify some of the basic characteristics of the feedstock and determine the suitable pyrolysis temperature(s) and heating rates to produce char fillers. The thermal analysis experiments were carried out using a Rheometric Scientific STA 1500 Simultaneous Thermal Analyser (Polymer Laboratories, TG/DSC), shown in Figure 3-3.

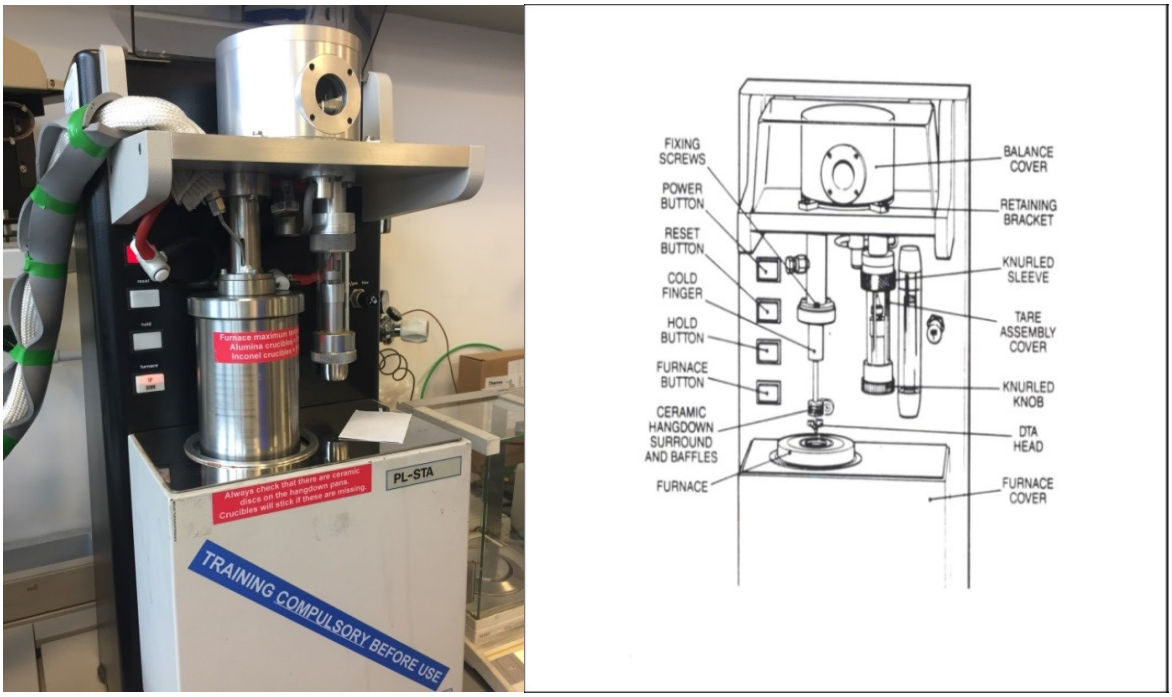


Figure 3-3 STA 1500 Simultaneous Thermal Analyser

For each analysis, around 10mg to 16mg of the ground sample was accurately weighed and loaded into an alumina crucible. Normally, the particle size of the sample needs to be less than 150 μm, since the results from thermal analysis could slightly change with the change of the particle size of sample (Kök et al., 1997). This crucible was placed on one side of the thermo-balance hang-down, along with an inert reference empty alumina crucible. The samples were then heated from room temperature (≈20°C) to the desired temperature (around 1000°C) under a continuous flow of nitrogen at 50ml/min flow rates. The inert nitrogen atmosphere is used to guarantee that the heat is well transferred through the sample so that the curve can be comparable to other works (Li et al., 2008) and to prevent oxidative changes in the sample. The furnace was equipped with a thermocouple for monitoring the accurate temperature of the sample which was heated at 10°C/min. The sample weight and temperature was monitored continuously with a data point recorded every 6 seconds (equivalent to every 1°C temperature rise). The derivative thermogravimetry (DTG), which shows the rate of weight change steps in TG curves was subsequently determined from the recorded TG data by the corresponding software in the machine.

3.3.1.2 Proximate Analysis

Using proximate analysis, the moisture content, volatile matters, fixed carbon and ash content of materials are determined. Since the use of thermogravimetry is easier and less time consuming, the STA 1500 thermal analyser is also used for the proximate analysis in this research.

During the course of coconut shell and raw sludge proximate analysis, around 15mg of feedstock was accurately weighed and loaded into the thermo-balance of the TGA analyser. The system was firstly programmed to heated up to 105°C from room temperature (≈ 20°C) at a heating rate of 40°C/min and held for 10 minutes at 105°C under an inert atmosphere of nitrogen to guarantee a non-oxidative environment. This step was to provide sufficient time to measure the losses of moisture content of the feedstock. As to the volatile matter content, the sample was them heated up to 950°C at 40°C/min heating rate and then held for 20 minutes under an inert nitrogen atmosphere. This isothermal stage provided enough time for the sample to reach a plateau in the weight loss curve. In order to measure the fixed carbon, the temperature was dropped to 600° C; at the same time, the gas flow was switched to air and was held there for 30 min (Bakisgan et al., 2009; Demirbas, 2004; San Miguel, 1999). The residue at the final stage was ash content of the sample. The proximate analysis of coconut shell or raw sewage sludge was performed using the protocol in Table 3-3.

Table 3-3 Proximate analysis protocol

Step	Temperature (°C)		Isotherm (min)	Heating rate (°C/min)	Atmosphere
	Start	End			
1	20	105	-	10	Nitrogen
2	105	105	10	-	Nitrogen
3	105	950	-	40	Nitrogen
4	950	950	20	-	Nitrogen
5	950	600	20	-	Air
6	600	600	-	30	Air
7	600	20	20	-	Air

3.3.1.3 Carbon Hydrogen Nitrogen Sulphur Analysis

CHNS analysis determined the C, H, N and S content of both the feedstock and the char filler samples. It was conducted by combustion analysis using a Carlo – Erba EA 1108-CHNS analyser by MEDAC Ltd, Surrey, UK. During the test, the sample is burned in excess of oxygen in the presence of a catalyst. Carbon is oxidised into carbon dioxide, hydrogen into water, nitrogen into nitrogen dioxide and sulphur into sulphur dioxide. The combustion products are then separated by gas chromatography and the components measured. The accuracy of this test can reach 0.30% with a detection limit less than 0.1%.

3.3.1.4 Conventional Thermal Pyrolysis

Pyrolysis is a thermal treatment by which organic materials are chemically decomposed by heat in the absence of oxygen. It is a promising method to sustainably recover valuable components from waste materials. By using waste materials such as biomass as feedstock, pyrolysis is a way to convert waste into energy. During the pyrolysis, large molecules break down into small molecules, resulting in carbonaceous residues containing carbon and char, combustible gases and condensable liquid hydrocarbons.

The char (carbonaceous residues), whose qualities are governed by the experimental conditions, can be applied in tyre manufacture, dye works wastewater decolourization and as a precursor for activated carbon and for the extraction of useful bio-chemicals (Mohan et al., 2006; Roy & Unsworth, 1989; Cunliffe & Williams, 1998). The oil and gases generated from pyrolysis of biomass can be used as renewable energy sources and fuel in the pyrolysis plants and existing industrial boilers and furnaces. They can also be used for generating electricity and heat if there is an excess (Environment Agency, 2004).

Various parameters can influence the pyrolysis process, including temperature, heating rate, pressure, retention time, atmosphere and type of reactor. A huge amount of research has been conducted to understand the correlation between the pyrolysis conditions and the pyrolysis output for pyrolysis performance indication (Arabiourrutia et al., 2007; Leung et al., 2002; Park & Atreya, 2010; Rofiqul Islam et al., 2008, Williams and Besler, 1996). For example,

with an increasing heating rate, the yield of char will decrease and the yield of oil and gas will increase (González et al., 2001; Wang et al., 2007). According to Sienkiewicz et al. (2012) it is obvious that there is a significant potential of pyrolysis treatment based on ongoing works in this field along with increasing cost of energy and petroleum and resources such as carbon black.

The pyrolysis of feedstock was performed in a Carbolite 11/150 laboratory scale rotary furnace (Carbolite, Hope Valley, UK) situated in a walk-in fume cupboard. As shown in Figure 3-4, a rotatory horizontal tubular quartz vessel with the capacity of almost 5 litres (containing 1 kg sample) is suspended by air-tight rotary fixtures inside an electrically heated box-furnace. The rotation is initiated from the left side, where the reactor vessel was attached to the furnace. The temperature is controlled by the thermal system with a thermocouple located within the box furnace; the temperature that can be reached is up to 1000°C. Nitrogen gas is introduced into the reaction vessel from the gas inlet ports at a controlled flow rate (San Miguel, 1999), which can be adjusted by a rotameter. The nitrogen flow maintaining in the vessel throughout the pyrolysis is to protect the char from oxidation and help to carry and remove the pyrolytic volatiles (oil and gas) towards the oil trap. The oil trap is located in the right end of the reactor vessel, in which the condensed oil can be collected. The non-condensable volatiles (gases) were vented from a small opening on the top of the oil trap to the fume cupboard.



Figure 3-4 Carbolite 11/50 rotary furnace

In each furnace run, around 300g of dried feedstock with the particle size smaller than 10mm was loaded into the quartz reactor vessel. Then, according to the results of the thermal analysis and proximate analysis of feedstock, and utilizing a Response Surface Methodology design of experiments procedure (described later), 30 samples were prepared in the furnace by varying the pyrolysis temperature between 400°C to 800°C; the heating rate from 5°C/min to 15°C/min and dwell time over 0 to 3 hours using selected nitrogen atmosphere flow rates from 100 to 1000ml/min. All samples were cooled to room temperature with continuous nitrogen flow before being removed from the furnace. The rotation rate of the furnace was held constant at 10rpm for each run. The char and oil produced were weighed to determine their yield and the gas yield was calculated by the difference from the total original feedstock mass. The char samples were stored in a sealed container in a desiccator for future analysis.

3.3.1.5 Response Surface Methodology (RSM) Design

In order to optimize the char filler production process from coconut shell or raw sewage sludge and explore the effect of different pyrolysis parameters focusing on the key characteristics of char fillers, response surface methodology (RSM) was applied in this research. In this study, a modified Central Composite Design (CCD) is used, where the alpha

value was decided as one resulting in three levels, lowest (-1), middle (0) and highest (+1). This design is more specifically known as Central Composite Face Centred Design (CCFD). Using the Central Composite Face Centred Design (CCFD), all the experiments were carried out based on a 2^4 full factorial design for the four identified design independent variables, namely; pyrolysis temperature, °C (X_1), heating rate, °C/min (X_2), holding time, min (X_3), and Nitrogen flow rate, ml/min (X_4). According to the preliminary results, three levels were selected as low -1, centre 0 and high +1 level. The total number of experimental runs was determined by the simple formula [$30 = 2^n + 2n + 6$], where n is the number of independent variables, in this study n equals to 4, 16 factorial points are included in the 2^4 full factorial CCFD and were augmented with 6 replicates at the centre point for the pure error.

The responses selected for full analysis of coconut shell char fillers were pH value and t-plot surface area. Whereas, the responses used in the sludge char RSM design were pH value, t-plot surface area and surface acidic groups. The design variables range are namely, X_1 [400 and 800°C], X_2 [5 and 15°C/min], X_3 [0 and 180min], and X_4 [100 and 1000ml/min]. Thus 600°C, 10°C /min, 90min, and 550mL/min for X_1, X_2, X_3, and X_4 respectively, as the zero level in this design was the central value (Table 3-4).

Table 3-4 Variables and their levels used in the experimental design

Variables	Symbol coded	Range and levels		
		Low level (-1)	Centre (0)	High level (+1)
Temperature (°C)	X_1	400	600	800
Heating rate (°C/min)	X_2	5	10	15
Holding time (min)	X_3	0	90	180
N_2 flow rate (ml/min)	X_4	100	550	1000

The statistical software Design Expert 8.0 (Stat-Ease Inc., Minneapolis, USA) was utilized for the experiment design, regression and graphical analyses of data obtained, statistical

analysis of the model to evaluate the analysis of variance (ANOVA) and the final optimization.

3.3.1.6 Post-pyrolysis Grinding by Wet TEMA Milling

All the char samples after the pyrolysis were ground by wet TEMA milling using a vibratory disc mill (Tema Machinery Company Ltd, UK). TEMA milling is steady and smooth, suitable for the extremely quick, loss free and reproducible grinding of medium-hard, brittle and fibrous material. It is also widely known that wet milling is considered more intensive and efficient than dry grinding. The energy provided by the mill acts on the solids suspended in distilled water to crush them, reducing them in size. It can break the char samples into finer particles in the micron & submicron (or nanometer) particle size. As a result, smaller particle size can be expected and guaranteed by wet milling. Additionally, it has been found that there is a trend in wet grinding which is clearer and follows an unvarying pattern. Whereas, the trend in dry grinding is vague and uncontrollable (maybe due to the heat generated during grinding with the oily sample). In other word, wet milling can cost-effectively create uniformly fine particles with limited or no contamination (Retsch, 2017). Based on several pre-tests, the optimum condition for wet TEMA milling were confirmed as 1:1 liquid and solid ratio, 1.5 minutes grinding time. Further milling afforded no change to the particle size of the char sample. After the milling process, the wet samples were dried at 105°C for 24 hours until constant weight. The dried samples were then lightly crushed to form powder suitable for further characterization tests.

3.3.2 Characterization Methods

3.3.2.1 Textural Characterization

Surface area and pore size distributions of the samples were characterized by liquid nitrogen (at 77K) adsorption and desorption method using the OMNISORP 100. In each test, the sample size of around 0.25g was accurately weighed into a glass sample tube. Before gas adsorption measurements, the samples were firstly degassed under vacuum conditions at 423K for a period of at least 4 hours until the pressure falls below 10^{-6} torr. Subsequently, the adsorption and desorption was conducted and the isotherm was obtained. Nitrogen adsorption isotherm was determined over a relative pressure (P/P_0) range from 0.0001- 0.95. Then the

BET surface area can be calculated with the isotherms by using the Brunauer–Emmett–Teller equation (See section 1.4.3.2). Slight adjustments of the region boundaries were made to ensure $R^2 \geq 0.9999$.

The t-plot method was used to find the micropore volume and the combined macropore and mesopore surface area. The significant surface areas were concluded from the difference between the BET surface area and the macropore and mesopore surface area and used to establish the relationship between pore size distribution and rubber uptake capacity of the fillers.

3.3.2.2 Toluene Extraction

ASTM D 1618-99 (Standard Test Method for Carbon Black Extractables - Transmittance of Toluene Extract) was applied for the toluene extraction test (ASTM, 2004). This test method covers the measurement of the degree of toluene discolouration by carbon black extractables and is useful in controlling the reaction process for the production of carbon black.

An adequate amount of filler sample was dried at 125°C for 60 minutes to constant weight in a gravity-convection oven before test. After the sample is cooled to room temperature in a desiccator, 2.00g of sample was transferred to a 125 cm^3 Erlenmeyer flask with a ground-glass stopper. To which 20cm^3 toluene was added to the sample and then the mixture was shaken vigorously without delay for 1 minute. The mixture was immediately poured as quickly as possible into the glass funnel with a filter paper in a second flask. After the filtration is complete, the flask needs to be stopped until ready to test. A visible spectrophotometer is adjusted to read 100% at the 425-nm wavelength when the cuvette with pure toluene is analysed. A portion of filtrate from the stoppered flask is poured into a clean cuvette which is placed into the spectrophotometer and the percent transmittance obtained at 425 nm to the nearest 0.1% is measured.

3.3.2.3 pH Value

Test Method A – Boiling Slurry of ASTM D1512-05 Standard Test Method for Carbon Black – pH value (ASTM, 2012) was applied in this pH value test. This test is used to indicate the pH of the filler sample surface by measuring the pH of water in contact with the carbon black because the surface pH value of a carbon black can affect the vulcanization of some rubber compounds.

Firstly, 5g of fine filler sample was weighed into a 100 cm^3 glass beaker and 50 cm^3 of boiling, distilled water was added. The glass beaker was covered with a watch glass and the mixture boiled for 15 minutes on a hotplate. A standardized electrode of pH meter was then placed in the sludge and rotated gently in alternate direction until a constant pH was obtain.

3.3.2.4 Boehm Titration

The Boehm titration is used in the project as a chemical method to investigate acidic and basic surface groups on carbon materials (Boehm, 1994). During the process, approximately 1.5g of char sample was added to 50.00 mL of one of three reaction bases of 0.05 M concentration: $NaHCO_3$, Na_2CO_3 and NaOH. Then the mixed samples were shake for 24 hours and filtered to remove the carbon. Aliquots of 10.00 ml were taken by pipette from the samples. The aliquots of the reaction base $NaHCO_3$ were then acidified by the addition of 20.00 mL of 0.05 M HCl, the aliquots of the reaction base Na_2CO_3 were mixed with the addition of 30.00 mL of 0.05 M HCl, to ensure complete neutralization of the base, which requires two protons. The acidified solutions were then back-titrated with 0.05 M NaOH. The aliquot of the NaOH reaction base was acidified by the addition of 20.00 mL of 0.05 M HCl and was back-titrated with 0.05 M NaOH. In all cases, CO_2 was removed from solution immediately by sparging the sample the sample with nitrogen gas for 1 hour before the titration (Goertzen et al., 2010).

3.3.2.5 Transmission Electron Microscopy

The microstructure (size and morphology) of the selected char filler samples was analysed through Transmission Electron Microscope (TEM). A high energy beam of electrons is

transmitted through an ultra-thin specimen, interacting with the specimen as it passes through. A significantly high resolution image is formed from the interaction of the electrons transmitted through the specimen; the image is magnified and focused onto an imaging device. Chemical information can also be obtained from TEM. Images of the selected chars in ethanol were obtained using TEM-2100 Plus Electron microscope in Material Department at Imperial College London, using x100, x4000 and x20000 magnification.

3.3.3 In-rubber Testing

Styrene-Butadiene Rubber (SBR) is a group of synthetic rubbers derived from styrene and butadiene (Pilla, 2004; Thomas & Maria, 2016). It is widely applied in tyre treads, as it provides wet skid and traction properties, as well as good abrasion resistance and good aging stability when protected by additives (Rodgers & Waddell, 2005). It is reported that more than 5.4 million tonnes of SBR were processed worldwide in 2012 (Arun et al., 2014). It is a commodity material which competes with natural rubber. The chemistry of SBR is very attractive, with different forms used for different purposes. The most common use of SBR is in pneumatic tyres with around 50% of car tyres being made from a range of types of SBR. The properties of the polymer is determined by the ratio of styrene and butadiene; with high styrene content, the rubbers are harder and less rubbery (Markovic & Visakh, 2016). It is also used by speaker driver manufacturers as the material for Low Damping Rubber Surrounds. Additionally, it also can be used in some rubber cutting boards (Zsigmond, 2016).

A widely used generic SBR formulation, shown in Table 3-5, was applied in the compounding process to investigate the performance of the char filler in rubber. Compounds were produced using a 60cc Brabender mixer set at 40˚C and 60rpm, following the procedure detailed in Table 3-6.

After compounding, the Moving Die Rheometer (MDR) test was conducted based on ASTM D5289, at 160°C for 30 mins. The results of the MDR were used to evaluate the cure characteristics of each compound and to allow preparation of cured sheet using a cure time of T90 + 5 minutes. Surface roughness maps (×250 magnification) were generated using a Hitachi TM3030 SEM fitted with an annular multi-segmented back-scattered electron detector to illustrate the dispersion property of the char fillers. Shore A hardness was tested

according ASTM D2240. Tensile Properties were determined following ASTM D412. Strain sweeps for Dynamic Mechanical Analysis (DMA) were conducted in tension at 40°C, 10Hz and double strain amplitude (DSA) range of ~ 0.06 to 6%. The in-rubber tests were conducted by Artis Limited (Melksham, UK.)

Table 3-5 SBR formulation

Ingredient	Past per hundred of rubber
SBR 1502	100
Char filler	60
TDAE Oil	10
Zinc Oxide	5
Stearic Acid	2
6PPD	1.5
TBBS	1.5
Sulphur	1.5

Table 3-6 Mixing procedure

Time (mins)	Step
Masterbatch Cycle	
/	Add polymer
0	Ram Down
0.5	Powders/Oil
1	Ram Down
2	Ram Bump
3	Ram Bump
5	Dump
Conversion Cycle	
/	Add Masterbatch
0	Ram Down
0.33	Add Curatives
0.5	Ram Down
2	Dump

3.3.4 Scanning Electron Microscopy

A Scanning Electron Microscope (SEM) (Auriga Cross Beam, Zeiss) was used to examine the surface morphology of the char filler filled rubber sample and to investigate the interaction between the char filler and rubber matrix. This is an important feature of the rubber to understand, since it indicates the mechanism of the char filler with the rubber matrix. Before the SEM, all the rubber samples were grounded using a liquid nitrogen Cyro-mill (CyroMill, Retsch) into fine powder to fulfil the size requirement of the SEM. All the samples were subsequently examined in the SEM under the secondary electron mode. It is reported that secondary electrons can knock electrons out of their orbits around an atom and finally escape from the sample with enough energy. The backscattered detectors produce an electron micrograph showing the difference in average atomic mass between the phases, and secondary detectors produce topographical micrographs of the sample (Bowen and Hall, 1975). Prior to SEM tests the sample surface were coated with a thin layer of gold to make them conductive.

3.3.5 Oil Calorific Value Analysis

Calorific value is a measurement of the heat released by a sample when burnt with oxygen in an enclosed combustion capsule (Parr Instrument Company, 2007). This information is very helpful when analyzing the energy balance of the process and when trying to determine whether the pyrolysis oil can be used to heat the system.

The calorific value analyses of pyrolysis oil from coconut and sludge was determined using a Parr 6100 Bomb Calorimeter, which is shown in Figure 3-5. Before the test, the equipment was calibrated with benzoic acid to determine the heat capacity of the calorimeter. Around 0.5 ± 0.001g of oil sample was placed and ignited in a bomb surrounded by water. The heat evolution resulted in a raised water temperature of the system, which was recorded. The calorific value of the oil sample per unit weight is calculated by multiplying the temperature change with the heat capacity of the calorimeter and diving by the sample's weight, which was automatically reported by 6100 calorimeter in the unit of MJ/kg. Each sample was tested in triplicate.



Figure 3-5 Parr 6100 Calorimeter

3.4 Summary

In the following chapters, the methods described above will be applied to evaluate the feedstock, develop and evaluate the char fillers, which will be applied as sustainable substitutes for carbon black in rubber.

Chapter 4 Coconut Shell Derived Char Fillers

The following results and discussion considers the study of the char filler derived from coconut shell. Firstly, the thermal behaviour, physical and chemical composition and the pyrolysis conditions of the coconut shell feedstock was identified through Thermal analysis and CHNS tests. Secondly, the production of the coconut shell char fillers through various pyrolysis temperatures, heating rates, holding times and nitrogen flow rates are discussed. Finally, the characteristics and application of the coconut char fillers were investigated in rubber testing.

4.1 Characterisation of Coconut Shell

4.1.1 Thermal Analysis of Coconut Shell

4.1.1.1 TGA-DTG Curves

It is well established from the literature that biomass can be converted into char by controlled thermal decomposition. Several steps are involved in this conversion: (1) up to 150°C, the desorption of adsorbed water takes place, (2) between 150°C and 260°C, structure and bound water splits up, (3) between 260°C to 400°C, water, CO and CO_2 will be released from chain scissions or depolymerisation and the breaking of C-C bonds within carbon rings, (4) above 400°C, the graphitic layers start to form due to aromatization reaction and (5) above 800°C, decomposition and the 1st stage carbon rearrangement reactions are almost finish with the carbon template structure as residues.

The thermal behaviour (TG and DTG analysis) of coconut shell is presented in Figure 4-1. According to the TGA plots, around 20% of "char yield" can be achieved by the coconut shell sample, irrespective of the real composition. The remaining residue is composed of fixed carbon ("carbon black"), some inorganic materials, and the carbonisation residue from the pyrolysis process as well (Kim & Park, 1995). There is a systematic order for the breaking down of some main components of biomass: 200 - 800°C (hemicellulose), 260 - 350°C (cellulose) and 280 - 500° (lignin) (Singh et al., 2009).

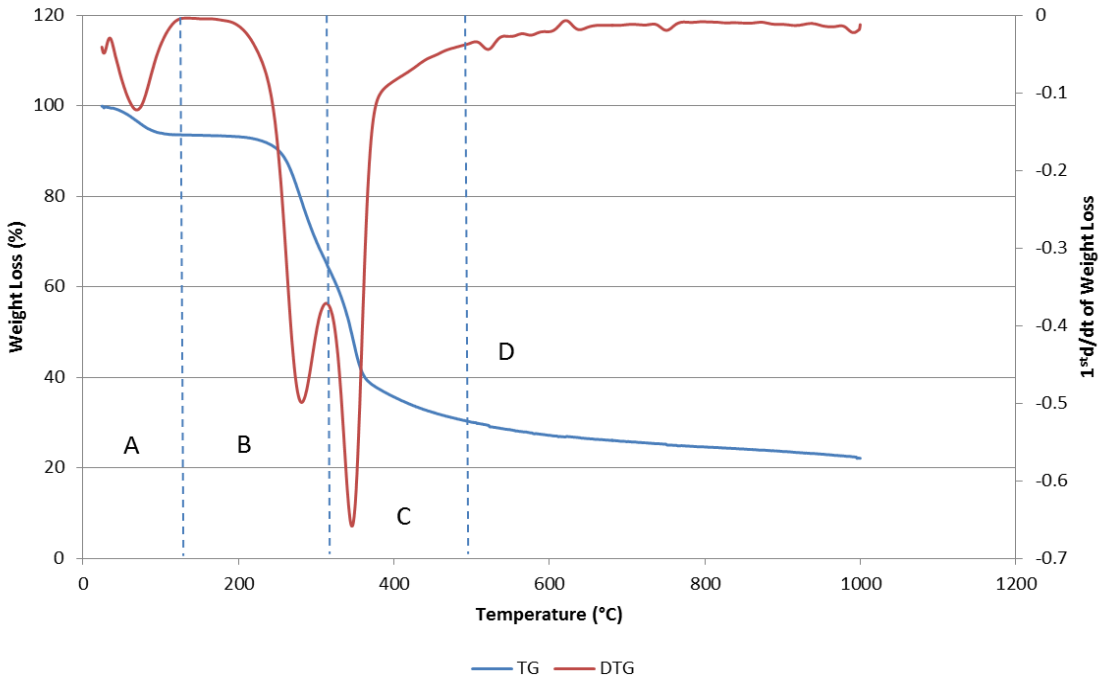


Figure 4-1 TG and DTG curves of coconut shell under N_2

It can be seen from the TGA plot (Figure 4-1) of coconut shell that 80 % of the total weight loss occurs between 250°C and 400°C, which may vary between 40% lignin to about 80% cellulose based on the evolution of H_2O, CO and volatile hydrocarbons from the fragmentation reaction of the polyaromatic components (Qian et al., 2004, Jain & Tripathi, 2014). It was reported by Cagnon (2004) that the coconut shell used in their study was composed of 35%wt. hemicellulose, 15%wt. cellulose and 50%wt lignin. Every valley on the DTG plot indicates a weight loss. It can be clearly observed from the DTG curve that there are three major weight loss stages occur during heating. As a result, the decomposition process of coconut shell can be divided into four regions associated with the effects described on the DTG and TG curves, which have been annotated as region A- D in Figure 4-1:

Region A, from room temperature to around 130°C, attributed to the removal of moisture content and hydrated compounds (Li et al., 2008, Cao et al., 2004).

The main pyrolysis took place between 250°C to 600°C. In this interval, two distinct peaks on the DTG curve can be seen clearly, which have been identified as Region B and Region C.

Region B, from approximately 200°C to 310°C with a peak in the DTG curve at around 280°C, indicates weight losses associated with the decomposition of the volatile constituents such as hemicelluloses and the partial breakdown of lignin (Orfão et al., 1999, Haykiri-Acma et al., 2010).

Region C, from 310°C to 400°C with the peak at around 345°C, represents mainly the lignin loss and cellulose loss, which can be regarded as the further degradation of hemicellulose (Gani & Naruse, 2007, Williams & Besler 1996, Cagnon et al., 2009). Since the lignin decomposition occurs at a wide range of temperature from 400°C to 600°C, the lignin loss happens in both Region C and Region D (Grønli et al., 1999, Orfão et al., 1999). According to Cagnon (2009), higher lignin content and higher char yield are obtained at the same time which means that in the present study lignin can be regarded as the main contributor to the final char yield.

In region D, at temperature above 500°C, the pyrolysis is essentially completed and further weight loss may be attributed to in-char structure rearrangement and the lignin decomposition with the occasional transformation of ash forming inorganics (San Miguel, 1999). According to Xie et al. (2009), the low decomposition rate of lignin can be attributed to its high level of aromaticity. No sharp decrease in weight was observed at later stages indicating that the inorganics have not melted or transformed dramatically at this heating rate (Haykiri-Acma et al., 2010). The DTG curve flattens and fluctuates very slightly to around the zero change value at around 600°C. It was confirmed by Cao et al. (2004) and Ning et al. (2006) that this temperature is suitable for carbonisation, given that the decomposition reactions are almost finished once this point has been reached.

Compared with the TG plots of the thermal analysis of several types of other woody biomass reported by Grønli et al. (2002), the thermal behaviour of coconut shell was found to match that of hard woods. This indicated that higher a lignin content can be expected compared with soft woods such as willow and redwood, which means that a higher carbon yield can be obtained from coconut shell char.

4.1.1.2 Proximate Analysis

The proximate analysis, determined according to the methodology described in Section 3.3.1.2 provides information on the compositions of the materials, such as moisture content, volatile matter content, ash content and fixed carbon content. Filled polymers, especially containing inorganic additives such as $Al(OH)_3$ and $CaCO_3$ for fire-retardant materials, are often estimated by the proximate analysis. During the decomposition process, several stages may appear on the plot. However, the residue at high temperature is always characteristic of the filler (Haines, 1995). Volatile matter components within the biomass can be liberated at a high temperature. High volatile content in biomass generally correlates to a high oil yield after thermal decomposition, while the char yield is related to the solid residue. Biomass typically consists of up to 80 – 90% of volatile content (including water content), and ash content ranging from 0.5 – 40% within rice husk and milfoil, respectively (Bakisgan et al., 2009; Demirbaş, 2004). The pyrolytic char contains two parts: fixed carbon (to become the carbon black substitute) and ash. By subtracting the percentage of moisture, volatile content and ash from the original mass of the biomass, the fixed carbon content can be determined.

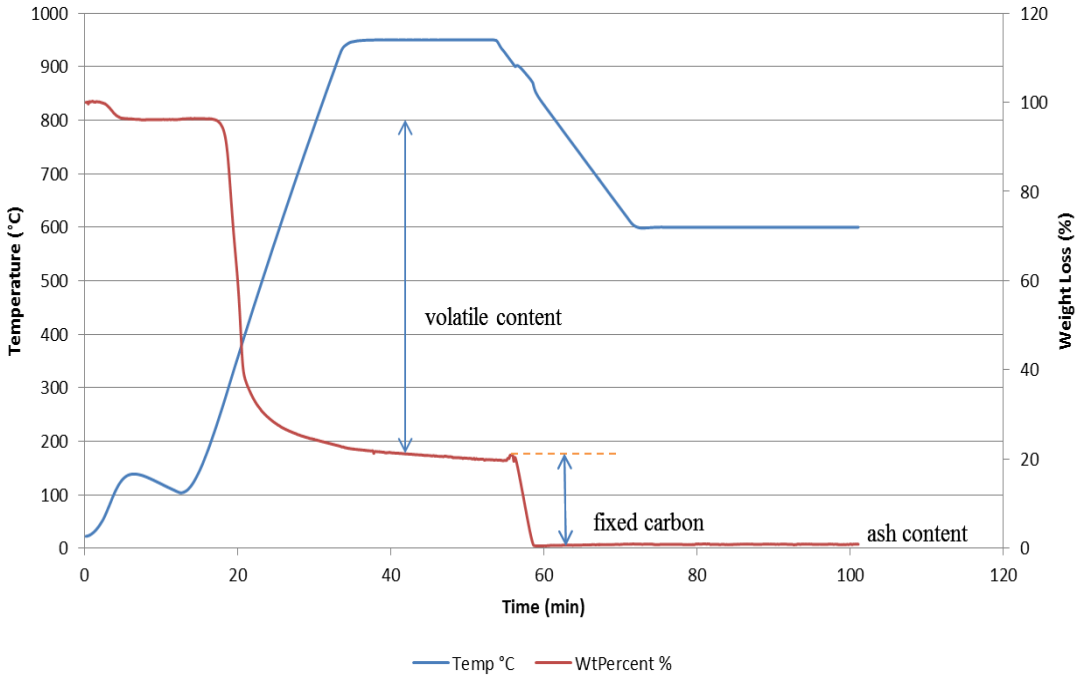


Figure 4-2 Proximate analysis of coconut shell

The proximate analysis result of coconut shell is shown in Figure 4-2. Similar thermal events to those in Figure 4-1 are evident. Between 20°C to 107°C the weight is lost due to removal of the 5% moisture content. As the temperature increased from 105°C to approximately 950°C, the loss of volatile matter content caused the sharp weight loss. About 75% of the coconut shell composition converts to volatile matter. In order to measure the fixed carbon ("potential carbon black"), the temperature is reduced to 600°C with the gas flow being switched to air. The remaining mass of material corresponds to the mineral ash content of the sample. The "potential carbon black" content within the coconut shell sample is around 20% of the total weight, whereas the ash content is only 0.2%. Given that commercial carbon black is made up by more than 95% of elemental carbon, this result was very encouraging as there is a high "potential carbon black" content and low ash content suggesting that coconut shell could be a suitable feedstock for a sustainable char filler.

4.2 Overview of Pyrolysis

The char yield, oil yield and gas yield from the pyrolysis process have been shown in Table 4-1. The data shown in Table 4-1 demonstrates that the char yield from coconut shells after pyrolysis ranges from 28.7 – 42.8 wt.%. This is a good yield and very encouraging in terms of the potential commercial opportunity for coconut shell to be used as a feedstock to produce a substitute carbon black. The oil yield from coconut shell pyrolysis was between 13.6 – 22.6 wt.%, which is beneficial, since the objective of this project is to produce char fillers, rather than oil. However, the gas yield is relatively high (38.0 – 57.7 wt.%). The implication of this high gas yield will be discussed later in Chapter 6.

Table 4-1 Char, oil and gas yield from pyrolysis

Run	Temperature (°C)	Heating rate (°C/min)	Holding time (min)	N_2 flow rate (ml/min)	Char yield (%)	Oil yield (%)	Gas yield (%)
1	800	5	180	1000	30.9	17.0	52.1
2	800	15	0	1000	29.2	14.4	56.4
3	600	10	90	550	31.5	15.8	52.7
4	400	15	0	100	39.4	14.4	46.2
5	800	5	0	100	30.3	22.6	47.1
6	600	5	90	550	32.6	20.5	46.9
7	400	15	180	1000	36.2	13.7	50.1
8	600	10	90	100	31.5	16.6	51.9
9	600	10	90	550	31.5	15.3	53.2
10	400	15	180	100	36.7	15.9	47.4
11	800	10	90	550	29.8	16.5	53.7
12	800	15	180	100	29.1	14.5	56.4
13	400	5	180	1000	38.7	15.4	45.9
14	800	5	180	100	30.7	20.7	48.6
15	800	15	180	1000	28.7	13.6	57.7
16	600	15	90	550	30.2	14.1	55.7
17	600	10	90	550	31.6	16.0	52.4
18	600	10	90	550	32.7	16.0	51.3
19	400	5	0	100	42.5	19.5	38.0
20	600	10	90	550	31.4	15.9	52.7
21	800	5	0	1000	31.3	16.6	52.1
22	600	10	0	550	31.6	16.4	52.0
23	600	10	90	1000	31.6	16.0	52.3
24	600	10	180	550	31.5	15.8	52.7
25	400	15	0	1000	39.9	14.2	45.9
26	600	10	90	550	31.6	16.7	51.7
27	400	5	0	1000	42.8	17.5	39.7
28	400	5	180	100	38.8	20.5	40.7
29	800	15	0	100	39.4	15.6	45.0
30	400	10	90	550	38.5	15.1	46.4

Perturbation plots have been constructed from the data presented in table 4-1 shown in Figure 4-3, where A represents pyrolysis temperature, B is heating rate, C is holding time and D is Nitrogen flow rate. The perturbation plot is applied to show the comparative effects of all independent pyrolysis factors on the char yield. The sharper the curvature of the variable, the more sensitive the response to the variable. The sharp curvature of the temperature indicates that the response (char yield) was very sensitive to temperature. For example, a high pyrolysis temperature mainly results in a low char yield. The comparatively flat heating rate, holding time and nitrogen flow rate curves presents a result of less sensitivity of char yield towards these variables. For example, Run27 with the highest char yield was produced at a lower temperature (400˚C) and zero dwell time. The reason for this observation was due to incomplete pyrolysis of the coconut shell. The other parameters have little impact upon char yield.

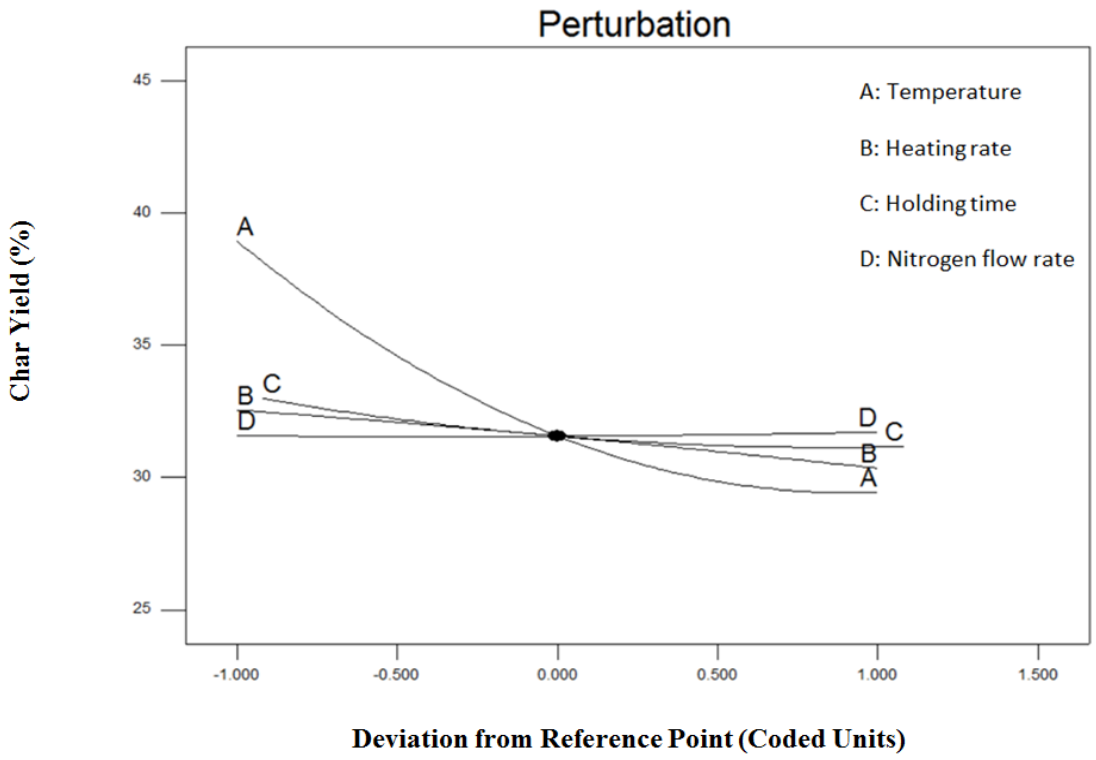


Figure 4-3 Perturbation plots with four pyrolysis parameters on char yield

4.3 Characteristics of Commercial Carbon Blacks and Char Fillers

Table 4-2 summarises the transmittance of toluene extract (T%), pH value, BET surface area, T-plot surface area and acidic groups and basic groups on the surface of both commercial

carbon blacks tested in this research, plus the coconut char fillers produced under the RSM procedure. The detailed results for the coconut char is presented in the RSM analysis in Table 4-3.

Toluene is a non-polar solvent, meaning that the leachable and unburned tarry or oil-residues on the surface of carbon black or the char can be dissolved into it. Thus, this is toluene transmittance correlates to the amount of tarry or leachable contents in the carbon black. This is very important for potential applications, since the presence of a high leachable (oily) content may cause contamination during processing into rubber or other applications and present problems in the appearance and performance of the final rubber products. As can be seen from Table 4-2, the toluene transmittance of N772 is 65.9%, which indicates that a significant amount of leachable components exist within N772. Although the result is acceptable, this has a limiting effect on the purposes to which N772 can be applied. In comparison, the T% of the N330 is much higher than N772, with a value of 99.5% which is typical of a high-grade carbon black which has little surface contamination. According to the data for the coconut chars in this study, it can be seen that all of the char samples have toluene transmittance values similar to N330 indicating that they are free from tarry residues and based upon this metric are comparable with high quality carbon black.

It is widely known that the T-plot surface area refers to the area of the meso and macro pores on the surface of absorbent (Do, 1998). Pores within solids are classified into three size ranges: Micropores (<2nm width) Mesopores (<2nm - <50nm with) and Macropores (>50nm width). Normally, if the pores (micropores and small mesopores) are significantly smaller than the very large (normally macro-pore size) rubber polymer chains, then the polymer molecules cannot access these pores. Therefore, the presence of many small pores may increase the surface area of the material, but not benefit the ability of the polymer to enter the carbon pores and in-turn not improve the reinforcement ability of the char. As a result, unlike micro-pores present in activated carbon, meso and macro pores may play the decisive role on the filler surface. From Table 4-2, the whole surface area (area of all pores) of N772 and N330 are 28.5 m^2/g and 71.5 m^2/g respectively, while the area of meso & macro pores is 26.6 m^2/g and 69.7 m^2/g.

Table 4-2 Characterization of carbon black and char filler

Run	T%	pH value	BET surface area (m^2/g)	t-plot surface area(m^2/g)	Acidic groups (mmol/g)	Basic groups (mmol/g)
1	99.43	5.52	7.76	7.05	1.278	0.168
2	99.77	9.78	304.89	141.57	0.008	0.430
3	99.90	9.94	301.89	118.82	0.170	0.210
4	100	8.97	205.83	130.27	0.265	0.258
5	99.91	9.74	323.14	118.76	0	0.457
6	99.93	9.67	247.43	202.80	0.003	0.329
7	99.57	6.22	ND*	ND	1.200	0.168
8	99.95	9.75	291.65	157.87	0	0.303
9	100	9.65	313.13	135.67	0.188	0.263
10	100	6.15	5.96	5.64	1.123	0.133
11	100	9.56	316.02	125.46	0.132	0.318
12	99.95	9.93	118.47	57.91	0	0.533
13	99.5	6.05	6.18	4.14	0.933	0.160
14	99.67	9.86	90.60	114.46	0	0.082
15	99.98	9.69	ND	ND	0	0.482
16	99.91	9.67	188.79	87.88	0	0.486
17	99.85	9.72	276.14	143.16	0	0.347
18	100	9.56	301.89	168.22	0.170	0.210
19	99.94	9.82	351.67	292.24	0.049	0.354
20	99.95	9.70	373.31	315.86	0.062	0.316
21	99.34	5.39	ND	ND	1.417	0.133
22	99.91	9.74	203.41	222.51	0.050	0.442
23	99.16	5.25	1.66	0.93	1.249	0.163
24	99.97	9.72	356.28	295.99	0.067	0.332
25	99.96	9.82	346.35	318.16	0	0.440
26	99.79	9.81	227.16	187.74	0.033	0.486
27	99.30	5.49	3.51	4.02	1.233	0.135
28	99.89	5.95	13.08	7.72	1.065	0.120
29	100	9.67	310.27	91.08	0	0.417
30	99.58	5.77	4.94	2.94	1.203	0.205
Coconut char filler	99.1 – 99.9	5.3 – 9.9	4.9 – 346.3	2.9 – 318.2	0 – 0.417	0.120 – 0.533
N772	65.9	8.5	28.5	26.6	0	0.079
N330	99.5	8.9	71.5	69.7	0.81	0.08

*ND = No data

The results indicate that meso and macro pores occupied most of the surface area of carbon black, which reaffirms previous statements about the importance of these pores in carbon black's application in the rubber industry. The surface area data of the coconut char samples follow the same trend as the commercial carbon blacks, although the surface areas are much greater for some of the samples. This data further supports the assertion that char samples can be used as an alternative rubber filler. For example, sample Run 20 and Run 21, which were produced from different conditions. The BET surface area for Run 20 and Run 21 are 373.31m^2/g and 346.35m^2/g, whereas the t-plot surface area are 315.86m^2/g and 318.16m^2/g respectively. It can be asserted from this result that the meso-pores contribute the majority of the surface area of the char samples.

Another important property of the filler is the surface pH value. It has been recognized that basic materials may accelerate vulcanization reactions whilst acidic ones may delay the vulcanization time of a rubber compound (ASTM, 2012; Boehm, 1994). Further, there is a correlation between the extent of free radicals of oxygen (hydrogen and hydroxyl etc.) on the surface of carbon black and the pH value. Free radicals can be helpful in the bonding process between rubber and fillers (Eirich et al., 1994). According to the above, a solution pH value close to 9 makes N772 and N330 better fillers for a wide range of application due to the reasonable vulcanization time and ideal amount of free radicals. It also can be implied that this higher pH value is generally beneficial towards the performance for all commercial carbon blacks and hence substitute carbon-based fillers too when applied within a rubber matrix. The pH value of many of the char samples was close to 9, which also supports the proposition that coconut shell could be a promising feedstock for rubber fillers. High numbers of surface group may make the carbon surface more active when mixing with the rubber matrix. The surface chemical groups on the surface of char filler are much more plentiful than the commercial carbon black, which may lead to a better interaction and hence reinforcement from coconut shell char.

4.4 RSM Process Optimization

The optimization in this research was conducted by using the pH value and t-plot surface area as response metrics.

4.4.1 Char Filler pH Value Response Analysis

4.4.1.1 Statistical Analysis

After completion of the 30 RSM experiments, the next stage was to produce a prediction model to assess the interaction among the design experimental variables and then optimize the pyrolysis process which would determine the local optimum design factors for the selected pH value of 9 and largest t-plot surface area.

The quadratic polynomial model has been chosen in this research for estimating the response surface of pH value, which is given in the equation:

$$Y_1 = \beta_0 + \sum_{i=1}^{4} \beta_i x_i + \sum_{i=1}^{3} \sum_{j=i+1}^{4} \beta_{ij} x_i x_j + \sum_{i=1}^{4} \beta_{ii} x_i^2$$

Where Y_1 is the pH value of char filler, β_0 is the value of the fixed response at the center point of the design, β_i, β_{ij}, and β_{ii} are the linear, interactive, and quadratic coefficients, respectively. x_i and x_j are the independent design variables.

4.4.1.2 Optimization of Pyrolysis Process on pH Value and Interaction between Independent Variables

The statistical design factors in both code and actual value as well as the experimental response and predicted values on pH value of char filler are all summarized in Table 4-3.

Table 4-3 Experimental design matrix with experimental and predicted values

Run	Temperature		Heating rate		Holding time		N2 flow rate		pH value		t-plot surface area	
	˚C		˚C/min		min		ml/min				m^2/g	
	X_1		X_2		X_3		X_4		Y_1		Y_2	
	Coded value	Actual value	Coded value	Actual value	Coded value	Actual value	Coded value	Actual value	Experimental data	Predicted data	Experimental data	Predicted data
1	-1	400	1	15	-1	0	-1	100	5.52	5.37	7.05	21.70
2	1	800	1	15	-1	0	1	1000	9.78	9.68	141.57	152.80
3	0	600	0	10	0	90	0	550	9.94	9.66	118.82	184.51
4	0	600	0	10	-1	0	0	550	8.97	9.13	130.27	136.82
5	1	800	-1	5	-1	0	-1	100	9.74	9.71	118.76	134.52
6	0	600	-1	5	0	90	0	550	9.67	9.73	202.80	265.04
7	-1	400	1	15	1	180	1	1000	6.22	6.18	ND*	ND
8	0	600	0	10	0	90	-1	100	9.75	9.84	157.87	195.39
9	0	600	0	10	0	90	0	550	9.65	9.66	135.67	184.51
10	-1	400	1	15	1	180	-1	100	6.15	6.21	5.64	41.50
11	0	600	0	10	1	180	0	550	9.56	9.53	125.46	106.38
12	1	800	1	15	1	180	-1	100	9.93	9.90	57.91	31.86
13	-1	400	-1	5	1	180	1	1000	6.05	6.04	4.14	17.82
14	1	800	-1	5	1	180	-1	100	9.86	9.80	114.46	105.08
15	1	800	1	15	1	180	1	1000	9.69	9.75	ND	ND

Table 4-3 Experimental design matrix with experimental and predicted values (continued)

16	1	800	0	10	0	90	0	550	9.67	9.80	87.876	101.37
17	0	600	0	10	0	90	0	550	9.72	9.66	143.16	184.51
18	0	600	0	10	0	90	0	550	9.56	9.66	168.22	184.51
19	0	600	0	10	0	90	1	1000	9.82	9.86	292.24	242.19
20	0	600	0	10	0	90	0	550	9.70	9.66	315.86	184.51
21	-1	400	1	15	-1	0	1	1000	5.39	5.46	ND	ND
22	1	800	-1	5	1	180	1	1000	9.74	9.75	222.51	206.30
23	-1	400	-1	5	-1	0	-1	100	5.25	5.25	0.93	0
24	0	600	1	15	0	90	0	550	9.72	9.79	295.99	221.24
25	1	800	-1	5	-1	0	1	1000	9.82	9.78	318.16	286.98
26	0	600	0	10	0	90	0	550	9.81	9.66	187.74	184.51
27	-1	400	-1	5	-1	0	1	1000	5.49	5.43	4.02	28.46
28	-1	400	-1	5	1	180	-1	100	5.95	5.98	7.72	-5.08
29	1	800	1	15	-1	0	-1	100	9.67	9.70	91.08	82.10
30	-1	400	0	10	0	90	0	550	5.77	5.78	2.94	0

*ND = No data

The regression equation characterizing the influence of different considered variables on pH value was concluded to be:

$$Y_1 = 9.66 + 2.01X_1 + 0.033X_2 + 0.20X_3 + 0.01X_4 - 0.033X_1X_2 - 0.16X_1X_3 - 0.028X_1X_4 + 0.027X_2X_3 - 0.024X_2X_4 - 0.031X_3X_4 - 1.87X_1^2 + 0.1X_2^2 - 0.33X_3^2 + 0.19X_4^2$$

Equation 1

Within this equation, a positive sign in front of the terms indicate a synergetic effect, whereas a negative sign indicates an antagonistic effect. Using the Pareto chart in Figure 4-4, the main and interaction effects of all the parameters to the response pH value can be interpreted more easily. According to the plot, the effect of pyrolysis temperature, the holding time and the quadratic effect of N_2 flow rate have highly significant positive influences on the char filler pH value. This means that with increasing pyrolysis temperature and holding time, the pH value increases. The N_2 flow rate has a relatively low significant positive effect on pH value.

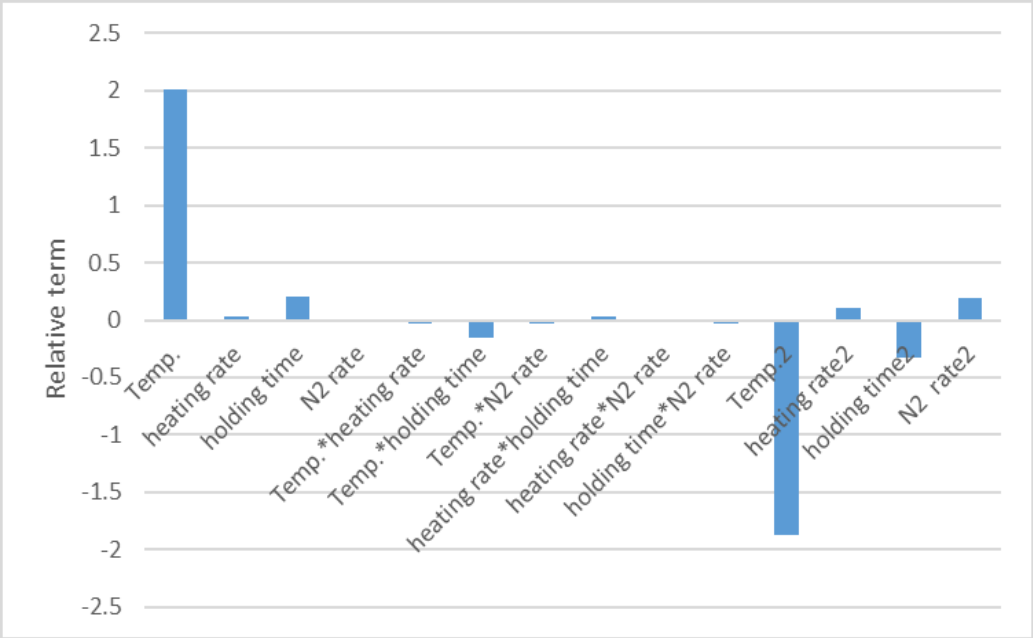


Figure 4-4 Pareto chart showing the effects of different independent variable on pH value

4.4.1.3 Statistical Analysis and Validation of Model

The validation of the fitted model was estimated and its statistical significance was determined by an F-test, which is an essential part of Analysis of Variance (ANOVA). It is often used to determine the fitness of the statistical model to the sampled data through

comparing if two populations having normal distribution have the same variances or standard deviation (Reviews, 2016). The Analysis of variance (ANOVA) for the response surface full quadratic model is presented in Table 4-4.

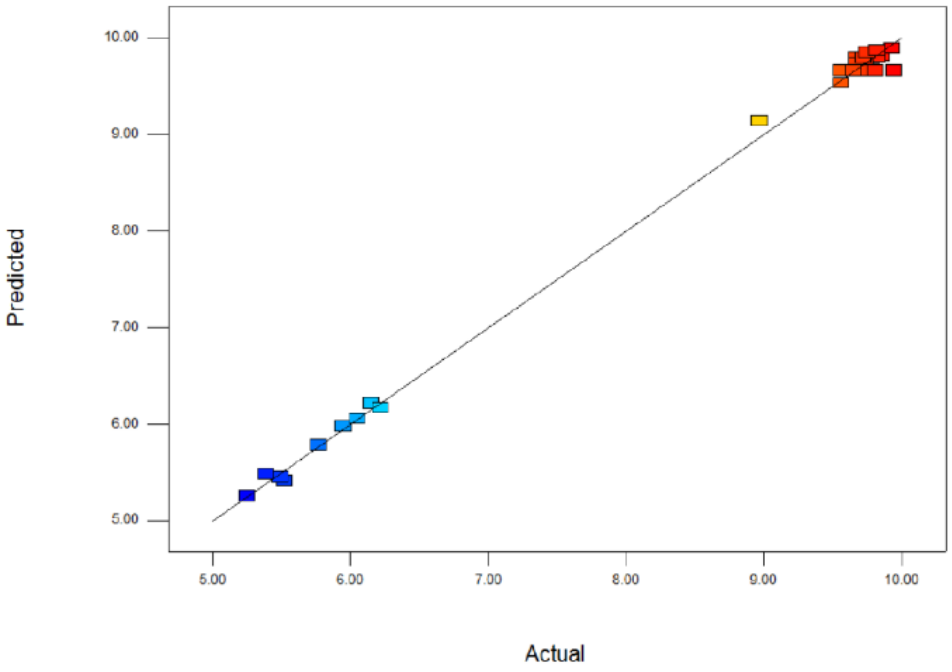
Table 4-4 Analysis of variance of the fitted quadratic regression model

Source	Sum of Squares	Mean Square	F-value	P-value	Remarks
Model	99.79	7.13	460.92	< 0.0001	significant
Residual	0.23	0.015	-	-	-
Lack of Fit	0.15	0.015	0.84	0.6227	not significant
Pure Error	0.087	0.017	-	-	-

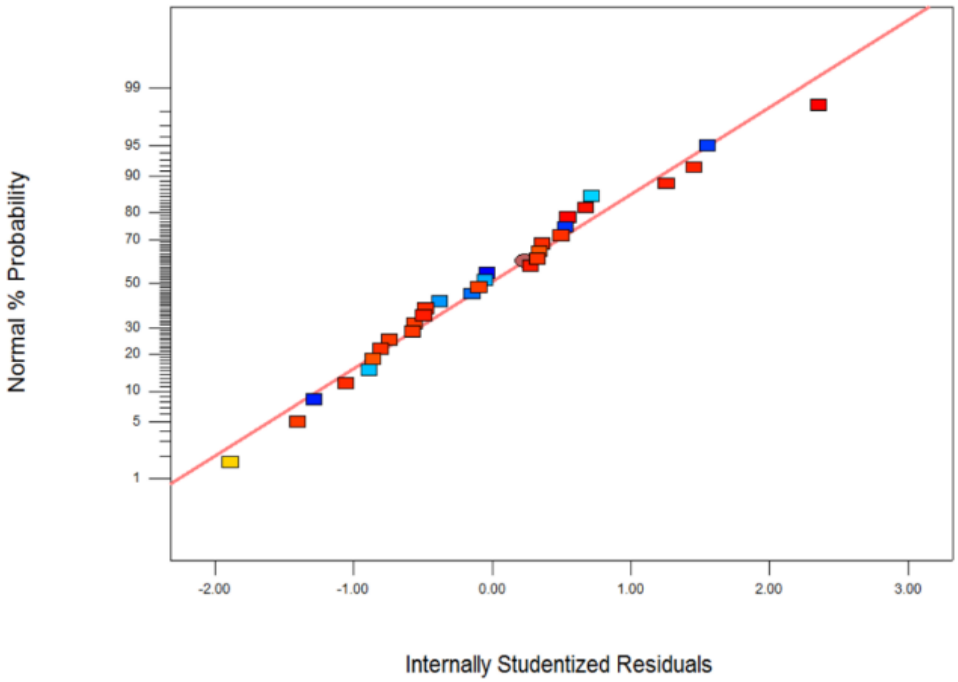
It can be seen that the model (see Equation 1 above) is highly statistically significant at 95% confidence level, with an F-value of 460.92, and very low probability P value of <0.0001. The values of the determination coefficients R^2 and R^2_{adj}, which measure the model fitting reliability, were calculated to be 0.9977 and 0.9955, respectively. This indicates that about 99.77% of the variance is attributed to the variables and suggests a high significance of the model. Therefore, only 0.0023 of the total variations is not fit for the model which ensures good alignment of the model with the experimental data. Confirmation of the adequacy of the regression model can also be assured by the good agreement between the experimental and predicted values of response pH value as shown in Table 4-3. The actual char pH value ranged from 5.25 to 9.94, while its corresponding predicted values are between 5.25 and 9.90. The difference between the level of the desired signal and the level of the background noise can be determined by the noise ratio. The large noise ratio indicates significant difference between the sample mean and the model value. It is reported that a noise ratio greater than 4 is desirable, which indicates that the difference is more than 4 times the size of the standard error (Frost, 2016). The ratio of 52.742 in this analysis implies an adequate signal and also indicated that this model is reliable and can be used to guide the design process. The lack of fit test is determined by comparing the viability of the current model residuals to the variability between observations at replicate setting of the factors. The lack of fit F-value of 0.84 implies this is not significant relative to the pure error. There is a 62.27% chance that a

lack of fit F-value this large could occur due to noise. Non-significant lack of fit is good, which suggests that all the systematic variations have been accounted for in the hypothesized model (El-Gendy et al., 2013).

The relationship between predicted and experimental values of the pH value of char fillers is presented in Figure 4-5(a). It is obvious that the correlation between the predicted and experimental values is high, indicating that the predicted and experimental values were of reasonable agreement. The data fits well using the model and a powerful estimate of response for the system with the experimental range can be achieved. The normal probability plot of the standardized residuals for pH value is shown in Figure 4-5(b). If the residuals follow a normal distribution, the points will show a straight line in the normal probability plot. Given that some scattering may occur even with the normal data, as can be seen in Figure 4-5(b), it can be assumed that the data is a normal distribution. As a result, a good validity for the approximation of the quadratic regression model can be assumed by the obtained normal probability plot.



(a)

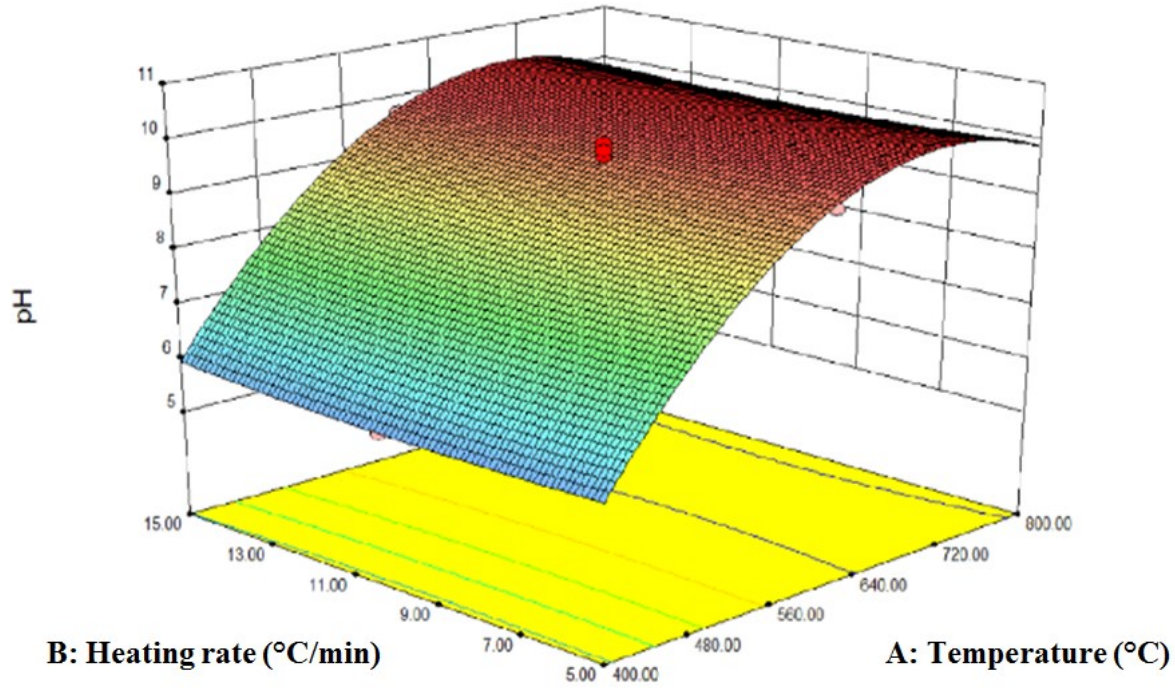


(b)

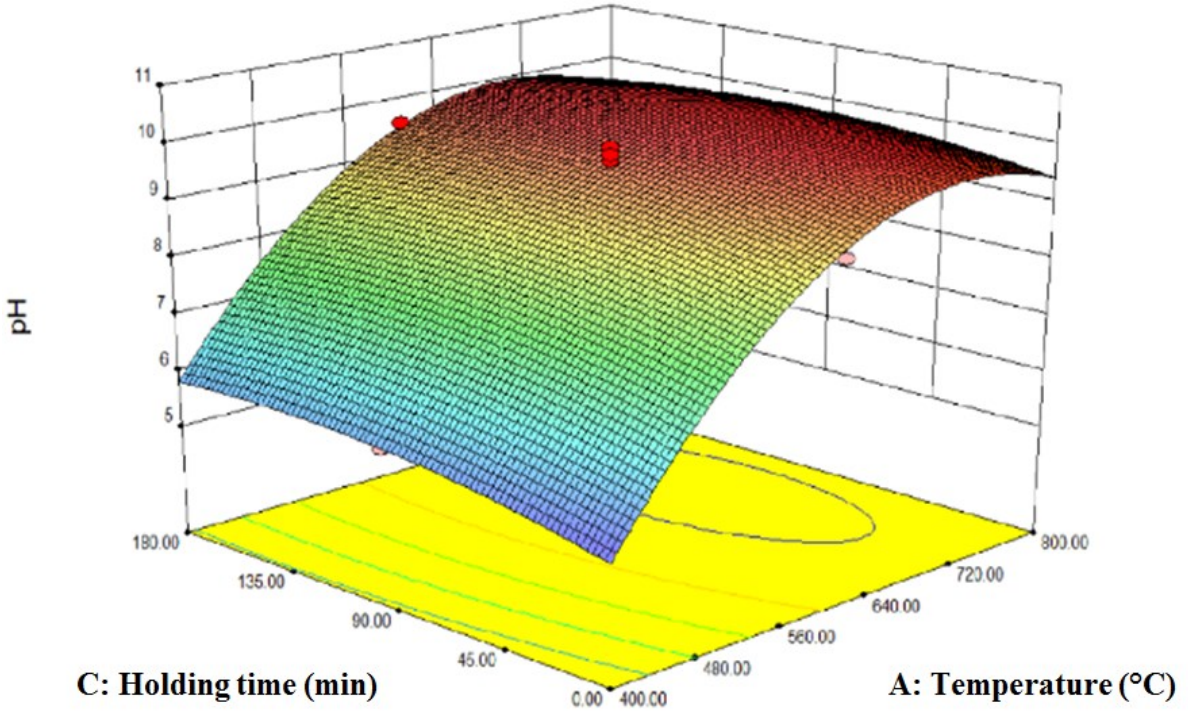
Figure 4-5 (a) Experimental values and predicted values for the model & (b) Normal probability plot of the residues

4.4.1.4 Interaction among Parameters Influencing Pyrolysis Process and pH Value

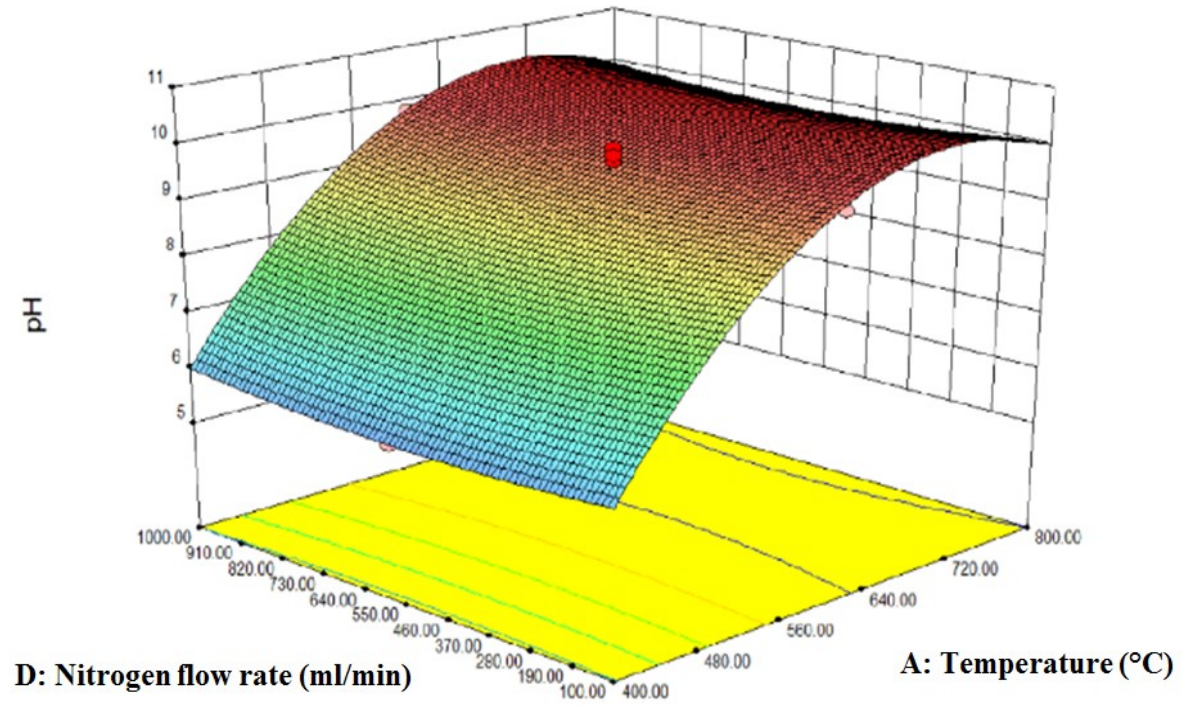
The empirical predicted quadratic model for response pH value in terms of process variables (temperature, heating rate, holding time and nitrogen flow rate) have been plotted in three-dimensional diagrams, shown in Figure 4-6. The red points represent the extreme value on each edge and the centre point. This enables the study of the interaction among the variables and to determine the optimum condition of each factor for optimum pH value. In this research the optimum pH value is selected as 9, which was discussed earlier (Section 4.3), and is considered to be a favorable pH value for the commercial reinforcing carbon blacks and the coconut shell chars. Figure 4-6(a) shows the interactive effect of temperature and heating rate on pH value at constant initial holding time of 90.00min and nitrogen flow rate at 550ml/min. It is clearly shown that with the increase of pyrolysis temperature above ≈720°C, the pH value increases. Figure 4-6(b) represents the effects of varying temperature and holding time on pH value at a constant heating rate of 10°C and nitrogen flow rate at 550ml/min. It is obvious that the initial temperature has a more powerful effect than holding time. However, an increase in pH value occurred with an increase in holding time over the temperature range from 400 to 720°C. Further increases in initial temperature did decrease the pH value.


pH
11
10
9
8
7
6
5
15.00
13.00
11.00
9.00
7.00
5.00
B: Heating rate (°C/min)
400.00
480.00
560.00
640.00
720.00
800.00
A: Temperature (°C)

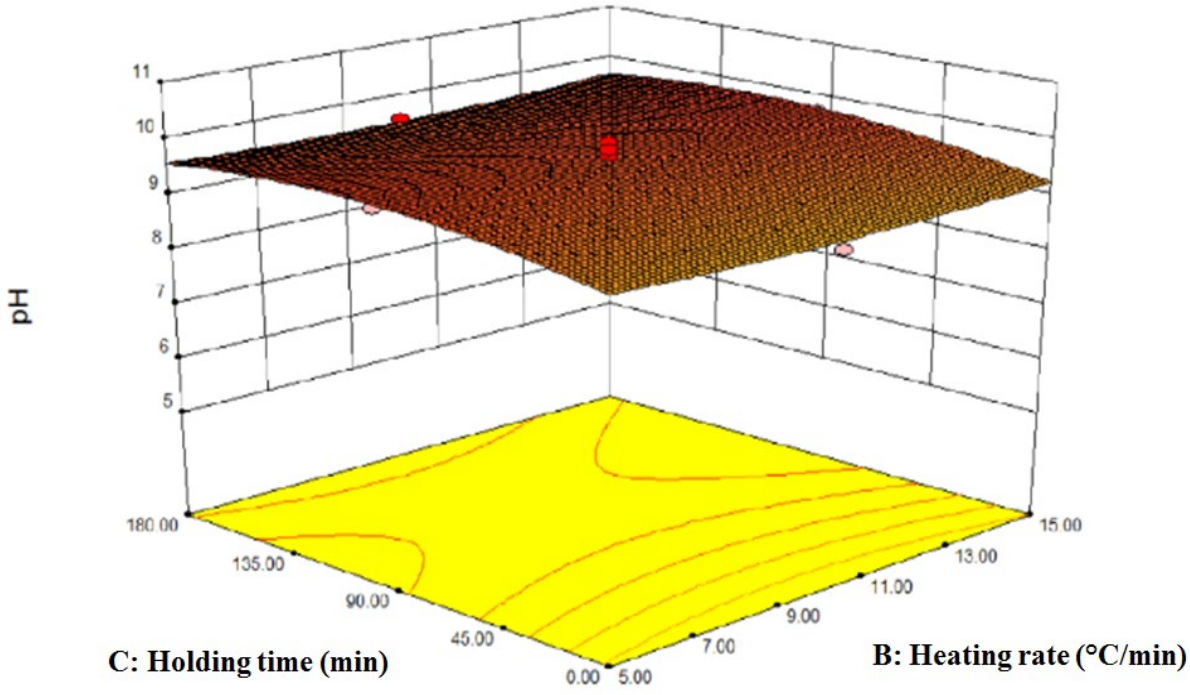
(a)


pH
11
10
9
8
7
6
5
180.00
135.00
90.00
45.00
0.00
C: Holding time (min)
400.00
480.00
560.00
640.00
720.00
800.00
A: Temperature (°C)

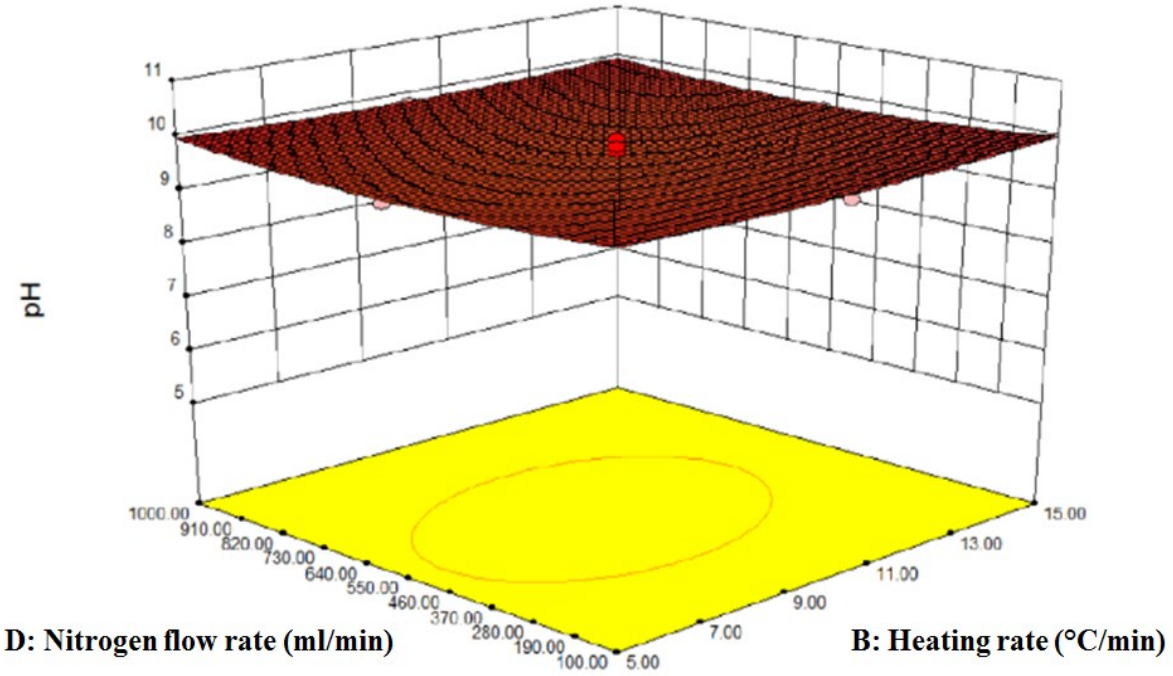
(b)


pH
11
10
9
8
7
6
5
1000.00
910.00
820.00
730.00
640.00
550.00
460.00
370.00
280.00
190.00
100.00
D: Nitrogen flow rate (ml/min)
400.00
480.00
560.00
640.00
720.00
800.00
A: Temperature (°C)

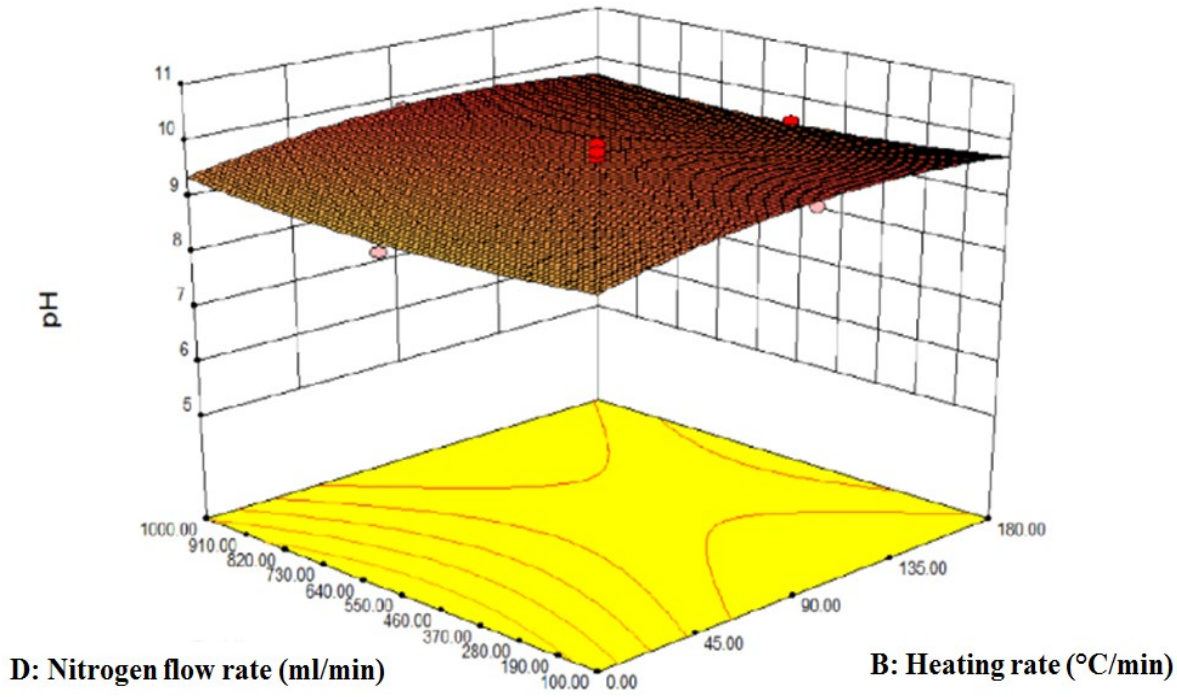
(c)


pH
11
10
9
8
7
6
5
180.00
135.00
90.00
45.00
0.00
C: Holding time (min)
5.00
7.00
9.00
11.00
13.00
15.00
B: Heating rate (°C/min)

(d)



(e)



(f)

Figure 4-6 (a-f) Response surface plots of pH value, illustrating the interaction between two variables: selected for temperature, heating rate, holding time and nitrogen flow rate

Figure 4-6(c) shows the effect of both nitrogen flow rate and temperature on pH value at a constant initial heating rate of 10°C/min and a holding time of 90min. A significant positive impact is detectable; that is, the pH value increased with the increase of temperature below 720°C. Nevertheless, with the increase of nitrogen flow rate below 550 ml/min, the pH value decreased. Then, after 550ml/min, the pH value increased with increasing nitrogen flow rate.

Figure 4-6(d), (e), (f) show the interactive effect of heating rate and holding time, heating rate and nitrogen flow rate and holding time and nitrogen flow rate. According to the plot, the effects on the three groups of factor are not as obvious (insignificant) compared to the groups with temperature.

4.4.1.5 Optimization of Pyrolysis Process based on pH Value and Model Verification

The optimization process was carried out to determine the optimum value of pH value, using the Design Expert 8.0 software. According to the software optimization step, the desired goal for each operational condition (X_1 temperature, X_2 heating rate, X_3 holding time, and X_4 nitrogen flow rate) was chosen "within" the studied range. The response (pH value) was defined as 9, to achieve the highest performance. The program combines the individual desirability into a single number and then searches to optimize this function based on the response goal. Accordingly, the optimum working conditions and respective pH value were established, and the results are presented in Table 4-5. An additional experiment was then performed to confirm the optimum results. As shown, the optimum pH value of 9 can be achieved at a temperature of 550°C, 6.5°C/min heating rate, 85min holding time, and 585ml/min nitrogen flow rate. The desirability function value was found to be 1.000 for these optimum conditions. The laboratory experiment agrees well with the predicted response value 8.97, with the standard deviation 0.0924 for validation of experiments. This indicates that process optimization by CCFD was suitable and reliable to optimize pH value from the coconut shell pyrolysis process.

Table 4-5 Optimum condition solution for optimum pH value

Number of trials	Temperature (°C)	Heating rate (°C/min)	Holding time (min)	N_2 flow rate (ml/min)	pH value	Desirability
1	546.45	6.46	83.26	585.27	9.0	1.000
2	546.11	11.21	89.81	562.70	9.0	1.000
3	540.69	5.44	172.21	881.70	9.0	1.000
4	560.77	6.40	7.31	988.80	9.0	1.000
5	542.57	5.47	171.99	221.34	9.0	1.000

4.4.2 Char Filler t-plot Surface Area Response Analysis

4.4.2.1 Statistical Analysis

The quadratic polynomial equation previously presented, was used to fit the response surface of the t-plot surface area of char samples. The only difference being that Y_1 was substituted for Y_2, which is the t-plot surface area of char filler.

4.4.2.2 Optimization of Pyrolysis Process on t-plot Surface Area and Interaction between Independent Variables

Based on CCFD analysis and experimental results, the statistical combinations of variables in coded and actual along with the predicted and experimental response focusing on t-plot surface area are presented in Table 4-3.

The regression equation for t-plot surface area of char samples characterizing the influence of different considered variables on surface area can be concluded as:

$$Y_2 = 184.51 + 62.22X_1 - 21.90X_2 - 15.22X_3 + 23.40X_4 - 29.95X_1X_2 - 17.51X_1X_3 + 19.58X_1X_4 - 5.20X_2X_3 - 20.44X_2X_4 - 12.81X_3X_4 - 145.36X_1^2 + 58.63X_2^2 - 62.91X_3^2 + 34.28X_4^2$$

Equation 2

The Pareto chart, shown in Figure 4-7, was used to investigate the main and interaction effects of all factors to the response t-plot surface area. Within the studied range of experiments, the effect of pyrolysis temperature and the quadratic effect of heating rate have a highly significant positive influence upon the char filler t-plot surface area. That is, with increments of pyrolysis temperature, the t-plot surface area value increases. While the quadratic effect of temperature and holding time have a highly significant inverse effect upon the t-plot surface area values.

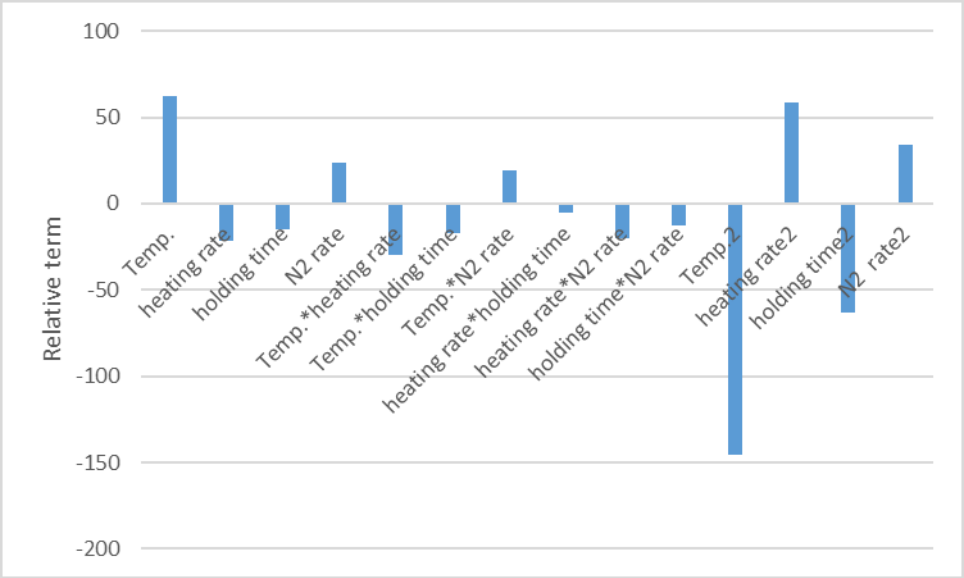


Figure 4-7 Pareto chart showing the effects of different independent variable on pH value

4.4.2.3 Statistical Analysis and Validation of the Model

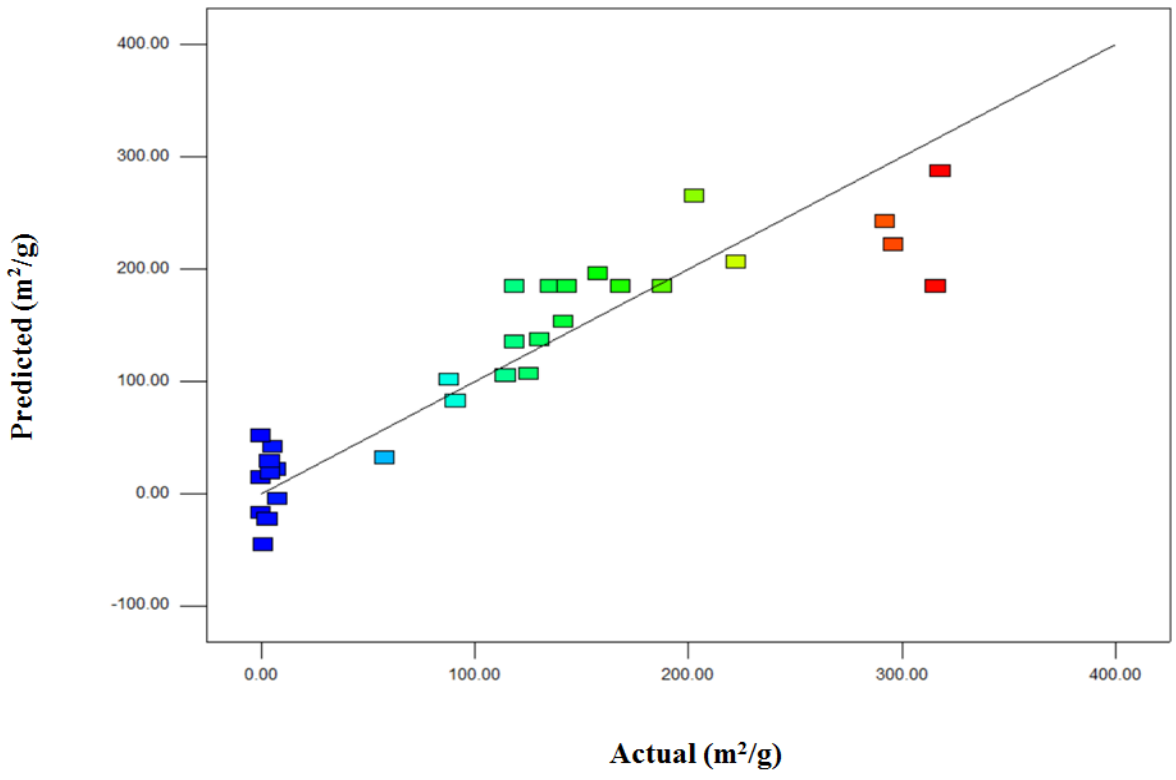
Table 4-6 shows the analysis of variance (ANOVA) for the response surface full quadratic model (see Equation 2 above). The model F-value is 5.40 with values of "Prob > F" less than 0.0500, which implies that model terms are significant. The R^2 and R^2_{adj} were calculated to be 0.8345 and 0.6800, respectively. This suggests that approximately 83.45% of the variance is attributed to the variables and indicated a high significance of the model. Confirmation of the adequacy of the regression model was reflected also by the good agreement between experimental and predicted values of response variables as shown in Table 6; the actual t-plot surface area values ranged from 0 to 318.16 and the corresponding predicted values were between 0 and 322.78m^2/g, respectively. The noise ratio is 8.085, greater than 4, indicating

that this model is reliable and can be used for further optimization. The "Lack of Fit F-value" of 0.49 implies the “Lack of Fit” is not significant relative to the pure error.

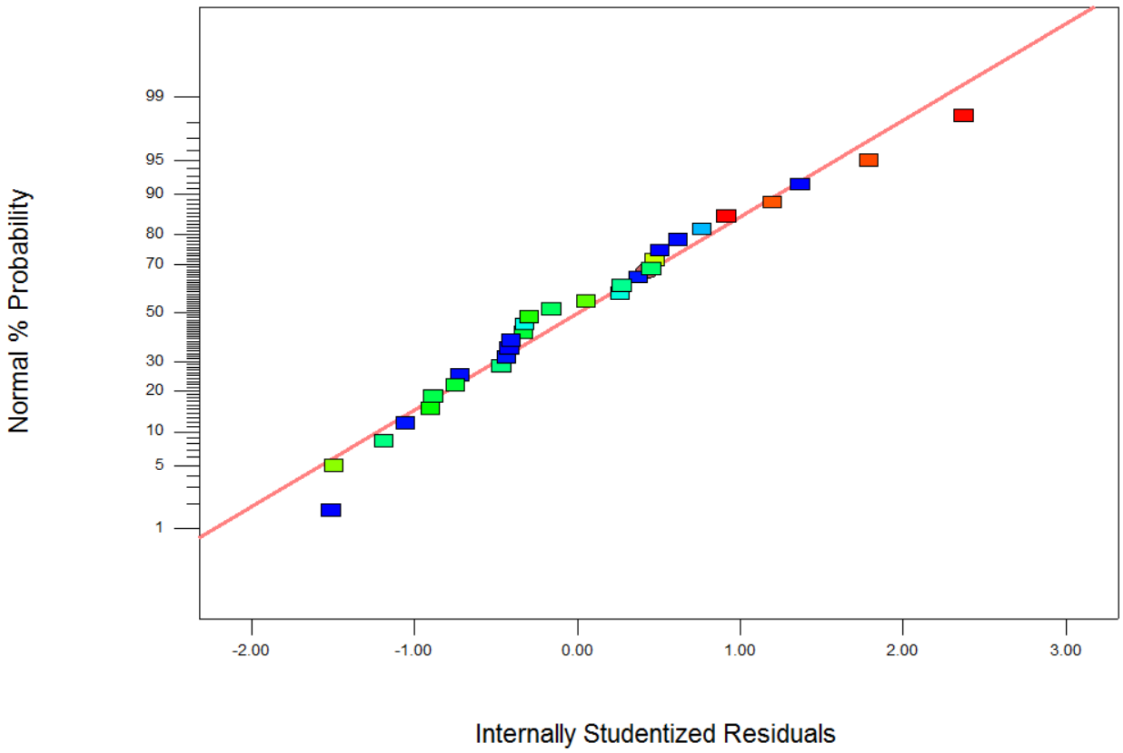
Table 4-6 Analysis of variance of the fitted quadratic regression model

Source	Sum of squares	Mean squares	F-value	p-value	Remarks
Model	2.561E+05	18290.61	5.40	0.0012	significant
Residual	50791.21	3386.08	-	-	-
Lack of Fit	25087.68	2508.77	0.49	0.8435	not significant
Pure Error	25703.52	5140.70	-	-	-

The relationship between predicted and experimental values of t-plot surface area can be seen from Figure 4-8(a). A reasonable agreement between the predicted and experimental values can be confirmed by the high correlation. The normal probability plots of the standardized residuals for t-plot surface area analysis is shown in Figure 4-8(b). The data is normally distributed indicating that a good validity for the approximation of the quadratic regression model.



(a)

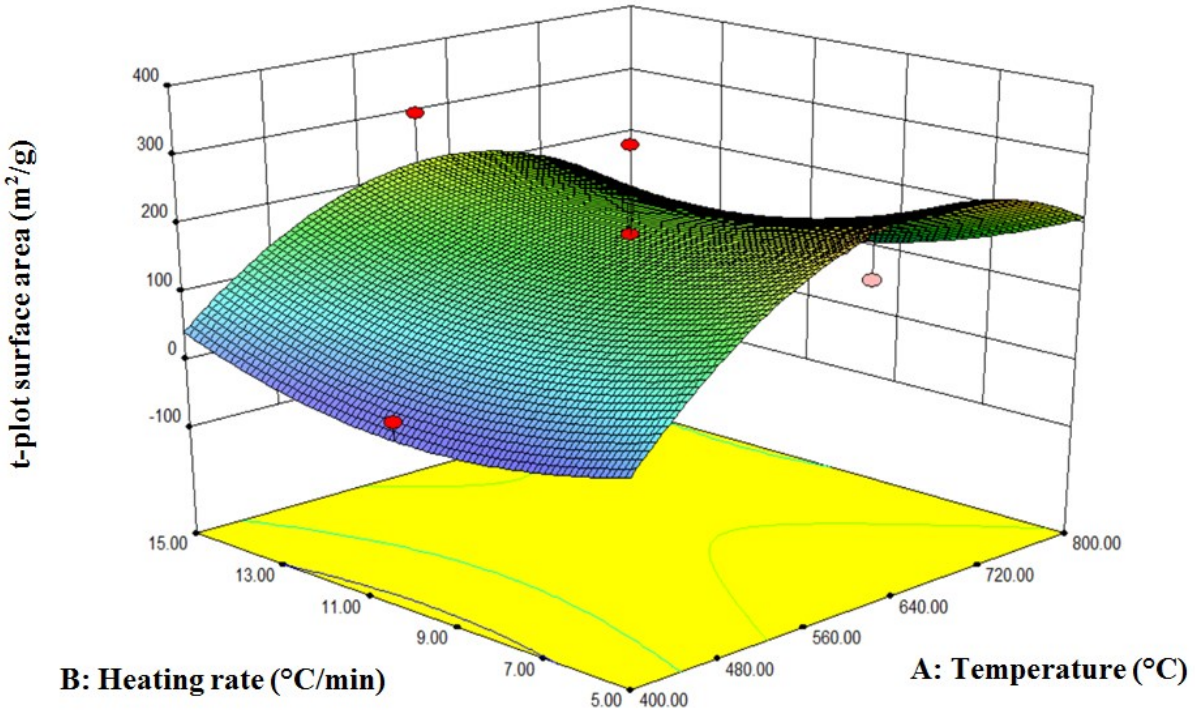


(b)

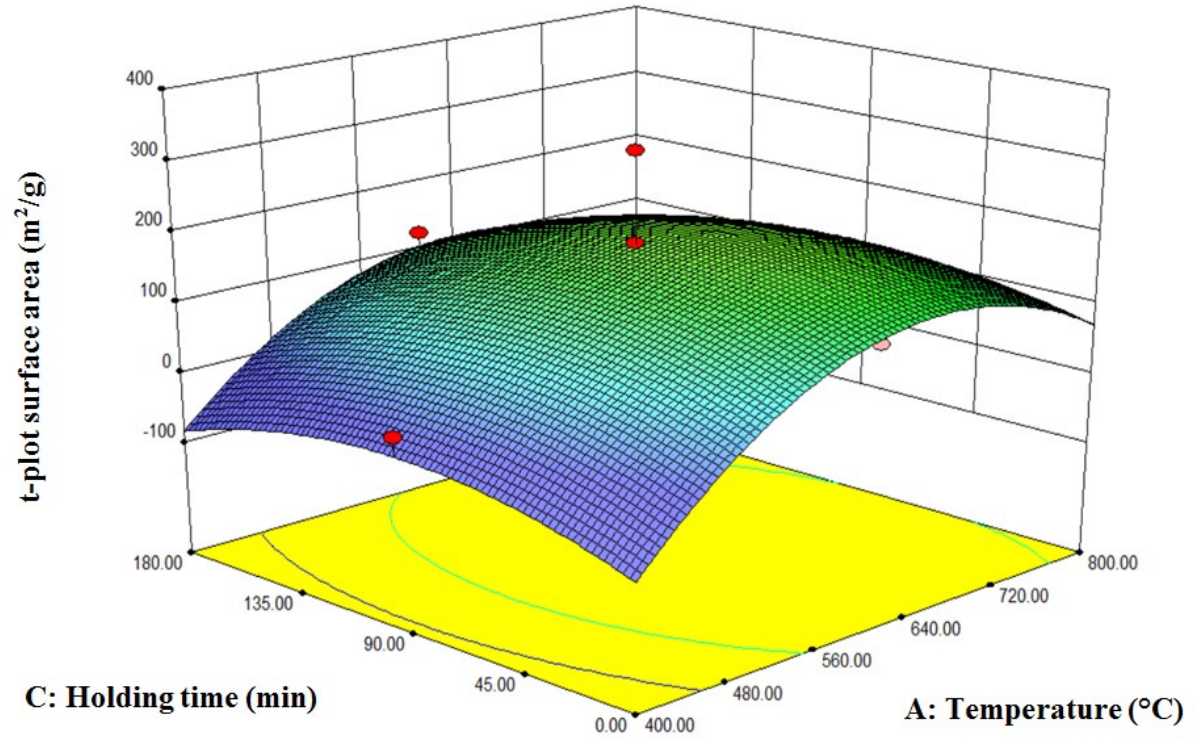
Figure 4-8 (a) Experimental values and predicted values for the model & (b) Normal probability plot of the residuals

4.4.2.4 Interaction among Parameters Influencing Pyrolysis Process and t-plot Surface Area

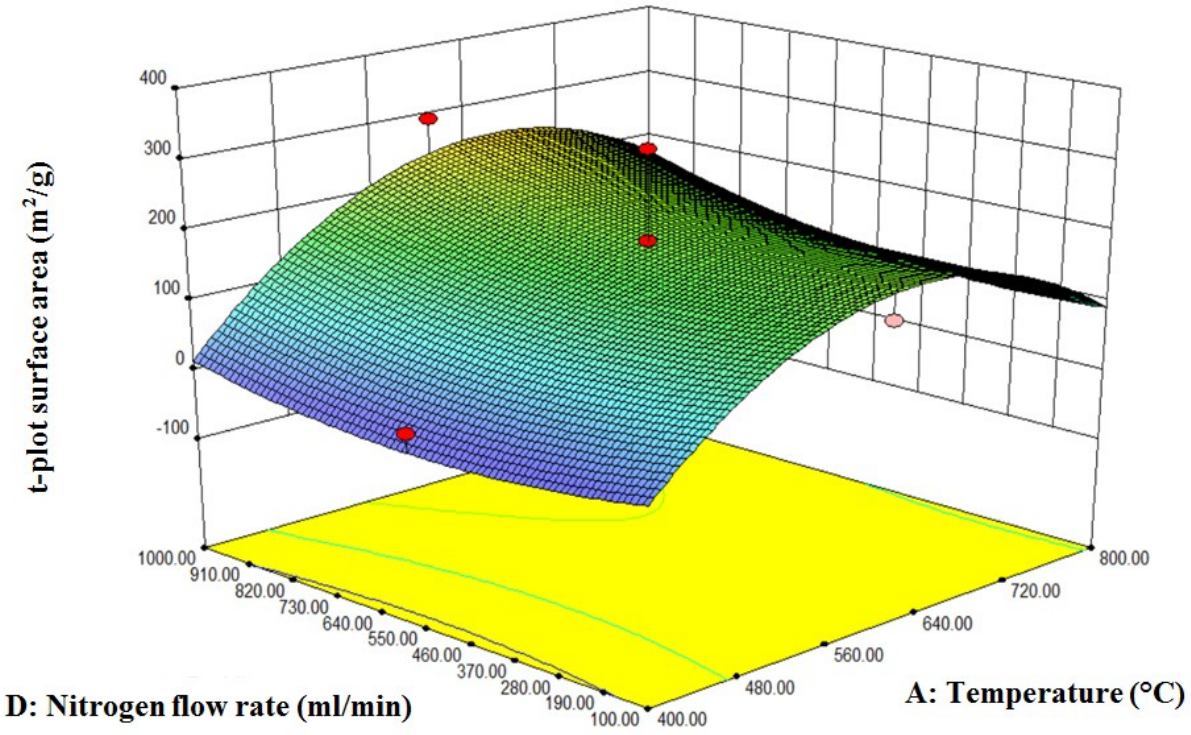
Figure 4-9(a) shows the cooperative effect of temperature and heating rate at a constant holding time of 90min and N_2 flow rate at 550ml/min. As shown in the plot, at low and high temperatures, the t-plot surface area decreases. Figure 4-9(b) illustrates the interactive effect of temperature and holding time on t-plot surface area at constant heating rate of 10°C/min and N_2 flow rate at 550ml/min. The positive interactive effect of temperature and holding time is obvious. The T-plot surface area is low at both low and high temperature and holding time. It grows with the increasing temperature between 400 to 640°C and over holding time ranges of 0 to 90 min.


t-plot surface area (m²/g)
400
300
200
100
0
-100
15.00
13.00
11.00
9.00
7.00
5.00
B: Heating rate (°C/min)
400.00
480.00
560.00
640.00
720.00
800.00
A: Temperature (°C)

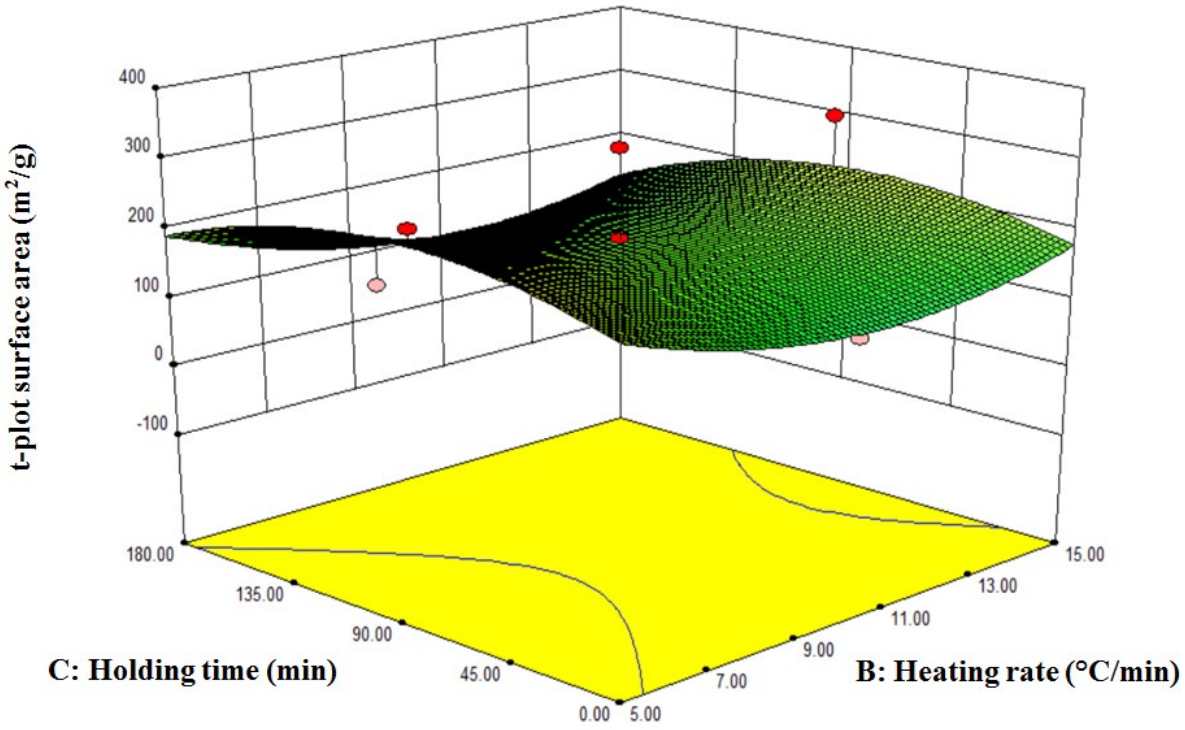
(a)


t-plot surface area (m²/g)
400
300
200
100
0
-100
180.00
135.00
90.00
45.00
0.00
C: Holding time (min)
400.00
480.00
560.00
640.00
720.00
800.00
A: Temperature (°C)

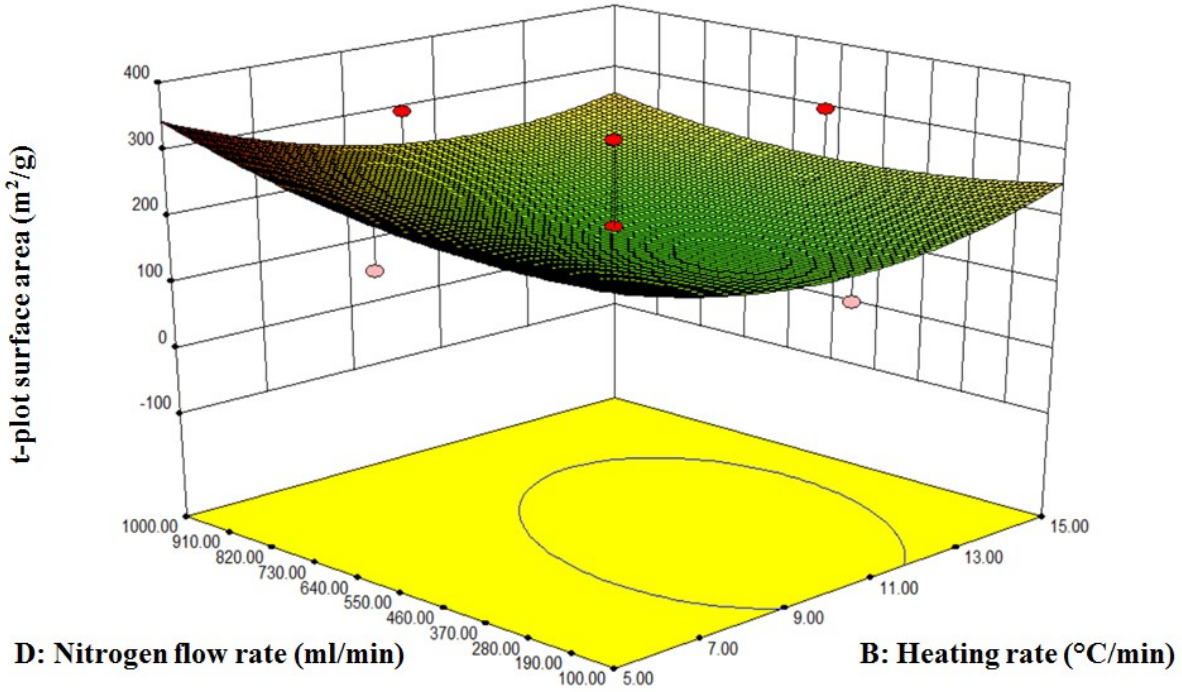
(b)


t-plot surface area (m²/g)
400
300
200
100
0
-100
1000.00
910.00
820.00
730.00
640.00
550.00
460.00
370.00
280.00
190.00
100.00
D: Nitrogen flow rate (ml/min)
400.00
480.00
560.00
640.00
720.00
800.00
A: Temperature (°C)

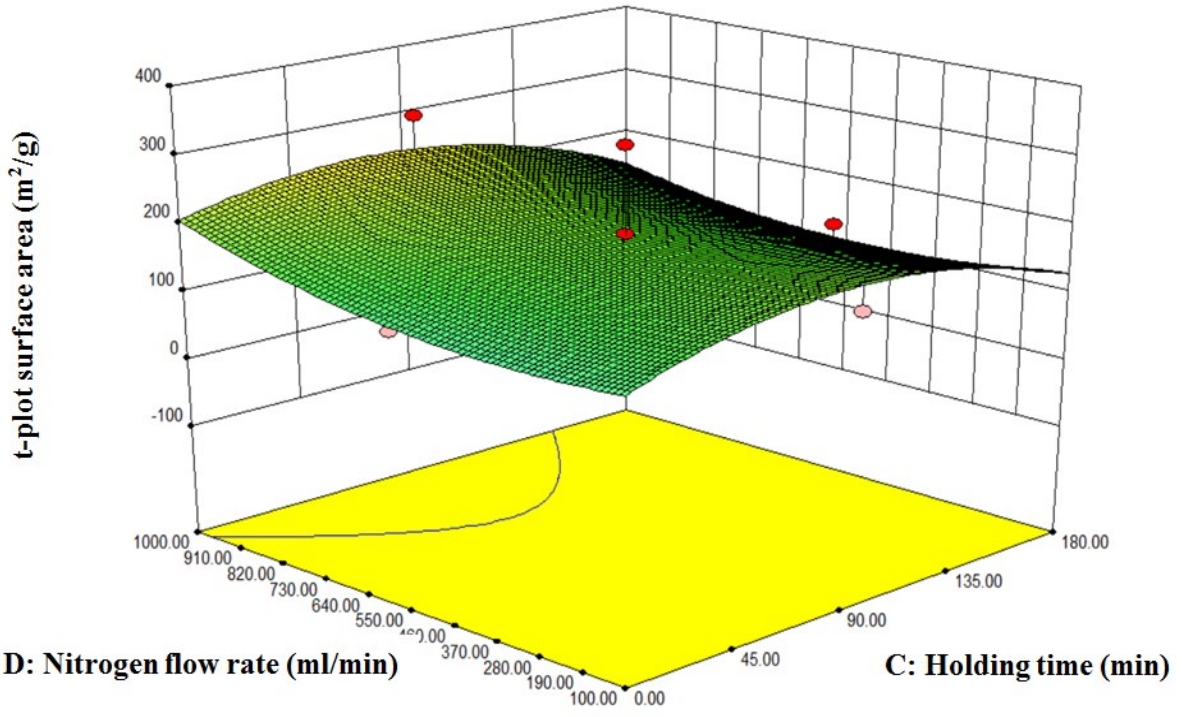
(c)


t-plot surface area (m²/g)
400
300
200
100
0
-100
180.00
135.00
90.00
45.00
0.00
C: Holding time (min)
5.00
7.00
9.00
11.00
13.00
15.00
B: Heating rate (°C/min)

(d)



(e)



(f)

Figure 4-9 (a-f) Response surface plots of t-plot surface area, illustrating the interaction between two variables: selected for temperature, heating rate, holding time and nitrogen flow rate

Figure 4-9(c) presents the interactive effect of temperature and nitrogen flow rate at a constant holding time of 90min and heating rate of 10°C/min. It can be seen that the t-plot surface area increases with the increase in temperature below 640°C. Figure 4-9(d) shows the cooperative effect of heating rate and holding time on t-plot surface area at constant 600°C temperature and 550ml/min N_2 flow rate. As shown in this plot, the t-plot surface area increases with an increasing holding time until 90min. Figure 4-9(e) and (f) present the interactive effect of heating rate and nitrogen flow rate and holding time and nitrogen flow rate. The planar nature of the plots indicate that the effects of the two groups of factor on t-plot surface area are not as influential as the interaction effects above, but more influential than upon pH when compared to figures 4-6(e) and 4-6(f).

4.4.2.5 Optimization of Pyrolysis Process based on t-plot Surface Area and Model Verification

According to the software optimization step, the response t-plot surface area was defined as maximum to achieve the best char performance. The program combines the individual desirability into a single number and then searches to optimize this function based on the response goal. Accordingly, the optimum working conditions and respective t-plot surface area are shown in Table 4-7. The maximum t-plot surface area which could be achieved is ≈339.923m^2/g, with the desirability function value to be 1.000.

Table 4-7 Optimum conditions solutions for t-plot surface area

Number of trials	Temperature (°C)	Heating rate (°C/min)	Holding time (min)	N_2 flow rate (ml/min)	t-plot surface area (m^2/g)	Desirability
1	635.01	5.4	44.4	656.74	321.85	1.000
2	639.99	6.18	65.14	823.85	326.02	1.000
3	638.69	5.69	58.69	794.36	339.92	1.000
4	600	5	90	550	322.78	1.000
5	638.44	14.94	73.59	996.2	318.81	1.000

4.5 Coconut Shell Derived Char Fillers In-rubber Tests

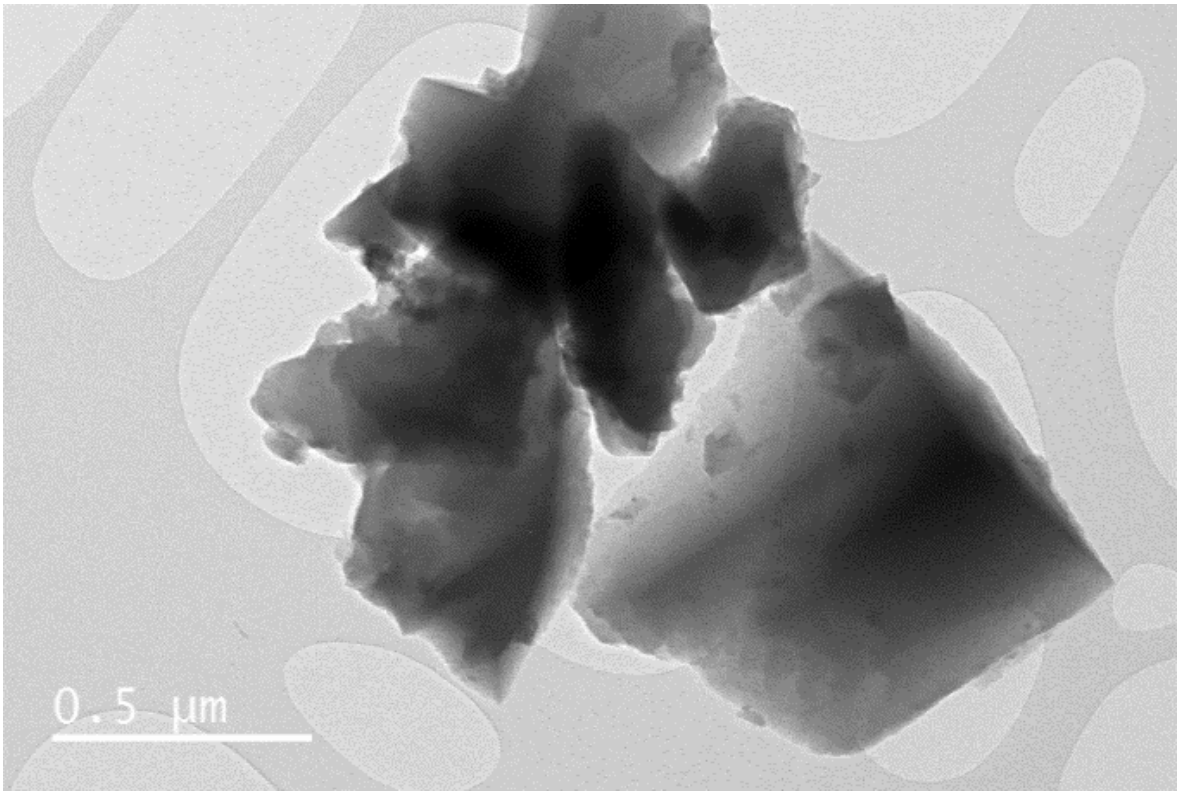
Based upon the physical and chemical properties obtained from the previously described results, and the regression and optimisation results from RSM method, eight pyrolytic coconut char fillers were selected to be mixed with an SBR rubber matrix and the performance of the final rubber products evaluated using standard rubber testing methodologies. The eight rubber samples tested contained char samples which had been prepared from the optimum pyrolysis condition (600˚C, 10˚C/min, 90min, 550ml/min N_2); from lowest and highest temperatures and char fillers that exhibited the "best" and the "worst" performance according to the physical and chemical tests detailed in Section 4.3. The eight pyrolysis conditions of the selected char fillers are shown in Table 4-8.

Table 4-8 Selection of coconut shell derived char fillers for in-rubber tests

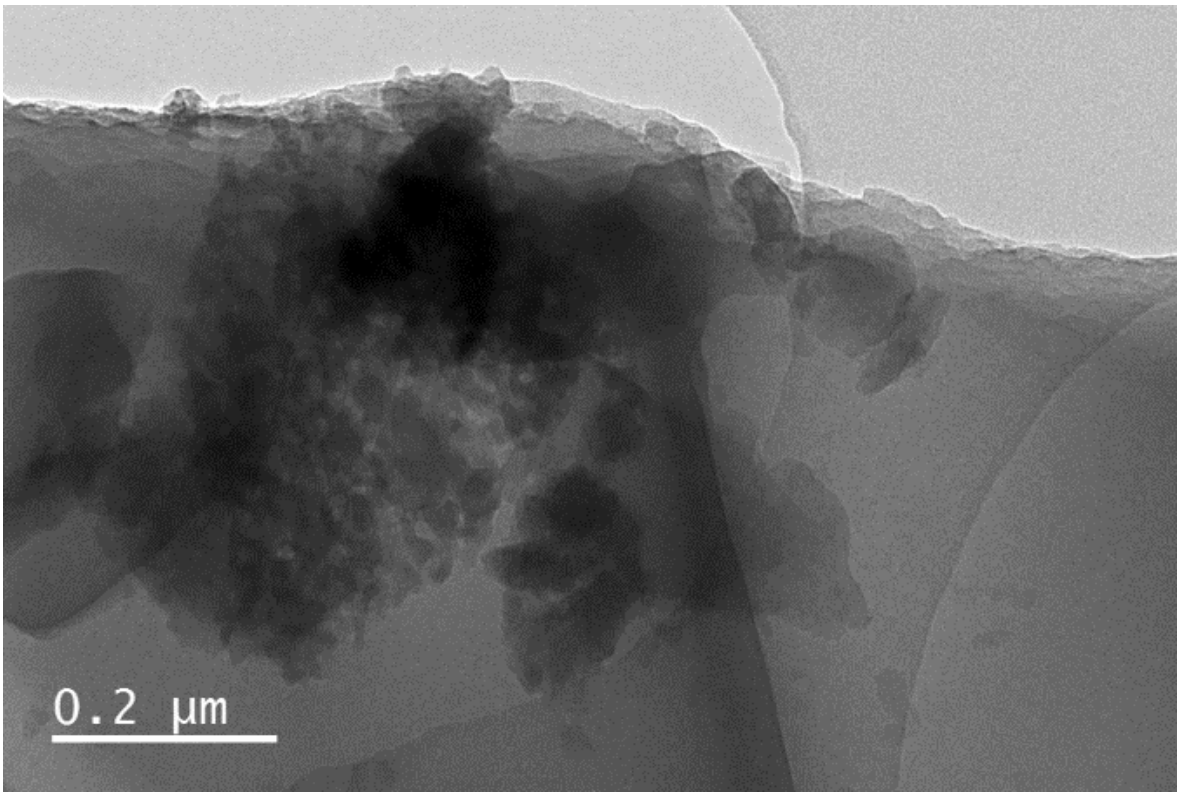
Run	Temperature (°C)	Heating rate (°C/min)	Holding time (min)	N_2 flow rate (ml/min)
4	600	10	0	550
16	800	10	90	550
19	600	10	90	1000
20	600	10	90	550
22	800	5	180	1000
24	600	15	90	550
25	800	5	0	1000
30	400	10	90	550

4.5.1 Transmission Electron Microscope (TEM) Results

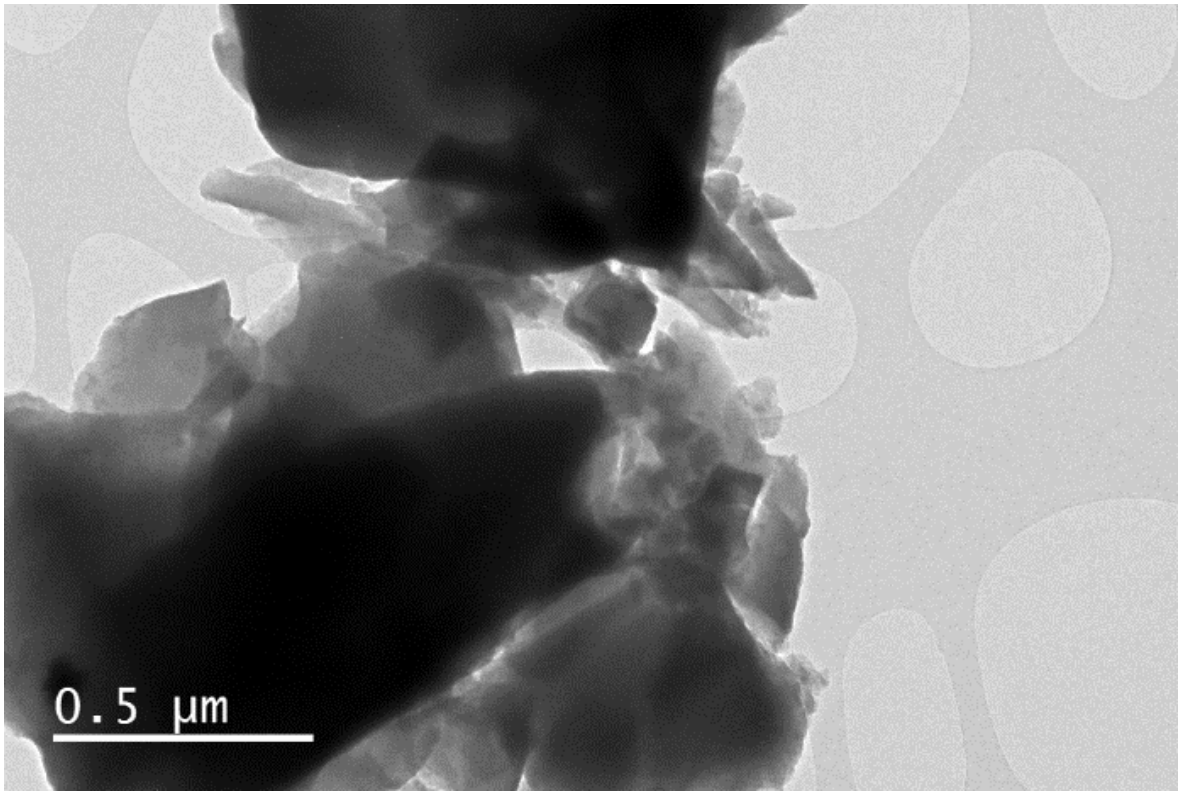
Two char samples were selected for TEM analysis, they were Run 20 and Run 30. Run 20 was the char sample which exhibited the best characteristics among the 30 runs, whereas Run 30 was less optimum compared to the other 29 samples. Commercial carbon black N330 and N772 were studied as reference materials. The TEM-micrographs of Run 20, Run 30, N330 and N772 at 6k and 25k magnifications are shown in Figure 4-10.



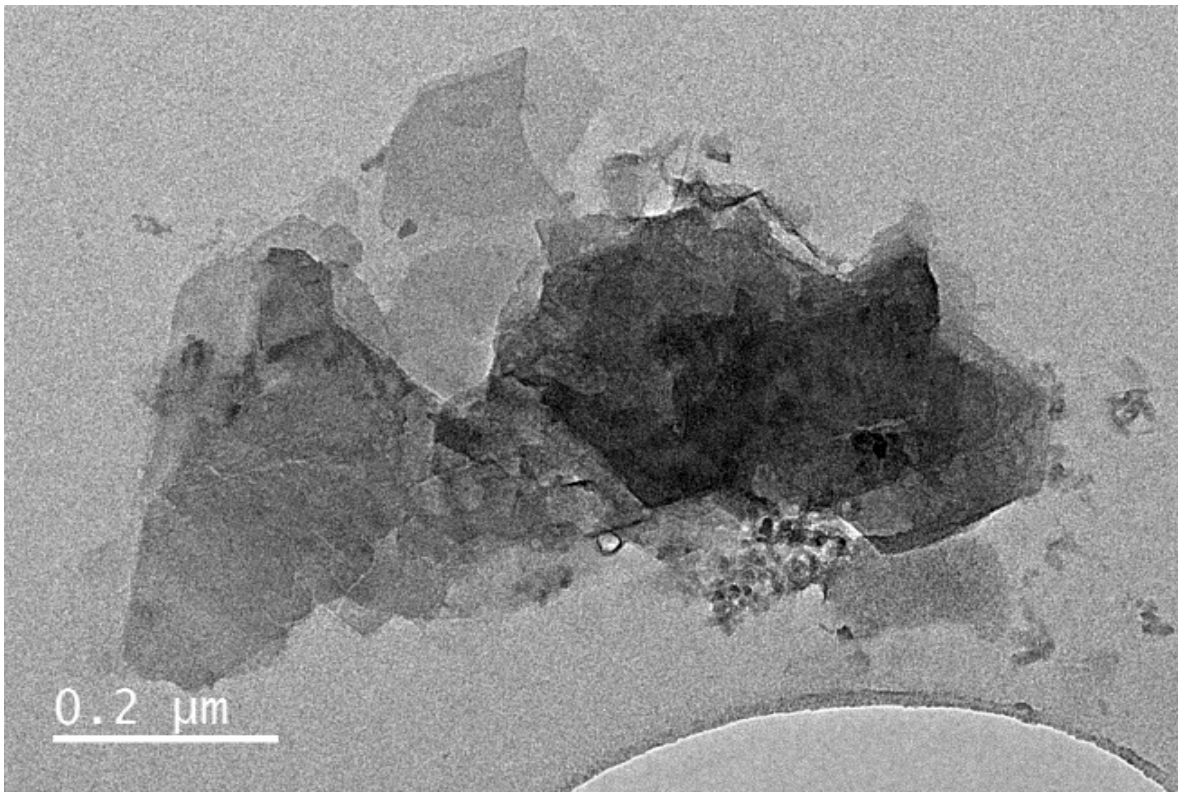
(a) TEM-micrograph of Run 20 at 6K magnification



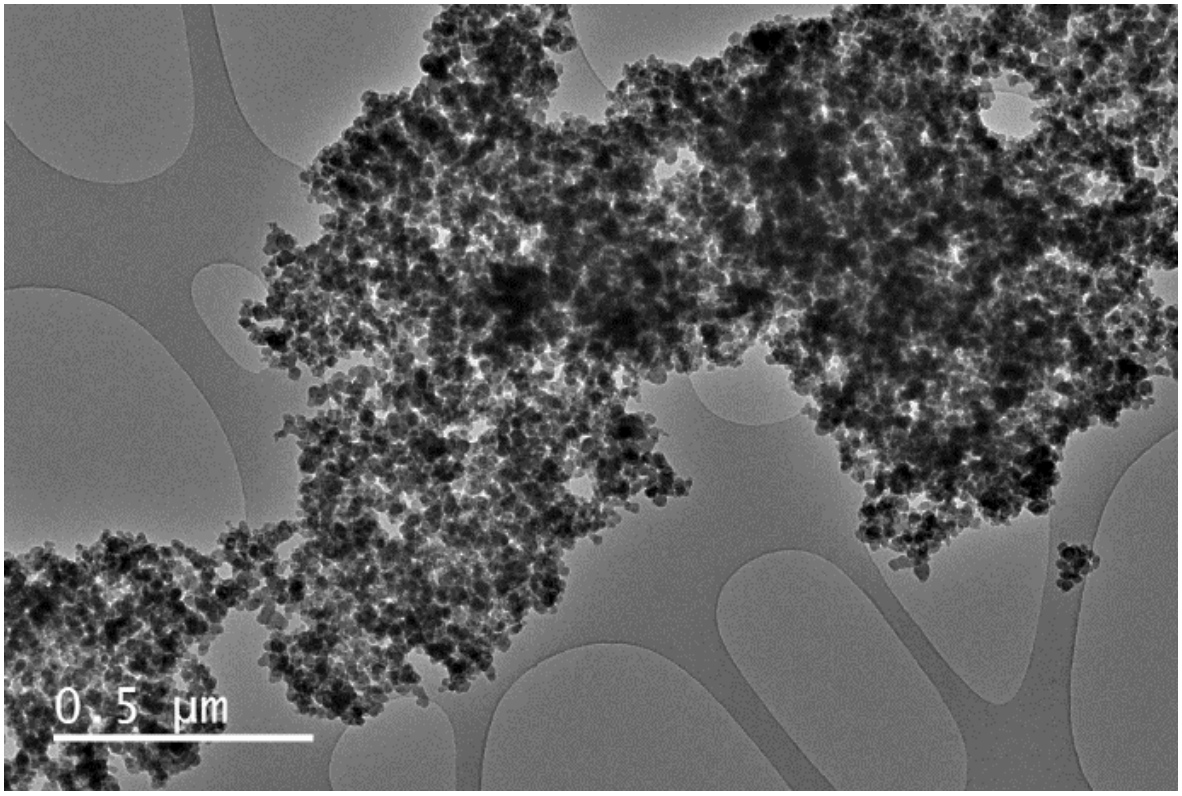
(b) TEM-micrograph of Run 20 at 25K magnification



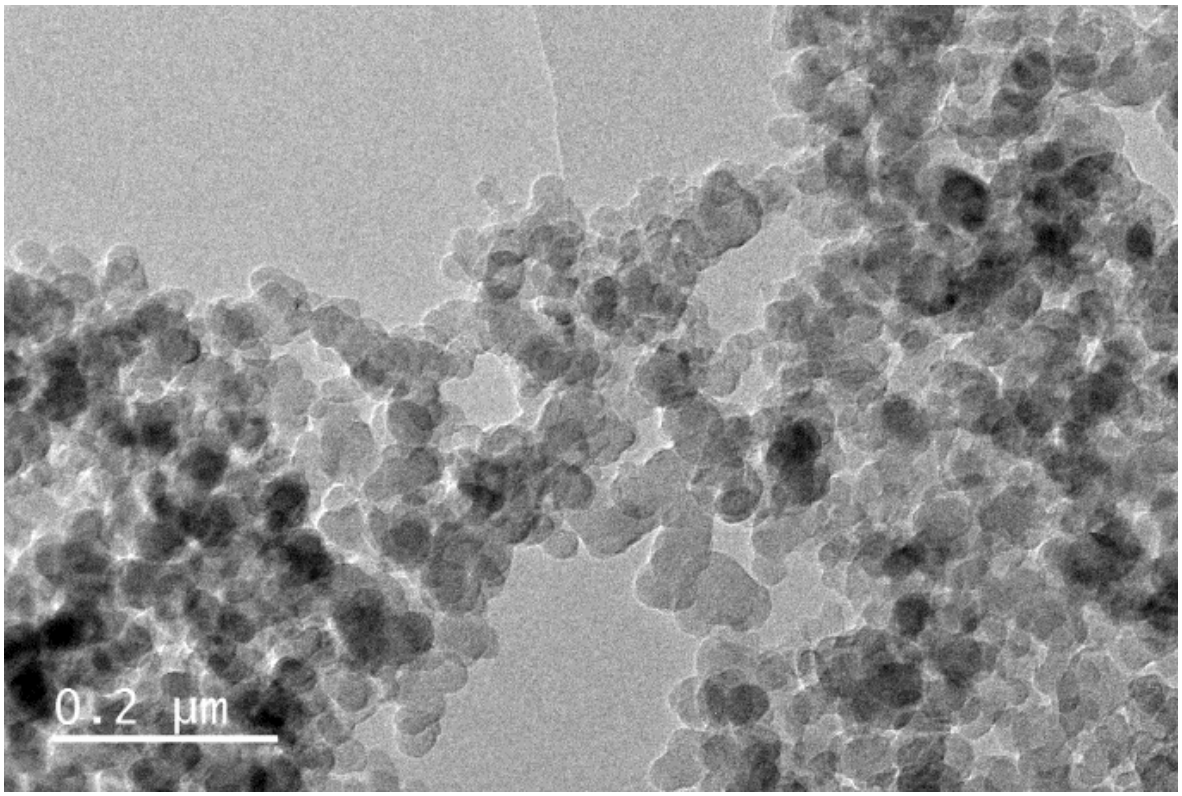
(c) TEM-micrograph of Run 30 at 6K magnification



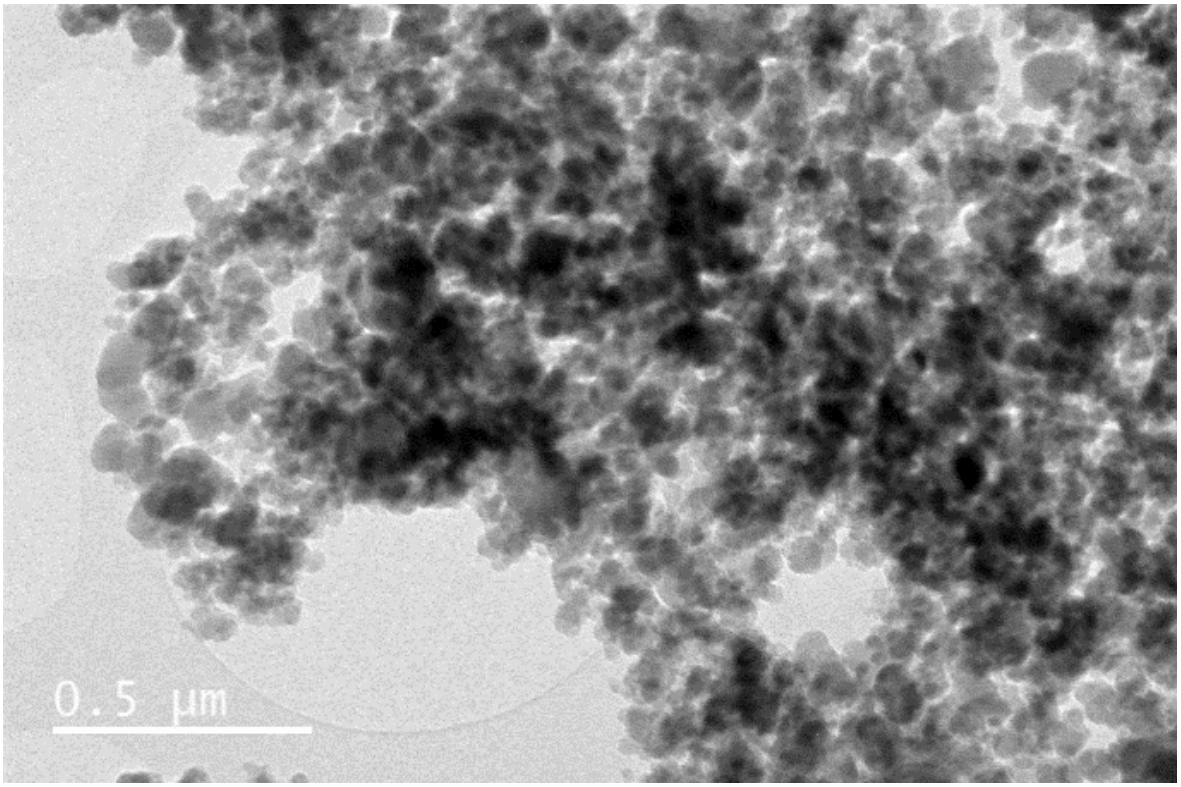
(d) TEM-micrograph of Run 30 at 25K magnification



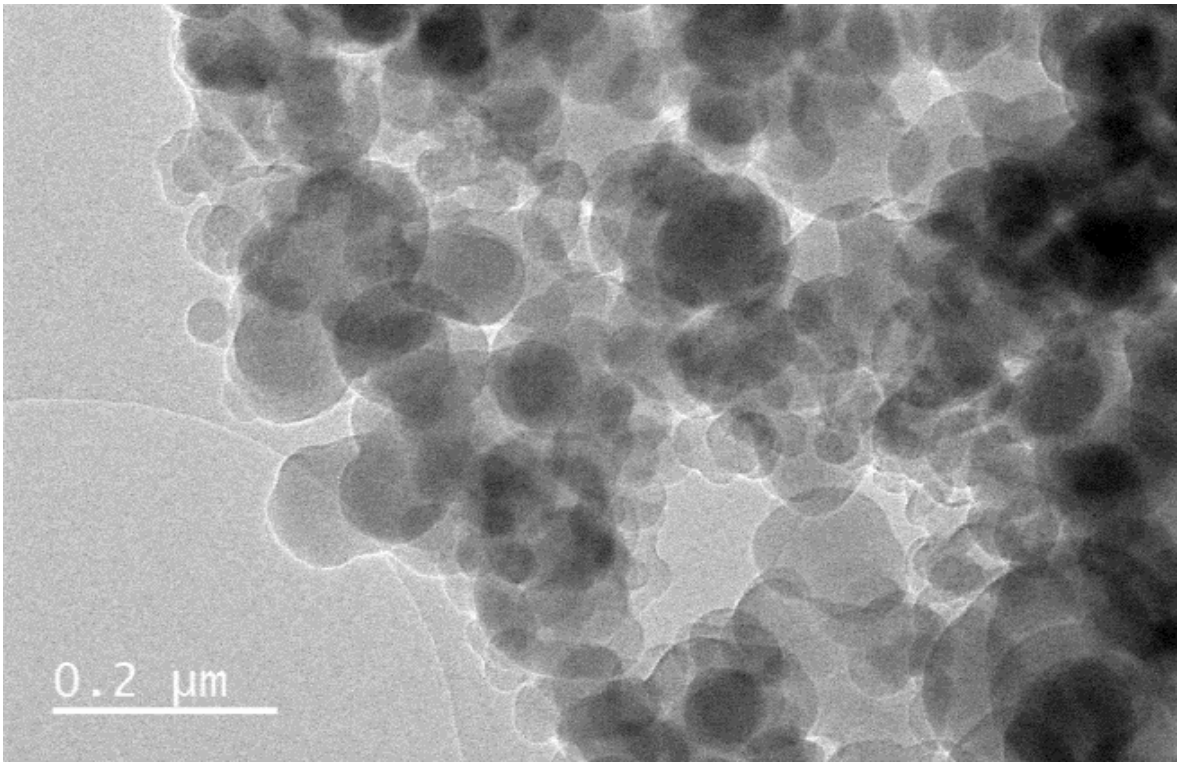
(e) TEM-micrograph of N330 at 6K magnification



(f) TEM-micrograph of N330 at 25K magnification



(g) TEM-micrograph of N772 at 6K magnification



(h) TEM-micrograph of N772 at 25K magnification

Figure 4-10(a-h) TEM-micrographs of Run 20, Run 30, N330 and N772 at 6K and 25K magnification, showing particle shape, size and distribution

It can be seen clearly from the TEM plots that neither Run 20 nor Run 30 appear to exhibit similar structure at 6K and 25K. Only a few grape-like clusters can be observed in the Run 20 sample at 25K, almost no cluster structure can be found within Run 30. Further, not only is the particle size of both Run 20 and Run 30 much larger than the commercial carbon blacks, but they show a larger variety of particle sizes. There are small particles, due to the ash, which are attached to the large particles making it one large agglomerated piece reducing the surface availability to which rubber would normally bond. Given the pyrolysis conditions used to prepare Run 20 and Run 30, a higher temperature is apparently preferred for obtaining smaller particle sizes, a uniform size distribution and clear structure. By comparing carbon black N330 and N772, it indicates that the nodules in N330 are better defined than in N772. The primary particles of N330 are smaller and with a more uniform size distribution to that of N772. There is also less overlap of the primary particles within the clusters in N330. It seems that the particles of N330 combine each other on the same plane making the working cluster easy to bond with the rubber matrix, whereas N772 is slightly blurry since more overlap occurs and less bonding results.

4.5.2 Carbon Hydrogen Nitrogen Sulphur Tests

Table 4-9 Elemental composition of coconut shell, char fillers and commercial carbon black

Sample	C (%)	H (%)	N (%)	S (%)	C/H ratio
Coconut shell	48.07	5.87	< 0.10	< 0.10	8.19
Run 4	82.97	2.94	< 0.10	< 0.10	28.22
Run 16	89.87	1.39	< 0.10	< 0.10	64.65
Run 19	87.35	2.42	< 0.10	< 0.10	36.09
Run 20	86.18	2.48	< 0.10	< 0.10	34.75
Run 22	90.47	1.47	< 0.10	< 0.10	61.54
Run 24	86.75	2.60	< 0.10	< 0.10	33.37
Run 25	88.94	1.92	< 0.10	< 0.10	46.32
Run 30	71.64	3.31	< 0.10	< 0.10	21.64
N330	96.84	0.99	< 0.10	0.46	97.82
N550	97.82	1.23	< 0.10	0.70	79.53
N772	94.43	0.86	< 0.10	0.91	109.80

The elemental composition, in terms of carbon, hydrogen, nitrogen and sulphur, of the coconut shell, char fillers and the commercial carbon black N330, N550 and N772 is presented in Table 4-9. Coconut shell contains 48.07% carbon, 5.87% hydrogen, <0.10% nitrogen and <0.10% Sulphur. Cagnon et al. (2004) has reported similar result: 48.7% carbon, 5.8% hydrogen, <0.3% nitrogen and <0.3% Sulphur. The C content of other nut shell such as hazelnut shells, walnut shells, and olive are similar to coconut shell, which ranges from 47 to 53% (Sharifan, 2014; Demirbaş, 2002, Aygün et al., 2003). The high C content makes coconut shell and lignocellulosic biomass very suitable as feedstock to produce carbonaceous materials (activated carbon etc). The H content of coconut shell is 5.87%, which directly influence the volatiles yield. The N content and S content were found to be less than 0.10%, comparable with a reported maximum of 0.5% N and S content for biomass (Demirbaş, 2004). The C content of commercial carbon blacks tested are all above 94%, confirming that carbon black is an extremely pure form of elemental carbon. The H content is around 1% and the N content is less than 0.10%. All the carbon black samples contain a small amount of Sulphur, which is one of the widely applied vulcanizing agent in rubber industry. According to Table

4-9, the C content of the pyrolytic coconut shell chars is around 90%, which is comparable with the commercial carbon blacks. The H content is slightly higher than the commercial carbon black indicating less aromaticity of the carbon structure. Both N and S content are lower than 0.10%. The C/H ratio has been calculated and shown in Table 4-9 as an indicative measurement of the aromaticity in the carbon structure. There is a big increase in C/H ratios of char samples compared to coconut shell, indicating the removal of H and N content and a development of aromatization of the carbon structure. It also can be concluded that high pyrolysis temperatures result in high C content, C/H ratio and low H content.

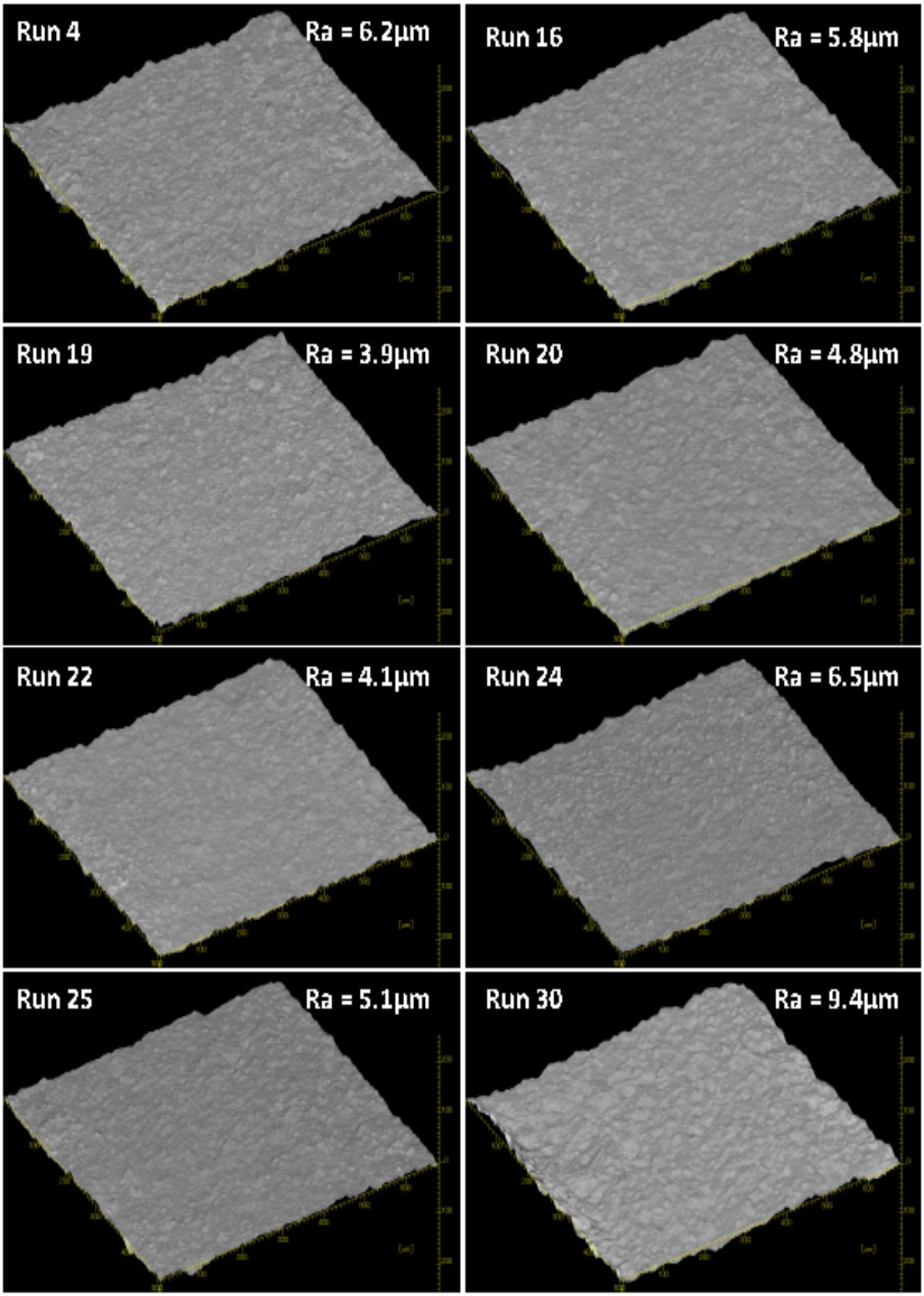
4.5.3 In-rubber Characterization

Following compounding within the SBR formulation (defined in Tables 3-5 and 3-6), the dispersion performance achieved with each of the selected char fillers was evaluated through SEM 3D surface roughness maps of freshly sectioned surfaces, shown in Figure 4-11. In this test, commercial carbon black N300 has been selected as the reference material. The optimum dispersion ability of the filler within the rubber compound is crucial, since it:

(1) Improves reinforcement, as the filler surface area available to the rubber matrix is increased.

(2) Improves fatigue performance, since large undispersed particles will act as stress concentrations, leading to premature failures.

(3) Improves surface finish and reduces the roughness of final rubber products, which is also important for extrusion application.


Run 4
Ra = 6.2µm
Run 16
Ra = 5.8µm
Run 19
Ra = 3.9µm
Run 20
Ra = 4.8µm
Run 22
Ra = 4.1µm
Run 24
Ra = 6.5µm
Run 25
Ra = 5.1µm
Run 30
Ra = 9.4µm

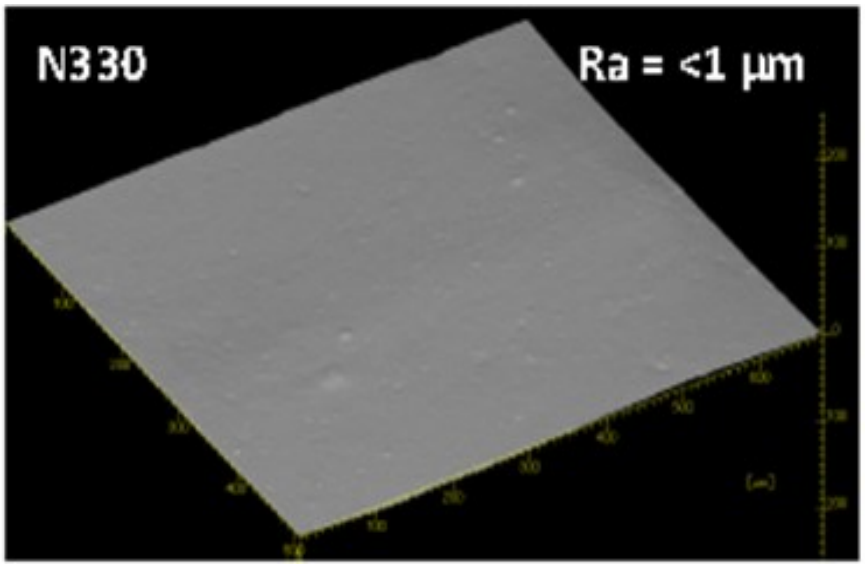
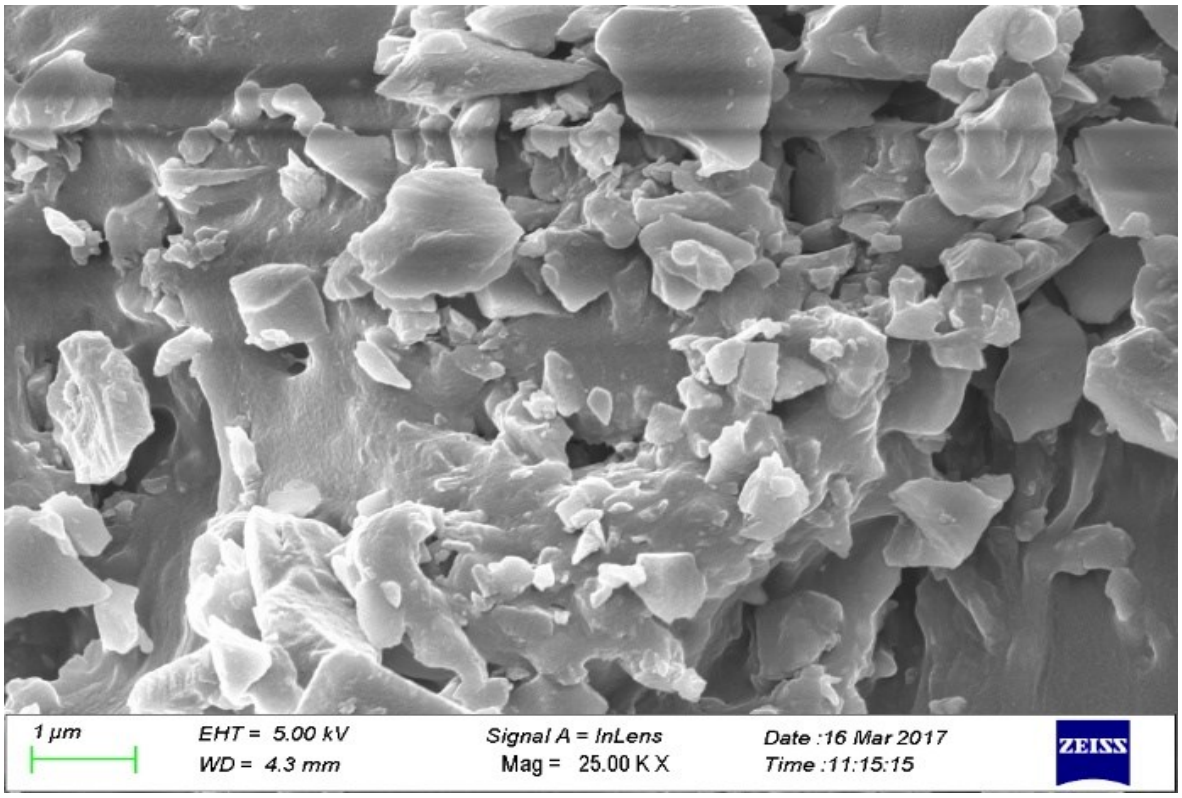


Figure 4-11 3D surface roughness maps highlighting filler dispersion, scale in micron

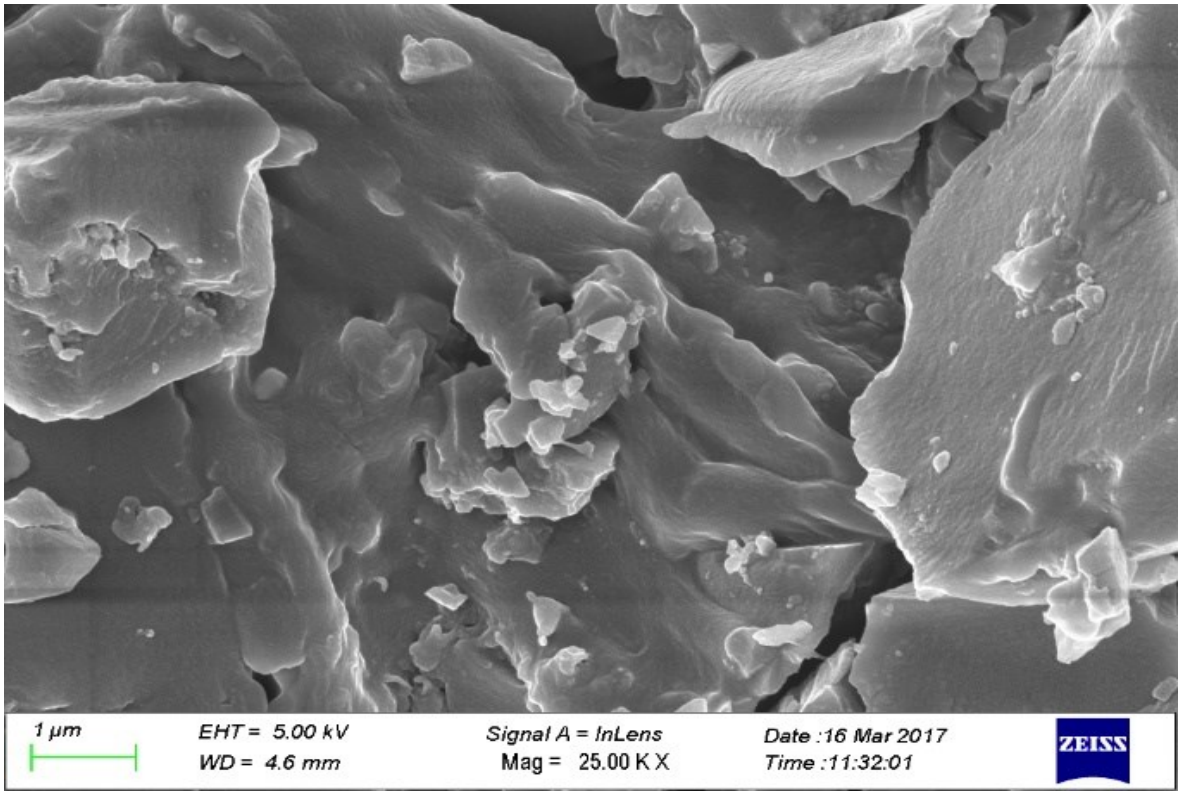
For conventional carbon black, dispersion is considered to be a function of both the filler surface area and the structure level. The greater the surface area to be wetted, the greater the energy required to achieve incorporation and dispersion. Conversely, greater structure levels increase the internal mixing shear force which lead to improved levels of dispersion. Given that the char samples chosen for evaluation have relatively high surface areas (see Table 4-3), it can be expected that these chars will be harder to disperse than a conventional N330. As can be seen in Figure 4-11, all the char samples had broadly similar dispersion levels except Run 30, which has the highest surface roughness value. The dispersion ability of coconut-derived char is found to be less than commercial carbon black and lower structure level can be expected based on the dispersion results. This also indicates a reduced fill-rubber interaction. Normally, the pelletized commercial carbon blacks will disintegrate during the rubber formulation mixing process. However, the coconut shell char particles resist break up when mixing with rubber, which contributed to an uneven dispersion of the char filler in the formed rubber product. Further research into alternative more efficient milling processes for the coconut shell char will need to be undertaken, based on this finding, to improve the dispersion of the char.

Figure 4-12 presents the SEM plots of coconut char compounded rubber sheet and N660 filled rubber sheet at 25K magnification. It can be seen from the images that the base layer is the rubber matrix, with the small particles of the filler (8 selected char samples and N660)

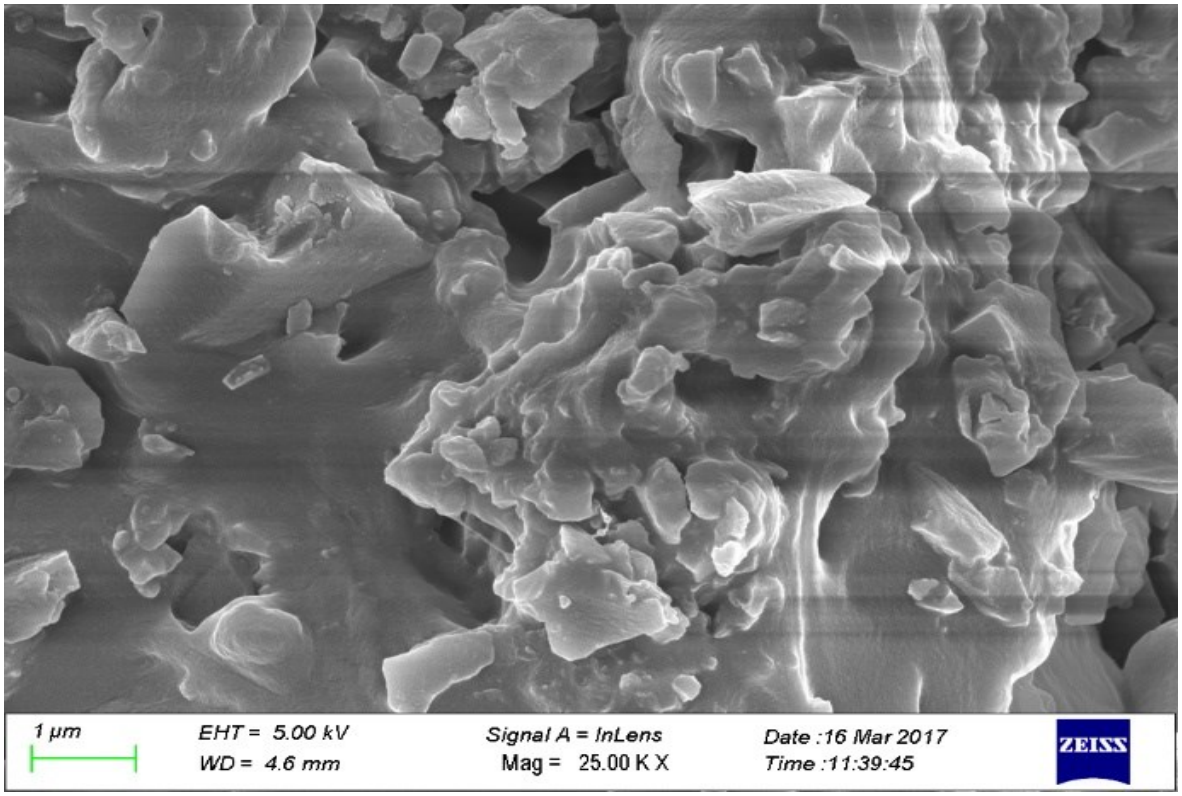
showing on the surface and as part of the rubber foundation. The coconut char and the carbon black samples show the filler is unevenly bound to the rubber surface, indicating that the mechanism of the char filler mixing and interaction with rubber is similar to conventional carbon black. The major difference between the char filler and carbon black are the particle shapes (angular), particle sizes and its distribution. Carbon black contains a smaller aggregate size and more uniform size distribution plus spheroid particles, so that more aggregates can attach to the rubber surface resulting in a good reinforcing ability. It is obvious that Run19 (Figure 4-12 (c)) has the best performance when used as a filler in rubber, which is supported by the dispersion test result above.



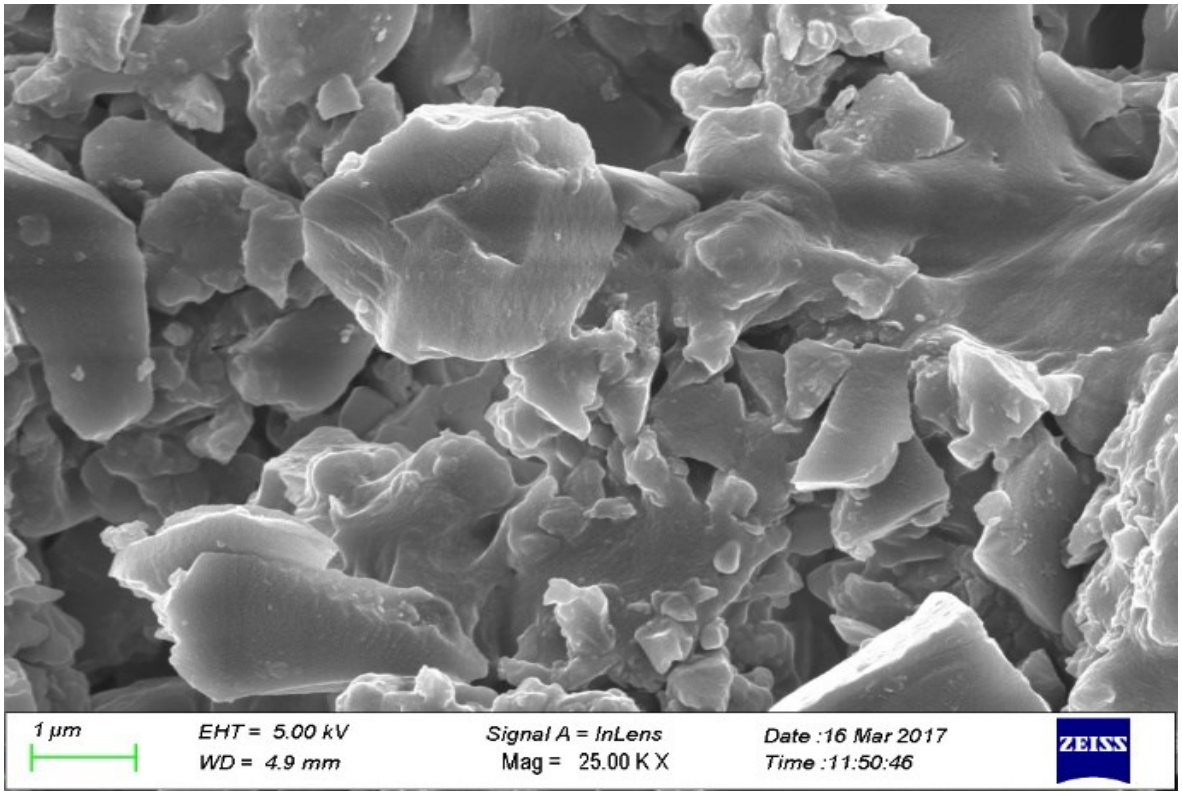
(a) SEM plot of Run 4 filled rubber sheet



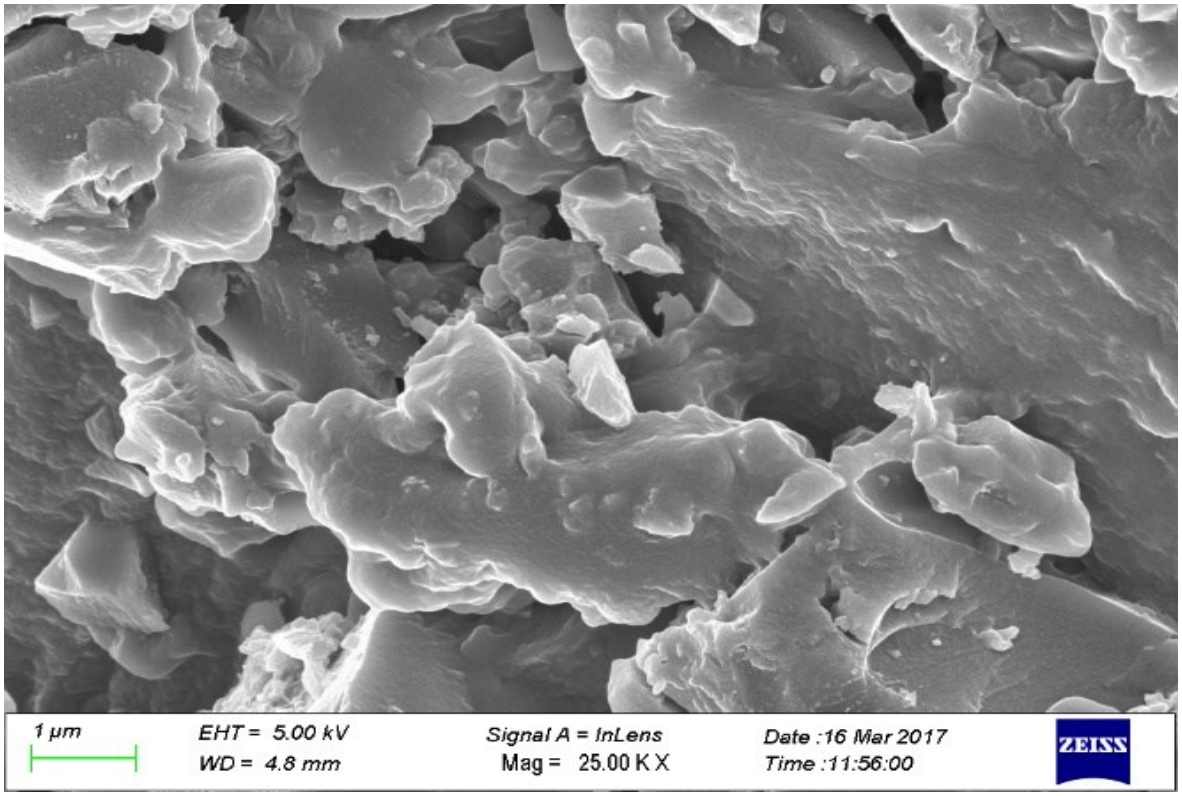
(b) SEM plot of Run 16 filled rubber sheet



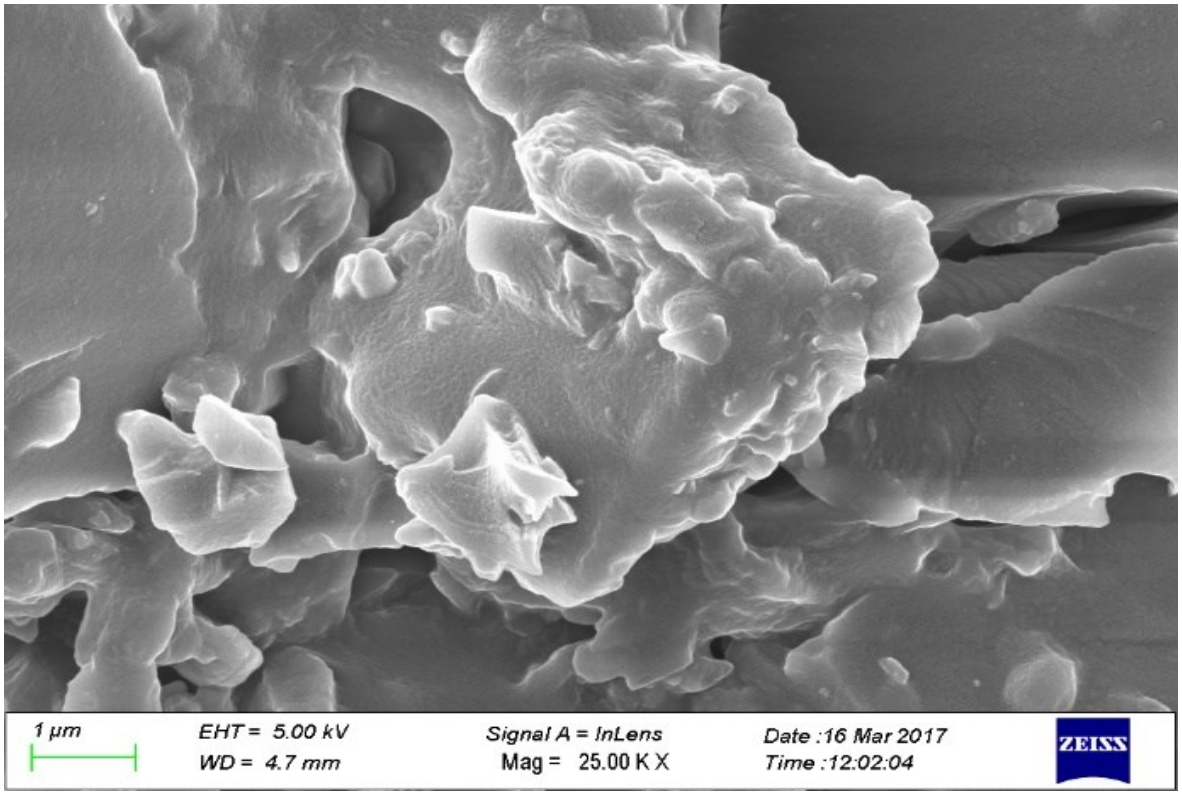
(c) SEM plot of Run 19 filled rubber sheet



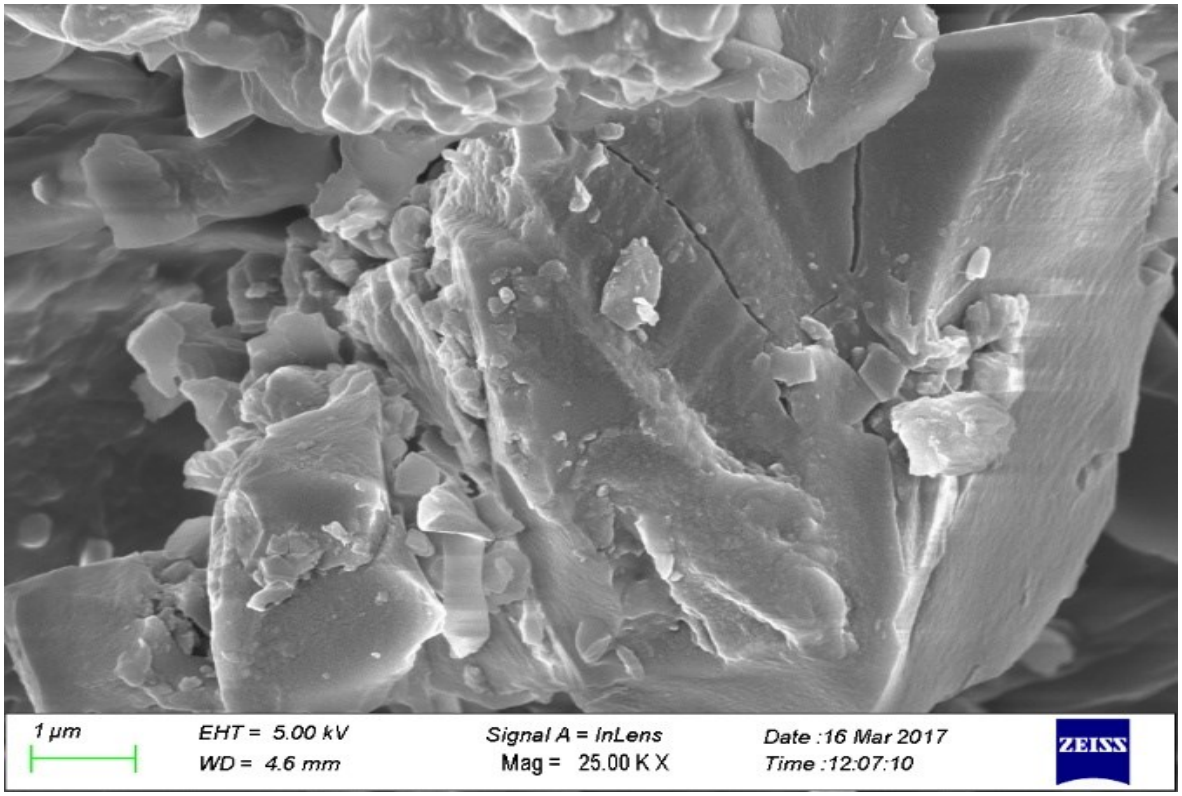
(d) SEM plot of Run 20 filled rubber sheet



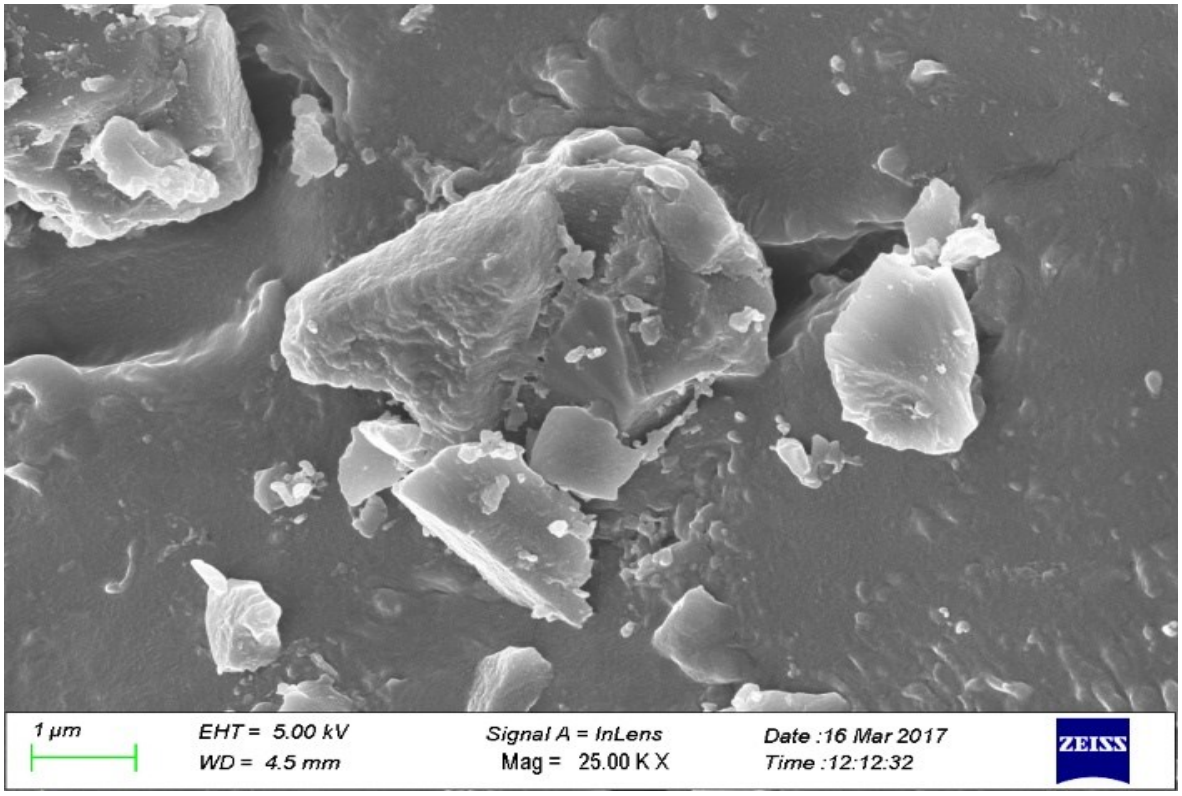
(e) SEM plot of Run 22 filled rubber sheet



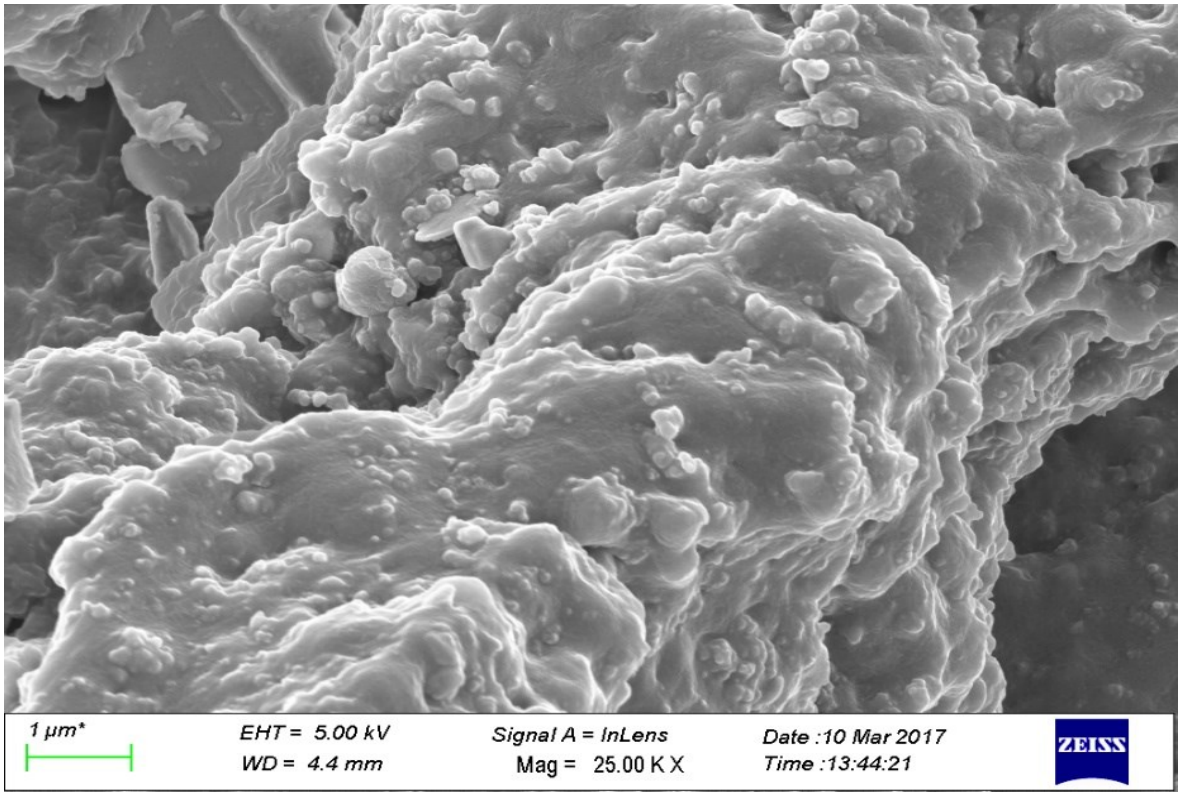
(f) SEM plot of Run 24 filled rubber sheet



(g) SEM plot of Run 25 filled rubber sheet



(h) SEM plot of Run 30 filled rubber sheet



(i) SEM plot of N660 filled rubber sheet

Figure 4-12(a-i) SEM plots of compounded rubber sheets at 25K magnification, illustrating rubber-filler bonding system

The cure and physical properties of the compounds are summarized in Table 4-10.

Table 4-10 Rheology and physical data of coconut shell chars

	Run 4	Run 16	Run 19	Run 20	Run 22	Run 24	Run 25	Run 30	CB N772	CB N330
MDR data (30mins @160˚C)										
Min (dNm)	1.21	0.96	1.13	1.16	1.00	1.15	1.02	1.3	1.23	2.14
Max (dNm)	14.55	14.11	14.35	14.42	14.16	14.36	14.32	13.99	13.66	17.30
Ts2 (mm:ss)	8.42	6.08	7.34	7.04	6.22	6.82	6.43	9.97	4.33	4.06
T90 (mm:ss)	15.73	11.94	14.07	13.48	12.05	13.05	12.79	18.95	9.19	9.13
Physical Properties										
Shore A (˚)	58	59	58	59	59	59	59	58	57	67
M 100% (MPa)	1.88	1.94	2.01	1.99	2.04	1.93	2.02	1.73	1.63	1.61
M 300% (Mpa)	2.77	2.89	2.93	2.82	3.02	2.71	2.98	2.57	9.3	17.0
Tensile Strength (Mpa)	4.3	5.53	4.95	5.68	4.76	3.06	5.08	4.1	20.4	25.9
Elongation at Break (%)	615	675	659	653	604	482	649	684	586	453

A compound's curing and processing behaviour is assessed by the Moving Die Rheometer (MDR) test. Firstly, a mixture is loaded into the cavity of the rheometer at room temperature. As the compound gets heated under pressure, the viscosity decreases and the torque exerted on the rotor drops. The lowest torque value measured in dNm, is called Moment Lowest (ML), noted as "Min" in Table 4-10. The stiffness of the uncured rubber compound at a given temperature can be indicated by ML. After the curing begins, the torque rises. When the torque increases 2 dNm unit above ML value, the time is recorded as Ts2. It provides information about at which point the curing process actually starts. With the curing progressing, the torque continues increasing. After some time, the torque reaches the maximum value and a plateau appears. The highest torque measured in dNm is regarded as Moment Highest (MH), also noted as "Max" in Table 4-10. The optimal vulcanization time is called T90, which is the time from the beginning of the test to the point where 90% of the MH value can be achieved. The hardness of the filled rubber compound is tested by the Shore A with ° unit. The M100% and M300% are the stresses required to produces an elongation of 100% and 300% of the test sample. The maximum tensile stress recorded in extending the test piece to a breaking point is shown as tensile strength; and the elongation at break is the tensile strain in the test length at breaking point (Saville, 1999).

According to Table 4-10, the time to onset of cure (Ts2) and cure times (T90) of the coconut char filled SBR were found to be comparable but slightly longer than expected for a conventional carbon black N772 and N330 respectively. This is an indication of differing surface chemistry that is likely having some level of interaction with the cure package utilised. This was particularly apparent for the material generated from Run 4 and 30. Both minimum and maximum torque values of char fillers are higher than the carbon black N772, but slightly lower than N330. As to the hardness tests, the value was similar to carbon black with equivalent surface area. The M100% values are considered to be higher than the commercial carbon blacks in the N200 to N300 series, which are outstanding reinforcing rubber fillers. Whereas the low tensile strength and high elongation to break values suggest that there are low filler-polymer interactions and structure levels, allowing for chain slippage over the filler surface, although these may be improved through modification of the rubber mix formulation (Fan et al., 2017).

Based on this data, the char sample from Run 20 was considered to be best performing char filler among the selected char samples, which agreed with the RSM optimization results. The sample can be considered as a semi to low-reinforcing filler with broadly similar cure characteristics to conventional carbon black.

The MDR cure curves are shown in Figure 4-13. The minimum torque values, which are regarded as an indication of compound viscosity, are considered fairly low, further indicating that the coconut shell char fillers have low structure levels.

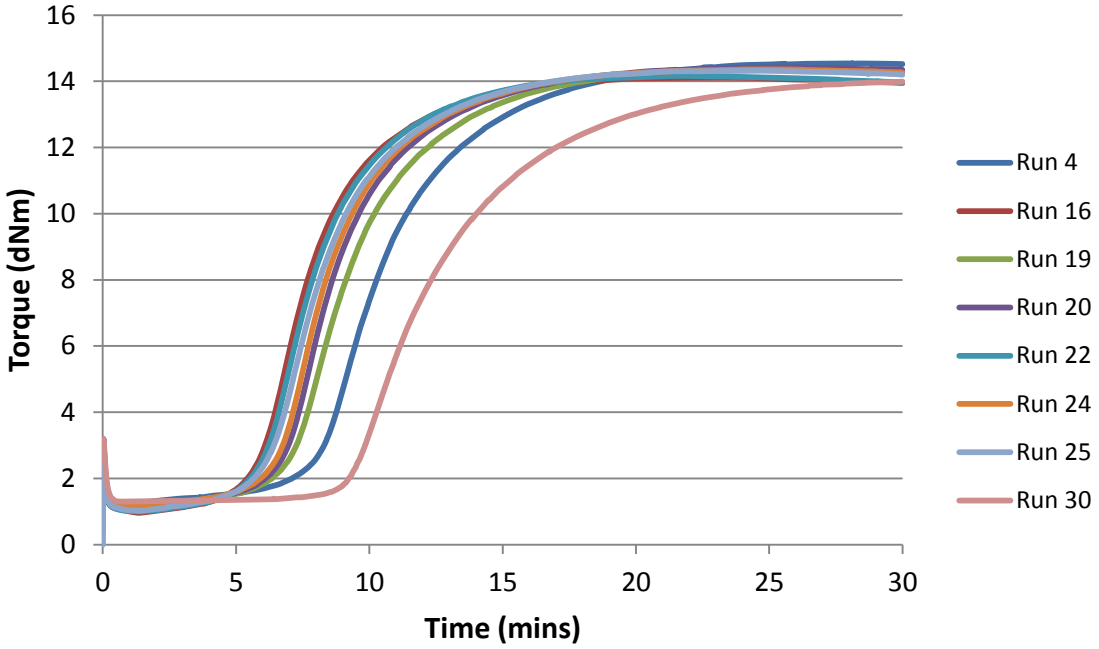


Figure 4-13 MDR cure profiles of coconut shell chars in the SBR system

When mixed in the rubber matrix, carbon black aggregates have a tendency to associate with each other to form agglomerates, owing to van der Waals type attraction forces between particles. Under dynamic loading, elastic modulus (E') decreases with increasing strain amplitude from a high plateau E'_0 to a low plateau E'_∞. This phenomenon is known as the Payne effect and provides a measure of the level of filler-filler interactions. Figure 4-14 shows the Payne effect as a plot of the elastic modulus against the double strain amplitude for N772 and coconut char filled vulcanisates (ERT, 2009).

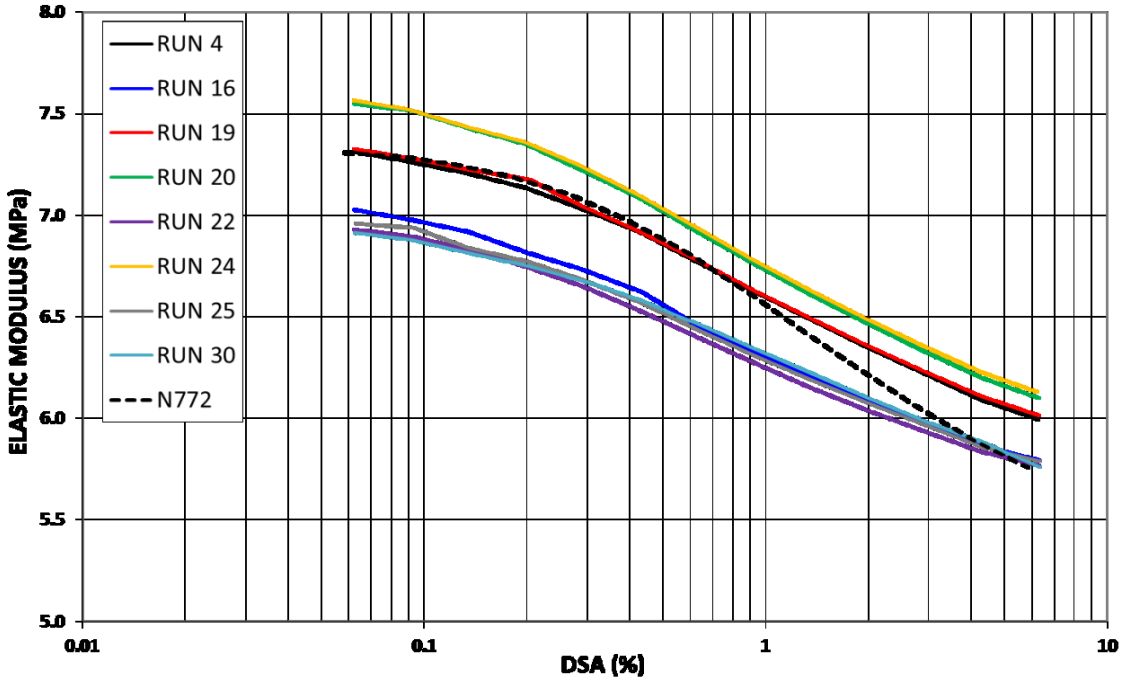


Figure 4-14 Elastic modulus plots against double strain amplitude of the compounds containing N772 and coconut char

Figure 4-15 illustrates the ΔE' networking efficiency versus surface area plot, where ΔE' (E'_0 - E'_∞) is a measurement of filler-filler interaction. The compound filled with N772 shows a higher Payne effect (ΔE'=1.55MPa) compared to the compounds filled with coconut chars (ΔE'<1.5MPa), which are considered to be slightly low given their high surface area, although the elastic modulus of coconut char filled rubber is higher than N772 filled compound. Normally, ΔE' directly increases with increasing surface area for commercial carbon black, however this was not the case for the coconut char sample, confirming weak filler-filler interaction. This is a very interesting characteristic, as such filler-filler interactions are associated with energy losses and, for example, high rolling resistance and poor fuel efficiency in a tyre tread. Graphitic crystallite ends are considered the dominant factor for filler-filler interactions for commercial carbon black, suggesting this feature is lacking within the coconut char sample (Norris et al., 2014).

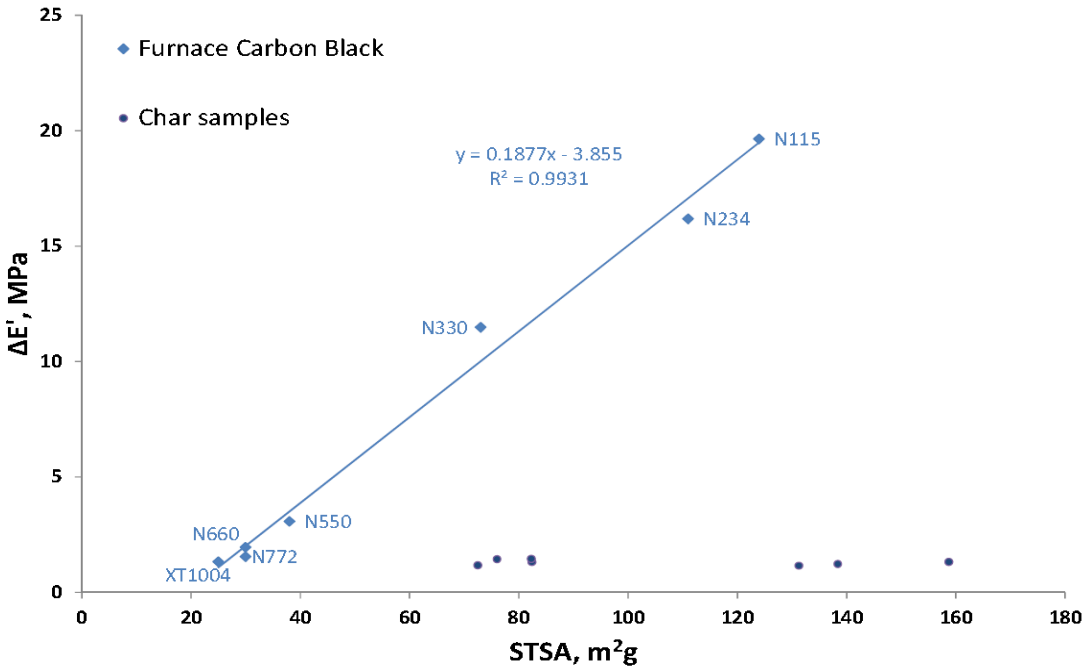


Figure 4-15 ΔE'networking efficiency versus surface area of coconut chars

At high dynamic strain, the effect of carbon black on reinforcement is a combination of the hydrodynamic effect and polymer-filler interactions only. This value (E'_{∞}) is low for all the char samples, confirming low levels of filler-polymer interactions. This is related to both surface activity and structure levels (Norris et al., 2014).

In summary, the char sample was found to have high external surface area values (in-line with N110 to N330 series carbon blacks), along with high levels of porosity and suitable surface pH properties. When compounded into a standard SBR formulation, dispersion was found to be sub-optimum, confirming that more efficient milling needs to be considered and optimization of the formulation/mixing procedure. The physical and dynamic data suggest that the char sample has limited filler-filler and filler-polymer interaction, resulting in relatively low levels of reinforcement. This is demonstrated in Figure 4-16, where char Run 20 is compared to a carbon black of similar surface area. If the level of filler-polymer interaction can be significantly increased, and the current level of filler-filler interactions maintained, the char filler would have very interesting properties with regard to low energy losses, such as tyre rolling resistance.

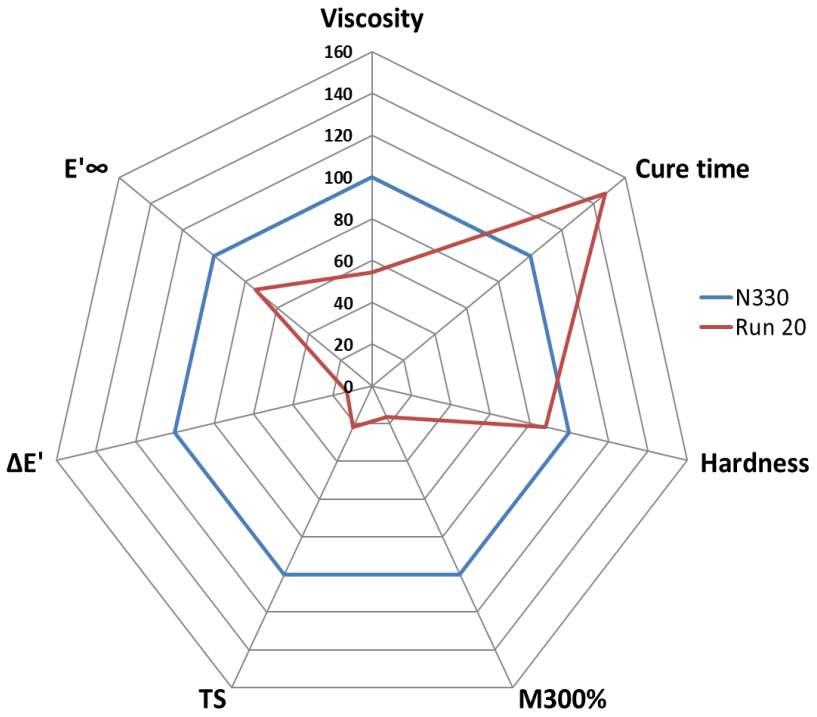


Figure 4-16 Coconut char Run 20 compared to N330

The current performance of the coconut char samples is considered closer to a mineral filler such as calcined clay, shown in Figure 4-17.

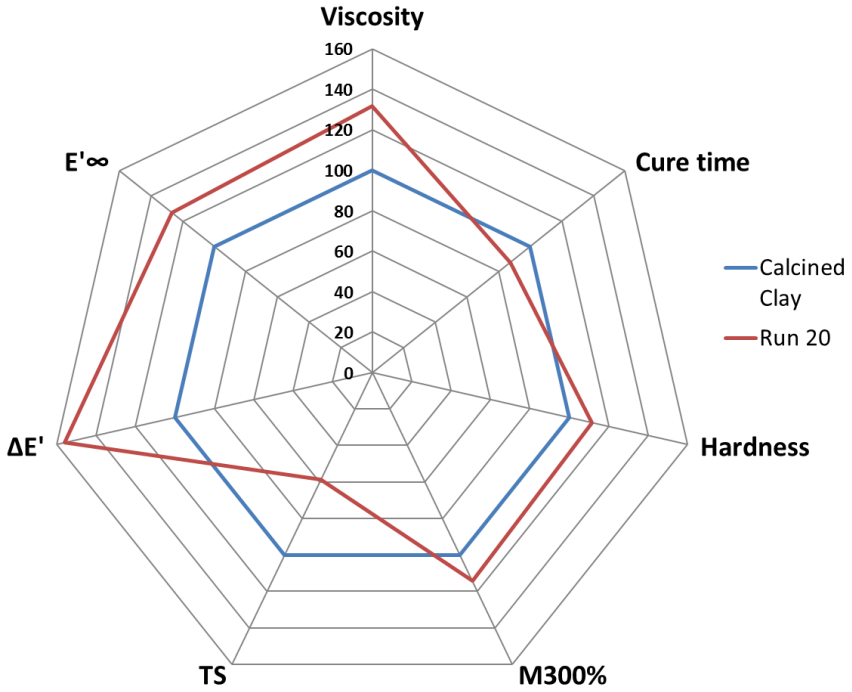


Figure 4-17 Coconut char Run 20 compared to calcined clay

4.6 Conclusion

Coconut shell, through the application of an RSM optimization methodology based upon the surface chemistry and porosity, has been successfully converted into a carbon black-like char filler. The char filler produced was comparable on a physico-chemical basis with the commercial semi-reinforcing carbon black. The surface area was much higher but the surface pH was similar. The results of in-rubber testing reveal that the semi-reinforcing carbon black can be partially replaced by the coconut char filler, since most of the performances testing of the rubber products were highly comparable. According to the Response Surface Methodology, temperature, heating rate and holding time have significant effects on the char quality. One of the optimum conditions for the coconut shell pyrolysis process can be confirmed as 600°C, 10°C/min heating rate, 90min holding time and 550ml/min Nitrogen flow rate. Further optimization of the post-production processing for the char has been identified alongside variations within the rubber formulation and mixing procedure to further improve the filler-rubber interaction, shorten the cure time and enhance the tensile strength.

Chapter 5 Raw Sewage Sludge Derived Char Filler

In this chapter, the char fillers derived from raw sludge has been introduced. This chapter can be divided in three parts. In the first part, the raw sewage sludge feedstock has been analysed for its thermal behaviour, physical and chemical composition using thermal analysis and CHNS test. The second reports the pyrolysis of the sewage sludge and the production of the char fillers through different temperatures, heating rates, holding times and nitrogen flow rates. In the third part, the performance and application of the char fillers has been investigated.

5.1 Characterisation of Raw Sewage Sludge

5.1.1 TGA-DTG Curves

The thermal behaviour of dried sewage sludge (TG and DTG curves) is shown in Figure 5-1, when heated at 10˚C/min from room temperature (≈ 20˚C) up to 1000˚C under a nitrogen atmosphere.

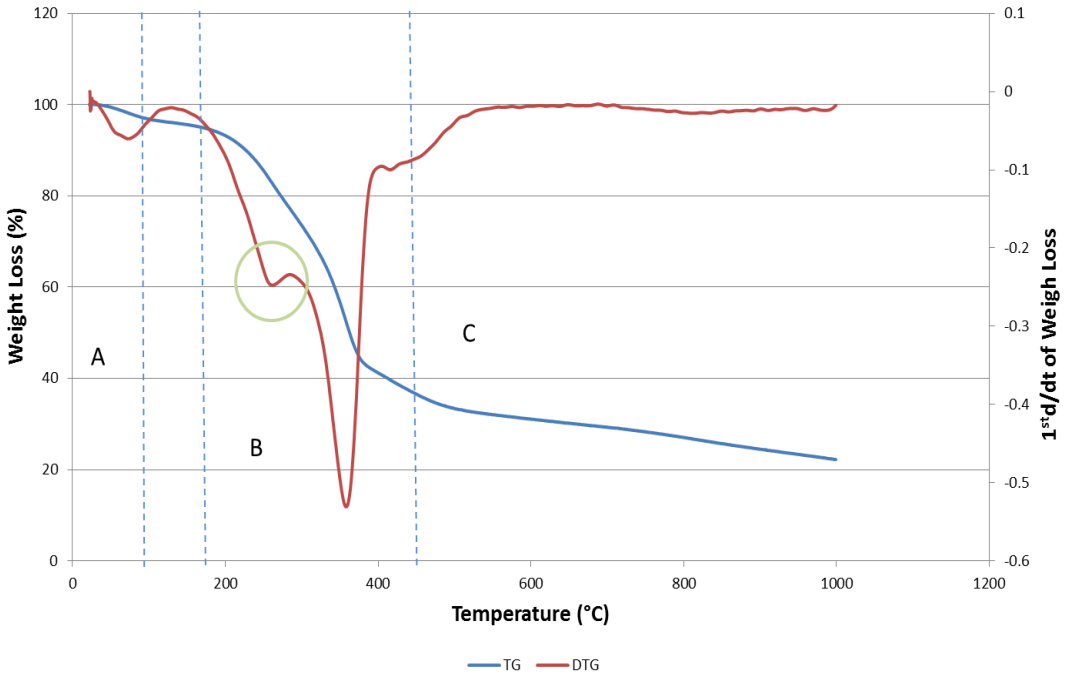


Figure 5-1 TG and DTG curves of sewage sludge under N_2

Three decomposition stages can be identified associated with the peaks on the DTG curve, which are noted as Region A, B and C in the plot. These three stages are: loss of water, main decomposition and final decomposition. The first stage (Region A), correspond to the drying and dehydration processes and takes place up to 100˚C. Then a rapid decrease in the weight of sludge sample initiates at around 200˚C (Region B), which is mainly caused by the decomposition of carbohydrates and lipids. The second pyrolysis stage finishes at around 450˚C, with an average 55 wt. % mass loss. It needs to be mentioned that there is an overlap of different decomposition reactions occurring during the second stage, due to the multitude of compounds present in sewage sludge making it difficult to accurately identify the exact decomposition reactions, which can be concluded from the small shoulder circled in the plot. The final, slow decomposition (Region C), associated with a sharp decrease in the decomposition rate, is most probably due to the secondary decomposition and reorganisation of the pyrolytic carbon layers (slow graphitisation of the char) (Kan et al., 2016; Pullket, 2015).

5.1.2 Proximate Analysis

The proximate analysis of sewage sludge was carried out using the process describes earlier in Section 3.3.1.2 and the result is shown in Figure 5-2.

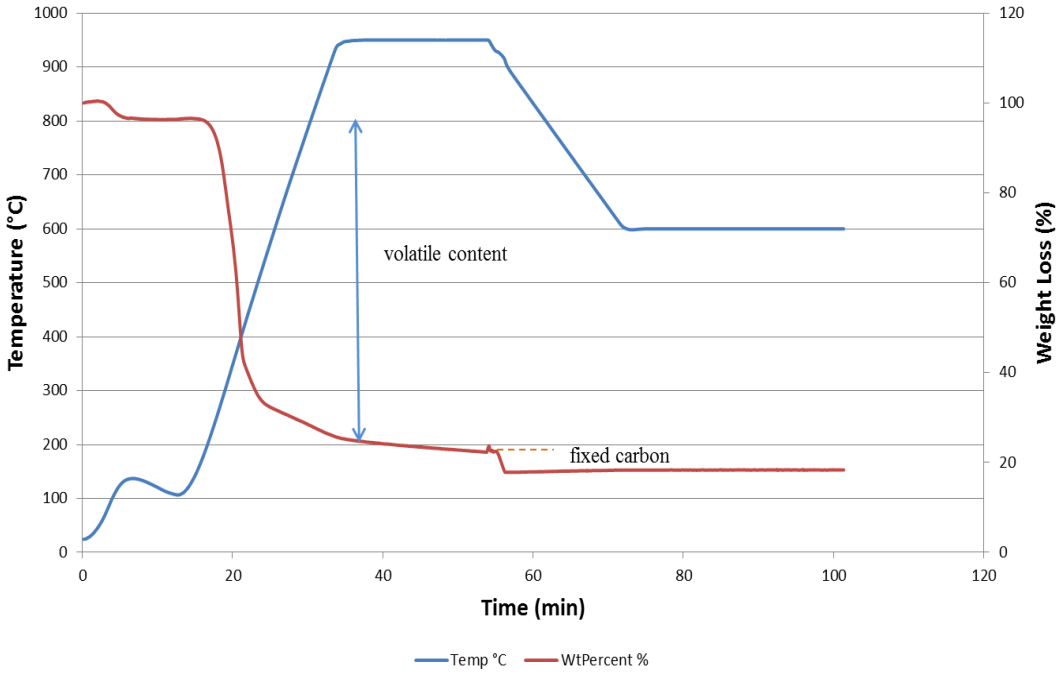


Figure 5-2 Proximate analysis of raw sewage sludge

The high volatile content within the sludge sample contributes to a high oil yield, whereas the solid residue content determined the char yield. It can be seen from the plot that about 70% of the total sludge weight is volatile content, and it is fully decomposed up to 900˚C. Then the gas flow was changed to air and the temperature decreased to 600˚C for determining the char black content. It has been labelled in the plot that the fixed carbon content within the sewage sludge contributes around 5% of the total sample weight. The remaining mass of material corresponds to 20% of the mineral ash content within the sludge feedstock which is found to be considerably higher than in carbon black N772. Further sludge char CHNS test will be undertaken later. This solid yield is higher than that achieved from biomass pyrolysis (Fan et al. 2017). This result was very encouraging, suggesting that the raw sewage sludge has the potential to be used as a suitable feedstock for a suitable char filler.

5.2 Overview of Pyrolysis of Raw Sewage Sludge

The pyrolysis conditions of raw sewage sludge, char yield and oil yield are presented in Table 5-1, the gas yield has been calculated by difference and is shown in the table. It can be seen from Table 5-1, that the solid (char) yield from raw sludge pyrolysis is between 29.4 – 64.2%, which is higher than the char yield from coconut shell, indicating sludge has the potential to produce a good yield of solid residue to be used for substitute rubber filler manufacture. The oil yields ranged from 20.5 to 34.6%, which are quite similar to coconut shell and similarly quite low. The oil and gas products will be discussed further in Chapter 6.

Table 5-1 Char, oil and gas yield from pyrolysis of sewage sludge

Run	Temperature (˚C)	Heating rate (˚C/min)	Holding time (min)	N_2 flow rate (ml/min)	Char yield (%)	Oil yield (%)	Gas yield (%)
1	600	10	90	550	33.6	31.4	35.0
2	400	15	0	1000	64.2	20.5	15.3
3	400	15	0	100	63.2	23.1	13.7
4	400	5	180	1000	38.5	29.1	32.4
5	600	10	90	550	34.7	29.6	35.7
6	600	10	180	550	34.7	29.0	36.3
7	600	15	90	550	29.9	25.6	44.5
8	800	5	180	100	30.0	34.6	35.4
9	400	15	180	100	40.9	32.5	26.6
10	600	10	0	550	36.6	29.3	34.1
11	600	10	90	550	35.1	28.3	36.6
12	400	5	0	1000	47.8	26.8	25.4
13	800	15	180	100	26.3	25.2	48.5
14	800	15	0	1000	32.1	24.6	43.3
15	600	10	90	100	33.8	25.8	40.4
16	800	10	90	550	30.7	27.6	41.7
17	800	15	0	100	34.1	22.4	43.5
18	400	15	180	1000	38.3	22.2	39.5
19	600	10	90	1000	33.7	25.5	40.8
20	600	10	90	550	34.8	26.6	38.6
21	400	5	0	100	49.8	30.0	20.2
22	800	5	180	1000	29.8	28.6	41.6
23	400	5	180	100	41.0	34.7	24.3
24	600	5	90	550	33.6	29.6	36.8
25	600	10	90	550	31.8	27.3	40.9
26	400	10	90	550	41.7	31.9	26.4
27	800	5	0	100	33.4	28.7	37.9
28	800	5	0	1000	29.4	31.9	38.7
29	800	15	180	1000	30.8	26.6	42.6
30	600	10	90	550	32.0	25.2	42.8

The perturbation plot for the sludge char yield is presented in Figure 5-3, where A is pyrolysis temperature, B represents heating rate, C is holding time and D is noted as Nitrogen flow rate. According to the perturbation plot, the effects of pyrolysis variables on the sludge char yield can be determined. It can be concluded from the data and plot that pyrolysis temperature and holding time have positive effects on the char yield, whereas heating rate and nitrogen flow rate have little influence on the char yield. High temperature and long holding time contribute to a complete pyrolysis avoiding volatile content remaining in the char sample, so that a lower char yield is achieved. Unlike coconut shell, not only temperature, but holding time can influence the char yield from pyrolysis of sewage sludge.

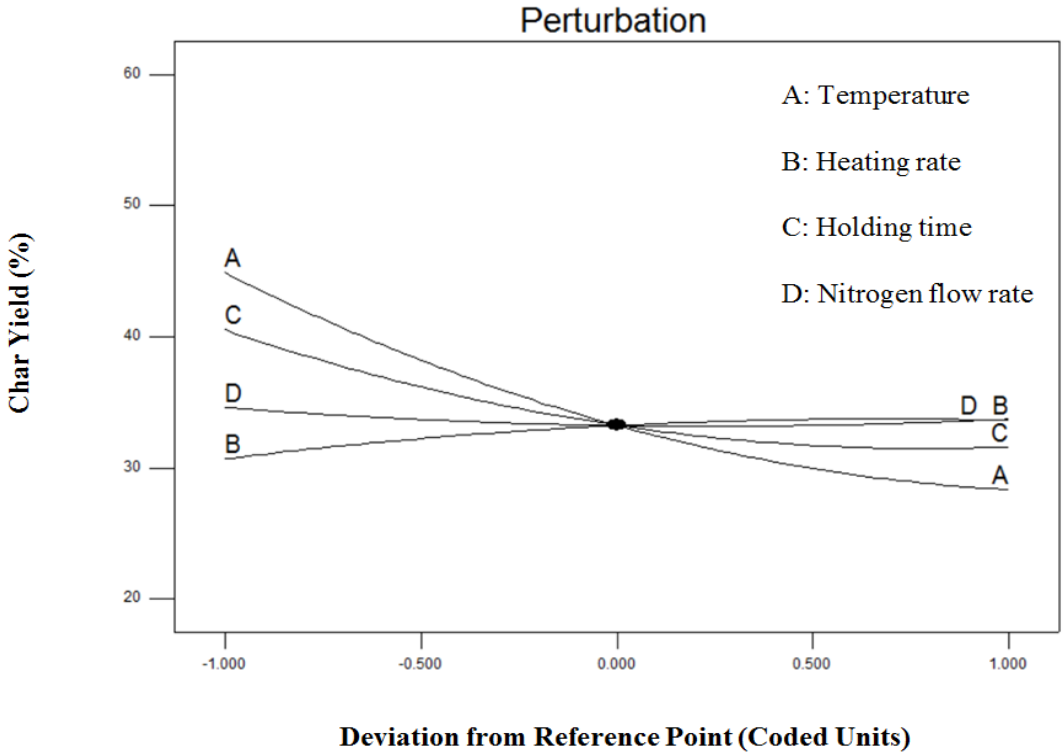


Figure 5-3 Perturbation plots with four pyrolysis parameters on the sludge char yield

5.3 Characteristics of Commercial Carbon Blacks and Sludge Char Fillers

The transmittance of toluene extract (T%), pH value, BET surface area, T-plot surface area and acidic and basic groups on the surface of both commercial carbon black N772 and N330, plus these values measured for the sludge char produced under the RSM design are summarised in Table 5-2.

Table 5-2 Characterization of carbon black and sludge char filler

Run	T%	pH value	BET surface area (m^2/g)	t-plot surface area(m^2/g)	Acidic groups (mmol/g)	Basic groups (mmol/g)
1	99.82	7.77	66.92	25.82	0.513	1.247
2	59.37	5.19	7.40	9.74	1.326	0.604
3	54.14	5.20	7.54	9.88	1.223	0.647
4	98.14	5.77	9.97	8.37	1.165	1.041
5	99.85	7.82	41.57	24.06	0.539	1.216
6	99.89	7.64	34.25	25.35	0.521	1.216
7	100	6.68	115.02	39.02	0.852	1.244
8	99.79	8.34	79.89	46.41	0.310	1.603
9	97.96	5.94	11.78	12.03	1.256	1.102
10	99.83	7.04	34.82	18.49	0.691	1.144
11	99.99	7.85	ND*	ND	0.444	0.486
12	84.73	5.58	5.19	6.26	1.385	0.847
13	99.73	7.21	160.21	98.63	0.917	1.425
14	99.92	8.28	57.23	37.37	0.432	1.550
15	100	6.94	117.02	37.00	0.767	1.188
16	100	8.14	108.78	63.28	0.480	1.517
17	99.69	7.33	103.7	47.64	0.833	1.252
18	100	6.36	107.34	40.90	1.317	1.192
19	100	6.62	77.39	27.12	0.915	1.117
20	100	7.10	72.60	26.44	0.683	1.123
21	84.08	5.40	10.03	11.38	1.375	0.783
22	100	8.27	52.44	29.68	0.524	1.525
23	98.34	5.91	11.80	12.03	1.269	0.933
24	99.84	7.06	128.65	39.39	0.647	1.236
25	100	6.66	109.54	45.49	0.868	1.202
26	84.10	5.30	11.38	14.40	1.403	0.894
27	100	7.77	147.75	57.99	0.725	1.338
28	99.96	6.85	151.03	60.99	0.913	1.355
29	99.84	8.25	97.55	58.72	0.478	1.523
30	99.74	6.77	123.51	44.61	0.852	1.210
Sludge char filler	54.14 – 100	5.19 – 8.34	5.19 – 160.21	6.26 – 98.63	0.31 – 1.403	0.486 – 1.603
N772	65.9	8.5	28.5	26.6	0	0.079
N330	99.5	8.9	71.5	69.7	0.81	0.08

*ND = No data

According to the data of the sludge char prepared as part of this research, it is obvious that most of the char samples have toluene transmittance values close to N330, indicating that they are essentially free from tarry residues and comparable with the higher quality carbon black.

As discussed in Section 4.3, the wider meso and macro pores are essential for bonding process between rubber and filler. In Table 5-2, results of the sludge char indicate that meso and macro pores occupied most of the surface area of carbon blacks, which is the same trend followed by carbon blacks and coconut chars, confirming that sludge char samples is suitable to be used as an alternative rubber filler.

The surface pH value is another essential property of the char filler since it correlates with the vulcanization time and the number of free radicals on the filler surface. According to the data in Table 5-2, unlike the commercial carbon black pH value around 9, the pH value of many of the char samples was around 7 which may not be sufficiently alkaline.

With regard to the quantities of acidic and basic groups on the surface of sludge char samples, they are much more prevalent than on both commercial carbon blacks and coconut shell chars. High numbers of surface groups may lead to a more active surface for char fillers, so that is helpful for development of the interaction between rubber and char fillers. This feature of the production process will be further analysed in the following RSM optimization section.

5.4 RSM Process Optimization

The optimization in this research was conducted by using the pH value, t-plot surface area and acidic groups on the surface of sludge chars as response metrics.

5.4.1 Sludge Char Filler pH Value Response Analysis

5.4.1.1 Statistical Analysis

The optimization for sludge was conducted by using the pH value as one of the main response metrics. The methodology applied has been described earlier, with the substitution of a pH value of 7 being used in the response value for the sludge chars. The linear model which was chosen in this study, for estimating the response surface of pH value, was given in the equation:

$$Y_1 = A + BX_1 + CX_2 + DX_3 + EX_4$$

Where Y_1 is the pH value of char filler, A is the value of the fixed response at the centre point of the design, B, C, D, E are the linear coefficients. X_1, X_2, X_3, X_4 are the independent design variables.

5.4.1.2 Optimization of Pyrolysis Process on the pH Value and Interaction between Independent Variables

The statistical design factors in both code and actual value, and the experimental response and predicted values on pH value, t-plot surface area and acidic surface groups of sludge char filler are summarized in Table 5-3.

The regression equation characterizing the influence of different considered parameters on pH value was concluded as:

$$Y_1 = 6.90 + 1.10X_1 - 0.028X_2 + 0.28X_3 + 0.063X_4$$

Equation 3

In this equation, the influences of pyrolysis temperature and holding time have relatively high significant positive influences on the char filler pH value. Thus, with increasing pyrolysis temperature and longer holding times, the pH value becomes more acidic.

Table 5-3 Experimental design matrix with experimental and predicted values

Run	Temperature		Heating rate		Holding time		N_2 flow rate		pH value		t-plot surface area		Acidic groups	
	˚C		˚C/min		min		ml/min				m2/g		mmol/g	
	X_1		X_2		X_3		X_4		Y_1		Y_2		Y_3	
	Coded value	Actual value	Coded value	Actual value	Coded value	Actual value	Coded value	Actual value	Experimental data	Predicted data	Experimental data	Predicted data	Experimental data	Predicted data
1	0	600	0	10	0	90	0	550	7.77	6.90	25.82	32.62	0.513	0.680
2	-1	400	1	15	-1	0	1	1000	5.19	5.56	9.74	9.26	1.326	1.239
3	-1	400	1	15	-1	0	-1	100	5.20	5.43	9.88	15.24	1.223	1.301
4	-1	400	-1	5	1	180	1	1000	5.77	6.17	8.37	8.26	1.165	1.255
5	0	600	0	10	0	90	0	550	7.82	6.90	24.06	32.62	0.539	0.680
6	0	600	0	10	1	180	0	550	7.64	7.18	25.35	36.64	0.521	0.506
7	0	600	1	15	0	90	0	550	6.68	6.87	39.02	37.14	0.852	0.735
8	1	800	-1	5	1	180	-1	100	8.34	8.25	46.41	55.98	0.310	0.419
9	-1	400	1	15	1	180	-1	100	5.94	5.99	12.03	23.28	1.256	1.401
10	0	600	0	10	-1	0	0	550	7.04	6.62	18.49	28.60	0.691	0.634
11	0	600	0	10	0	90	0	550	7.85	6.90	ND*	ND	0.444	0.680
12	-1	400	-1	5	-1	0	1	1000	5.58	5.61	6.26	0.22	1.385	1.519
13	1	800	1	15	1	180	-1	100	7.21	8.19	98.63	65.02	0.917	0.771
14	1	800	1	15	-1	0	1	1000	8.28	7.76	37.37	51.00	0.432	0.573
15	0	600	0	10	0	90	-1	100	6.94	6.84	37.00	35.61	0.767	0.822

Table 5-3 Experimental design matrix with experimental and predicted values (continued)

16	1	800	0	10	0	90	0	550	8.14	8.00	63.28	53.49	0.480	0.570
17	1	800	1	15	-1	0	-1	100	7.33	7.63	47.64	56.98	0.833	0.763
18	-1	400	1	15	1	180	1	1000	6.36	6.12	40.90	17.3	1.317	1.295
19	0	600	0	10	0	90	1	1000	6.62	6.96	27.12	29.63	0.915	0.798
20	0	600	0	10	0	90	0	550	7.10	6.90	26.44	32.62	0.683	0.680
21	-1	400	-1	5	-1	0	-1	100	5.40	5.49	11.38	6.20	1.375	1.333
22	1	800	-1	5	1	180	1	1000	8.27	8.37	29.68	50.00	0.524	0.433
23	-1	400	-1	5	1	180	-1	100	5.91	6.05	12.03	14.24	1.269	1.113
24	0	600	-1	5	0	90	0	550	7.06	6.93	39.39	28.10	0.647	0.699
25	0	600	0	10	0	90	0	550	6.66	6.90	45.49	32.62	0.868	0.680
26	-1	400	0	10	0	90	0	550	5.30	5.80	14.40	11.75	1.403	1.250
27	1	800	-1	5	-1	0	-1	100	7.77	7.69	57.99	47.94	0.725	0.731
28	1	800	-1	5	-1	0	1	1000	6.85	7.81	60.99	41.96	0.913	0.789
29	1	800	1	15	1	180	1	1000	8.25	8.32	58.72	59.04	0.478	0.537
30	0	600	0	10	0	90	0	550	6.77	6.90	44.61	32.62	0.852	0.680

*ND = No data

5.4.1.3 Statistical Analysis and Validation of Model

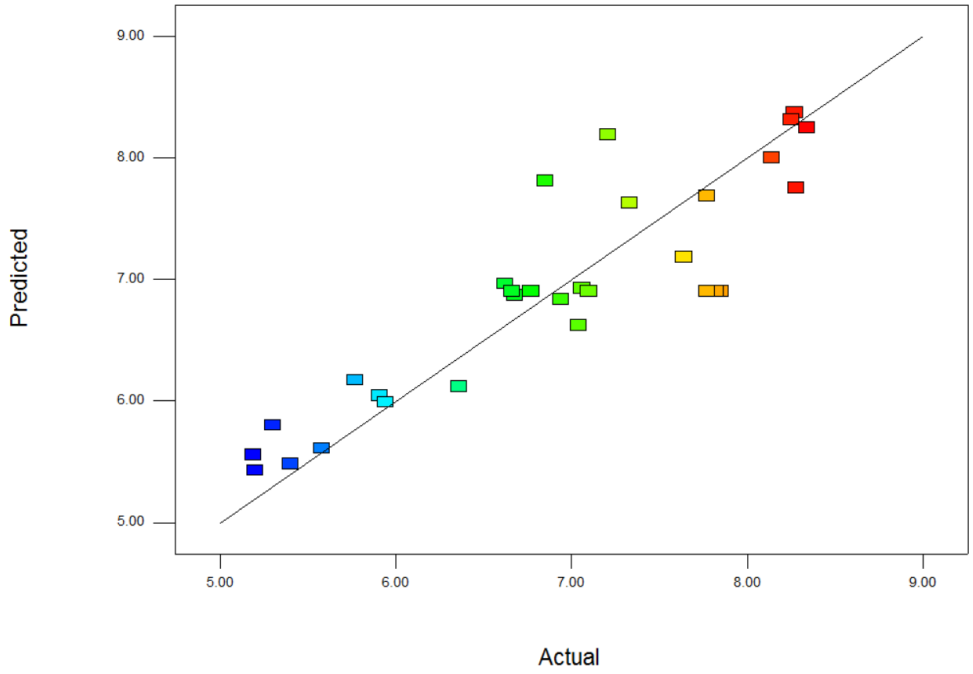
The validation of the fitted model (see Equation 3 above) was calculated and its statistical significance was evaluated by an F-test. The investigation of variance (ANOVA) for the response surface linear model is shown in Table 5-4. According to the data in the table, the model is highly statistically significant at 95% confidence level, with an F-value of 23.55, and low probability P value of less than 0.0001. The value of the determination coefficients R^2 and R^2_{adj} were estimated as 0.7903 and 0.7567 respectively. This means that about 79.03% of the variance is attributed to the variables and indicates a highly significant. The adequacy of the regression model can also be confirmed from the good agreement between the experimental and predicted values of response pH value shown in Table 5-3. The actual char pH value ranges from 5.19 to 8.34, whereas the corresponding predicted values are from 5.43 and 8.37. The noise ratio is 14.503, which is greater than 4 and indicates an adequate signal. This model can be considered to be suitable to be used to navigate the design space. The lack of fit F-value of 0.77 shows that lack of fit is not significant relative to the pure error. There is a 69.89% possibility that a lack of fit F-value this large could occur due to noise, which is make the model usable.

Table 5-4 Analysis of variance of the fitted linear regression model

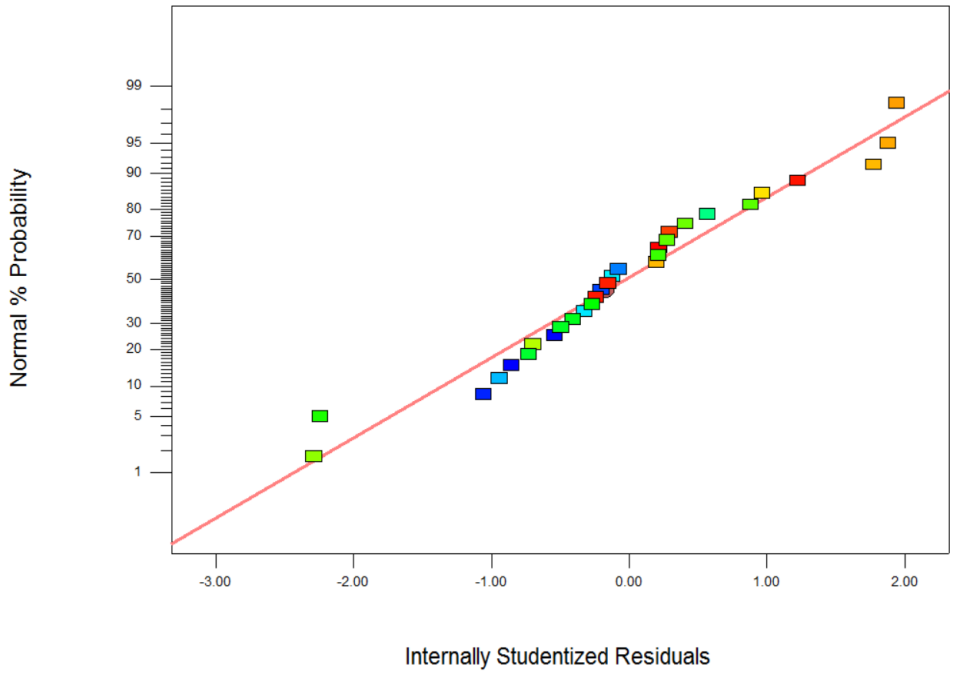
Source	Sum of Squares	Mean Square	F-Value	P-value	Remarks
Model	23.26	5.82	23.55	< 0.0001	significant
X_1	21.76	21.76	88.11	< 0.0001	significant
X_2	0.014	0.014	0.059	0.8108	not significant
X_3	1.42	1.42	5.74	0.0244	not significant
X_4	0.071	0.071	0.29	0.5967	not significant
Residual	6.17	0.25	-	-	-
Lack of Fit	4.65	0.23	0.77	0.6989	not significant
Pure Error	1.52	0.30	-	-	-

The relationship between predicted and experimental values of the pH value of sludge char fillers is presented in Figure 5-4(a). It is evident that the correlation between the predicted

and experimental values is good, which indicates that the predicted and experimental values were in reasonable agreement. The data fits well using the model and a powerful estimate of response for the system with the experimental range was achieved.



(a)

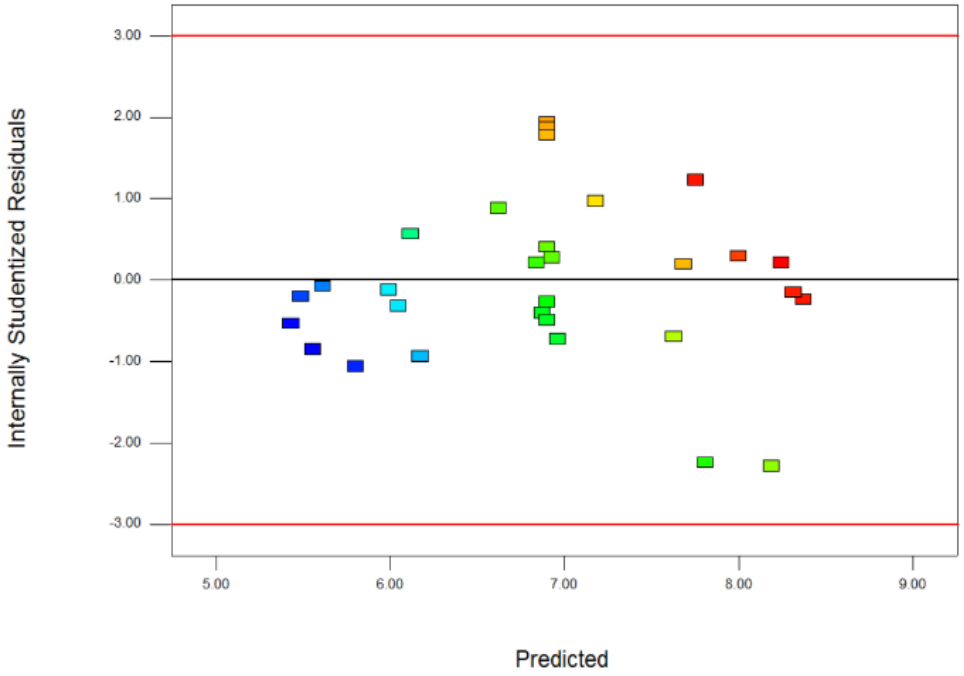


(b)

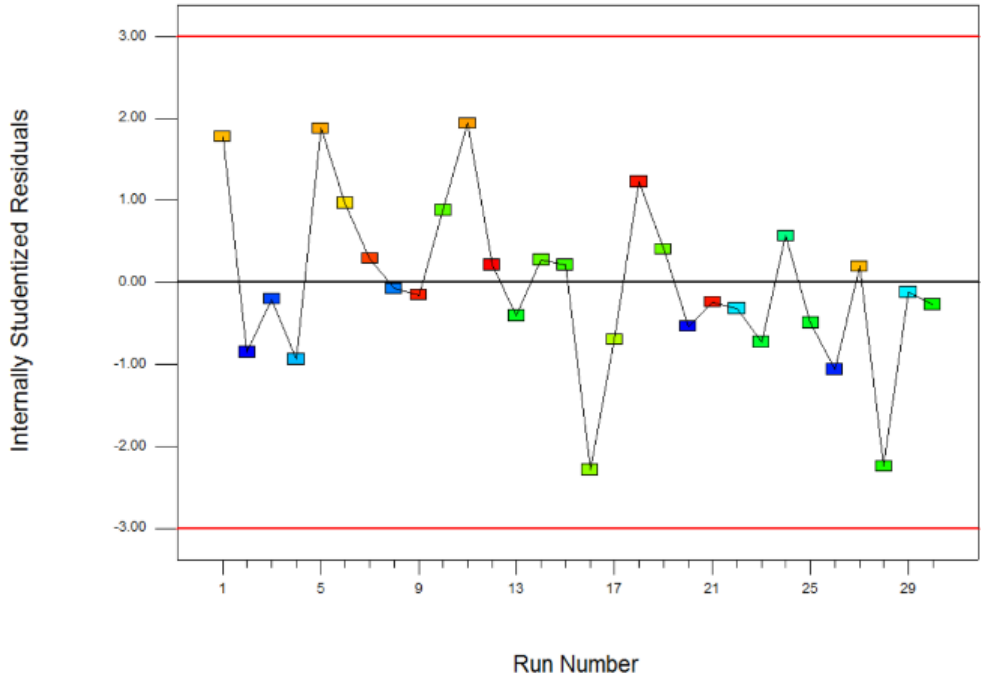
Figure 5-4 (a) Experimental pH values and predicted pH values for the model & (b) Normal probability plot of the residues

The normal probability plot of the standardized residuals for pH value of sludge chars is shown in Figure 5-4(b). It has been mentioned before that the points would show a straight line in the normal probability plot, when the residuals follow a normal distribution. It can be assumed from the figure that the data is a normal distribution, regardless of some scattering which may occur even with the normal data. Therefore, a good validity for the approximation of the quadratic regression model can be assumed by the obtained normal probability plot.

The plot of residual versus predicted values for pH is shown in Figure 5-5(a). According to the randomly scattered observed points in the constant range of residuals, there is no obvious pattern and unusual structure to be followed. Therefore, the model is regarded as adequate and the violations of the independence or constant variance assumption in all runs is confirmed. Figure 5-5(b) presents the plot of the standardized residuals versus runs. The points are located randomly within ±3, which indicates that the errors were normally distributed and insignificant.



(a)



(b)

Figure 5-5 Diagnostic plots for pH value (a) residual versus predicted pH value and (b) residual versus run number

5.4.1.4 Optimization of Pyrolysis Process based on pH Value and Model Verification

The optimization process was carried out to determine the optimum value of pH 7 through the Design Expert 8.0 software. Accordingly, the optimum working conditions and respective pH value were established. The results are presented in Table 5-5. All the desirability function values of the five conditions were found to be 1.000 for these optimum conditions. The laboratory experiment (temperature 600˚C, 10˚C/min heating rate, 90min pyrolysis holding time and 550mL/min nitrogen flow rate) agrees well with the predicted response value of 7.1, which indicates that process optimization by CCFD was a suitable and reliable methodology to optimize the process at the chosen pH value for the sludge pyrolysis process.

Table 5-5 Optimum condition solution for optimum pH value

Number of trial	Temperature °C	Heating rate °C/min	Holding time min	N2 flow rate ml/min	pH value	Desirability
1	610.58	9.38	99.82	595.58	7.0	1.000
2	602.37	10.19	98.26	987.04	7.0	1.000
3	605.00	5.18	103.28	567.52	7.0	1.000
4	622.83	9.45	98.65	142.00	7.0	1.000
5	574.70	10.80	168.66	528.86	7.0	1.000

5.4.2 Sludge Char Filler t-plot Value Response Analysis

5.4.2.1 Statistical Analysis

The linear model has been selected for analysing the response surface for the t-plot, shown in the equation:

$$Y_2 = A + BX_1 + CX_2 + DX_3 + EX_4$$

Where Y_2 is the t-plot surface area of sludge char filler, A is the value of the fixed response at the centre point of the design, B, C, D, E are the linear coefficients. X_1, X_2, X_3, X_4 are the independent design variables (Temperature, heating rate, holding time and nitrogen flow rate).

5.4.2.2 Optimization of Pyrolysis Process on the t-plot Surface Area and Interaction between Independent Variables

The regression equation characterizing the influence of different considered parameters on pH value was concluded as:

$$Y = 32.62 + 20.87X_1 + 4.52X_2 + 4.02X_3 - 2.99X_4$$

Equation 4

From this equation, the response of pyrolysis temperature has a highly significant positive effect on the sludge char filler t-plot surface area. Heating rate and holding time have slightly positive influences while the nitrogen flow rate has a negative influence on the sludge char t-

plot surface area. The experimental response and predicted values calculated from the equation for the t-plot surface area can be seen from Table 5-3.

5.4.2.3 Statistical Analysis and Validation of Model

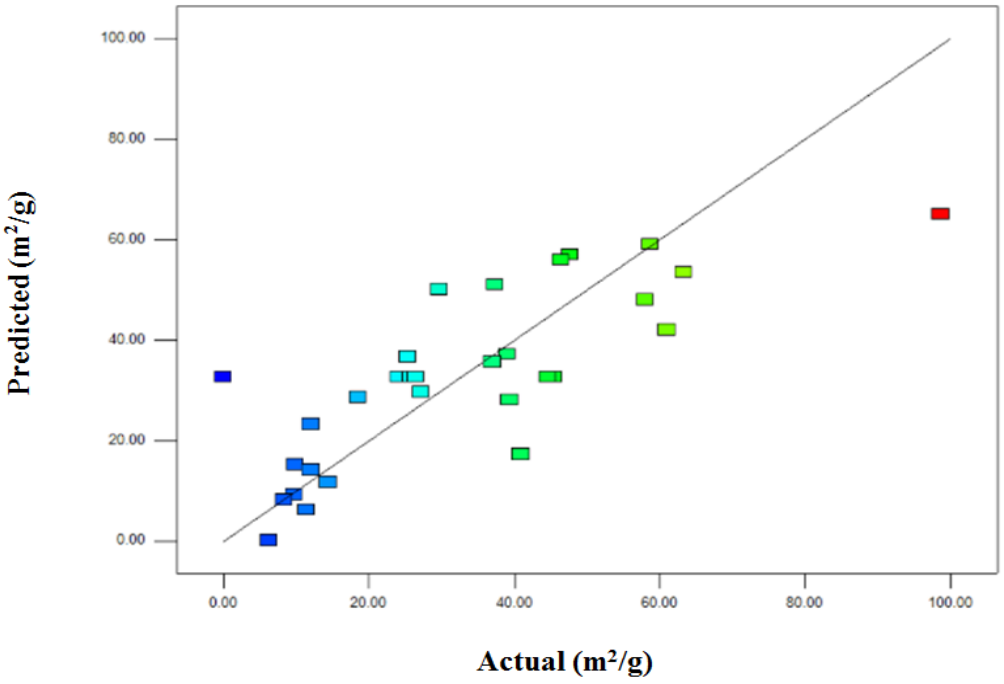
The ANOVA for the t-plot surface area response surface linear model (see Equation 4 above) is presented in Table 5-6. It can be seen that the model F-value is 10.50 and the P-values are less than 0.0500, implying the model and terms are significant. The "Lack of Fit F-value" of 0.68 indicated that the Lack of Fit is not significant relative to the pure error. The R^2 and R^2_{adj} were calculated as 0.6269 and 0.5672. In other words, 62.69% of the variance is based on the factors, so that a high significance for the model can be achieved. The noise ratio is 11.057 in this analysis, which is higher than 4, confirming an adequate signal. Thus, this model can be used to navigate the design space.

Table 5-6 Analysis of variance of the fitted linear regression model

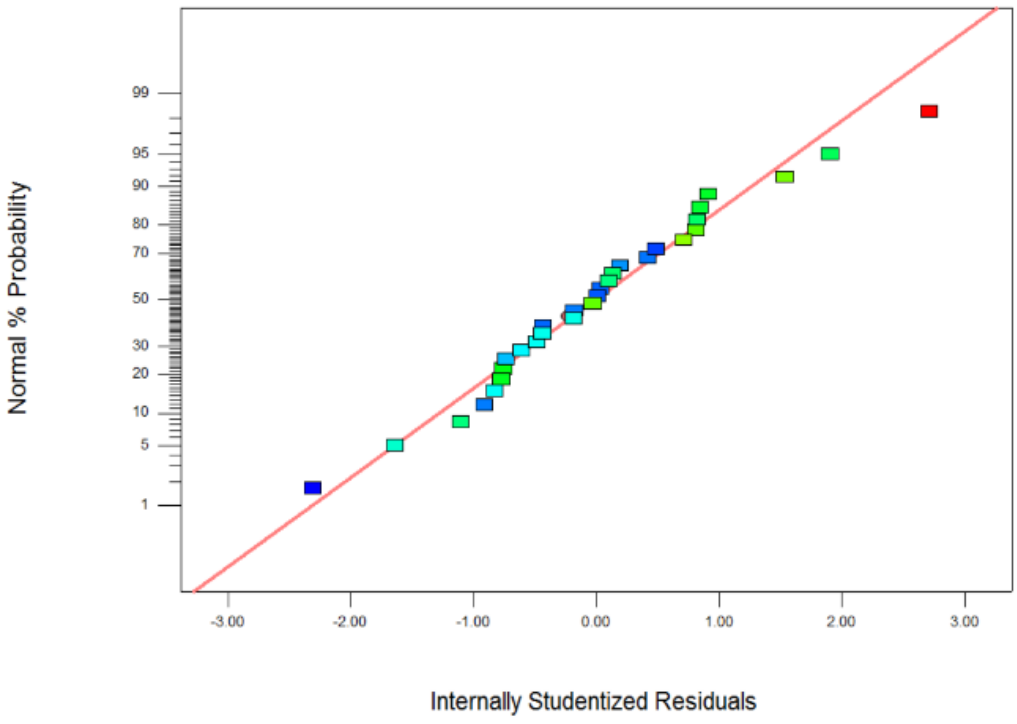
Source	Sum of Squares	Mean Square	F-Value	P-value	Remarks
Model	8663.03	2165.78	10.50	< 0.0001	significant
X_1	7842.68	7842.68	38.03	< 0.0001	significant
X_2	368.40	368.40	1.79	0.1934	not significant
X_3	290.93	290.93	1.41	0.2461	not significant
X_4	161.03	161.03	0.78	0.3853	not significant
Residual	5154.95	206.20	-	-	-
Lack of Fit	3766.72	188.34	0.68	0.7577	not significant
Pure Error	1388.23	277.65	-	-	-

The agreement of the model on t-plot surface area can also be confirmed by Figure 5-6. Figure 5-6(a) shows the good regression between predicted and experimental values of the t-plot surface area. The normal probability plot of the standardized residuals for t-plot surface area analysis is presented in Figure 5-6(b). All the points are located in one line indicating the

data is normally distributed and offers a good validity for the approximation of the linear model.



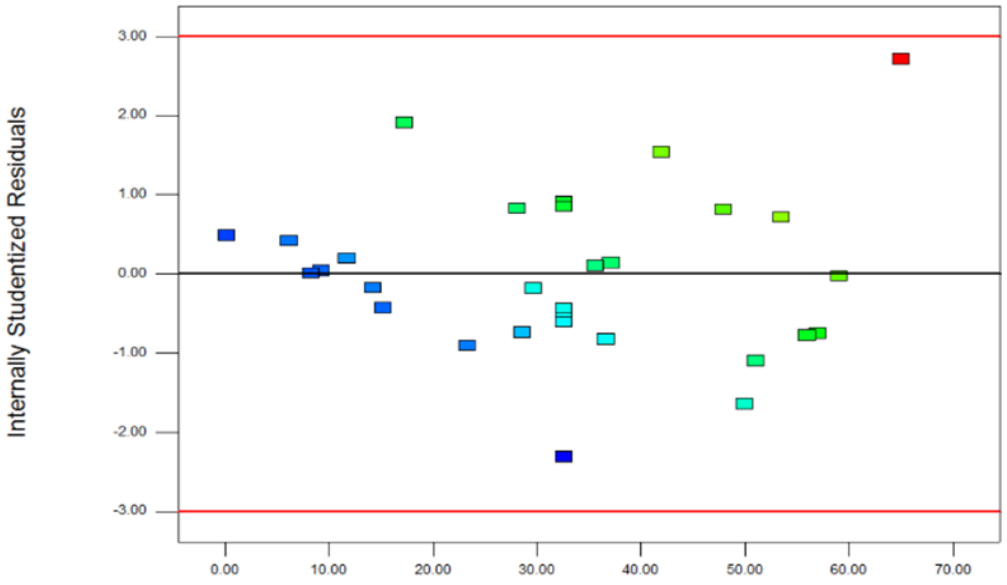
(a)



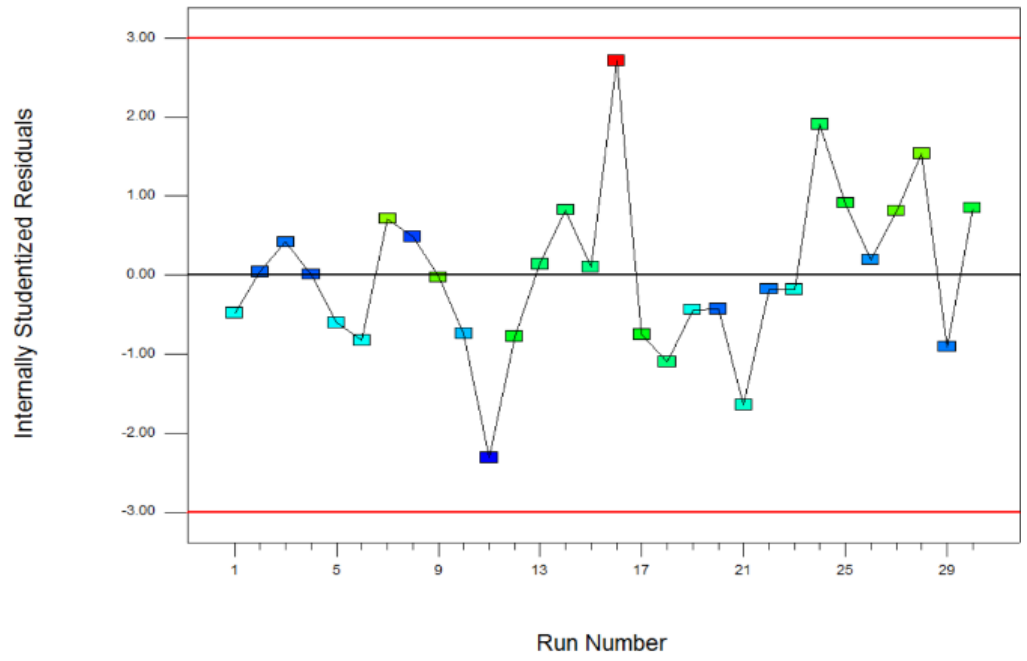
(b)

Figure 5-6 (a) Experimental t-plot surface area values and predicted t-plot surface area values for the model & (b) Normal probability plot of the residuals

The plot of residual versus predicated values for t-plot surface area are shown in Figure 5-7(a), while Figure 5-7(b) shows the standardised residuals against runs. The randomly located points can be seen in both of the plots, which imply that the model is adequate and fits the data. The errors are not significant.



(a)



(b)

Figure 5-7 Diagnostic plots for t-plot surface area value (a) residual versus predicated value and (b) residual versus run number

5.4.2.4 Optimization of Pyrolysis Process based on t-plot Surface Area and Model Verification

The optimization process was carried out to ensure that the optimum value of t-plot surface area is maximum through the software. The results are presented in Table 5-7. The desirability function values of the five conditions are all found to be 1.000 for these optimum conditions. The laboratory experiment (temperature 800˚C, 15˚C/min heating rate, 180min pyrolysis holding time and 100mL/min nitrogen flow rate) agrees well with the predicted largest response value, which indicates that process optimization by CCFD was a suitable and reliable methodology for the sludge pyrolysis process.

Table 5-7 Optimum condition solution for optimum t-plot surface area

Number of trial	Temperature °C	Heating rate °C/min	Holding time min	N_2 flow rate ml/min	t-plot surface area m^2/g	Desirability
1	799.98	14.99	179.95	101.30	65.00	1.000
2	799.99	15.00	179.79	106.75	64.97	1.000
3	800.00	14.97	179.25	100.00	64.97	1.000
4	799.97	15.00	176.80	100.00	64.88	0.998
5	799.07	15.00	178.10	100.00	64.84	0.998

5.4.3 Sludge Char Surface Acidic Groups Response Analysis

Unlike the coconut shell char samples, there are a significant number of acidic groups on the surface of the sludge char. Therefore, an RSM analysis on the surface acidic groups is required for sludge char.

5.4.3.1 Statistical Analysis

A quadratic polynomial model was required for evaluating the response surface of acidic groups, which is described by the equation:

$$Y_3 = \beta_0 + \sum_{i=1}^{4} \beta_i x_i + \sum_{i=1}^{3} \sum_{j=i+1}^{4} \beta_{ij} x_i x_j + \sum_{i=1}^{4} \beta_{ii} x_i^2$$

Where Y_3 is the surface acidic groups, β_0 is the value of the fixed response at the center point of the design, β_i, β_{ij}, and β_{ii} are the linear, interactive, and quadratic coefficients, respectively. x_i and x_j are the independent design variables.

5.4.3.2 Optimization of the Pyrolysis Process on Surface Acidic Groups and Interaction Between Independent Variables

The regression equation illustrating the influnece of the 4 pyrolysis factors on surface acidic groups was shown as:

$$Y_1 = 0.68 - 0.34X_1 + 0.018X_2 - 0.064X_3 - 0.012X_4 + 0.016X_1X_2 - 0.023X_1X_3 - 0.032X_1X_4 + 0.08X_2X_3 - 0.062X_2X_4 - 0.011X_3X_4 + 0.23X_1^2 + 0.037X_2^2 - 0.11X_3^2 + 0.13X_4^2$$

Equation 5

According to the sign in front of the terms in the equation and the Parato chart shown in Figure 5-8, the main influence of the pyrolyisis variables to the response surface acidic groups can be interpreted. The negative effect of pyrolysis temperature is highly significant in terms of the numbers of acidic groups created and destroyed. With increasing temperature, the number of the acidic groups will decrease sharply. However, the quadratic effect of temperature and nitrogen flow rate have a relative significant positive effect upon acidic groups.

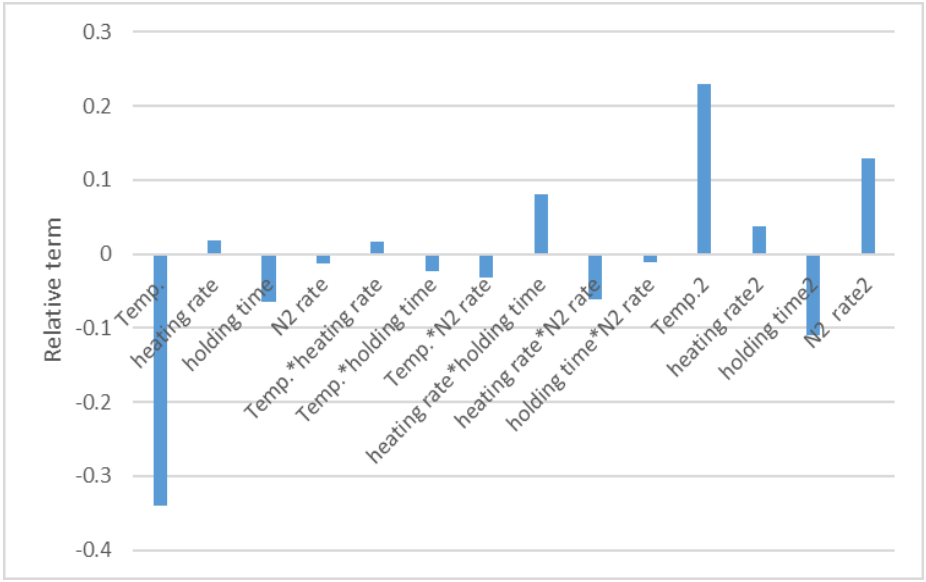


Figure 5-8 Pareto chart showing the effects of different independent variables on surface acidic groups

5.4.3.3 Statistical Analysis and Validation of the Model

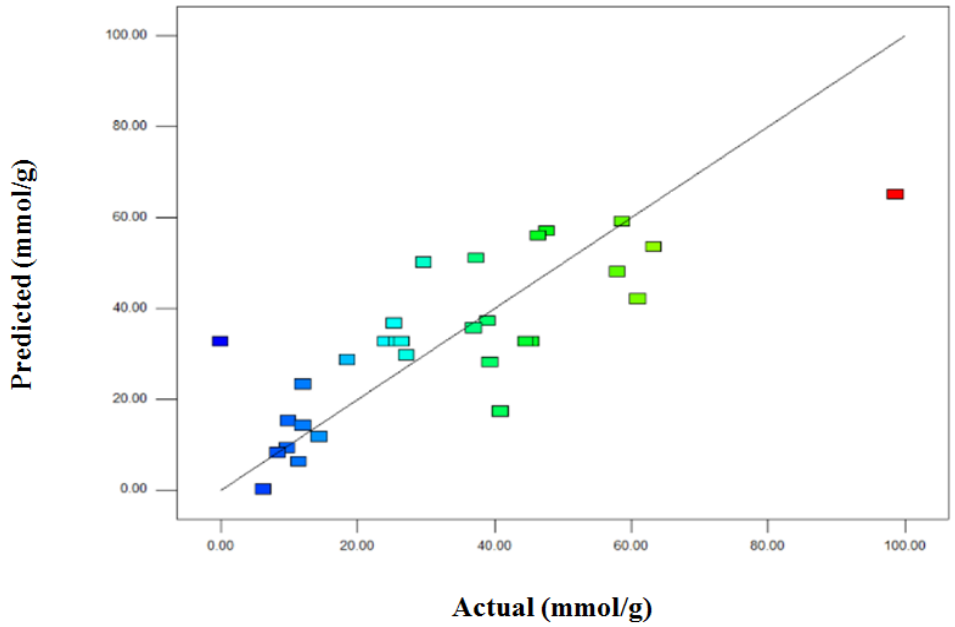
The validation of the fitted model (see Equation 5 above) and its statistical significance were estimated by F-test. The ANOVA for the response surface full quadratic model is shown in Table 5-8. According to the table, the model is highly statistically significant at 95% confidence level, with an F-value of 7.71 and low probability P-value 0.0002. The values of the determination coefficients R^2 and R^2_{adj} for model fitting reliablity were calcualted to be 0.8780 and 0.7642 respectively. This means that about 87.80% of the variance is correlated to the variables and suggests a high significance for the model.

Table 5-8 Analysis of variance of the fitted quadratic regression model

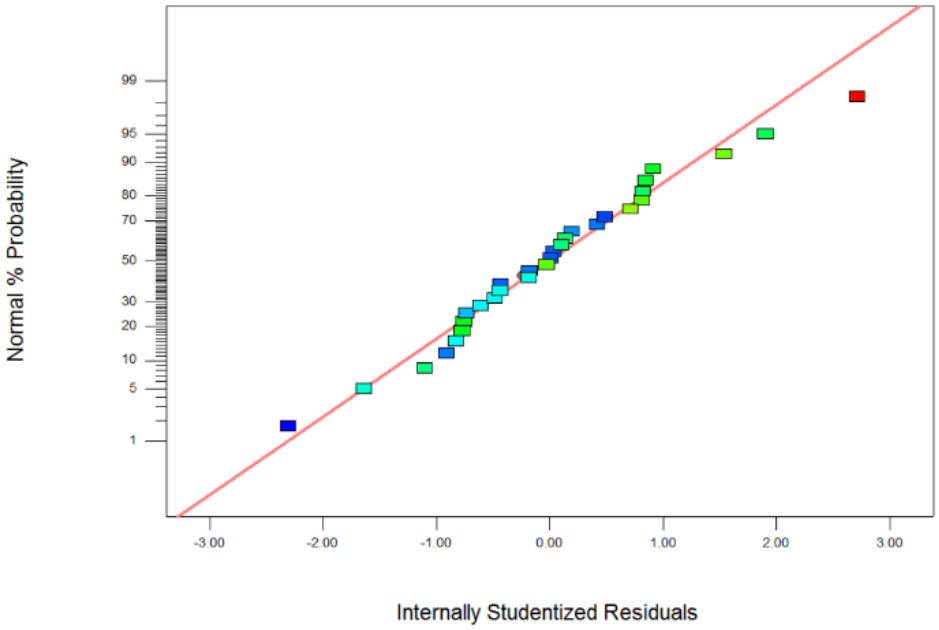
Source	Sum of Squares	Mean Square	F-Value	P-value	Remarks
Model	2.94	0.21	7.71	0.0002	significant
X_1	2.07	3.07	76.03	< 0.0001	significant
X_2	5.724E-003	5.724E-003	0.21	0.6533	not significant
X_3	0.073	0.073	2.68	0.1226	not significant
X_4	2.689E-003	2.689E-003	0.099	0.7578	not significant
X_1X_2	4.225E-003	4.225E-003	0.16	0.6993	not significant
X_1X_3	8.649E-003	8.649E-003	0.32	0.5815	not significant
X_1X_4	0.016	0.016	0.59	0.4537	not significant
X_2X_3	0.10	0.10	3.78	0.0708	not significant
X_2X_4	0.061	0.061	2.22	0.1569	not significant
X_3X_4	1.764E-003	1.764E-003	0.065	0.8026	not significant
X_1^2	0.14	0.14	4.99	0.0412	significant
X_2^2	3.560E-003	3.560E-003	0.13	0.7228	not significant
X_3^2	0.029	0.029	1.08	0.3158	not significant
X_4^2	0.043	0.043	1.57	0.2292	not significant
Residual	0.41	0.027			
Lack of Fit	0.25	0.025	0.75	0.6714	not significant
Pure Error	0.16	0.033			

A good alignment of the model also can be concluded by the positive agreement between the experimental and the predicted values for response acidic groups, as shown in Table 5-3. The actual concentrations of acidic groups formed are between 0.31 and 1.375, whereas the corresponding predicted values ranged from 0.419 to 1.333. The noise of ratio is 11.057, which is higher than 4, indicating an adequate signal and implying that this model is sufficiently reliable to be used to guide the design process. The lack of fit F-value is 0.75, which means that the lack of fit is not significant relative to the pure error. There is a 67.14% chance that a "Lack of Fit F-value" this large could occur due to noise.

The comparasion between experimental and predicted values of the surface acidic groups is shown in Figure 5-9(a). It can be clearly seen that the correlation between the two values is acceptable, which indicating a reasonable agreement of the model. All the points are located in one line in the normal probability plots of the standardized residuals for t-plot surface area analysis in Figure 5-9(b) indicating the data is normally distribution and a good validity for the approximation of the linear model.



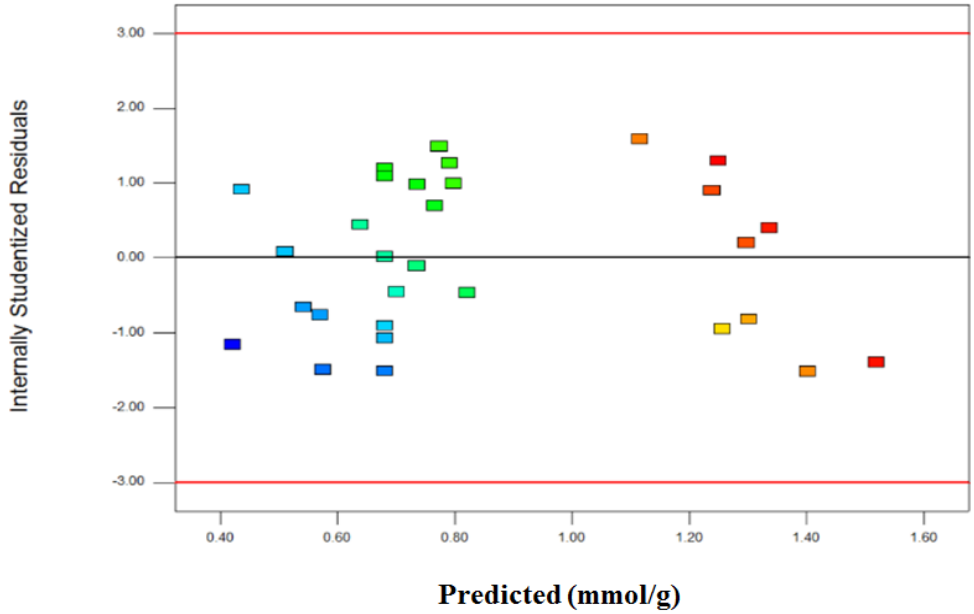
(a)



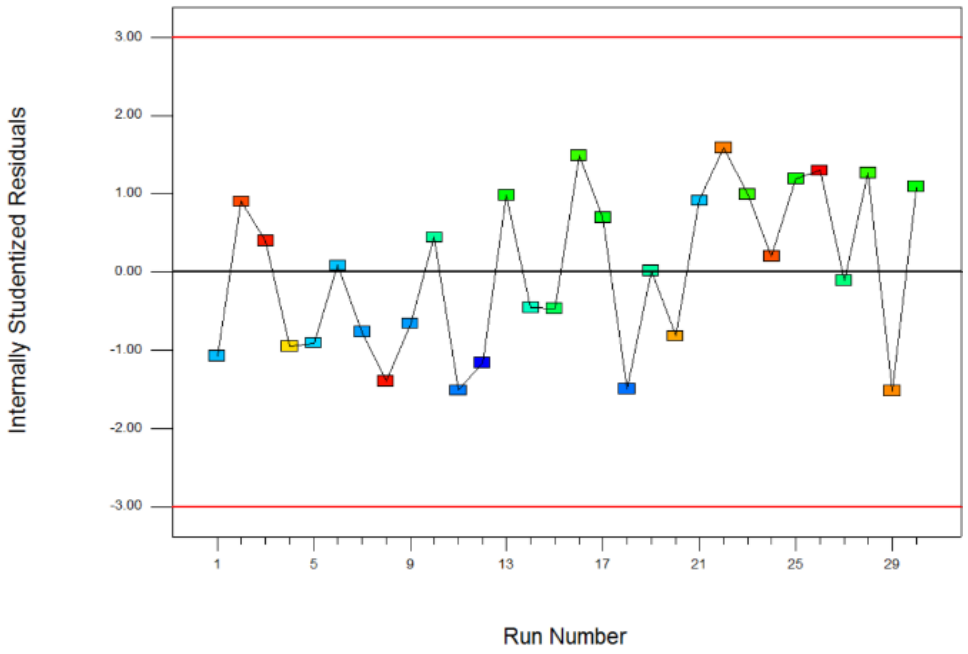
(b)

Figure 5-9 (a) Experimental surface acidic group values and predicted surface acidic group values for the model & (b) Normal probability plot of the residues

According to the randomly scattered points on the plot of residuals versus predicted acidic groups value in Figure 5-10(a), the model is suitable and there is no need to suspect any violation of the independence or constant variance assumption in any of the runs. From Figure 5-10(b), it can be concluded that the errors of the experiments were normally distributed and not significnat.



(a)



(b)

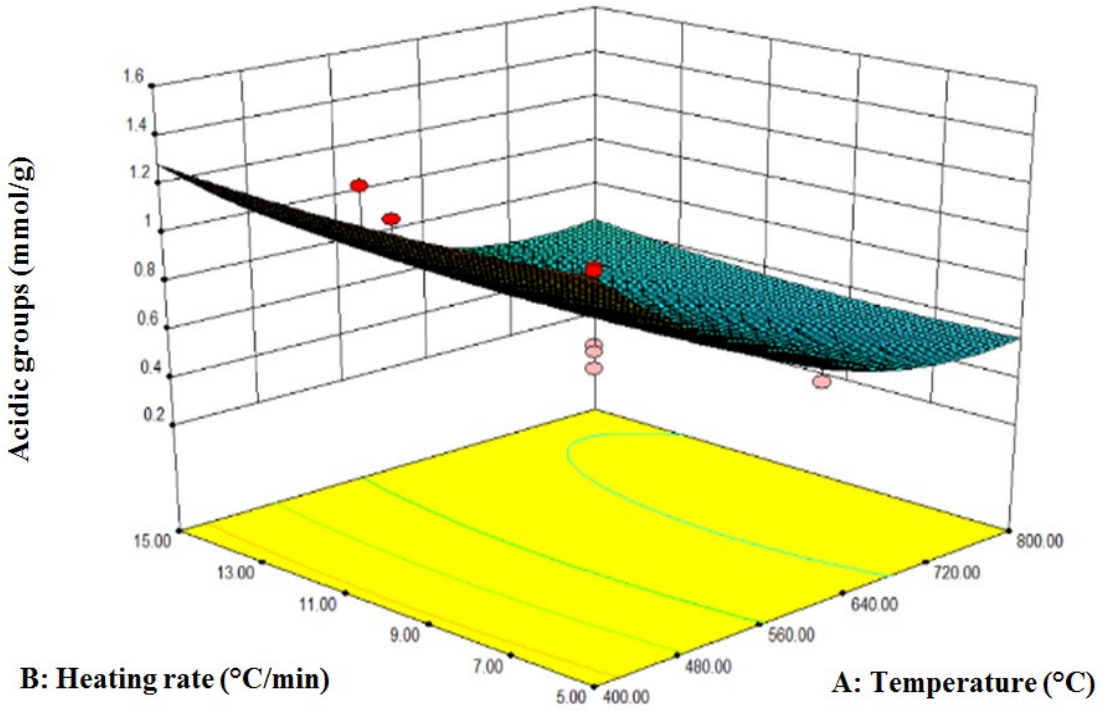
Figure 5-10 Diagnostic plots for surface acidic group value (a) residual versus predicted value and (b) residual versus run number

5.4.3.4 Interaction among Parameters Influencing the Pyrolysis Process and the Surface Acidic Group Values

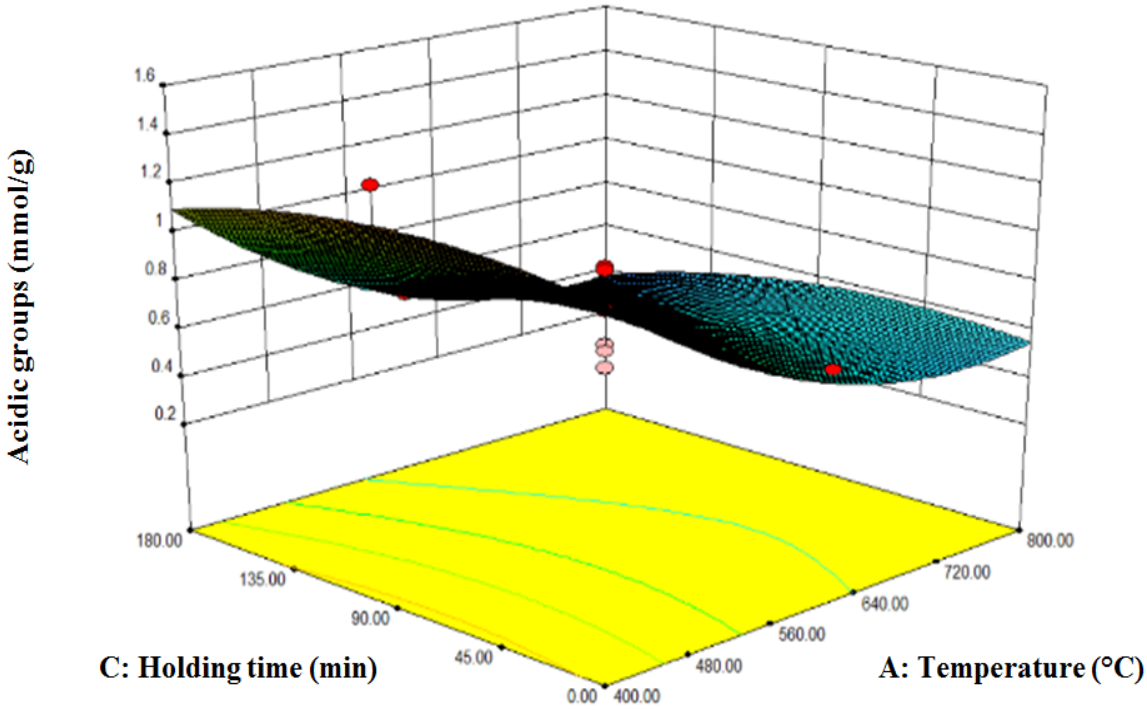
In order to understand the interaction among variables and to decide the optimum pyrolysis condition for each of the factors necessary for optimum creation of surface acidic groups, the empirical predicted quadratic model for the response surface acidic groups in terms of pyrolysis factors (temperature, heating rate, holding time and nitrogen flow rate) were plotted in three-dimensinal diagrams, which are shown in Figure 5-11(a-f). The optimum surface acidic groups was set as the parameter to maximise.

Figure 5-11(a) shows the interactive effect of temperature and heating rate on surface acidic groups at a constant residence time of 90.00min and a nitrogen flow rate of 550ml/min. It can be clearly seen that there is little interaction between temperature and heating rate for the final acidic group value. The number of acidic groups decreases only with increasing temperature, regardless the heating rate. The effect of temperature and holding time on the acidic groups, when heating rate is set at 10˚/min and the nitrogen flow rate is 550ml/min is shown in figure 5-11(b). It is obvious that the acidic groups values increase with an

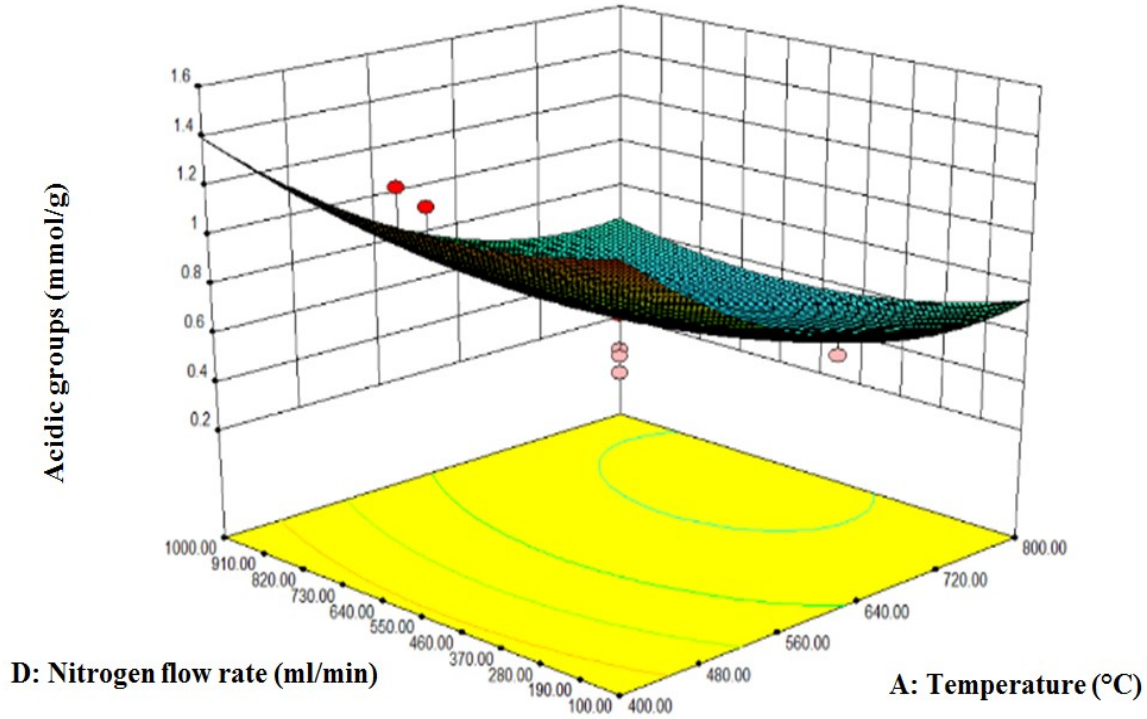
increasing holding time until 90min, so that the maximum acidic groups value can be achieve when the temperature is 400˚C and holding time is 90min. Figure 5-11(c) represents that interactive effect of temperature and nitrogen flow rate on acidic group value at constant heating rate of 10˚C/min and 90min holding time. When the nitrogen flow rate is below 550ml/min, the acidic groups value decreases with an increasing nitrogen flow rate. The minimum number of acidic groups are reached when the nitrogen flow rate is 550ml/min and the temperature is 800˚C. The interactive effects on heating rate and holding time, heating rate and nitrogen flow rate, holding time and nitrogen flow rate are shown in Figure 5-11(d), (e) and (f). Due to the planar nature of the plots, the effects of these three groups of variables on acidic groups value are regarded as significant influential as the interaction effects discussed above.



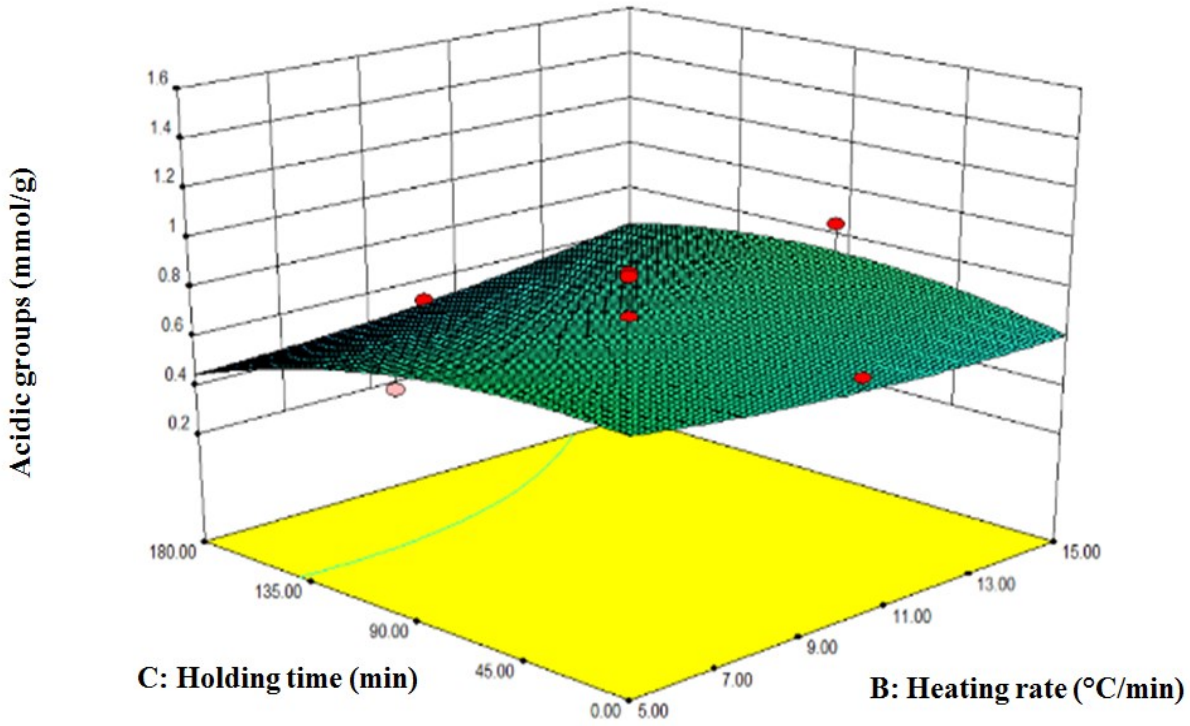
(a)


Acidic groups (mmol/g)
1.6
1.4
1.2
1
0.8
0.6
0.4
0.2
180.00
135.00
90.00
45.00
0.00
C: Holding time (min)
400.00
480.00
560.00
640.00
720.00
800.00
A: Temperature (°C)

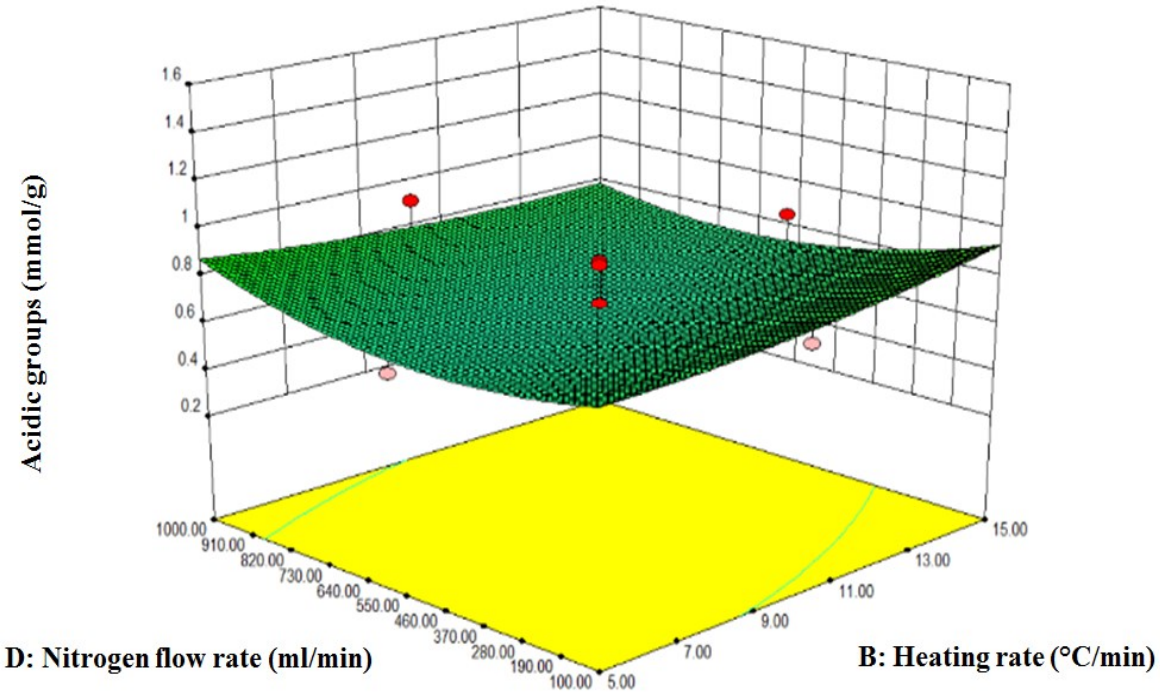
(b)


Acidic groups (mmol/g)
1.6
1.4
1.2
1
0.8
0.6
0.4
0.2
1000.00
910.00
820.00
730.00
640.00
550.00
460.00
370.00
280.00
190.00
100.00
D: Nitrogen flow rate (ml/min)
400.00
480.00
560.00
640.00
720.00
800.00
A: Temperature (°C)

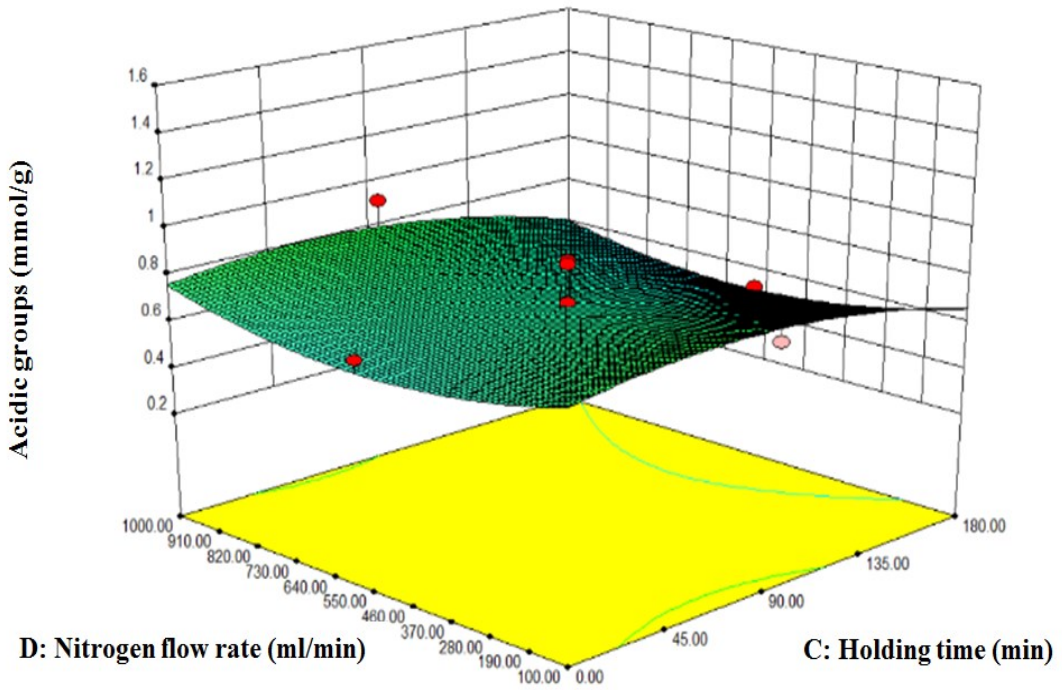
(c)


Acidic groups (mmol/g)
1.6
1.4
1.2
1
0.8
0.6
0.4
0.2
180.00
135.00
90.00
45.00
0.00
C: Holding time (min)
5.00
7.00
9.00
11.00
13.00
15.00
B: Heating rate (°C/min)

(d)


Acidic groups (mmol/g)
1.6
1.4
1.2
1
0.8
0.6
0.4
0.2
1000.00
910.00
820.00
730.00
640.00
550.00
460.00
370.00
280.00
190.00
100.00
D: Nitrogen flow rate (ml/min)
5.00
7.00
9.00
11.00
13.00
15.00
B: Heating rate (°C/min)

(e)



(f)

Figure 5-11 (a-f) Response surface plots of surface acidic groups, illustrating the interaction between two variables: selected for temperature, heating rate, holding time and nitrogen flow rate

5.4.3.5 Optimization of the Pyrolysis Process based on Acidic Groups Value and Model Verification

The response surface for the acidic group formation was determined as a maximum to achieve the best char performance during the optimization process. Accordingly, five optimum pyrolysis conditions and the resultant acidic group values are displayed in Table 5-9. The maximum acidic group value which could be achieved was 1.5313mmol/g, which is in relative close agreement with 1.385mmol/g from the 400˚C temperature, 5˚C/min heating rate, 0min holding time and 1000ml/min nitrogen flow rate run (Run 8). Exact agreement with the RSM was not expected. The reason being that sewage sludge is a relatively heterogeneous material, so unlike coconut shells, there is batch-batch compositional variance. Further, the Boehm titration is very sensitive to slight variations in iner-sample titration values. Nevertheless, the sample-optimisation agreement is considered to be very good.

Table 5-9 Optimum conditions solution for acidic group value

Number of trial	Temperature °C	Heating rate °C/min	Holding time min	N_2 flow rate ml/min	Acidic groups mmol/g	Desirability
1	400.16	5.03	25.28	998.94	1.531	1.000
2	400.37	5.00	48.42	999.02	1.530	1.000
3	400.10	5.01	52.55	999.90	1.530	1.000
4	400.38	5.00	26.40	999.57	1.532	1.000
5	400.00	5.00	12.90	1000.00	1.529	0.999

5.5 Raw Sewage Sludge Derived Char Fillers In-rubber Test

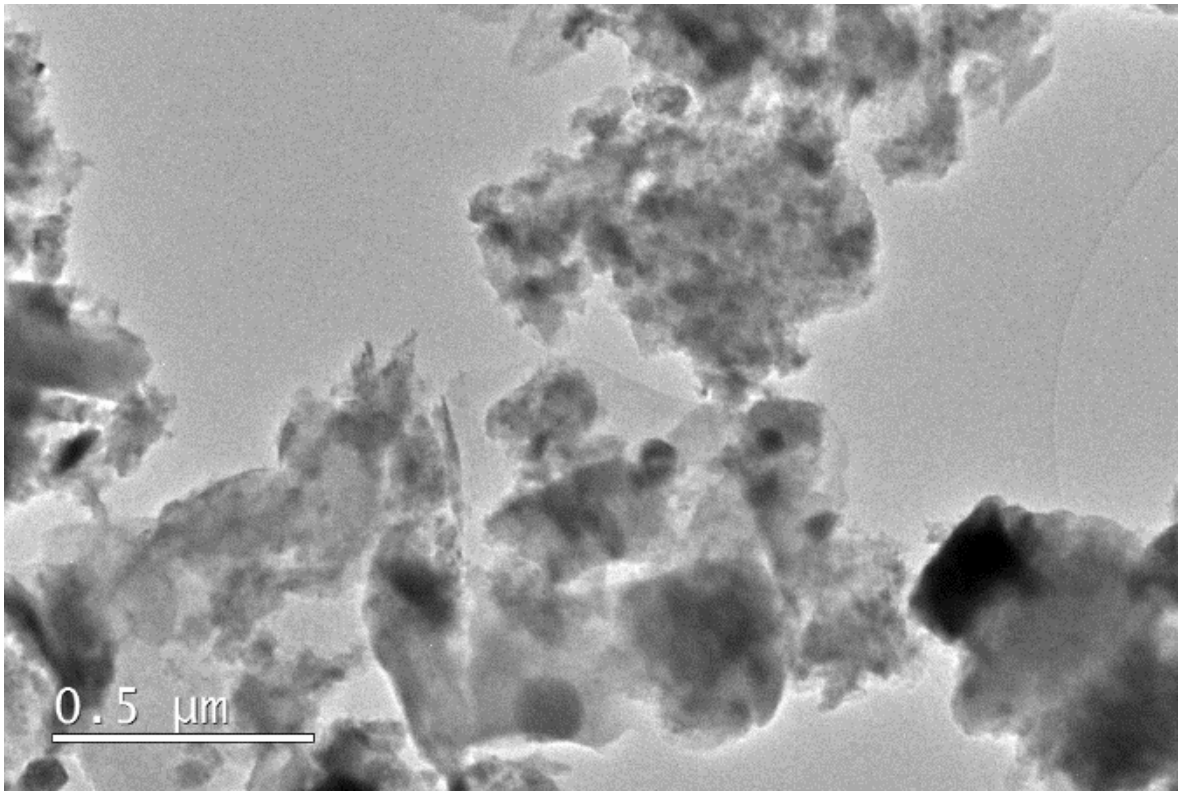
According to the results on the the physical and chemical properties obtained and the RSM optimization, nine sludge char samples were selected to be mixed in an SBR rubber matrix and the performance of the final rubber products evaluated. The nine char filler samples include the char from the optimum pyrolysis condition (600˚C, 10˚C/min, 90min, 550ml/min N_2) based upon pH, plus from different temperatures and char fillers that offered the "best" and the "worst" performance according to the previous physical and chemical tests. The nine pyrolysis conditions of the selected char fillers are tabulated in Table 5-10.

Table 5-10 Selection of coconut shell derived char fillers for in-rubber tests

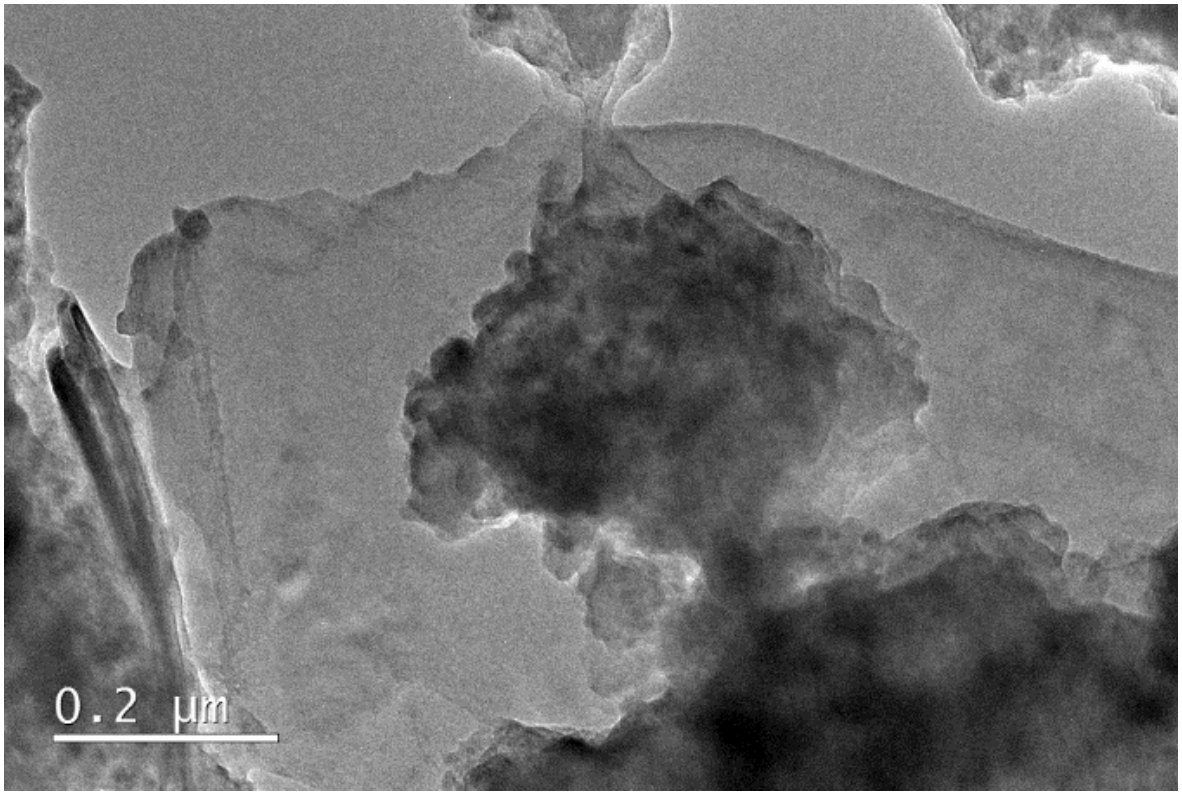
Run	Temperature (°C)	Heating rate (°C/min)	Holding time (min)	N_2 flow rate (ml/min)
8	800	5	180	100
13	800	15	180	100
14	800	15	0	1000
16	800	10	90	550
18	400	15	180	1000
19	600	10	90	1000
20	600	10	90	550
21	400	5	0	1000
29	800	15	180	1000

5.5.1 Transmission Electron Microscope (TEM) Result

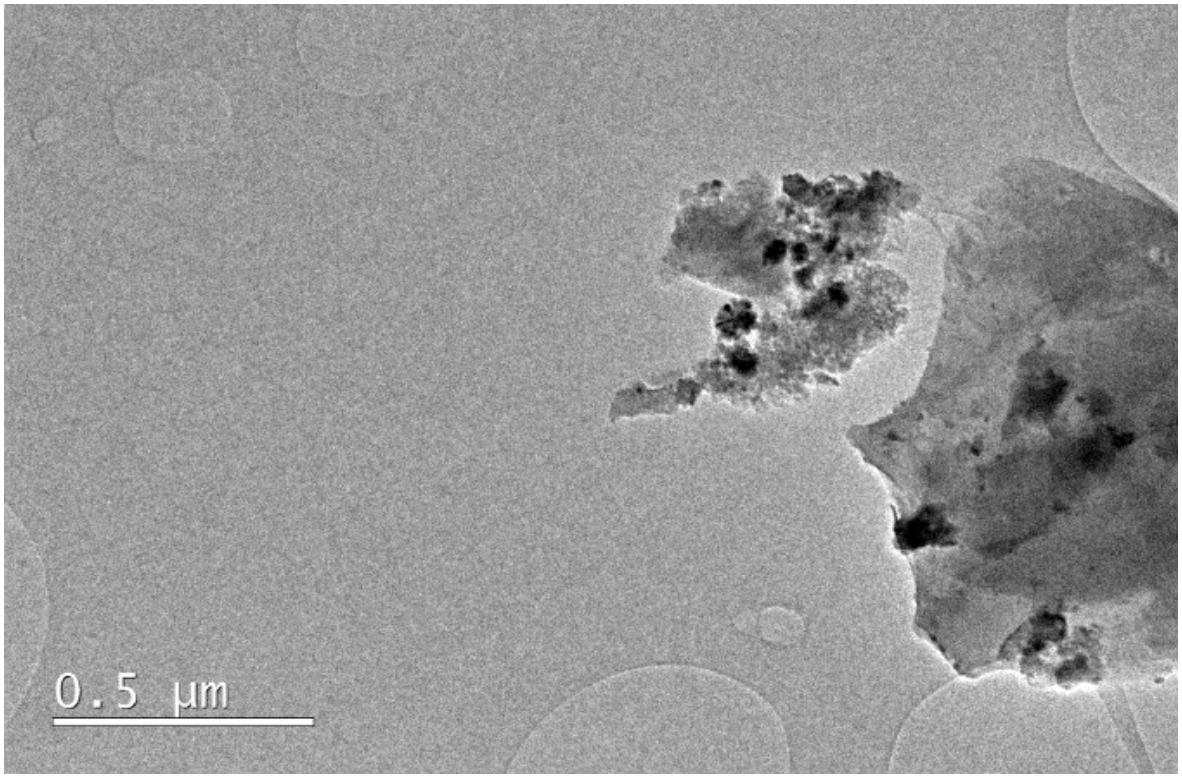
Among the 30 runs, Run 20 achieved the best performance when mixed with rubber matrix, whereas the rubber product filled with Run 13 did not exihibt a satisfactory reinforcement result. TEM anaysis was applied to better understand the morphological properties of the char samples, such as the particle and aggregate size and their shape. Figure 5-12 shows the TEM-micrographs at 6K and 25K magnifications of the chars from both Run 20 and Run 13. The TEM-micrographs of reference materials N330 and N772 can be found in Figure 4-10.



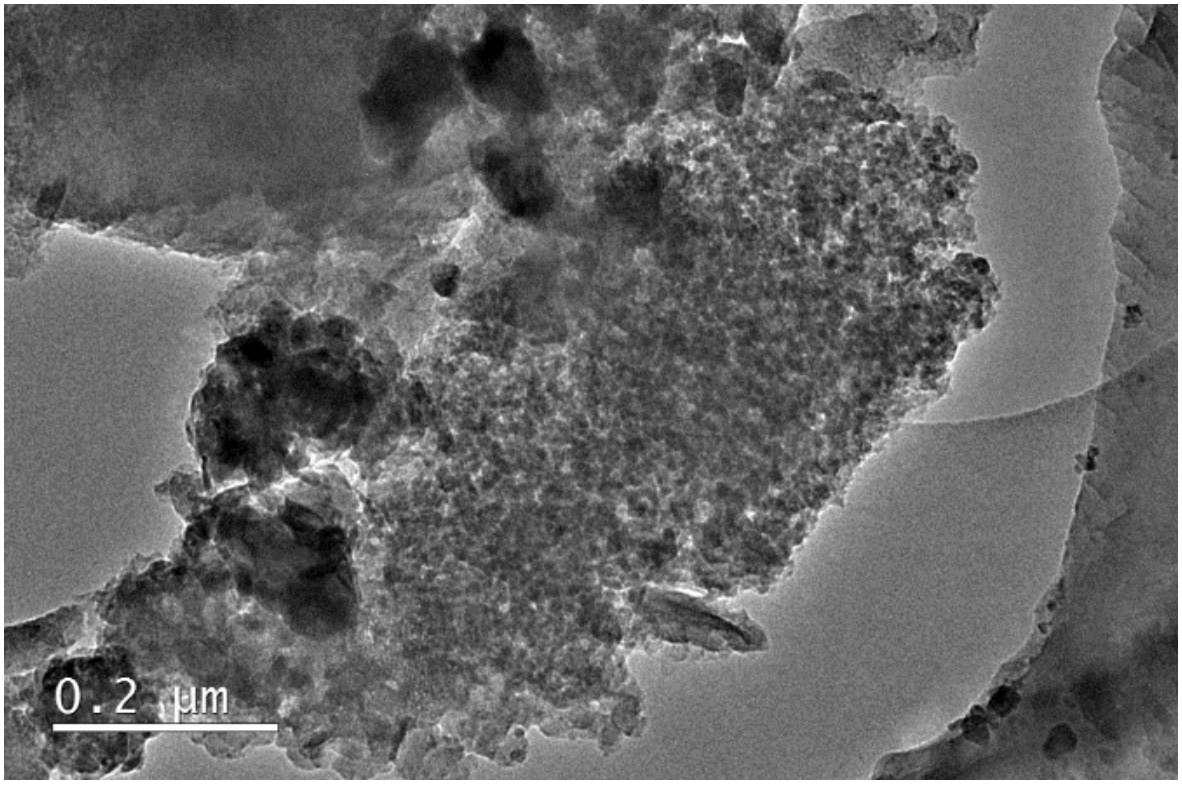
(a) TEM-micrograph of Run 13 at 6K magnification



(b) TEM-micrograph of Run 13 at 25K magnification



(c) TEM-micrograph of Run 20 at 6K magnification



(d) TEM-micrograph of Run 20 at 25K magnification

Figure 5-12 TEM-micrographs of Run 13 and Run 20 at 6K and 25K magnification, showing particle shape, size and distribution

According to the TEM analysis, the shape and size of the sludge char fillers are much more like carbon black and consequently behave much better than coconut shell char filler. There are several clusters shown in the sludge char sample TEM plots. The particle size of Run 20 is smaller than Run 13, and size distrbution is more uniform than Run 13 as well. The aggregates shown in Figure 5-12(d) is highly desirable, the clusters are very similar to the ones shown in Figure 4-10(e) and (f). Based on the TEM resluts, it can be seen that the morphological properties of char fillers made from sewage sludge are close to the high quality commercial carbon black and hence have significant potential to be used as carbon black subsititutes.

5.5.2 Carbon Hydrogen Nitrogen Sulphur Tests

Table 5-11 shows the results of Carbon Hydrogen Nitrogen and Sulphur tests of the raw sewage sludge and the nine selected sludge char filler samples.

Table 5-11 Elemental composition of sewage sludge and sludge char fillers

Sample	C (%)	H (%)	N (%)	S (%)	C/H ratio
Raw sewage sludge	42.70	6.43	3.31	1.64	6.64
Run 8	33.78	0.75	1.45	2.35	45.04
Run 13	21.04	0.84	1.10	1.84	25.05
Run 14	37.15	0.96	2.44	1.74	38.70
Run 16	34.73	0.83	1.60	1.77	41.84
Run 18	31.14	2.08	3.97	1.81	14.97
Run 19	28.63	1.56	2.99	1.60	18.35
Run 20	32.69	1.41	3.00	1.40	23.18
Run 21	39.17	3.60	3.99	1.61	10.88
Run 29	35.39	0.92	1.52	1.90	38.47

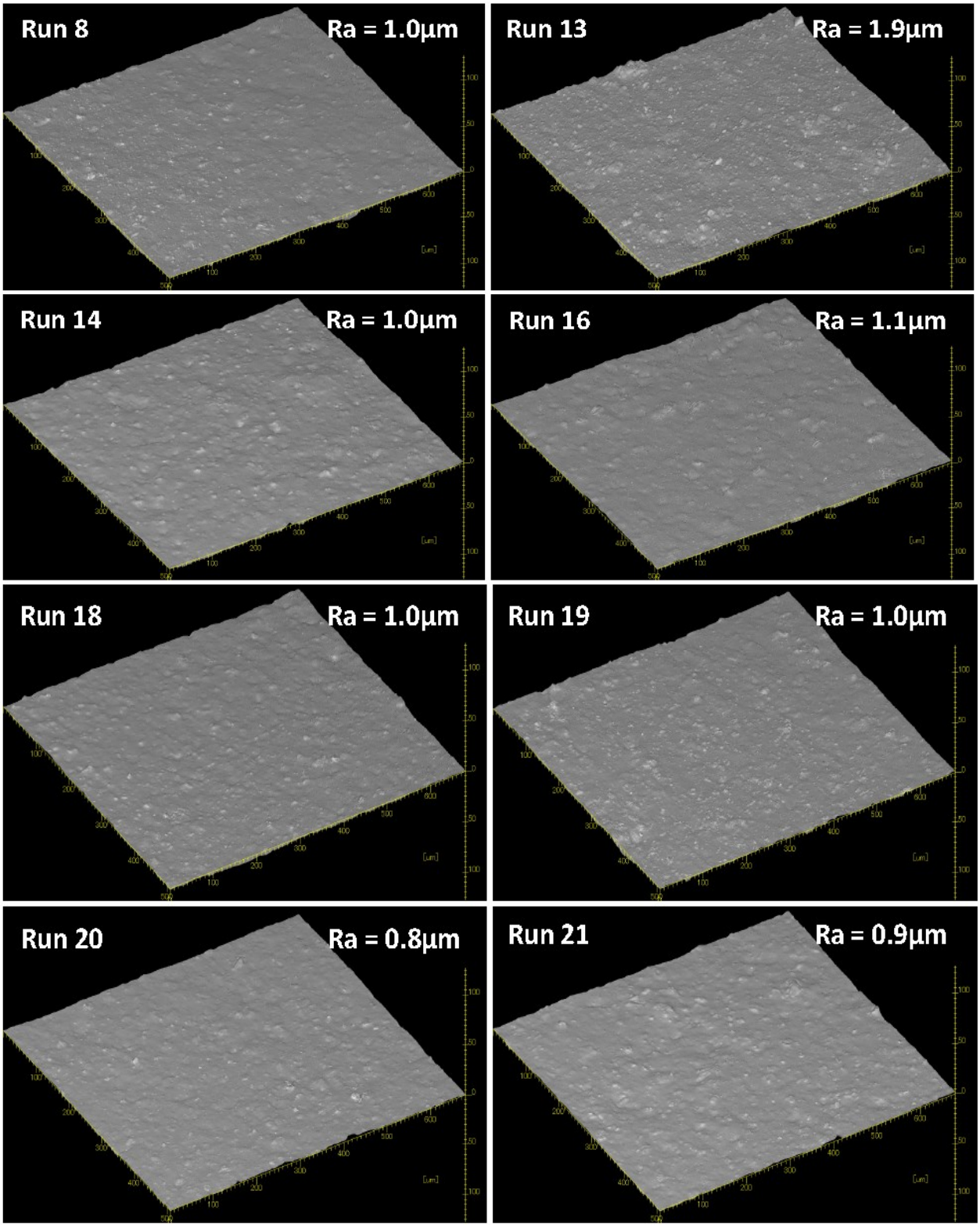
The reference data of the commercial carbon black N330, N550 and N772 can be found in Table 4-9. There are 42.70% C content, 6.43% H content, 3.31% N content and 1.64% S content within raw sewage sludge. Due to the gas and oil release from the feedstock during the pyrolysis process, the C content decreased in the final char filler samples to around 30%. The H and N content also decreased, but were still higher than commercial carbon black because of the feedstock property. The S content is much higher than the commercial carbon blacks, which is a widely used vulcanizing agent in rubber manufacture, leading to the potential for a better bonding process between rubber and the filler during the mixing and vulcanisation period. Although the C content in the sludge chars is lower than the commercial carbon black making sludge chars softer than coconut chars, which may be helpful for better tensile strength and elongation properties for the final rubber products.

C/H ratios of char samples witnessed a drop compared to both coconut shell char and commercial carbon black, indicating an insufficient removal of H and N content, and a reduced development of aromatization of the carbon structure. It also can be concluded that

high pyrolysis temperatures result in high C content, C/H ratio and sulphur content and low H and N content.

5.5.3 In-rubber Characterization

The selected SBR formulation which has been utilised (shown in Table 3-5) was selected to assess the performance of the novel rubber filler systems, whilst allowing the performance of the char samples to be benchmarked. After compounding within the SBR formulation the dispersion level achieved with each of the sludge char samples was assessed. SEM 3D surface roughness maps of freshly dispersion sectioned surfaces are provided in Figure 5-13. All the char samples had similar dispersion levels apart from Run 13, which has the highest surface roughness value and contained a higher proportion of larger undispersed particles (Ra = 1.9μm). The sludge char from Run 13 had the highest surface area and correspondingly, was harder to disperse. It is worth to noting that the levels of dispersion achieved were significantly improved compared to the coconut shell derived chars (see Figure 4-11).


Run 8
Ra = 1.0µm
Run 13
Ra = 1.9µm
Run 14
Ra = 1.0µm
Run 16
Ra = 1.1µm
Run 18
Ra = 1.0µm
Run 19
Ra = 1.0µm
Run 20
Ra = 0.8µm
Run 21
Ra = 0.9µm

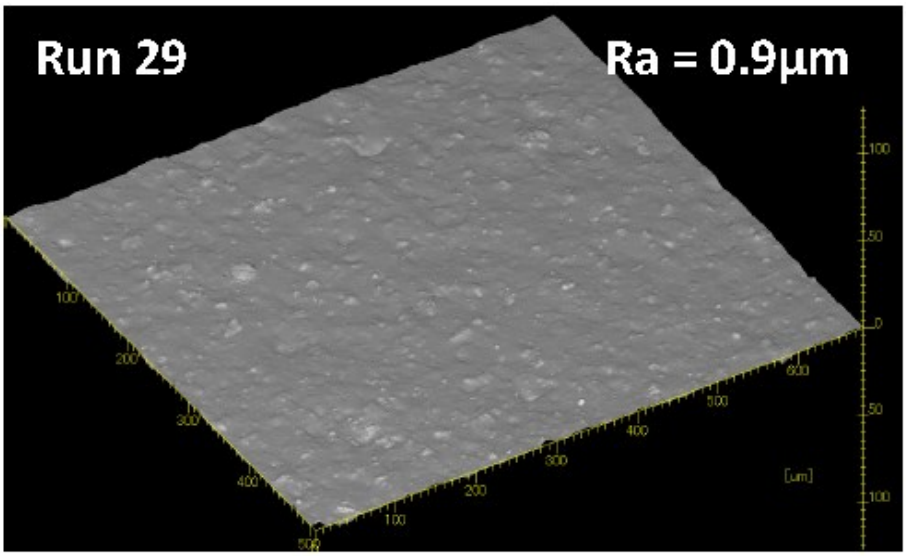
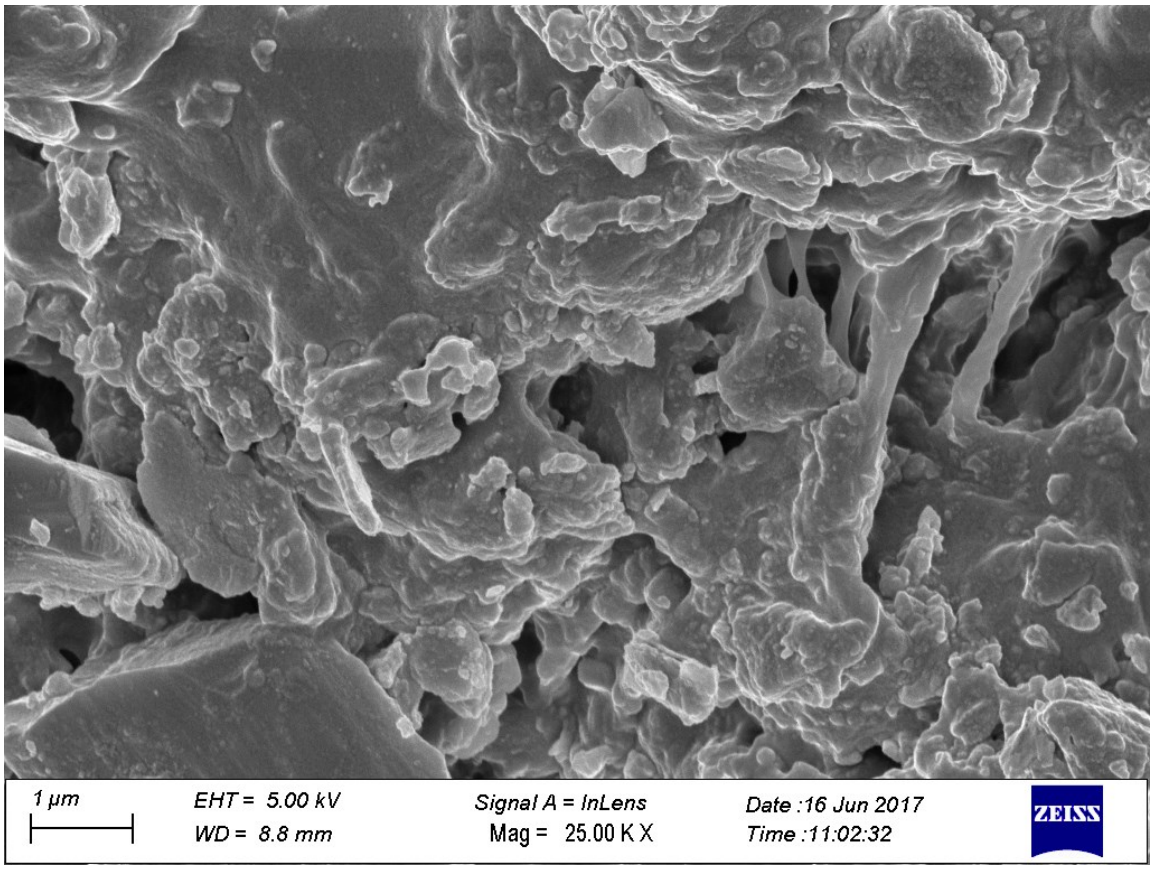
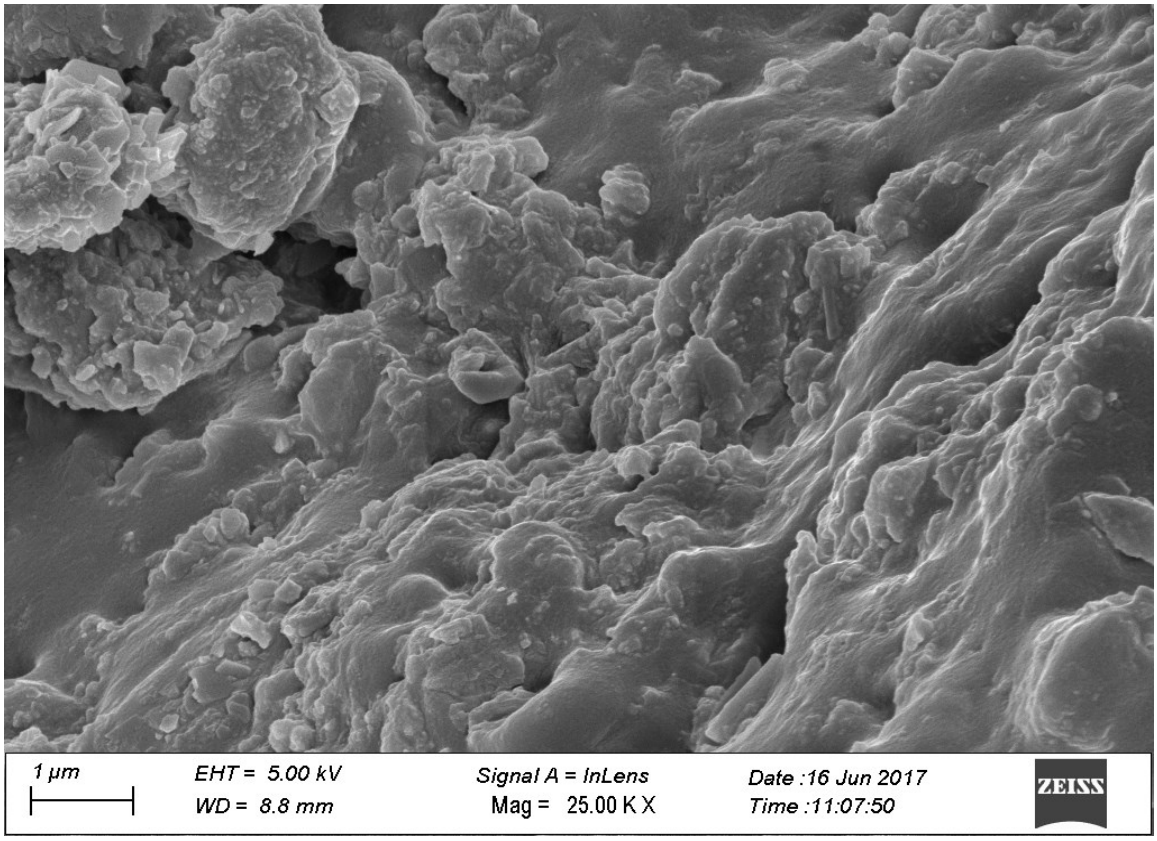


Figure 5-13 3D surface roughness maps highlighting filler dispersion, scale in micron

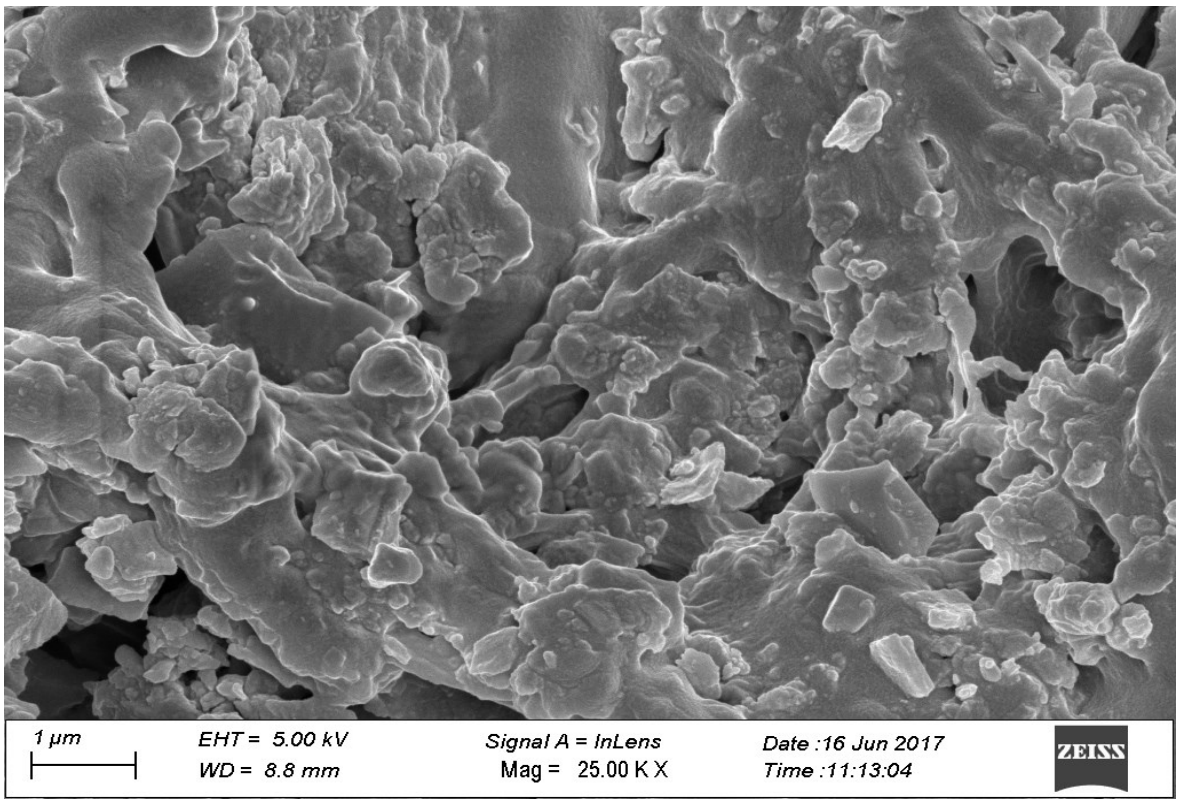
The dispersion test can be further developed by the SEM analysis, shown in Figure 5-14(a-j). 25K magnification was selected in the char sludge SEM plots.



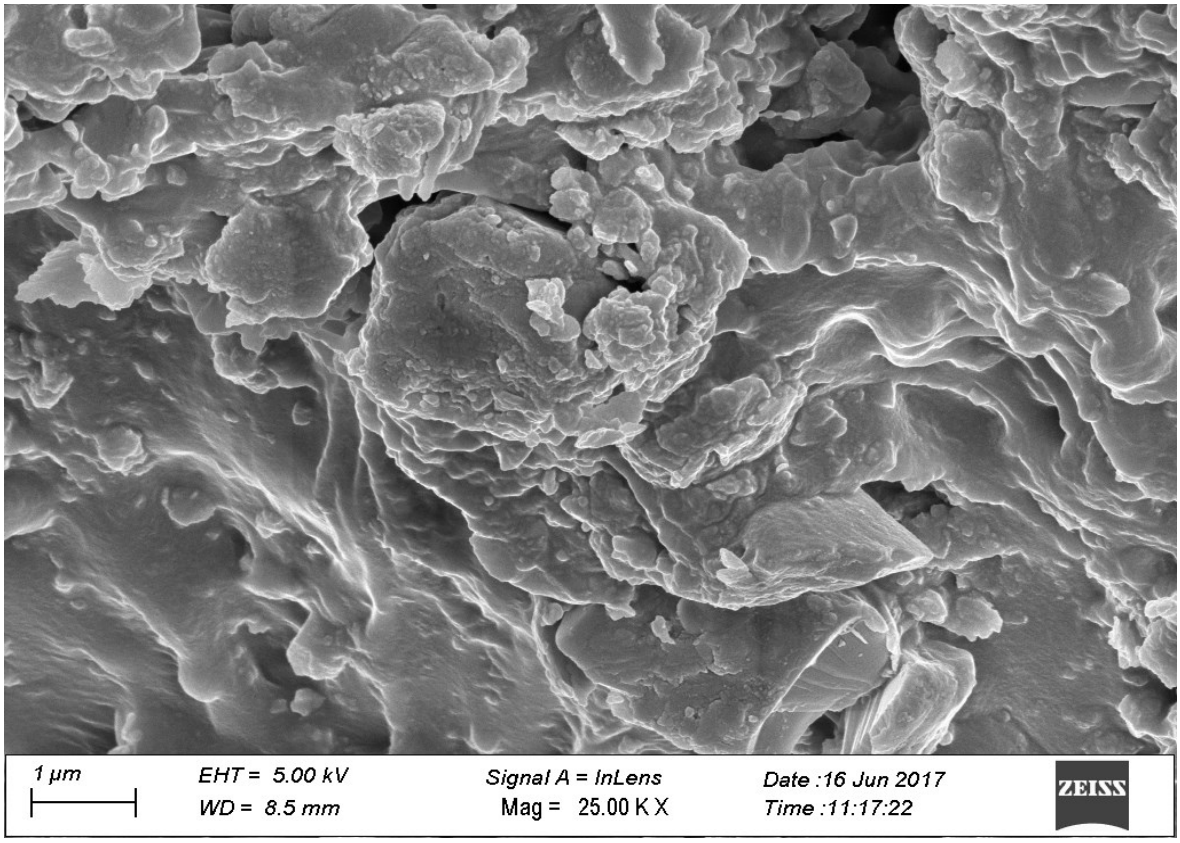
(a) SEM plot of Run 8 filled rubber sheet



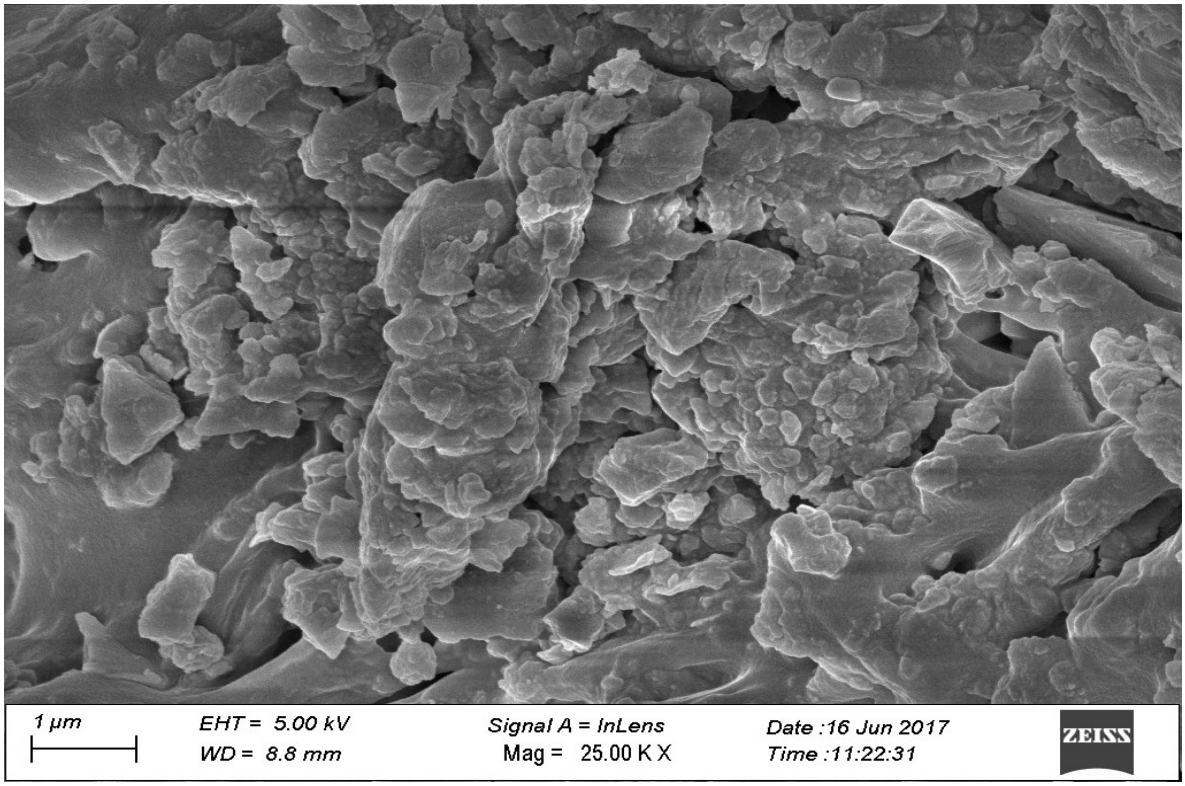
(b) SEM plot of Run 13 filled rubber sheet



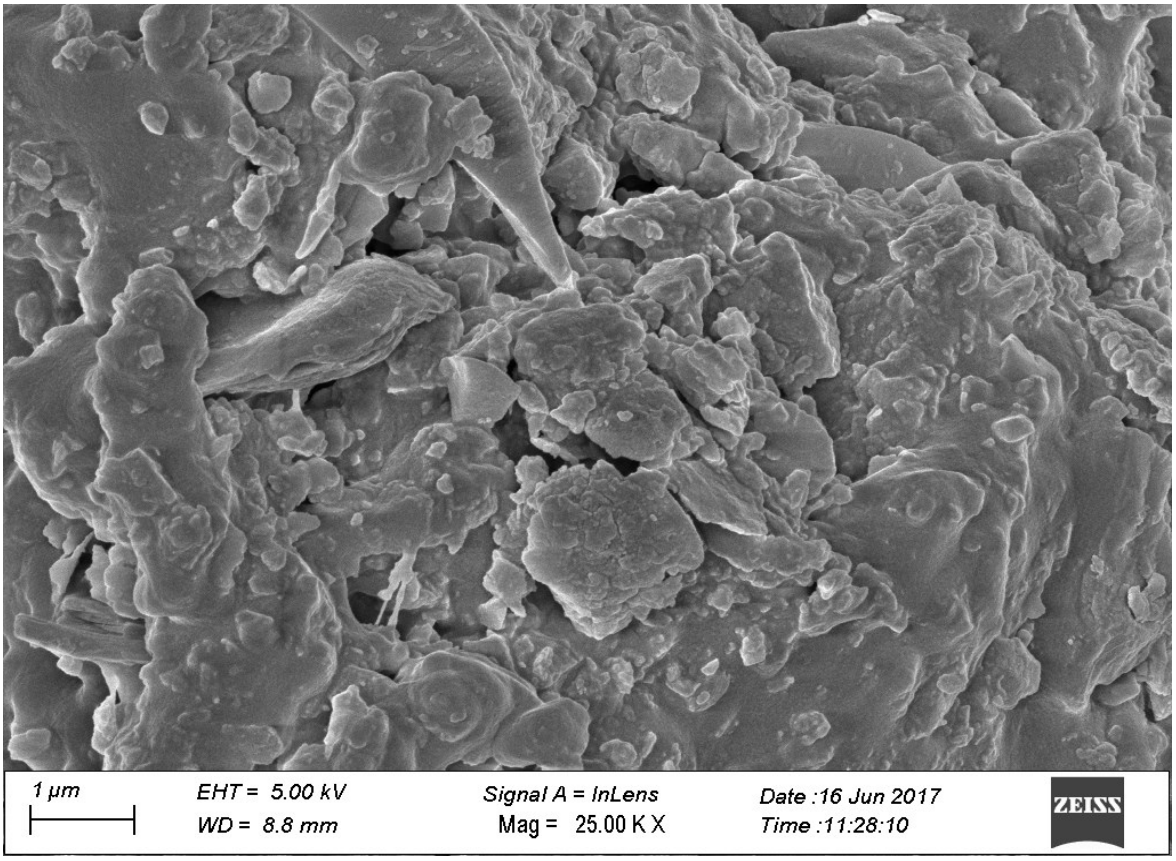
(c) SEM plot of Run 14 filled rubber sheet



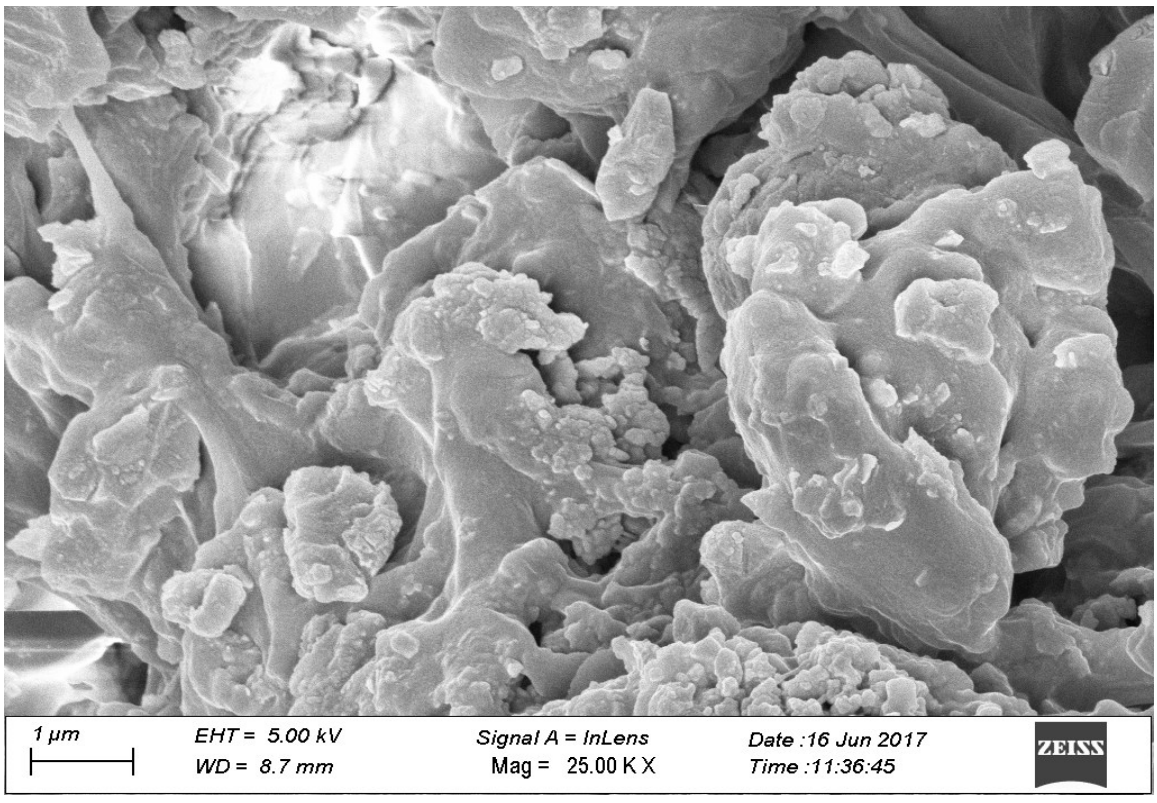
(d) SEM plot of Run 16 filled rubber sheet



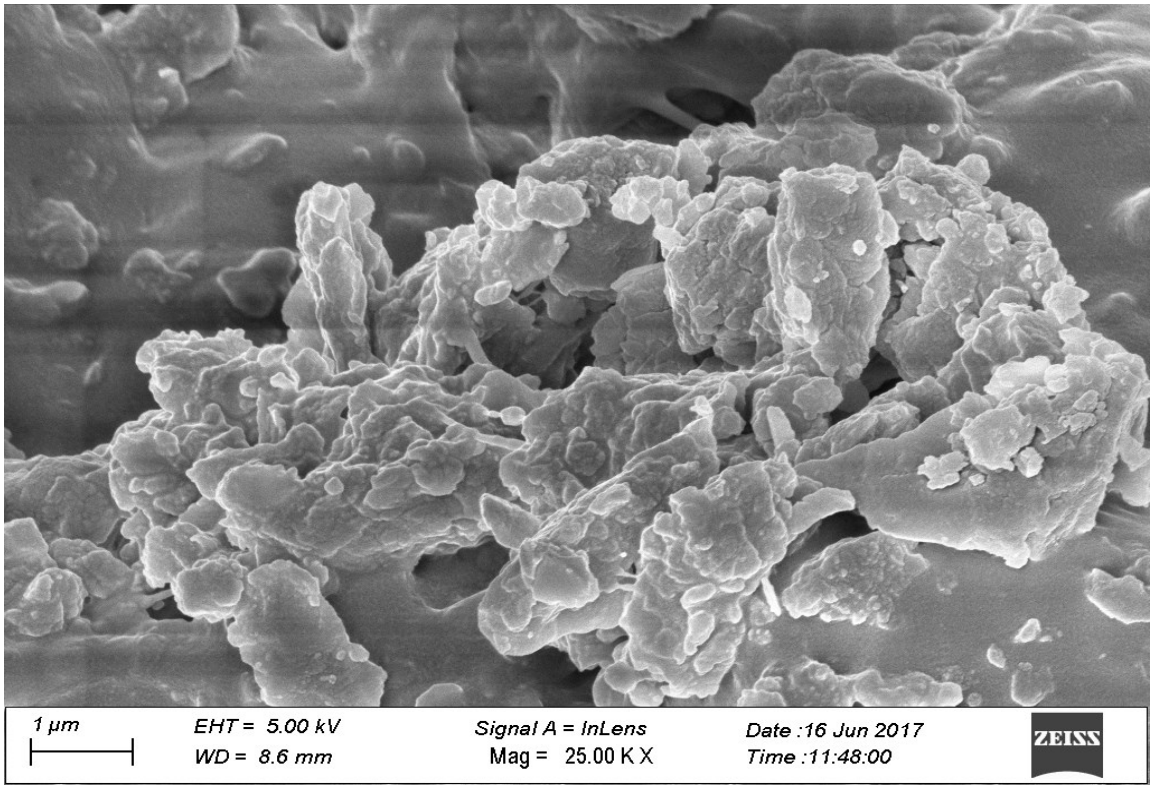
(e) SEM plot of Run 18 filled rubber sheet



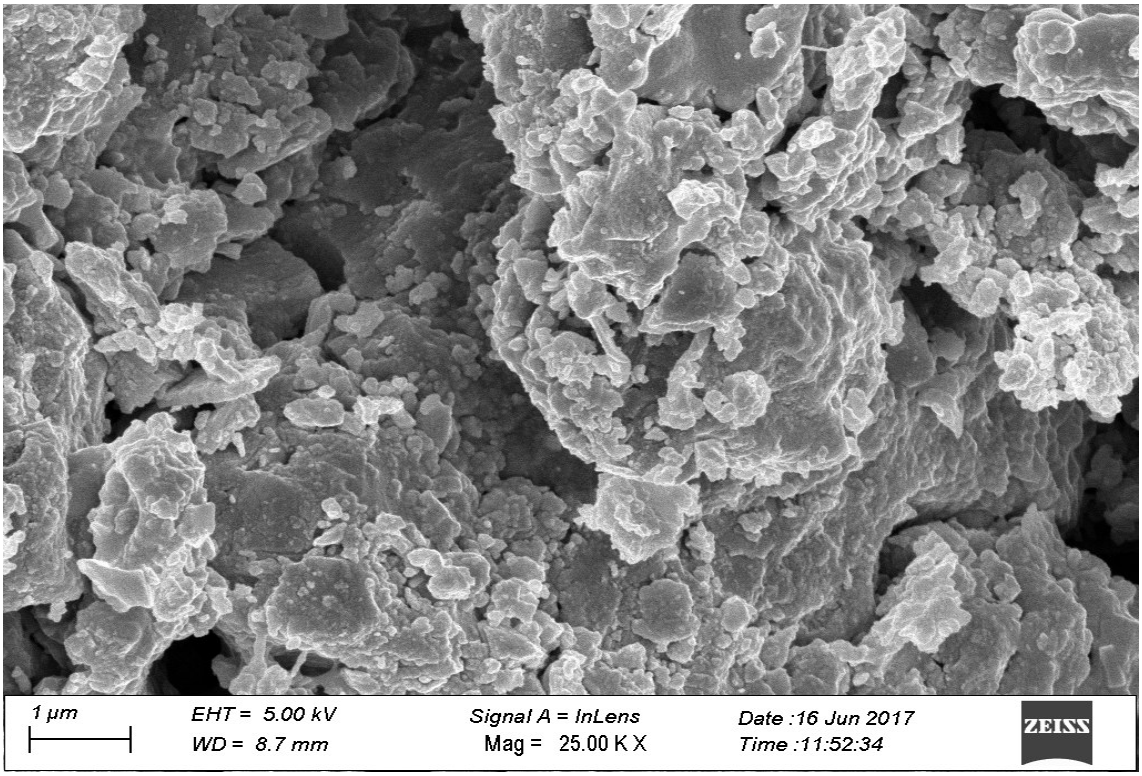
(f) SEM plot of Run 19 filled rubber sheet



(g) SEM plot of Run 20 filled rubber sheet



(h) SEM plot of Run 21 filled rubber sheet



(i) SEM plot of Run 29 filled rubber sheet

Figure 5-14(a-i) SEM plots of compounded rubber sheets at 25K magnification, illustrating rubber-filler boning system

All the sludge char samples behaved better than coconut char fillers. The particle size is much smaller and more evenly distributed than coconut char samples. It is also shown by the SEM analysis, that Run 13 has the less suitable particle size and dispersion ability, as there were seldom any filler particles can be seen in Figure 5-13(b). From the SEM micrographs of Run 20, Run 21 and Run 29, it can be easily seen than the small sludge char filler particles are attached evenly to the rubber surface and are very similar to the N660 filled rubber sheet in Figure 4-12.

The cure and physical properties of the char filled rubber compounds are tabulated in Table 5-12. The MDR cure curves are shown in Figure 5-15. The time to onset of cure (Ts2) and cure times (T90) for Run 8, 16 and 29 were found to be close to the reference N772 carbon black. The other char samples had longer cure times, indicating that differing surface chemistry most likely to be having some level of interaction with the cure package applied. The minimum torque values, which is regarded as an indication of compound viscosity, are considered fairly low, implying that the structure levels of the rubber imparted by the char fillers are low (Hewitt & Ciullo, 2007).

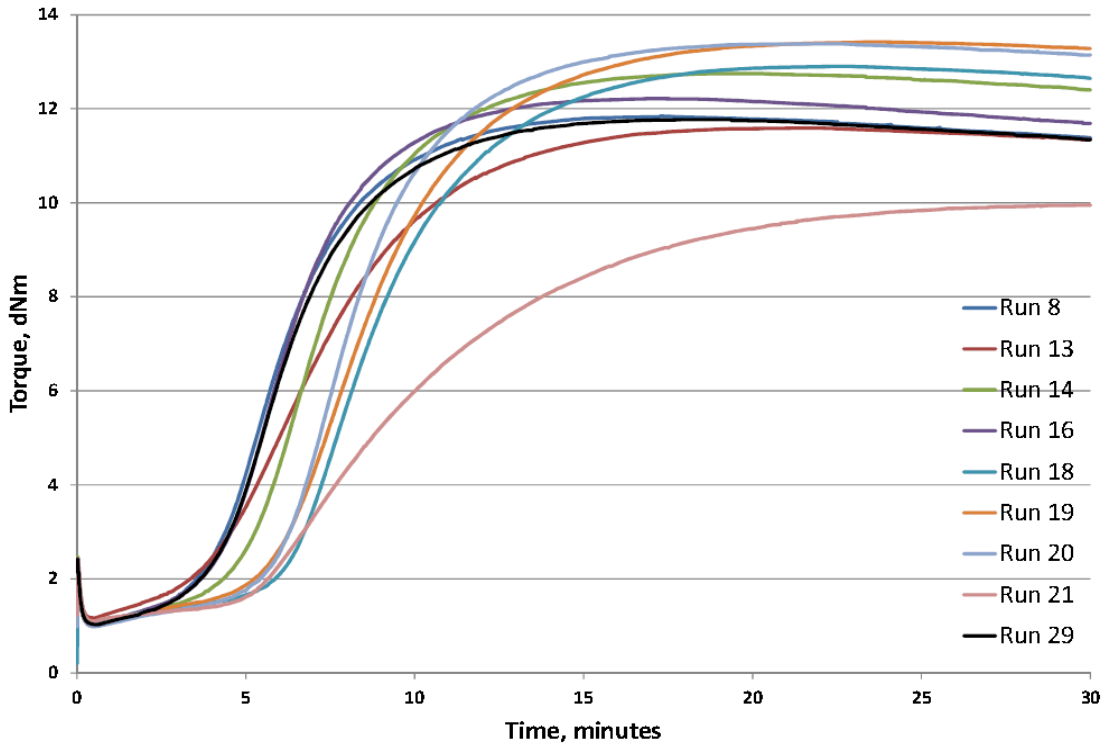


Figure 5-15 MDR cure profiles of sludge chars in the SBR system

Table 5-12 Rheology and physical data of sludge chars

	Run 8	Run 13	Run 14	Run 16	Run 18	Run 19	Run 20	Run 21	Run 29	CB N772
MDR data (30mins @160˚C)										
Min (dNm)	1.02	1.17	1.03	1.04	1.07	1.00	0.99	1.10	1.03	1.23
Max (dNm)	11.84	11.59	12.75	12.21	12.90	13.42	13.38	9.96	11.77	13.66
Ts2 (mm:ss)	4.40	4.71	5.30	4.58	6.78	6.28	6.28	6.79	4.55	4.33
T90 (mm:ss)	9.65	11.86	10.97	9.60	13.38	13.31	12.07	17.61	9.96	9.19
Physical Properties										
Shore A (˚)	53	53	56	55	56	57	57	52	55	57
M 100% (MPa)	1.42	1.47	1.64	1.50	1.64	1.69	1.65	1.32	1.48	1.63
M 300% (Mpa)	2.88	3.06	3.29	3.03	3.03	3.25	2.99	1.81	3.01	9.3
Tensile Strength (Mpa)	6.27	9.56	7.72	8.51	8.37	7.70	8.51	8.12	8.10	20.4
Elongation at Break (%)	639	757	664	715	698	633	676	962	716	586

The results of the hardness property studied by the Shore A test were similar for all the 9 samples, between 53 and 57˚. As to the modulus, the M100% values are considered similar to the reference N772 carbon black, whereas the M300% values were significantly lower indicating that the reinforcing ability provided by the char samples are low, which corroborates the rubber structure observations previously. Low tensile strength and high elongation to break values are associated with low filler-polymer interaction and structure levels, allowing for chain slippage over the filler surface.

According to the data, sludge char sample produced from Run 20 was the best performing char filler among the selected 9 samples, which is in agreement with the RSM optimization results. The sample can be considered as a semi-reinforcing filler with broadly similar cure characteristics and technical performance to a conventional carbon black.

Figure 5-16 shows the Payne effect as a plot of the elastic modulus against the double strain amplitude for N772 and sewage sludge filled vulcanisates.

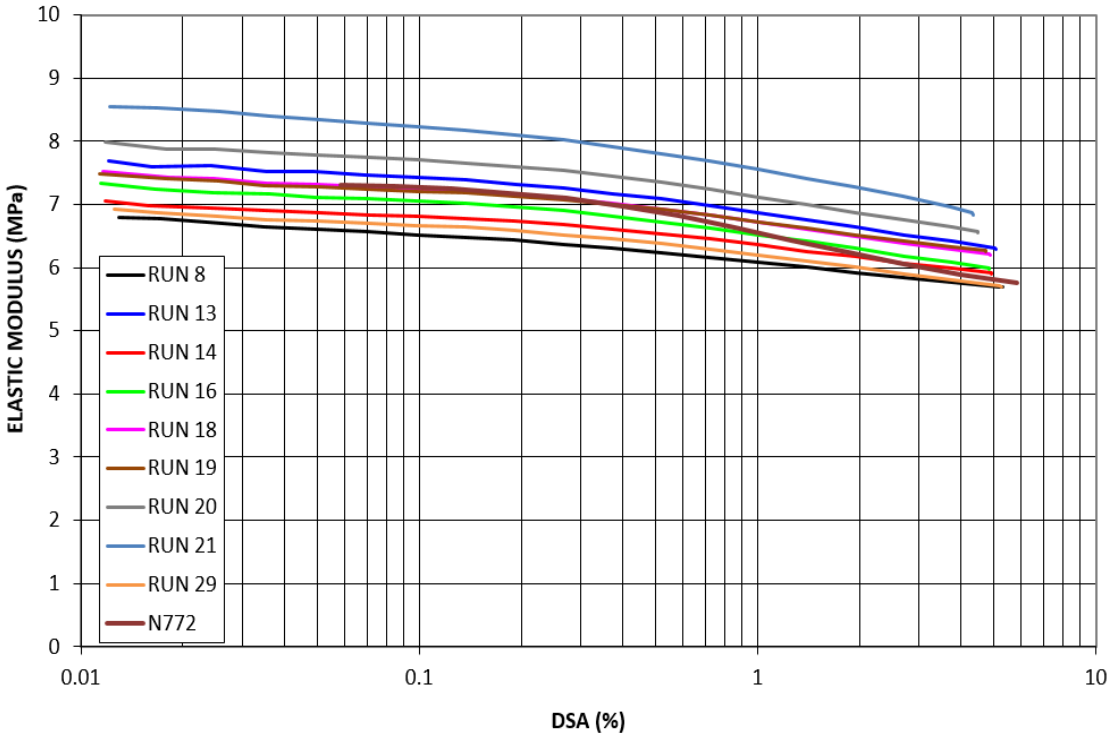


Figure 5-16 Elastic modulus plots against double strain amplitude of the compounds containing N772 and sludge chars

Figure 5-17 shows the ΔE' networking efficiency versus surface area plot of char fillers and N772 and N326 carbon blacks, where ΔE' (E'_0 - E'_∞) is a measurement of filler-filler interaction. The ΔE' value of char fillers was measured as < 1.7 MPa for the sludge char samples, which is similar to N772, but still considered to be low given their surface area. N326 has a ΔE' values of 13.5Mpa when mixed with the same SBR formulation. Unlike conventional carbon blacks, the ΔE' value of the char sample doesn't increase with increasing surface area. As a result, it can be concluded that there is a reduced filler-filler interaction compared to carbon black. This is a very interesting characteristic as it is similar to that observed for coconut char as such filler-filler interactions are correlated to energy losses and, for example, high rolling resistance and poor fuel efficiency in a tyre tread. Graphitic crystallite ends are considered the fundamental factor for filler-filler interactions for conventional carbon black, indicating this feature is absent within the sludge char samples as may be expected given the low-temperature manufacturing process. The high strain elastic modulus (E'∞) is low for all the sludge char samples, confirming low levels of filler-polymer interactions. This is associated to both surface activity and structure levels.

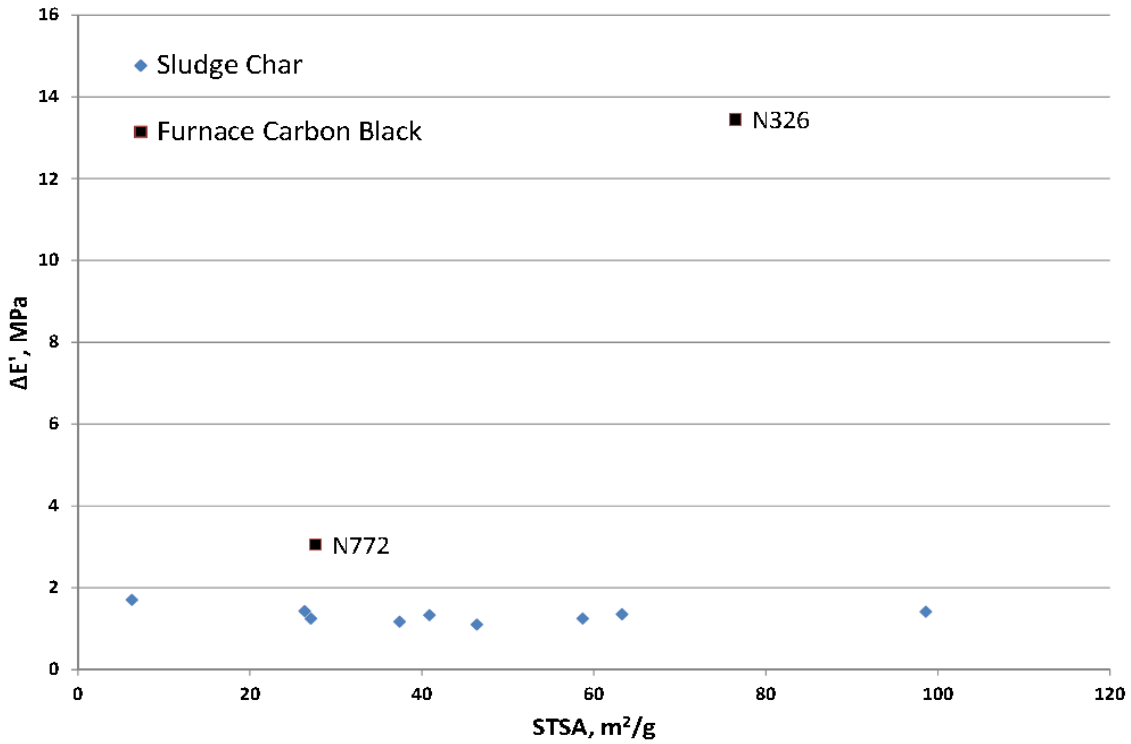


Figure 5-17 ΔE'networking efficiency versus surface area

To sum up, the sludge char fillers were found to offer significantly improved dispersion compared with the coconut shell derived variants. The sludge chars were also slightly more reinforcing, with Run 20 offering the best propertied of those evaluated, as shown in Figure 5-18.

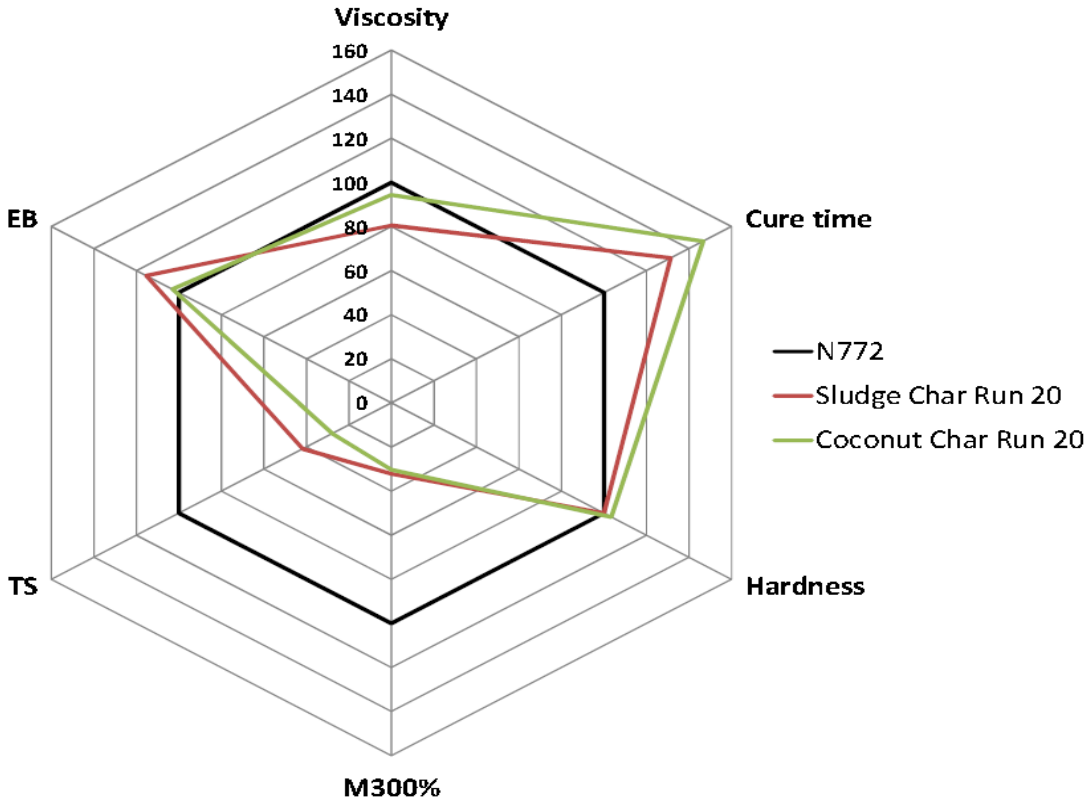


Figure 5-18 Char samples compared to N772

Further size reduction, ideally to less than 1μm, may produce an interesting filler that could potentially replace N990, shown in Figure 5-19, in a number of rubber applications.

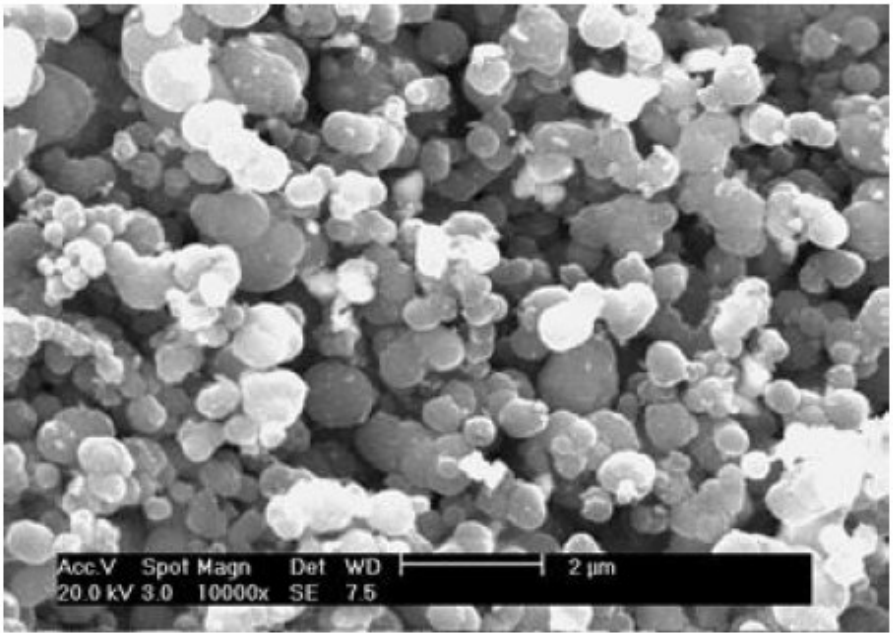


Figure 5-19 Carbon black N990 appearance

5.6 Conclusion

Raw sewage sludge has been fully evaluated as a carbon black-like char filler, through the application of an RSM optimisation methodology using surface chemistry and surface area as optimisation parameters. The resultant char filler was comparable with commercial semi-reinforcing carbon blacks. The in-rubber testing revealed that the semi-reinforcing carbon black can be partially replaced by the sewage sludge char filler, given that most of the performance testing of the rubber products were comparable. Based upon the Response Surface Methodology analysis, temperature, heating rate and pyrolysis holding time have been identified as having significant effects on char quality. The optimum conditions required to produce a suitable carbon black-like substitute from raw sewage sludge, were identified as: 600°C temperature, 10°C/min heating rate, 90min holding time and 550ml/min Nitrogen flow rate. Although these results are not too dissimilar from the coconut fillers studied in the previous chapter, the sewage sludge fillers appear to offer advantages over coconut shell fillers due to exhibiting better particle structure and rubber-filler interaction to a more favourable porosity. Nevertheless, it has been identified that there is a need to undertake optimisation of the post-production processing for the char alongside modification to the rubber formulation and mixing procedure to further improve the filler-rubber interactions, enabling this material to be developed as a viable replacement for carbon black as a filler in rubber.

Chapter 6 Environmental Impact Evaluation

6.1 Calculation of Energy Consumption

6.1.1 Life Cycle Assessment

The aim of this part of the research is to undertake an analysis of the energy and emissions associated with filler manufacture from coconut shell and raw sewage sludge. The production of carbon black has significant requirements in terms of heat input (energy) and consequentially high CO_2 emissions. Through the use of renewable materials, it should be expected that lower energy consumption and reduced environmental impacts will result. Two essential factors are required to be met for a sustainable waste management system: (1) the recovery of either products or energy value from the waste, and (2) the reduction of the environmental impacts after the treatment and disposal of the waste. A limited Life Cycle Assessment (LCA) has been conducted and is presented in this chapter to quantify the potential environmental impacts of waste materials pyrolysis systems, based on energy and CO_2 requirements for filler manufacture, which will provide a basis for a better-informed decision making process.

LCA was first introduced in the 1960s and 1970s to evaluate industrial production along with the rise of sustainable development requirements. It was then further developed from 1980 to 1990 (Yoshida et al., 2013; Guinee et al., 2011). LCA has been widely used in the solid waste management industry, including sewage sludge management. It has been reported that more than 300 peer-viewed articles on LCA on different sectors of solid waste management have been published and 50 LCA models were specifically targeting solid waste treatment technologies in Europe (Gentil et al., 2010; Pires et al., 2011). According to British Standard BS EN ISO 14044:2006, life cycle is defined as "*consecutive and interlinked stages of a product system, from raw material acquisition or generation from natural resources to final disposal*", and LCA refers to "*compilation and evaluation of the inputs, outputs and the potential environmental impacts of a product system throughout its life cycle*". The life cycle of a waste management process is considered as the waste from its generation, treatment,

potential end-use and eventual disposal. By using life cycle assessment to measure the environmental performance of a process, some targets can be achieved:

(1) Improving resources and energy use efficiency,

(2) Providing quantitative comparison basis for different systems,

(3) Supporting strategy formulation,

(4) Providing quantitative data for assessing environmental impacts and sustainability requirement.

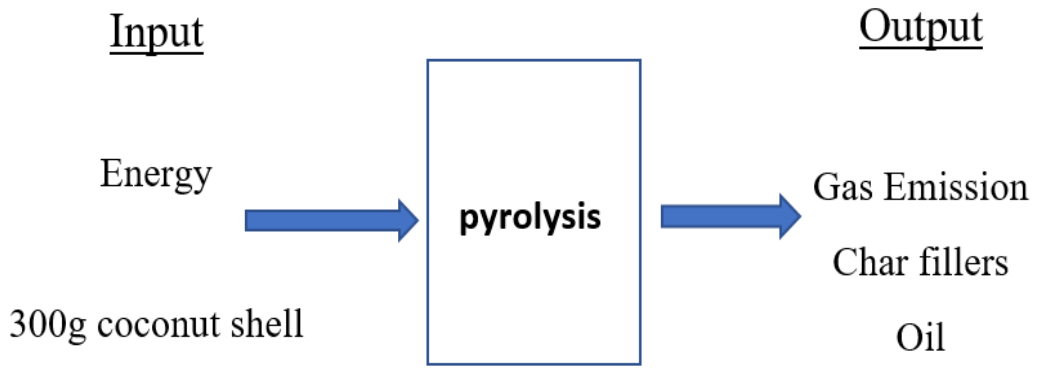
Four steps need to be undertaken when using LCA, (1) goal and scope definition, (2) inventory analysis, (3) impact assessment, and (4) interpretation (Abbe, 2009).

6.2 Methodology

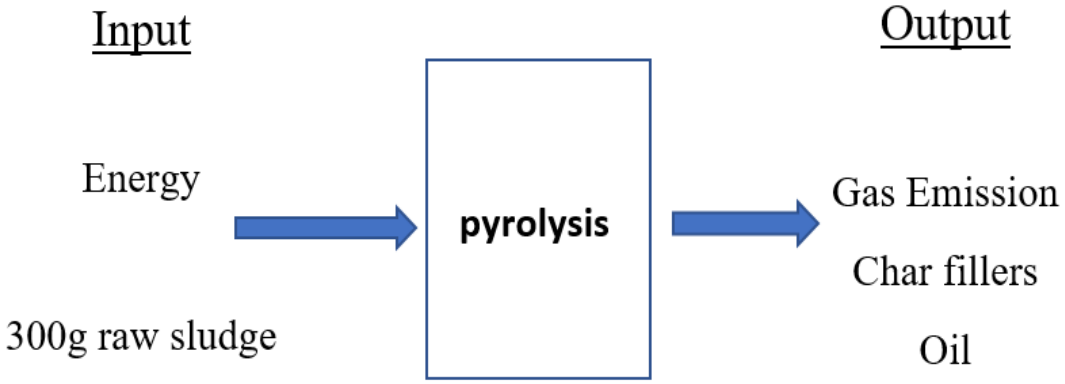
The goal of LCA applied in this study was to evaluate the environmental impacts (energy usage and CO_2 emission) of the carbon black substitute production from coconut shell and raw sewage pyrolysis, compared with the performance of the commercial carbon black manufacture. It was assumed that all the other process steps involved in the carbon black manufacture (grinding, pelletizing, packing, shipping etc.) would be common, irrespective of the feedstock. Thus, the scope of this assessment was a simplified environmental impact evaluation of the two processes.

The system boundary defines which individual technical sub-systems are included in the assessment as well as the inputs and outputs. When considering the system boundary, a representative and acceptable pyrolysis process of 300g feedstock was selected with 600˚C temperature, 10˚C/min heating rate, 90min holding time and 550ml/min nitrogen flow rate.

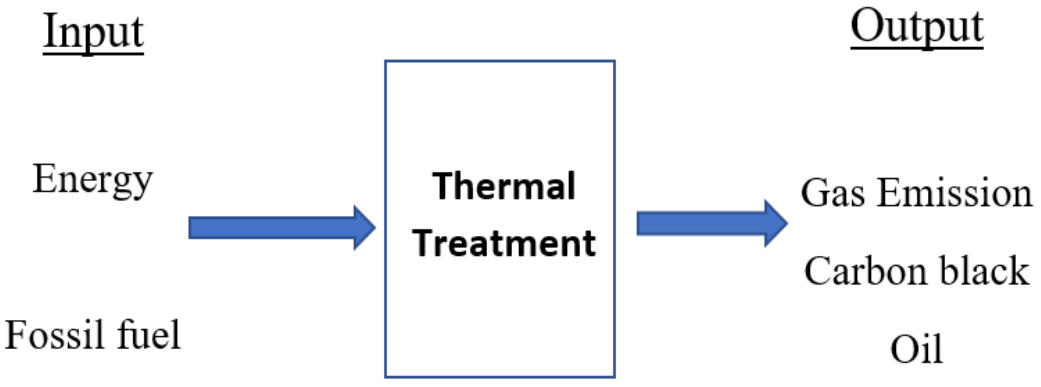
Three systems have been assessed in this evaluation, as shown in Figure 6-1. System (a) is the 300g coconut shell pyrolysis process under 600˚C temperature, 10˚C/min heating rate, 90min holding time and 550ml/min nitrogen flow rate, (b) is the same system but using raw sewage sludge as feedstock, while (c) is the manufacture process of commercial carbon black.



(a)



(b)



(c)

Figure 6-1 Three systems in this study

6.3 Energy Assessment

6.3.1 Energy Consumption Assessment

A theoretical approach has been utilised to calculate the energy consumption during the pyrolysis process of the feedstock using the experimental data and the laboratory-scale furnace (a Carbolite HTR-11/175 rotary furnace, described in Section 3.3.1.4). The total energy consumption during the process can be simplified into three parts: feedstock pyrolysis, mechanical energy consumption and energy (heat) loss. The sources of energy consumption and their calculation equations are summarised in Table 6-1 (Sharifan, 2014).

Table 6-1 The energy consumption sources during pyrolysis

Source of energy consumption	Calculation equation
Rotation of quartz reactor	Rotating motor power
Pyrolysis of feedstock (coconut shell and sludge)	$E = m \times C_p \times \Delta T$
Heat loss	1. Convention through insulation, natural convention 2. Radiation from the external steel cover 3. Radiation through wall openings

Table 6-2 summarizes the energy usage of coconut shell and raw sludge pyrolysis. Based on the calculation assumption from Sharifan (2014), the rotation of the quartz reactor and the heat loss are estimated as 0.1MJ and 2.8MJ, respectively. The energy for coconut shell (300g) pyrolysis can be calculated as (Fono-Tamo & Koya, 2013):

$$E = m \times C_p \times \Delta T = 0.3kg \times 2.1KJ/kgK \times (600 - 20) = 0.37MJ$$

In the equation, m is the mass of the material, C_p is the specific heat value of the material, and ΔT is the change of temperature.

Whereas the energy consumption of raw sludge (300g) pyrolysis can be calculated as (Xu & Lancaster, 2009):

$$E = m \times C_p \times \Delta T = 0.3kg \times 1.95KJ/kgK \times (600 - 20) = 0.34MJ$$

Table 6-2 Energy usage of feedstock pyrolysis

Source of energy consumption	Energy usage (MJ per 300g sample)
Rotation of quartz reactor	0.1
Pyrolysis of feedstock (coconut shell)	0.37
Pyrolysis of feedstock (raw sewage sludge)	0.34
Heat loss	2.8

6.3.2 The Calorific Value of Oil Output

Table 6-3 presents the calorific value of the oil from both 300g coconut shell and raw sludge pyrolysis process. The average oil yield of the six centre point experiment in RSM design (600°C temperature, 10°C/min heating rate, 90min holding time and 550ml/min nitrogen flow rate) can be calculated as 15.9%, which is used for the calculation of the oil output during the coconut shell pyrolysis. The average oil yield is 28.1% from raw sludge pyrolysis process. As a result, the total energy contained within the oil has been calculated and tabulated in Table 6-4.

Table 6-3 Calorific value of oil output

Coconut pyrolysis oil		
Measurement	Sample weight (g)	Calorific value (MJ/kg)
1	0.5114	13.2098
2	0.5082	13.3866
3	0.5098	13.2684
Average	13.2883	
Oil from raw sludge pyrolysis		
Measurement	Sample weight	Calorific value
1	0.5068	25.1930
2	0.5071	24.7179
3	0.5012	24.3319
Average	24.7476	

Table 6-4 Energy obtained from oil output per 300g sample

	Weight (g per 300g sample)	Energy obtained from oil (MJ per 300g sample)
Coconut oil	47.7	0.63
Sludge oil	84.3	2.09

According to the data above, the final net energy consumption has been calculated and shown in Table 6-5. It has been assumed that all the energy provided by the oil product is completely reused in the pyrolysis system. It can be deduced from this data that the production of char filler from raw sludge, using the same production conditions and furnace arrangement, is more energy-effective than coconut shell pyrolysis using the same pyrolysis conditions.

Table 6-5 Final net energy consumption

	Final net energy consumption (MJ per 300g sample)
Coconut shell pyrolysis	+2.64
Raw sludge pyrolysis	+1.15

The main gaseous products formed during the coconut shell pyrolysis process are methane, carbon monoxide, carbon dioxide, water vapor, hydrogen and a wide range of organic vapors (Rout, 2013). Whereas, the vapors released from the raw sewage sludge pyrolysis are mainly methane, carbon monoxide, carbon dioxide, water vapor, hydrogen and C_2H_6 (Pullket, 2015). The gases from both of the two feedstock are highly similar and among this water vapor and CO attributes to the majority of the gaseous products. These gases can be regarded as a mixture of energy-rich gases, since carbon monoxide, hydrogen, methane and a broad range of other VOCs within them are combustible constituents. These gases can be used for thermal and fuel purpose directly, to generate electricity or as a heat source.

6.4 Energy Analysis

In this section, the real industry production is considered, in which several assumptions have been used to derive the numbers:

(1) The heat loss of the furnace has been ignored and is assumed to be zero, since the energy consumed to pyrolyse the huge amount of feedstock is very high compare to the overall (negligible) heat loss in the real treatment plant.

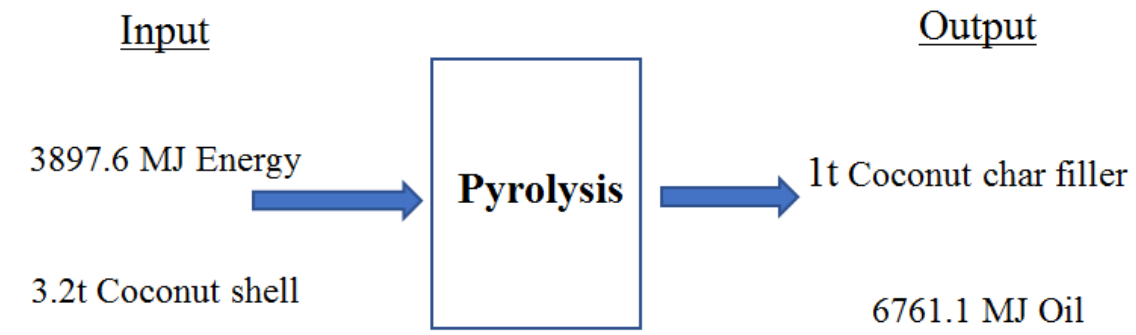
(2) The contribution to the energy value from the gas emissions has been neglected in the coconut shell and raw sludge pyrolysis, since the heat value is quite low compared with oil.

(3) The functional unit is to produce 1 tonne of carbon black substitute.

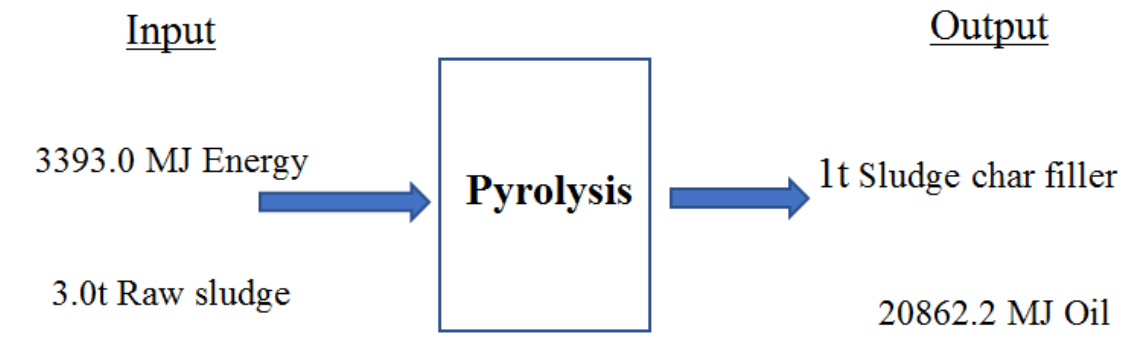
(4) The energy for removing the water content within the sample before pyrolysis is not considered in this analysis.

(5) According to the centre point experiment in RSM, the average char yield from coconut shell pyrolysis and raw sludge pyrolysis can be calculated as 31.7% and 33.7% respectively.

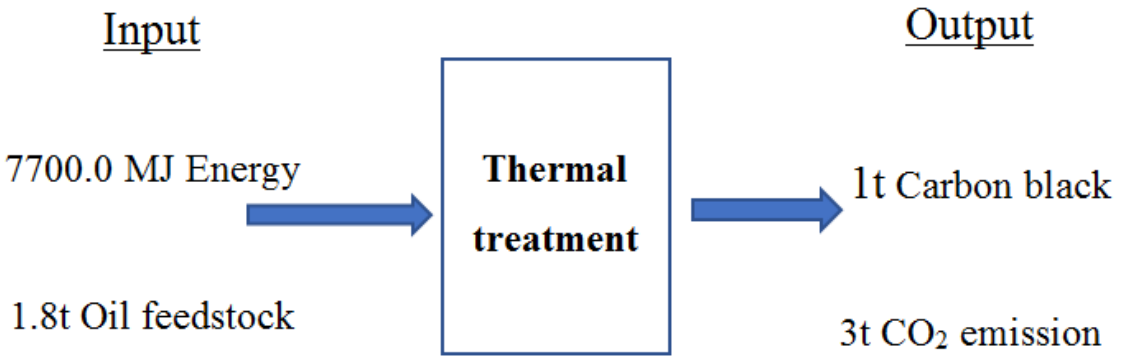
The inputs and output of the three production processes are shown in Figure 6-2.



(a)



(b)



(c)

Figure 6-2 The input and output of the three production processes

It is clearly shown in Figure 6-2, that in order to produce 1t of rubber filler, using a crude oil products as the feedstock for pyrolysis, needs the most energy input at 7700.0MJ/t. Coconut shell and sewage sludge pyrolysis only need 3897.6MJ/t and 3393.0MJ/t respectively. Further,

no reusable oil output is produced from a commercial carbon black manufacturing process, but significant quantities (3t) of CO_2 emission result (Nicolas, 2009; EC, 2007).

6.5 Carbon Dioxide Emission Saving

In order to calculate the net carbon dioxide saving, a method explored by Cebrian Gomez (2008) is used in this study. The 2012 UK Grid Electricity Year factor 0.35 $kgCO_2/kWh$ (DECC & Defra, 2012) is used as a conversion factor, the resulting CO_2 emission values are calculated and shown in Table 6-6.

Table 6-6 Carbon dioxide emissions of the different system

System	Energy (MJ/ton)	Energy (kWh/ton)	Emissions ($kgCO_2$/ton)
Coconut shell pyrolysis	3897.6	1091.3	382.0
Raw sludge pyrolysis	3393.0	950.0	332.5
Carbon black manufacture from oil feedstock	7700.0	2156.0	754.6

It can be concluded that the carbon black substitute production through pyrolysis of coconut shells or sewage sludge has a much lower carbon footprint than the conventional method. The energy input to the waste materials system use only half of the energy needed in the fossil fuel process for commercial carbon black manufacture. In addition, the oil and gas production from each of the pyrolysis systems can also be used in the system as the heating resource, which makes the pyrolysis process much more energy efficient and for practical purposes, almost carbon neutral (based on fossil-carbon emissions). However, it needs to be noted that in this study the raw sewage sludge is dried sludge. Therefore, when considering using raw sludge in the industry, the energy used in the dewatering process also needs to be calculated.

6.6 Conclusion

It has been calculated that the reduction in fossil-fuel carbon dioxide emissions is a significant benefit when using pyrolysis of the coconut shell and raw sewage sludge to prepare carbon black substitute fillers. It indicates that reusing these waste materials in the production of a carbon black replacement will reduce the overall environmental impact in terms of the greenhouse gas emission (as CO_2) compared to the current commercial carbon black manufacture. The result of this Life Cycle Impact Assessment is helpful in the first-step decision making and assessing the viability and sustainability of the suggested waste materials treatment.

To sum up, the pyrolysis of coconut shell and raw sludge for sustainable rubber filler production uses less energy, has a lower carbon footprint and results in a significant heat value by-product (oil).

Chapter 7 Conclusions and Future Work

7.1 Conclusions

The aim of this research has been to evaluate new types of sustainable fillers for rubber and related materials, based on the char produced from pyrolysis of two, high-volume problematic waste materials: coconut shell (biomass) and raw sewage sludge. Through pyrolysis, the waste materials can be converted into high quality bio-char products, and high heat value, renewable energy materials (mainly oil and some gases) at relatively small scale. Thus, global fossil fuel-derived emissions worldwide can be improved through the ability of biochar to sequester the carbon contained in these materials by conversion into a stable and non-available form. This type of process is regarded as major sector with growth potential in the global carbon market with a controllable, clean and simple manufacturing process.

The key outputs from this study can be summarised as follows:

(1) The in-depth physical and chemical characterization of two waste materials: coconut shell and dried raw sewage sludge have been undertaken. These materials have been converted in a pyrolytic char and the products have been compared to commercial carbon blacks: N115, N220, N330, N550, N660 and N772. The surface area of the commercial carbon blacks are typically between 18.5 – 94.5m^2/g; the toluene transmittance are all around 99% except N772 (≈ 65%), showing that carbon blacks are mostly oil-free product, which is corroborated by the toluene transmittance test and proximate analysis. The pH value ranges from 8.37 to 10.09. Through the Boehm titration analysis, the acidic groups on the surface are more prevalent than basic groups. The SEM analysis of the compounded rubber sheet with N660, and TEM of N330 and N772 has been studied to confirm the mechanism of filler and rubber interaction.

(2) The pyrolysis process is a powerful alternative method for the thermochemical treatment of waste carbonaceous materials. The relatively high fixed carbon content of coconut shell contributes to the ability to produce a solid residue which offers much opportunity to apply it as a sustainable carbonaceous rubber filler. Through a careful analysis of the thermal behaviour of coconut shell (powder), the pyrolysis temperature and heating rate were

established. This information was subsequently used to construct a Response Surface Methodology experimental design. Through the application of a Central Composite Face Centred Design (CCFD), all the experiments were undertaken using four identified variables, namely; pyrolysis temperature (°C) (400 – 800°C), heating rate (°C/min) (5 – 15°C/min), holding time (min) (0 – 180min), and Nitrogen flow rate (ml/min) (100 – 1000ml/min); three levels were selected as low -1, centre 0 and high +1 level. The total number of experimental runs was 30 runs.

The char yield (28.7% - 42.5%) of the coconut shell was considered to be good and suggested that the pyrolysis of coconut shell is a suitable methodology to be used on coconut shells as a means of treatment for recovery of reusable products. The coconut char samples generated from conventional pyrolysis have high external surface area values up to 318.6m^2/g, in-line with N100 to N300 series carbon blacks, which are considered to be high quality carbon blacks. The coconut chars also exhibit high levels of porosity. The Boehm titration shows that only when the pyrolysis temperature drops below 400°C, are there more acidic functional groups (up to 0.417mmol/g) than basic groups on the surface of char samples. Otherwise, the char samples with high pyrolysis temperature (600°C and 800°C) have more basic functional groups on their surface. The pH values of the char samples confirm the results of the Boehm titration, in that most of the chars have a basic surface, which is also consistent with the data of the commercial carbon blacks. From the results from toluene transmittance test, all of the char samples from pyrolysed coconut shell are as clean as the commercial carbon black (95 to 97 T%); in other words, almost no oily residues on the surface. According to TGA results, the lower ash content (20%) within the char samples is more acceptable than other chars from woods and textile. Based upon the response of surface area, and pH value, the optimizations of the pyrolysis of coconut shell, within the selected parameters, have been achieved using RSM.

When compounded into the SBR formulation, dispersion was found to be sub-optimum, confirming that more efficient milling would be desirable. The physical and dynamic data generated suggest that the char samples have limited filler-filler and filler-polymer interactions, resulting in relatively semi-reinforcement, indicating that the rubber mix may need optimisation.

(3) It has been confirmed that the pyrolysis of dried raw sewage sludge provides a flexible and suitable way of converting sludge into char fillers, which offers much promise as a sustainable rubber filler to replace commercial carbon black. The experiment design share the same RSM parameters as the previous coconut shell pyrolysis study. The surface area (up to 160m^2/g) is slightly lower than coconut shell derived char fillers, but is still higher than commercial carbon black. The toluene transmittance tells that most of the sludge char filler are as clean as commercial carbon black. Both acidic groups (up to 1.403mmol/g) and basic groups (up to 1.603mmol/g) on the surface of the char filler are observed to be much more than coconut char and the correlation to the pH value can be seen as well. Based on the response of surface area, pH value and surface acidic groups, the optimization of the pyrolysis of raw sewage sludge have been achieved using RSM.

After having been compounded with a rubber matrix using the SBR formulation, the rubber products performed much better than the coconut shell char filled rubber sample, based upon their technological performance. The sludge chars displayed much better dispersion characteristics and better filler-rubber interaction. It was very evident from the samples prepared that the sludge char fillers show great potential to be used as a replacement of commercial carbon black N990 as a sustainable semi-reinforcing rubber filler. Once again, there was highlighted the need to optimise the rubber-mix formulation to better enhance the filler-rubber bonding, but the benefits imparted by undertaking this process would be significant.

(4) The TEM analysis shows that the morphological features of the sludge derived char fillers are very similar to commercial carbon black, with a prevalence of “spheroidal” particles present in the images. The presence of the ash component in the sludge char provided an interesting added feature. Given that it is increasingly common to add silica to rubber mixes as an alternative filler to carbon black in rubber, the char-ash matrix offered by sewage sludge char appears to offer an opportunity to provide single filler materials with added benefits.

(5) Utilisation of the SEM analysis of the rubber samples prepared using the different carbon materials filled with carbon black N660, coconut shell char fillers and sludge char fillers, enabled an assessment of the mechanism of the interaction between filler and rubber to be observed. The interaction between coconut shell char and rubber may correlates to the physical Van der Waals force (simply entrapment), whereas there are apparently chemical reactions occurring which may contribute to the interaction between the rubber and sludge char fillers, akin to those observed for carbon black (N660 etc.). This indicates that sewage sludge is a very promising feedstock for carbon black filler replacement production.

(6) The LCA assessment has revealed that to produce the same quantity of rubber filler (1t), the energy consumption of coconut shell (3897.6MJ) and raw sewage sludge (3393.0MJ) is much less than commercial carbon black manufacture process (7700.0MJ) and the carbon dioxide emissions associated with the processes are much lower using shells or sludge, compared to oil.

7.2 Contributions to Knowledge

(1) This is the first study which has analysed and tested the potential for converting coconut shell and raw sewage sludge into sustainable carbon black substitutes through the application of conventional pyrolysis and the subsequent in-depth analysis of the chars specifically for in-rubber applications.

(2) The development and application of a modified Central Composite Design (Central Composite Face Centred Design) has been used to design and analyse the pyrolysis process enabling a thorough understanding of the influence of key process variables and their effects on the properties of the char products.

(3) The mixing and testing of the interactions between the rubber and this new class of rubber fillers has provided a new understanding of key factors which influence the filler-polymer bonding, including particle size coupled with surface chemistry, as applied to non-carbon

black materials. Due to the similar thermal behaviour of biomass, this char filler production process has demonstrated the potential to extend the methodology to other biomass for carbonaceous filler materials production.

(4) Through Life Cycle Assessment and the thermodynamic analysis, the energy consumption throughout the pyrolysis production system has been evaluated and the potential for the process to be significantly less energy and emission intensive, than current carbon black production processes has been validated with experiment.

7.3 Future Work

This thesis has shown that the beneficial recovery of value from biomass and raw sewage sludge can be achieved by the solid product obtained from the pyrolysis process being used as a carbon black substitute in rubber manufacture. There are still further investigations needed. According to the results obtained from this research, the following investigations have been identified for future research:

(1) It has been recognised that a more efficient milling method would be desirable to further modify the particle size of these novel rubber fillers. This should significantly increase the level of filler-polymer interaction. If the filler-polymer interaction can be increased, and the current level of filler-filler interactions maintained, the char filler would have very interesting properties with regard to low energy losses and better reinforcement, widening their application.

(2) Further optimisation of the post-production processing for the char needs to be investigated. Factors such as char surface chemical modification using KOH or HCl for removing ash content and introducing more functional groups and changing the surface activity to the char surface, further enhancing the filler-polymer bonding should be undertaken.

(3) The coconut and sludge char fillers are an entirely new types of rubber filler. The lack of experience within the rubber industry with non-carbon black fillers means that mix optimisation must be undertaken for further future improvements. The reformulation of rubber mixes is a key step to be considered to maximise benefit of alternative fillers and widen their applicability.

(4) A wider, whole life cycle assessment should be further developed to find and reach the balance between yield, CO_2 emission and the quality of these substitute carbon blacks compared to current carbon blacks, as applied within the rubber system.

(5) Due to the more efficient (volumetric) heating mechanism associated with microwave pyrolysis, the production of chars using this technology has the potential to produce different products which may have different and interesting surface properties. The obvious capability to save energy when heating due to the molecular (atomic)-scale heating caused by microwave ovens would influence the LCA and therefore, a suitable optimised microwave system need to be developed and evaluated. The manufacture of traditional carbon black is not feasible using microwaves; hence, this technology may be a major step-forward as far as rubber-filler production is concerned.

(6) In order to commercialize the alternative sustainable rubber filler, economic analysis needs to be considered in later stage. It is necessary to weigh the cost of the new rubber filler manufacture process against the benefits it will bring.

References

Abbe, O. E. (2009) *Recovery of Value from Oil Drill Cuttings – A Sustainable Waste Management Solution for the Oil and Gas Exploration and Production Industry*. PhD thesis. Imperial College London.

Agrafioti, E., Bouras, G., Diamadopoulos, E., & Kalderis, D. (2013) Biochar production by sewage sludge pyrolysis. *Journal of Analytical and Applied Pyrolysis*. 101, 72-78.

Ahmed, K., Nizami, S. S. & Raza, N. Z. (2012) Characteristics of natural rubber hybrid composites based on marble sludge/carbon black and marble sludge/rice husk derived silica. *Journal of Industrial and Engineering Chemistry*. 19(4), 1169-1176.

Ali Shah, A., Hasan, F., Shah, Z., Kanwal, N. & Zeb, S. (2013) Biodegradation of natural and synthetic rubbers: A review. *International Biodeterioration & Biodegradation*. 83, 145-157.

Andrews, S., (2014) Cooper Tire Perspective. [Presentation] Carbon Black World 2014, 20th October.

ANRPC (Association of Natural Rubber Producing Countries). (2017) Available from: http://www.anrpc.org/html/market-news-details.aspx?ID=26&PID=28&NID=966 [Accessed 7th August 2017]

Arabiourrutia, M., Lopez, G., Elordi, G., Olazar, M., Aguado, R., Bilbao, J. (2007) Product distribution obtained in the pyrolysis of tyres in a conical spouted bed reactor. *Chemical Engineering Science*. 62(18), 5271-5275.

References

Arayapranee, W., Na-Ranong, N., & Rempel, G. (2005). Application of Rice Husk Ash as Fillers in the Natural Rubber Industry. *Journal of Applied Polymer Science*. 98(1), 34-41.

Arun, P. S., Sathish, S. & Narendhar, C. (2014) Fabrication of polystyrene composite reinforced with silicon carbide nanoparticles. *International Journal of Current Engineering and Technology*. Available from:

http://inpressco.com/wp-content/uploads/2014/02/Paper44247-249.pdf [Accessed 1st August 2017].

Arundel, J. (2000) *Sewage and Industrial Effluent Treatment*. United States, Wiley-Blackwell Publishing.

ASTM Standard D1506-99 (2013) *Standard Test Methods for Carbon Black- Ash Content*. West Conshohocken, ASTM International.

ASTM Standard D1512-05 (2012) *Standard Test Methods for Carbon Black – pH Value* . West Conshohocken, ASTM International.

ASTM Standard D1618-99 (2004) *Standard Test Methods for Carbon Black Extractables-Transmittance of Toluene Extract*. West Conshohocken, ASTM International.

ASTM Standard D1765-17 (2017) *Standard Classification System for Carbon Blacks Used in Rubber Products*. West Conshohocken, ASTM International.

ASTM Standard D2414-16e1 (2016) *Standard Test Method for Carbon Black – Oil Absorption Number (OAN)*. West Conshohocken, ASTM International.

References

ASTM Standard D6556-16 (2016) *Standard Test Method for Carbon Black—Total and External Surface Area by Nitrogen Adsorption*. West Conshohocken, ASTM International.

Athanassiades, E., (2013) *Waste tyre pyrolysis: Sustainable recovery and reuse of a valuable resource*. PhD thesis. Imperial College London. U.K.

Aujame, L., Seguin, D., Droy, C. & Hessler, C. (2000) Experimental design optimization of filamentous phage transfection into mammalian cells by cationic lipids. *Biotechniques*. *28*.

Aygün, A., Yenisoy-Karakaş, S. & Duman, I. (2003) Production of granular activated carbon from fruit stones and nutshells and evaluation of their physical, chemical and adsorption properties. *Microporous and Mesoporous Materials*. 66(2), 189-195.

Bakisgan, C., Dumanli, A. G. & Yürüm, Y. (2009) Trace elements in Turkish biomass fuels: Ashes of wheat straw, olive bagasse and hazelnut shell. *Fuel*. 88(10), 1842-1851.

Banks, J. (1998) *Handbook of simulation: modelling, estimation and control*. US, John Wiley and Sons Inc.

Bezerra, M. A., Santelli, R. E., Oliveira, E. P., Villar, L. S. & Escaleira, L. A. (2008) Response surface methodology (RSM) as a tool for optimization in analytical chemistry. *Talanta*, 76(5), 965-977.

Blanchard, A. F. & Parkinson, D. (1948) Structures in rubber reinforced by carbon black. *Second Rubber Technology Conference*, London, Great Britain.

References

Blanchard, A. & Parkinson, D. (1952) Breakage of Carbon-Rubber Networks by Applied Stress. *Industrial & Engineering Chemistry*. 44(4), 799-812.

Bloomfield, M. S. & Butler, W. C. (2000) Robustness testing, using experimental design, of a flow-through dissolution method for a product where the actives have markedly differing solubility properties. *International Journal of Pharmaceutics*. 206(1), 55-61.

Blow, C. M. (1975). *Rubber Technology and Manufacture*. U.K., Butterworth-Heinemann.

Boehm, H. P. (1994) Some aspects of the surface chemistry of carbon blacks and other carbons. *Carbon*. 32(5), 759 – 769.

Bolton, S. & Bon, C. (2010) *Pharmaceutical Statistics: Practical and Clinical Applications*, fifth ed., New York, CRC Press.

Bowen, D. K. & Hall, C. R. (1975) *Microscopy of materials- Modern imaging methods using electron, X-Ray and ion beams*. Great Britain, MacMillan Press Ltd.

Box, G. E. P. & Wilson, K. B. (1951) On the Experimental Attainment of Optimum Conditions. *Journal of the Royal Statistical Society*. Series B (Methodological). 13, 1-45.

British Standards, BS EN ISO 14044:2006. (2006) *Environmental management. Life cycle assessment. Requirements and guidelines*.

Bueche, F. (1960) Molecular basis for the mullins effect. *Journal of Applied Polymer Science*. 4(10), 107-114.

References

Bueche, F. (1961) Mullins effect and rubber–filler interaction. *Journal of Applied Polymer Science*. 5(15), 271-281.

Bueche, F. (1965) In: Kraus G. (ed.) *Reinforcement of elastomer.* New York, Wiley.

Cagnon B.; Py X.; Guillot A. (2004) *Carbonization kinetics of coconut shells and plum stones*. Proceedings of Carbon 2004 Conference. Brown University, Providence, RI (Paper K023).

Cagnon, B.; Py, X.; Guillot, A.; Stoeckli, F. & Chambat, G. (2009) Contributions of hemicellulose, cellulose and lignin to the mass and the porous properties of chars and steam activated carbons from various lignocellulosic precursors. *Bioresource Technology*. 100(1), 292-298.

Cao, Q., Xie, K., Bao, W. & Shen, S. (2004) Pyrolytic behavior of waste corn cob. *Bioresource Technology*. 94(1), 83-89.

Caramia, M. & Dell´Olmo., P. (2008) *Multi-objective Management in Freight Logistics. Increasing Capacity, Service Level and Safety with Optimization Algorithms*. London, Springer.

Cebrián-Gómez, M. G. (2008) *Environmental impacts of and material recovery from biodegradable waste*. PhD thesis. Imperial College London.

Chaudhary, D., Jollands, M. & Cser, F. (2004) Recycling rice hull ash: A filler material for polymeric composites? *Advances in Polymer Technology*. 23(2), 147-155.

Chen, X., Jeyaseelan, S. & Graham, N. (2002) Physical and Chemical Properties Study of Activated Carbon made from Sewage Sludge. *Waste Management*. 22, 755-760.

Chiang, C. (2013) *Natural rubber biosynthesis: Perspectives from polymer chemistry*. PhD thesis. The University of Akron.

Conesa, J. A., Marcilla, A., Prats, D. & Rodriguez-Pastor, M. (1997) Kinetic Study of the Pyrolysis of Sewage Sludge. *Waste Management & Research*. 15(3), 293-305.

Costa, H. M. D., Visconte, L. L. Y., Nunes, R. C. R. & Furtado, C. R. G. (2000) The effect of coupling agent and chemical treatment on rice husk ash- filled natural rubber composites. *Journal of Applied Polymer Science*. 76(7), 1019-1027.

Costa, H. M. D., Visconte, L. L. Y., Nunes, R. C. R. & Furtado, C. R. G. (2002) Mechanical and dynamic mechanical properties of rice husk ash–filled natural rubber compounds. *Journal of Applied Polymer Science*, 83(11), 2331-2346.

Council Directive 1999/31/EC of 26 April 1999 on the landfill of waste. (1999) Brussels. pp. 1-19

Council Directive 86/278/EEC of 12 June 1986 on the protection of the environment, and in particular of the soil, when sewage sludge is used in agriculture. (1986) Brussels.

Council Directive 91/271/EEC of 21 May 1991 concerning urban waste-water treatment. (1991) Brussels.

Crompton, T. R. (2012) Physical Testing of Plastics. Shropshire, Smithers Rapra Technology Ltd, pp. 1-102.

Cunliffe, A. M. & Williams, P. T. (1998) Properties of chars and activated carbons derived from the pyrolysis of used tyres. *Environmental Technology*. 19(12), 1177 – 1190.

Dannenberg, E. M. (1966) Molecular slippage mechanism of reinforcement. *Transactions of the Institution of the Rubber Industry*. 42, 26.

Dasgupta, M., Kar, S., Gupta, S. D., Mukhopadhyay, R. & Bandyopadhyay, A. (2013) Effect of fly ash as filler in rubber – A comprehensive study of the vulcanisate properties of styrene butadiene rubber compounds. *Progress in Rubber, Plastics and Recycling Technology*. 29(3), 151-168.

Deb, K. (2005) *Multi-objective optimization. In Burke, E. and Kendall, G. (Eds.) Search methodologies*. US, Springer.

DECC & Defra (2012) *2012 Guidelines to Defra / DECC's GHG Conversion Factors for Company Reporting.* Available from: https://www.gov.uk/government/uploads/system/uploads/attachment_data/file/69568/pb13792-emission-factor-methodology-paper-120706.pdf [Accessed 3rd August 2017].

Demirbas, A. (2004) Combustion characteristics of different biomass fuels. *Progress in Energy and Combustion Science*. 30(2), 219-230.

Demirbaş, E., Kobya, M. Öncel, S. & Şencan, S. (2002) Removal of Ni(II) from aqueous solution by adsorption onto hazelnut shell activated carbon: Equilibrium studies. *Bioresource Technology*. 84(3), 291-293.

References

Department for Environment, Food and Rural Affairs (Defra). (2011) *Environmental permitting guidance: The landfill directive*. Available from: http://webarchive.nationalarchives.gov.uk/20130403065019/http://archive.defra.gov.uk/environment/policy/permits/documents/ep2010landfill.pdf [Accessed 3rd August 2017]

Department for Environment, Food and Rural Affairs (Defra). (2017) *Sewage sludge on farmland: code of practice for England, Wales and Northern Ireland***.** Available from: https://www.gov.uk/government/publications/sewage-sludge-on-farmland-code-of-practice/sewage-sludge-on-farmland-code-of-practice [Accessed 9th July 2017].

Department of Environment, Transport and the Regions (DETR). (2000) *Waste Strategy 2000*. HMSO, London, UK.

Directive 2000/76/EC of the European parliament and of the council of 4 December 2000 on the incineration of waste. (2000) Brussels.

Directive 2008/98/EC of the European parliament and of the council of 19 November 2008 on waste and repealing certain Directives. (2008) Brussels.

Do, D. (1998). *Adsorption analysis: Equilibria and kinetics* (Series on chemical engineering; v.2). London, Imperial College Press.

Domínguez, A., Menéndez, J. A., Inguanzo, M. & Pis, J. J. (2005) Investigations into the characteristics of oils produced from microwave pyrolysis of sewage sludge. *Fuel Processing Technology*. *86*(9), 1007-1020.

References

Domínguez, A., Menéndez, J. A., Inguanzo, M. & Pis, J. J. (2006) Production of bio-fuels by high temperature pyrolysis of sewage sludge using conventional and microwave heating. *Bioresource Technology*. 97(10), 1185-1193.

Donnet, J., Bansal, R. C. & Wang, Meng-Jiao. (1993). *Carbon black : Science and technology* (2nd ed., revised and expanded ed.). New York: Dekker.

Eddy, M., Techobanoglous, G., Burton, F.L. & Stensel, D. H. (2003) *Wastewater Engineering: Treatment and Reuse*. New York, McGraw-Hill Higher Education.

Edwards, D. (1990) Polymer-filler interactions in rubber reinforcement. *Journal of Materials Science*. *25*(10), 4175-4185.

Eirich, F., Mark, James E, & Erman, Burak. (1994). *Science and technology of rubber* (2nd ed.). San Diego; London: Academic Press.

El-Gendy, N., Madian, H., & Amr, S. (2013) Design and Optimization of a Process for Sugarcane Molasses Fermentation by Using Response Surface Methodology. *International Journal of Microbiology*. 2013, 9.

Environment Agency. (2004) *Life Cycle Assessment of the Management Options for Waste Tyres. Environment Agency R&D Report Ref. No. P1 437/TR, Environment Agency, Bristol.*

ERT (Elastomer Research Testing B.V.). (2009) *Measuring the Payne effect in filled rubber*. [Presentation] VKRT meeting, 14th May.

References

European Commission. (1991) Directive 91/676/EEC of the European Parliament on implementation of the Council concerning the protection of water against pollution caused by nitrates from agricultural sources for the period 2000–2003 SEC(2007)339/COM/2007/0120 final. Brussels.

European Commission. (2007) *Large Volume Inorganic Chemicals – Solids and Others industry*. August 2007. pp. 208-215.

European Community. (2009) Directive 2009/28/EC of the European Parliament and of the Council of 23 April 2009 on the promotion of the use of energy from renewable sources and amending and subsequently repealing Directives 2001/77/EC and 2003/30/EC. *L140/16-62: Official Journal of the European Union*.

Fan, Y., Fowler, G. D., & Norris, C. (2017) Potential of a Pyrolytic Coconut Shell as a Sustainable Biofiller for Styrene-Butadiene Rubber. *Industrial and Engineering Chemistry Research*. 56(16), 4779-4791.

Ferreira, S. L. C., Bruns, R. E., Ferreira, H. S., Matos, G. D., David, J. M., Brandão, G. C., Da Silva, E. G. P., Portugal, L. A., Dos Reis, P. S., Souza, A. S. & Dos Santos, W. N. L. (2007) Box-Behnken design: An alternative for the optimization of analytical methods. *Analytica Chimica Acta*. 597(2), 179-186.

Ferreira, S. L. C., Dos Santos, W. N. L., Quintella, C. M., Neto, B. B. & Bosque-Sendra, J. M. (2004) Doehlert matrix: A chemometric tool for analytical chemistry—review. *Talanta*, 63(4), 1061-1067.

Fono-Tamo, R. S. & Koya, O.A. (2013) Characterisation of Pulverised Palm Kernel Shell for Sustainable Waste Diversification. *International Journal of Scientific & Engineering Research*. 4(4), 6-10.

References

Food and Agriculture Organization of the United Nations. (2017) *Crops – coconuts*. Available from: http://www.fao.org/faostat/en/#data/QC/visualize [Accessed on 29th July 2017].

Food and Agriculture Organization of the United Nations. (2017) *Crops and livestock products – Groundnuts shelled in 2013*. Available from: http://www.fao.org/faostat/en/#data/TP [Accessed on 6th August 2017].

Forrest, M. J. (2001) *Rubber Analysis - Polymers, Compounds and Products: (Report No. 139), Volume 12*. Smithers Rapra Technology.

Frost, J. (2016) *Understanding t-Tests: 1-sample, 2-sample, and Paired t-Tests*. Available from: http://blog.minitab.com/blog/adventures-in-statistics-2/understanding-t-tests:-1-sample,-2-sample,-and-paired-t-tests [Accessed 7th August 2017].

Fuad, M. Y. A., Ismail, Z., Mansor, M. S., Ishak, Z. A. M. & Omar, A. K. M. (1995) Mechanical Properties of Rice Husk Ash/Polypropylene Composites. *Polymer Journal*. 27(10), 1002-1015.

Fytili, D. & Zabaniotou, A. (2008) Utilization of sewage sludge in EU application of old and new methods—A review. *Renewable and Sustainable Energy Reviews*. 12(1), 116-140.

Ganguly, S., Bhattacharya, P. & Banerjee, A. N. (2005) Effect of surface modification of carbon black by 1,2 Dihydroxy benzene and 1,2,3 trihydroxy benzene on a natural rubber-carbon black composite. Indian Journal of Chemical Technology. 12, 695-700.

References

Ganguly, S., Bhattacharya, P., Banerjee, A. N. & Chakraborty, S. (2003) 1,3,5-trihydroxy benzene as a surface modifier of carbon black and its effect on the filler–rubber interaction. *Journal of Applied Polymer Science*. 87(14), 2272-2278.

Ganguly, S., Chakraborty, S., Banerjee, A. N. & Bhattacharya, P. (2002) Effect of meta - dihydroxy benzene as a surface modifier on filler–filler and filler–polymer interaction of carbon black polymer composite. *Journal of Applied Polymer Science*. 85(9), 2025-2033.

Gani, A. & Naruse, I. (2007) Effect of cellulose and lignin content on pyrolysis and combustion characteristics for several types of biomass. *Renewable Energy*. 32(4), 649-661.

Genieva, S., Turmanova, D., Dimitrova, C. & Vlaev, A. (2008) Characterization of rice husks and the products of its thermal degradation in air or nitrogen atmosphere. *Journal of Thermal Analysis and Calorimetry*. 93(2), 387-396.

Gent, A. & Hwang, N. (1990) Internal failures in model elastomeric composites. *Journal of Materials Science*. 25(12), 4981-4986.

Gent, A. N. & Tompkins, D. A. (1969) Nucleation and Growth of Gas Bubbles in Elastomers. *Journal of Applied Physics*. *40*(6), 2520-2525.

Gentil, E. C., Damgaard, A., Hauschild, M., Finnveden, G., Eriksson, O., Thorneloe, S., Kaplan, P. O., Barlaz, M., Muller, O., Matsui, Y., Li, R. & Christensen, T. H. (2010) Models for waste life cycle assessment: Review of technical assumptions. *Waste Management*. 30(12), 2636-2648.

Goertzen, S. L., Thériault, K. D., Oickle, A. M., Tarasuk, A. C. & Andreas, H. A. (2010) Standardization of the Boehm titration. Part I. CO_2 expulsion and endpoint determination. *Carbon*. 48(4), 1252-1261.

González, J. F., Encinar, J. M., Canito, J. L. & Rodríguez, J. J. (2001) Pyrolysis of automobile tyre waste. Influence of operating variables and kinetics study. *Journal of Analytical and Applied Pyrolysis*. 58, 667-683.

Gopalan Nair, K. & Dufresne, A. (2003) Crab shell chitin whisker reinforced natural rubber nanocomposites. 2. Mechanical behaviour. *Biomacromolecules*. 4(3), 666-674.

Gregg, S. J. & Sing, K. S. W. (1982) Adsorption, Surface Area and Porosity, London, Academic Press.

Grønli, M., Antal, M. J. & Várhegyi, G. (1999) A round-robin study of cellulose pyrolysis kinetics by thermogravimetry. Industrial & Engineering Chemistry Research. 38(6), 2238-2244.

Grønli, M., Várhegyi, G., & Di Blasi, C. (2002) Thermogravimetric analysis and devolatilization kinetics of wood. *Industrial and Engineering Chemistry Research*. 41(17), 4201-4208.

Guinée, J. B., Heijungs, R., Huppes, G., Zamagni, A., Masoni, P., Buonamici, R., Ekvall, T. & Rydberg, T. (2011) Life cycle assessment: Past, present, and future. *Environmental Science & Technology*. 45(1), 90-96.

Guth, E. & Gold, O. (1938) On the hydrodynamical theory of the viscosity of suspensions. *Physical Review*. 53, 322.

References

Guth, E. (1945). Theory of Filler Reinforcement. *Journal of Applied Physics*. 16(1), 20-25.

Haines, P., & Reading, M. (1995). *Thermal methods of analysis: Principles, applications and problems*. London, Blackie Academic.

Han, K. (2000). Identification of Natural Rubber and Characterization of Rubber Biosynthetic Activity in Fig Tree. *Plant Physiology*. 123(3), 1133-1142.

Haykiri-acma, H., Yaman, S. & Kucukbayrak, S. (2010) Comparison of the thermal reactivities of isolated lignin and holocellulose during pyrolysis. *Fuel Processing Technology*. 91(7), 759-764.

Hewitt, N. & Ciullo, P. (2007) *Compounding Precipitated Silica in Elastomers: Theory and Practice*. New York, William Andrew. p.553.

Hosler, D., Burkett, S. & Tarkanian, M. (1999). Prehistoric Polymers: Rubber Processing in Ancient Mesoamerica. *Science*. 284(5422), 1988-1991.

Ikram, A. (2002) *Natural rubber bioderadation in soil in relation to the waste disposal of used latex products*. Available from: http://www.rubbernews.com/article/20020101/DATA/301019985/natural-rubber-biodegradation-in-soil-in-relation-to-the-waste [Accessed 1st July 2017]

Intergovernmental Panel on Climate Change (IPCC). (2007) *Fourth Assessment Report: Climate Change 2007 (AR4): Synthesis Report*.

References

International Carbon Black Association (ICBA). (2016) *Carbon Black User's Guide*. Available from: http://www.carbon-black.org/images/docs/2016-ICBA-Carbon-Black-User-Guide.pdf [Accessed 27th June 2017].

International Energy Agency (IEA). (2007) *Tracking Industrial Energy Efficiency and CO_2 Emissions*. Available from: https://www.iea.org/publications/freepublications/publication/tracking_emissions.pdf [Accessed 3rd August 2017].

Intharapat, P., Kongnoo, A. & Kateungngan, K. (2013) The Potential of Chicken Eggshell Waste as a Bio-filler Filled Epoxidized Natural Rubber (ENR) Composite and its Properties. *Journal of Polymers and the Environment*. 21(1), 245-258.

Ishak, Z. A. M. & Bakar. A. A. (1995) An investigation on the potential of rice husk ash as fillers for epoxidized natural rubber (ENR). *European Polymer Journal*. 31(3), 259-269.

Ismail, H., Nizam, J. M. & Abdul Khalil, H. P. S. (2001) The effect of a compatibilizer on the mechanical properties and mass swell of white rice husk ash filled natural rubber/linear low density polyethylene blends. *Polymer Testing*. 20(2), 125-133.

Jain, A. & Tripathi, S. K. (2014) Fabrication and characterization of energy storing supercapacitor devices using coconut shell based activated charcoal electrode. *Materials Science & Engineering B*. 183, 54-60.

Jha, V. (2008) *Carbon Black Filler Reinforcement of elastomers*. PhD Thesis. University of London. U.K.

Jong, L. (2007) Effect of soy spent flakes and carbon black co-filler in rubber composites. *Composites Part A*. *38*(2), 252-264.

Kan, T., Strezov, V. & Evans, T. (2016) Effect of the Heating Rate on the Thermochemical Behavior and Biofuel Properties of Sewage Sludge Pyrolysis. *Energy and Fuels*. 30(3), 1564-1570.

Kim, S., & Park, J. (1995). Pyrolysis kinetics of scrap tire rubbers. 1: Using DTG and TGA. *Journal of Environmental Engineering*. 121(7), 507-514.

Kincl, M., Turk, S. & Vrečer, F. (2005) Application of experimental design methodology in development and optimization of drug release method. *International Journal of Pharmaceutics*. 291(1), 39-49.

Kök, M. V.m Özbas, E., Hicyilmaz, C. & Karacan, Ö. (1997) Effect of particle size on the thermal and combustion properties of coal. *Thermochimica Acta*. 302(1), 125-130.

Konak, A., Coit, D. W. & Smith, A. E. (2006) Multi-objective optimization using genetic algorithms: A tutorial. *Reliability Engineering & System Safety*. 91, 992-1007.

Kroschwitz, J. I., Mark, H. F., Bikales, N., Overberger, C. G. & Menges, G. (1985) *Encyclopedia of polymer science and engineering.* New York, John Wiley and Sons.

Kühner, G. & Voll, M. (1993) Manufacture of carbon black. In: Donnet J., Bansal R. C. & Wang M. (ed.) *Carbon Black, Science and technology,* Second Edition, Revised and Expanded, pp. 1-66.

References

Kuratani, K., Okuno, K., Iwaki, T., Kato, M., Takeichi, N., Miyuki, T., Awazu, T., Majima, M. & Sakai, T. (2011) Converting rice husk activated carbon into active material for capacitor using three-dimensional porous current collector. *Journal of Power Sources*. 196(24), 10788-10790.

Lashof, D.A. & Ahuja, D.R. (1990) Relative contributions of greenhouse gas emissions to global warming. *Nature*. 344, 529-531.

Laturnus, F., Groen, C., & Von Arnold, K. (2007) Organic Contaminants from Sewage Sludge Applied to Agricultural Soils - False Alarm Regarding Possible Problems for Food Safety? *Environmental Science and Pollution Research International*. 14(1), 53-60.

Lee, E. Y., Ryu, G. H. & Lim, S. T. (1990) Effects of processing parameters on physical properties of corn starch extrudates expanded using supercritical CO_2 injection1. *Cereal Chemistry Journal*. 76, 63-69.

Lenntech. (2017) *Sludge sorts*. Available from: http://www.lenntech.com/library/sludge/sorts/sludgesorts.htm [Accessed 1st August 2017]

Leung, D., Yin, X., Zhao, Z., Xu, B. & Chen, Y. (2002) Pyrolysis of tire powder: Influence of operation variables on the composition and yields of gaseous product. *Fuel Processing Technology*. 79(2), 141-155.

Li, W., Yang, K., Peng, J., Zhang, L., Guo, S. & Xia, H. (2008) Effects of carbonization temperatures on characteristics of porosity in coconut shell chars and activated carbons derived from carbonized coconut shell chars. *Industrial Crops & Products*. 28(2), 190-198.

References

Li, Z., Zhang, J. & Chen, S. (2008). Effects of carbon blacks with various structures on vulcanization and reinforcement of filled ethylene-propylene-diene rubber. *Express Polymer Letters*. 2(10), 695-704.

Lin, J. (2002) Identification of the surface characteristics of carbon blacks by pyrolysis GC–MASS. *Carbon*. 40(2), 183-187.

Liyana-Pathirana, C. & Shahidi, F. (2005) Optimization of extraction of phenolic compounds from wheat using response surface methodology. *Food Chemistry*, 93(1), 47-56.

Loadman, M. J. R. (1998) *Analysis of Rubber and Rubber-like Polymers*. Netherlands, Springer Netherlands, p. 278.

MacMillan, A. (2015) *Global Warming 101*. Available from: https://www.nrdc.org/stories/global-warming-101 [Accessed 2nd July 2017].

Manna, A. K., De, P. P., Tripathy, D. K., De, S. K. & Peiffer, D. G. (1999) Bonding between precipitated silica and epoxidized natural rubber in the presence of silane coupling agent. *Journal of Applied Polymer Science*. 74(2), 389-398.

Mark, E. J., Erman, B. & Eirich, F. R. (2005) *Science and technology of rubber* (3rd ed.). San Diego; London: Elsevier Academic Press, p. 368.

Mark, E. J., Erman, B. & Roland, C. M. (2013) *The Science and Technology of Rubber* (4th ed.). Waltham, Academic Press.

Markovic, G. & Visakh, P. M. (2016) *Rubber Nano Blends: Preparation, Characterization and Applications*. Russia, Springer, p. 211.

Massart, D. L., Vandeginste, B. G. M., Buydence, L. M. C., De Jong, S., Lewi, P. J. & Smeyers-verbeke, J. (1997) *Handbook of chemometrics and qualimetrics*. Netherlands, Elsevier Science.

Maya, K. S. (2007) *Studies on in situ precipitated silica filled rubber composites with special reference to NR, NBR and SBR*. PhD Thesis. Cochin University of Science and Technology. India.

McAllister, J. (2015) Factors Influencing Solid-Waste Management in the Developing World. *All Graduate Plan B and other Reports*. Paper 528.

Medalia, A. I. & Kraus, G. (1994) Reinforcement of elastomers by particulate fillers. In: Mark J. E., Erman B. & Eirich F. R. (ed.) *Science and Technology of Rubber*. 2nd Edition, Academic Press, pp. 387-418.

Mettler Toledo. (2012) *Introduction to TGA*. [Lecture] Queen University Belfast, 16th February.

Mohan, D. U., Pittman Jr., C. H. & Steele, P. (2006) Pyrolysis of wood/biomass for bio-oil: A critical review. *Energy and Fuels*. 20(3), 848-889.

Montgomery, D. C. (1976) *Design and analysis of experiments*. London, John Wiley.

Mooney, M. (1940) A Theory of Large Elastic Deformation. *Journal of Applied Physics*. 11(9), 582-592.

Morton, M. (1963) *Introduction of Rubber Technology*. New York, Reinhold Publishing Corporation.

Mullins, L. & Tobin, N. (1965) Stress softening in rubber vulcanizates. Part I. Use of a strain amplification factor to describe the elastic behavior of filler-reinforced vulcanized rubber. *Journal of Applied Polymer Science*. 9(9), 2993-3009.

Myers R. H., Montgomery D. C. & Anderson-Cook C. M. (2009) *Response Surface Methodology – Process and Product Optimization Using Designed Experiments.* 3rd ed. New Jersey, John Wiley & Sons.

Myers, R. H. & Montgomery, D. C. (2002). *Response surface methodology: Process and product optimization using designed experiments*. 2nd ed. New York: Wiley.

Nashar, D., Abd-El-Messieh, S., & Basta, A. (2004) Newsprint paper waste as a fiber reinforcement in rubber composites. *Journal of Applied Polymer Science*. 91(1), 469-478.

Nicolas, P. (2009) *Carbon Black*. Available from: https://www.promes.cnrs.fr/uploads/pdfs/solhycarb/Carbon_Black-N_Probst.pdf [Accessed 7th August 2017].

Ning, P., Yang, Y., Peng, J. & Zhang, S. (2006) Pyrolysis and Charring of Coconut Shell by Thermal Analysis. *Chemistry and Industry of Forest Products*. 26(1), 49-52.

Norris, C. J., Hale, M. & Bennett, M. (2014) Pyrolytic carbon: Factors controlling in-rubber performance. *Plastics, Rubber and Composites*. 43(8), 245-256.

Orfão, J. J. M., Antunes, F. J. A. & Figueiredo, J. L. (1999) Pyrolysis kinetics of lignocellulosic materials-three independent reactions model. *Fuel*. 78(3), 349-358.

Orion Engineered Carbons (OEC). (2015) *What is Carbon Black*. Available from: https://www.thecarycompany.com/media/pdf/specs/orion-what-is-carbon-black.pdf [Accessed 7th July 2017].

Park, S. J. & Kim. J. S. (2000) Role of Chemically Modified Carbon Black Surfaces in Enhancing Interfacial Adhesion between Carbon Black and Rubber in a Composite System. *Journal of Colloid And Interface Science*. 232(2), 311-316.

Park, S. J., Kim, H. C. & Kim, H. Y. (2002) Roles of Work of Adhesion between Carbon Blacks and Thermoplastic Polymers on Electrical Properties of Composites. *Journal of Colloid And Interface Science*. 255(1), 145-149.

Park, W. C. & Atreya, A. (2010) Experimental and theoretical investigation of heat and mass transfer processes during wood pyrolysis. *Combustion and Flame*. 157(3), Combustion and Flame, 2010, Vol.157(3).

Parr Instrument Company. (2007) *Introduction to Bomb Calorimetry (No. 484M)* Available from: http://www.parrinst.com/support/downloads/manuals/ [Accessed 3rd August 2017].

Payne, A. (1962) The dynamic properties of carbon black-loaded natural rubber vulcanizates. Part I. *Journal of Applied Polymer Science*. 6(19), 57-63.

Pena, J., Allen, N., Edge, M., Liauw, C., Santamaria, F., Noiset, O. & Valange, B. (2001). Factors affecting the adsorption of stabilisers on to carbon black (flow micro-calorimetry and FTIR studies). Part I Primary phenolic antioxidants. *Journal of Materials Science (USA)*. 36(12), 2885-2898.

Pilla, S. D. (2004) *Slip and Fall Prevention: A Practical Handbook*. US, CRC Press.

Pires, A., Martinho, G. & Chang, N. (2011) Solid waste management in European countries: A review of systems analysis techniques. *Journal of Environmental Management*. 92(4), 1033-1050.

Prifysgol Bangor University, Water UK & ADAS. (2014) *Biosolid nutrient management matrix*. Available from: http://www.adas.uk/Downloads/Biosolids_Nutrient_Management_Matrix.pdf [Accessed 25th June 2017].

Public health, England and Wales, Public health, Scotland. (1989) *The Sludge (Use in Agriculture) Regulations 1989*.

Pullket, S. (2015) *Sewage sludge as source of activated carbon for the thermal of endocrine disrupting chemicals in wastewater*. PhD Thesis. Imperial College London. U.K.

Puskas, J. E., Gautriaud, E., Deffieux, A. & Kennedy, J. P. (2006) Natural rubber biosynthesis—A living carbocationic polymerization? *Progress in Polymer Science*. 31(6), 533-548.

Qian, J. M., Wang, J. P. Qiao, G. J. & Jin, Z. H. (2004) Preparation of porous SiC ceramic with a woodlike microstructure by sol-gel and carbothermal reduction processing. *Journal of the European Ceramic Society*. 24(10-11), 3251-3259.

Retsch. (2017) *Vibratory Disc Mill RS 200*. Available from: http://www.retsch.com/products/milling/disc-mills/rs-200/function-features [Accessed 7th July 2017]

Reviews, C. (2016). *Introduction to Statistics and Data Analysis*. US, Cram101 Textbook Reviews.

Rio, S., Faur-Brasquet, C., Le Coq, L. & Le Cloirec, P. (2005) Structure characterization and adsorption properties of pyrolyzed sewage sludge. *Environmental Science and Technology*. 39(11), 4249-4257.

Rivlin, R. S. (1956). In: Eirich, F.R. (ed.) *Rheology.* New York, Academic Press.

Rodgers, B. & Waddell, W. (2005) The science of rubber compounding. In: Mark J. E., Erman B. & Eirich F. R. (ed.) *Science and Technology of Rubber*. (3rd ed.). Burlington, Elsevier Academic Press, pp. 401-454.

Rofiqul Islam, M., Haniu, H., & Rafiqul Alam Beg, M. (2008) Liquid fuels and chemicals from pyrolysis of motorcycle tire waste: Product yields, compositions and related properties. *Fuel*. 87(13), 3112-3122.

Rout, T. K. (2013) *Pyrolysis of coconut shell*. MTeeh thesis. National institute of technology, Rourkela. India.

Roy, C. & Unsworth, J. (1989) Pilot plant demonstration of used tyres vacuum pyrolysis. In: Ferrero G. L., Maniatis K., Buckens A. & Bridgewater A. V. (ed.) *Pyrolysis and Gasification*. London, Elsevier Applied Science, pp. 180-189.

Sae-oui, P., Rakdee, C. & Thanmathorn, P. (2002) Use of rice husk ash as filler in natural rubber vulcanizates: In comparison with other commercial fillers. *Journal of Applied Polymer Science*. 83(11), 2485-2493.

Sae-oui, P., Sirisinha, C. & Thaptong, P. (2009) Utilization of limestone dust waste as filler in natural rubber. *Journal of Material Cycles and Waste Management*. 11(2), 166-171.

Samolada, M. C. & Zabaniotou, A. A. (2014) Comparative assessment of municipal sewage sludge incineration, gasification and pyrolysis for a sustainable sludge-to-energy management in Greece. *Waste Management*. 34(2), 411-420.

San Miguel, G. (1999) *Activated carbon produced by pyrolysis and physical activation of waste tyres*. PhD Thesis. Imperial College London. U.K.

San Miguel, G., Fowler, G. D. & Sollars, C. (1998) Pyrolysis of tire rubber: Porosity and adsorption characteristics of the pyrolytic chars. *Industrial and Engineering Chemistry Research*. 37(6), 2430-2435.

Sareena, C., Ramesan, M. & Purushothaman, E. (2012) Utilization of coconut shell powder as a novel filler in natural rubber. *Journal of Reinforced Plastics and Composites*. 31(8), 533-547.

Saville, B. P. (1999) *Physical Testing of Textiles*. Netherlands, Elsevier, pp. 116-118.

Schmidt, E. (1951) Effect of Colloidal Noncarbon Pigments on Elastomer Properties. *Industrial & Engineering Chemistry*. 43(3), 679-683.

Setua, D., Shukla, M., Nigam, V., Singh, H., & Mathur, G. (2000) Lignin reinforced rubber composites. *Polymer Composites*. 21(6), 988-995.

Sharifan, S. (2014) *A comparative optimisation study of activated carbon production from hazelnut shells by thermal and microwave heating methods*. PhD Thesis. Imperial College London. U.K.

Shen, L. & Zhang. D. K. (2005) Low-temperature pyrolysis of sewage sludge and putrescible garbage for fuel oil production. *Fuel*. 84(7), 809-815.

Shen, W., Guo, Q., Wang, H., Yang, X., Liu, Y. & Zhang, Y. (2008) Product Composition of Pyrolyzed Sewage Sludge and Adsorption of Methylene Blue by Porous Material Derived from It. *Environmental Engineering Science*. 25(1), 99-105.

Sienkiewicz M., Kucinska-Lipka J., Janik H. & Balas A. (2012) Progress in used tyres management in the European Union: A review. *Waste Management*. 32(10), 1742-1751.

Singh, K., Risse, M., Das, J. & Worley. (2009) Determination of composition of cellulose and lignin mixtures using thermogravimetric analysis. *Journal of Energy Resources Technology*. 131(2), 6.

Slack, C. (2003) *Noble Obsession: Charles Goodyear, Thomas Hancock, and the Race to Unlock the Greatest Industrial Secret of the Nineteenth Century*. New York, Hyperion.

Smith, K. M., Fowler, G. D., Pullket, S. & Graham, N. J. D. (2009) Sewage sludge-based adsorbents: A review of their production, properties and use in water treatment applications. *Water Research*. 43(10), 2569-2594.

Strange, K. (2002) Overview of waste management options: Their efficacy and acceptability. In: Hester, R. E., & Harrison, R. M. (eds.) *Environmental and Health Impact of Solid Waste Management Activities*. Royal Society of Chemistry, pp. 1-51.

Stuart, A. S., John, S. D., John, F., D. & Allan, N. H. (2006) Thermogravimetric measurements of the kinetics of pyrolysis of dried sewage sludge. *Fuel*. 85(9), 1248-1253.

Tchobanoglous, G., Burton, F. L. & Stensel, H. D. (2003) *Wastewater engineering: Treatment and reuse* (4th ed., International ed., McGraw-Hill series in civil and environmental engineering). Boston, London, McGraw-Hill.

Thomas, S. & Maria, H. J. (2016) *Progress in Rubber Nanocomposites*. India, Woodhead Publishing, pp. 42-44.

Treloar, L. R. G. (1943) The statistical length of paraffin molecules. *Proceedings of the Physical Society*. 55(5), 345-361.

Tsechansky, L. & Graber, E. R. (2014) Methodological limitations to determining acidic groups at biochar surfaces via the Boehm titration. *Carbon*. 66, 730-733.

Wampler W. A., Carlson T. F. & Jones W. R. (2004) Carbon Black. In: Rodgers B. (ed) *Rubber Compounding, Chemistry and Applications*, Marcel Dekker, pp. 239-284.

References

Wang, M. J., Gray, C. A., Reznek, S. A., Mahmud, K. & Kutsovsky Y. (2000) Carbon Black. In: *Kirk-Othmer Encyclopedia of Chemical Technology*. (5th ed.). John Wiley & Sons Inc., Hoboken, pp. 761-803.

Wang, Z., Guo, Q., Liu, X. & Cao, C. (2007) Low temperature pyrolysis characteristics of oil sludge under various heating conditions. *Energy and Fuels*. 21(2), 957-962.

Water UK & BRC (British Retail Consortium). (1998) *The Safe Sludge Matrix.* Available from: http://adlib.everysite.co.uk/adlib/defra/content.aspx?doc=94726&id=94737 [Accessed 3rd August 2017].

Water UK. (2016) *Biosolids: Good Practice Guidance Leaflet*. Available from: https://dl.dropboxusercontent.com/u/299993612/Publications/Reports/Waste%20recycling/UKWIR%20biosolids%20good%20practice%20leaflet.pdf [Accessed 5th July 2017].

Water UK. (2017) *Sludge management*. Available from: http://www.water.org.uk/policy/environment/waste-and-wastewater/sludge [Accessed 1st August 2017]

Williams, P. T. & Besler, S. (1996) The influence of temperature and heating rate on the slow pyrolysis of biomass. *Renewable Energy*. 7(3), 233-250.

Xie, X., Goodell, B., Zhang, D., Nagle, D. C., Qian, Y., Peterson, M. L. & Jellison, J. (2009). Characterization of carbons derived from cellulose and lignin and their oxidative behavior. *Bioresource Technology*. 100(5), 1797-1802.

Xiong, W., Liu, M., Gan, L., Lv, Y., Li, Y., Yang, L., Xu, Z., Liu, H. & Chen, L. (2011) A novel synthesis of mesoporous carbon microspheres for supercapacitor electrodes. *Journal of Power Sources*. 196(23), 10461-10464.

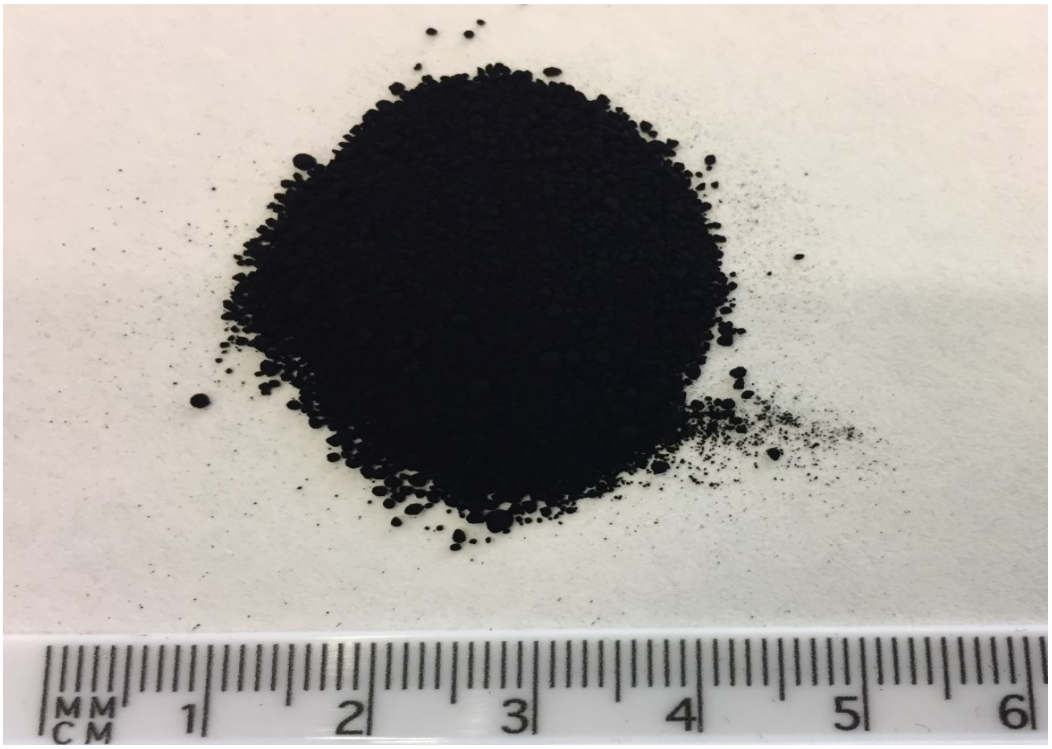
Xu, C. & Lancaster, J. (2009) Treatment of secondary pulp and paper sludge for energy recovery. *Energy recovery.* New York, Nova Science Publishers Inc., pp. 187-212.

Yoshida, H., Christensen, T. H. & Scheutz, C. (2013). Life cycle assessment of sewage sludge management: A review. *Waste Management and Research*. 31(11), 1083-1101.

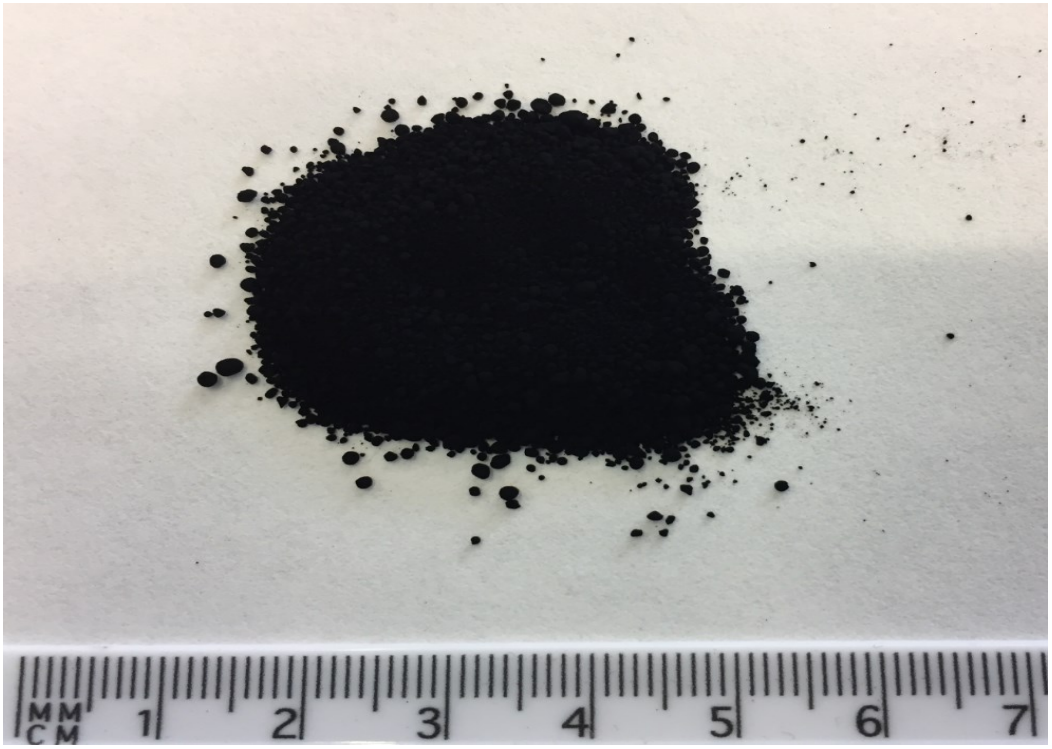
Zhou, X., Li, L., Dong, S., Chen, X., Han, P., Xu, H., .Yao, J., Shang, C., Liu, Z. & Cui, G. (2012) A renewable bamboo carbon/polyaniline composite for a high-performance supercapacitor electrode material. *Journal of Solid State Electrochemistry*. 16(3), 877-882.

Zsigmond, A. (2016) *The effect of electrode binders to electrochemical properties of negative electrode materials*. Bachelor Thesis. Brno University of Technology. Czech Republic.

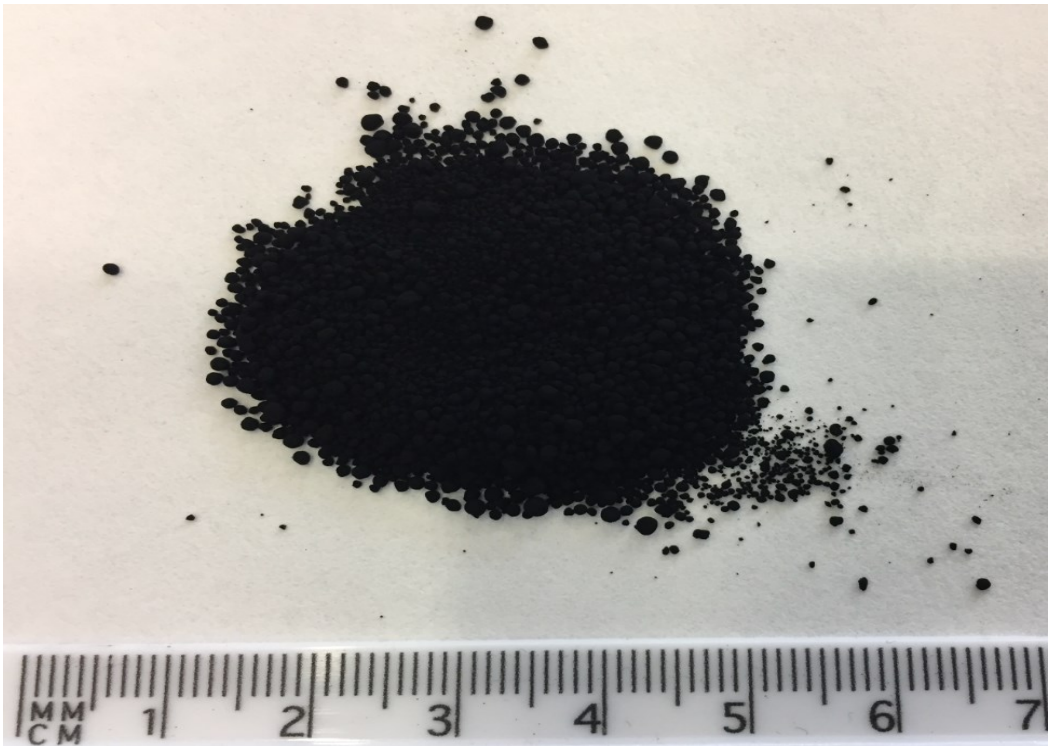
Appendix I Commercial Carbon Black



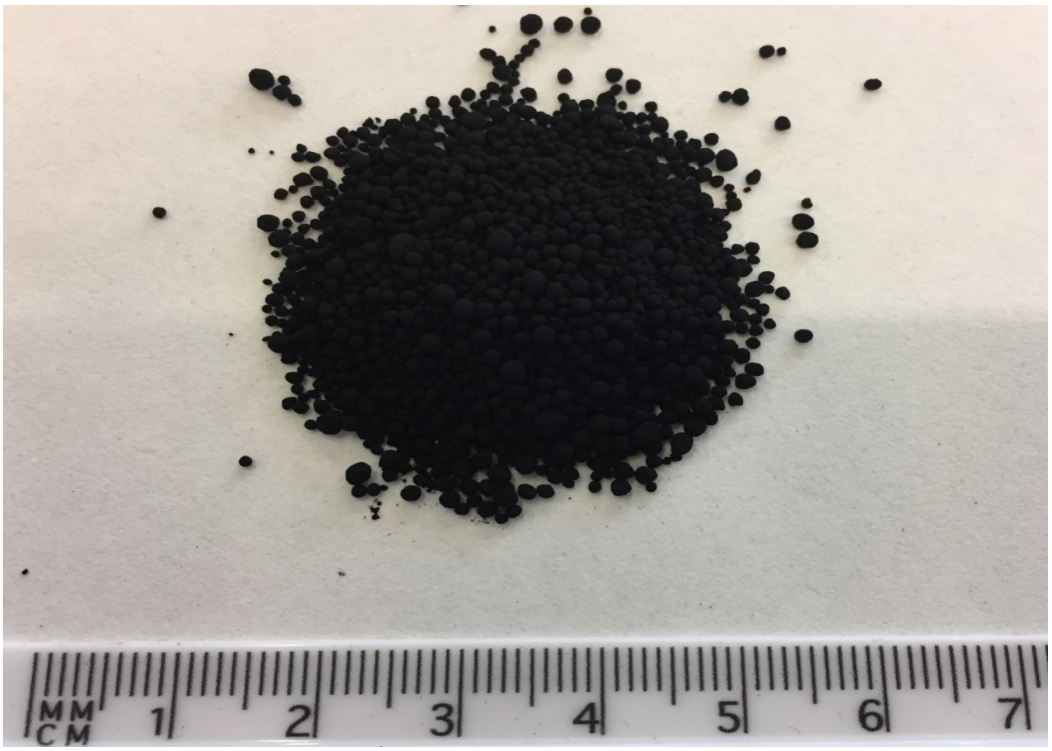
Carbon black N115



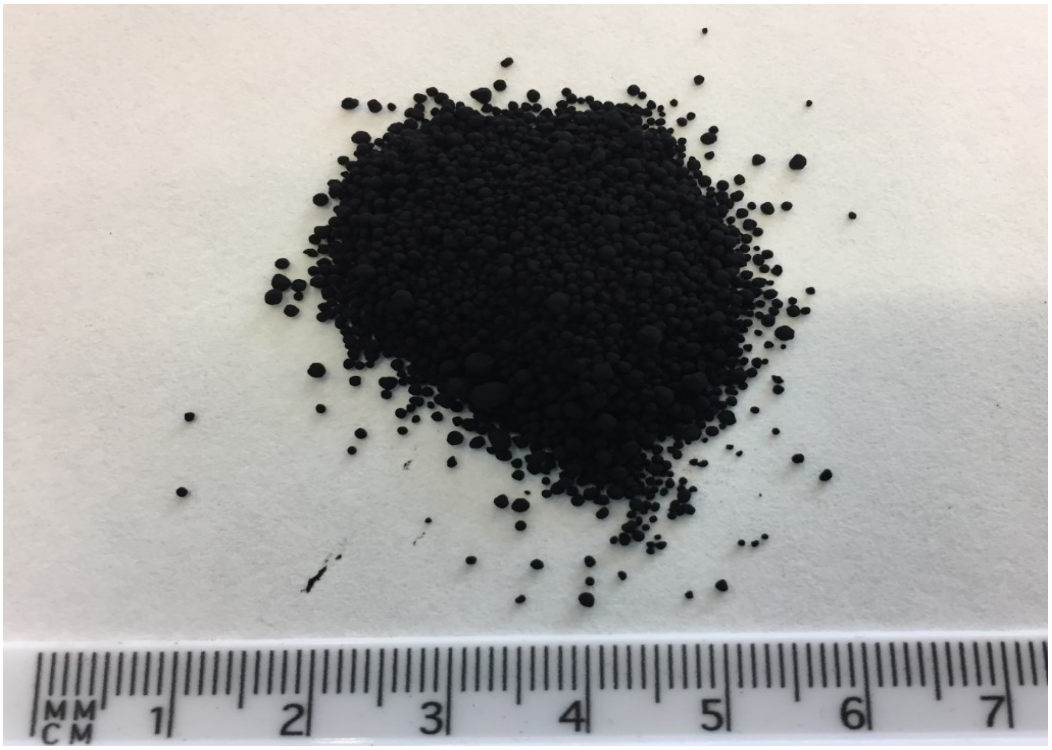
Carbon black N220



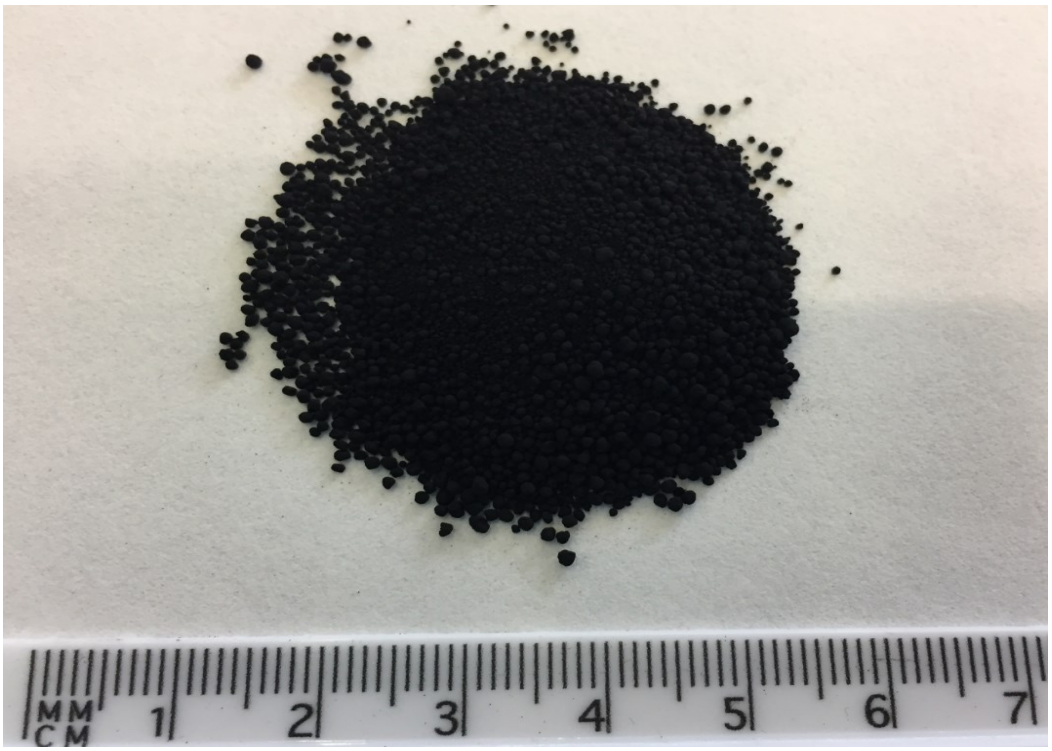
Carbon black N330



Carbon black N550



Carbon black N660



Carbon black N772

Figure I. Commercial carbon black N115, N220, N330, N550, N660 and N772

Appendix II

Publications arising from this research

1. Fan, Y., Fowler, G. D., & Norris, C. (2017) Potential of a Pyrolytic Coconut Shell as a Sustainable Biofiller for Styrene-Butadiene Rubber. *Industrial and Engineering Chemistry Research*. 56(16), 4779-4791.

2. Article "Potential of a Pyrolytic Coconut Shell as a Sustainable Biofiller for Styrene–Butadiene Rubber" was included in the Virtual Special Issue "Invited Papers from ACS Philadelphia" in *Industrial & Engineering Chemistry Research*. Virtual Special Issue: http://pubs.acs.org/page/iecred/vi/philadelphia-national-meeting2016.

Oral Presentations

1. *Potential of a Pyrolytic Coconut Shell as a Sustainable Biofiller for Styrene-Butadiene Rubber*. Presented at the 252nd ACS National Meeting in Philadelphia, August, 2016. Identified as "Best Presentation" in the ENVR session.

2. *The Potential of Pyrolytic Raw sewage sludge as a Sustainable Bio-filler for styrene-butadiene rubber*. Presented at IWA Specialist Conference On sludge Management SludgeTech 2017, 9th – 13th July, 2017.